

Division of Pharmaceutical Biosciences

Drug Research Program

Faculty of Pharmacy

University of Helsinki

Finland

Doctoral Programme in Drug Research (DPDR)

Enhancing oncolytic adenovirus therapy by simultaneously activating multiple immune effector populations

Firas Hamdan

ACADEMIC DISSERTATION

To be presented for public discussion with the permission of the Faculty of Pharmacy of the University of Helsinki, in Lecture hall 2041, Biocenter 2, on the 14th of July, 2023 at 12:15

Helsinki 2023

Supervisors

Professor Vincenzo Cerullo, PhD

Division of Pharmaceutical Biosciences
Drug Research Program
Faculty of Pharmacy
University of Helsinki
Finland

Thesis Committee

Pia Siljander, PhD

Extracellular Vesicle Research Group
Molecular and Integrative Research Program,
Faculty of Biological and Environmental Sciences
CURED, Drug Research Program, Faculty of Pharmacy
University of Helsinki
Helsinki, Finland

Professor Satu Mustjoki, MD, PhD

Hematology Research Unit
Department of Clinical Chemistry and Hematology
University of Helsinki
Helsinki, Finland

Pre-Examiners

Professor Sirpa Jalkanen, MD, PhD

Academician
Director of InFLAMES Flagship
University of Turku
Turku Finland

Professor Kalle Saksela, MD, PhD

Professor, Department of Virology
Doctoral Program in Biomedicine
HUSLAB
University of Helsinki
Helsinki, Finland

Opponent

Professor Richard Vile, PhD

Department of Molecular Medicine
Department of Immunology
Mayo Clinic
Rochester MN, USA

Custos

Professor Vincenzo Cerullo, PhD

Division of Pharmaceutical Biosciences
Drug Research Program
Faculty of Pharmacy
University of Helsinki
Finland

© Firas Hamdan Hissaoui

ISBN 978-951-51-9334-6 (softcover)

ISBN 978-951-51-9335-3 (PDF)

Unigrafia/Hansaprint Oy

Helsinki 2023

“ Sometimes science is more art than science “

Rick Sanchez from Dimension C-132

“ ان كنت تعرف شياء " فقد غابت عنك أشياء ”

Murmured by Samir Hamdan countlessly

Table of Contents

Acknowledgements	9
Abstract	14
List of Original publications	17
Personal contribution to original publications	18
Abbreviations	19
1. Introduction	21
2. Cancer Immunotherapies	22
2.1. Passive immunotherapies	23
2.1.1. Cytokines	24
2.1.2 Adoptive cell therapy (ACT).....	25
2.2.3 Antibody Therapy	26
2.2 Active Immunotherapy	36
2.2.1 Checkpoint inhibitory therapy	36
2.2.2 Cancer Vaccines	43
2.2.3 Oncolytic viruses.....	44
3. Adenoviruses and their roles as cancer therapies	44
3.1 Adenoviruses	45
3.1.1 Adenovirus genome, replication, and machinery behind it.....	46
3.1.2 Adenovirus-host cell interactions and selective replication	48
3.1.3 Arming oncolytic adenoviruses	49
3.1.4 Construction of adenoviral vectors.....	52
4. Aims of the Study	53
5. Methods and Materials	54
5.1 Cell lines.....	54
5.2 Oncolytic adenoviruses	54
5.3 Transgene insertion into Adenovirus genome	55
5.4 Amplification and purification of oncolytic adenoviruses	56
5.5 Particle titering	56
5.6 Infectivity assay	57
5.7 Viability assay	57
5.8 PBMC migration assay.....	57
5.9 Determining concentrations of biological molecules	58
5.10 Competition assay.....	58
5.11 PBMC, PMN, monocyte and complement active serum isolation.....	58
5.12 Mixed leukocyte reaction (MLR).....	59

5.13 Complement dependent cytotoxicity.....	59
5.14 Antibody dependent cell mediated cytotoxicity	59
5.15 Antibody dependent cell mediated phagocytosis	60
5.16 Trogocytosis	60
5.17 Real-time quantitative analysis (xCELLigence assay)	60
5.18 Live cell imaging	61
5.19 Whole blood assays.....	61
5.20 Patient derived cancer organoid cultures	61
5.21 Immunofluorescence and flow cytometry analysis on organoids	62
5.22 Organoid viral infection, PBMC co-culture and ADCC experiments.....	62
5.23 Syngenic mice models	63
5.24 <i>In-vivo</i> immune cell depletion	63
5.25 Humanized mice studies.....	64
5.26 Flow cytometry	64
5.27 Statistical analysis	64
6. Results and Discussions.....	65
6.1 Study I. GAMER-Ad: An enhanced and faster cloning method for oncolytic adenoviruses....	65
6.1.1 Designing and executing the GAMER-Ad cloning method	65
6.1.2 Quality control of assembled adenovirus genome products	66
6.1.3 Oncolytic fitness and functionality of adenovirus engineered by GAMER-Ad	67
6.2 Study II: Activating multiple immune effector populations using a cross-hybrid IgGA Fc fusion peptide against PD-L1.....	69
6.2.1 Characterizing oncolytic adenovirus expressing cross-hybrid IgGA Fc fusion peptide.....	69
6.2.2 Ad-Cab induces Fc-effector mechanisms of both IgG1 and IgA1.....	70
6.2.3 Activation of multiple effector mechanisms elicit high tumor killing.....	72
6.2.4 In-vivo efficacy of Ad-Cab with CT26 and A549 tumor models.....	74
6.2.5 Ad-Cab does not solely require CD8+ T cells like conventional checkpoint inhibitory therapy.....	76
6.2.6 Generation and testing of patient derived organoids with Ad-Cab.....	76
6.3 Study III: Controlled release of enhanced cross-hybrid IgGA Fc fusion peptide against PD-L1	78
6.3.1 Cab FT induces high tumor killing at lower concentrations when PBMCs are added	78
6.3.2 Cab and Cab FT do not induce cell death of certain leukocyte population while blocking the PD-L1/PD1 axis	79
6.3.3 Engineering Fc-fusion peptides into oncolytic adenoviruses for controlled release and induction of Fc-effector mechanism.....	80
6.3.4 Kinetics of tumor cell killing with Ad-Cab and Ad-Cab FT using XCELLigence.....	81
6.3.5 Lower amounts and dosages are required for Ad-Cab FT for <i>in vivo</i> efficacy.	82
7. Conclusions and Future Prospects	84
<i>References.....</i>	<i>Error! Bookmark not defined.</i>
<i>Original publications</i>	<i>Error! Bookmark not defined.</i>

Acknowledgements

The following work presented in this thesis was carried out at the University of Helsinki, Faculty of Pharmacy, Division of Pharmaceutical Bioscience in the Doctoral Programme of Drug Research under the IVTLab. I want to express my eternal gratitude for the Faculty of Pharmacy for providing me the facilities to conduct my research. Also, this work would have not been possible with the financial support of the University of Helsinki Research foundation.

I am forever grateful to Prof. Richard Vile for accepting the role of thesis Opponent and travelling from the USA. Very early on in my scientific path I was truly amazed with your work and having you read and debate my research is truly humbling. I truly have to thank Prof. Satu Mustjoki and Dr. Pia Siljander for their indispensable input concerning my thesis work, this work would have not been the same without your guidance. Prof. Kalle Saksella and Prof. Sirpa Jalkanen, I am very thankful for reading my thesis and helping me shape it to its final form.

I would like to thank Prof. Vincenzo Cerullo for being my mentor and supervisor during this thesis. You have guided me through this scientific journey in a manner I would have never imagined. Other than guiding me through a scientific way, you have showed me what creativity looks like and how important it is in science. Also, you have witnessed many of my turning live events and have helped me through these tough times. For this I will be eternally grateful! If I ever reach to a PI position, I hope I have the same passion, ambition and love of science as you do.

A big thank you to all the IVT members that I have had the pleasure to work with. Starting with Cristian Cappasso, thank you for grilling me with questions and giving me a clear picture of the IVTLab during my interview. Manlio, I have nothing to say but thank you for always helping me during the hardest times and showing me what caring means. Also, I will miss our talks about what science should look like. Sara thanks for giving me an example of what hard work and motivation is. It provided me with a framework that I wish to follow in the future. Jacopi, we share the same b-day, almost the same phone numbers and almost first author

paper in the same academic journal. That I will always remember but also showing me what hard work, dedication and the art of questioning can result in! I know that you will be doing great things in the future. Erkko, you are truly an example of what a scientist should be like. Smart and humble! Your creativity is something so unique that I was able to learn so much from. Thank you Katarina for helping me out in the IVT Lab, without you I would have been lost through my PhD. Bea, you also have huge thank you in not letting me get lost in this lab! I know for sure that Netherlands gained an amazing scientist with you. Gabi, thank you for sharing your love of food, organizing and cleaning skills with me. Hopefully one day I will put them to good use and say I have learned from the best. Salvatore, thank you for being part of this lab and for showing us what ambition is. Keep feeding your ambition with reading everyday (as you are doing) and you will go far I am sure. Otto, I am so happy that you joined the IVT Lab. As a lab we have so many things to learn from you when it comes to coordinating projects. Inesiii even though you are not officially part of the IVT Lab, we all know that you are one of us. You have taught me what resilience is and how important that is in science but also in life! Eres grande!

One of the biggest “thank you” I should be giving in my scientific career is to Mitchell Evers. Mitchell, thanks to you and your mentoring I learned to always ask, be curious and be extremely analytical in my work. You taught me how to be independent, formulate scientific questions and watch out for small chili peppers. Because of my mentor, I realized how important is to be a supervisor in someone’s scientific path. I have been truly lucky with mentoring the best students I can ask for and I truly hope I have guided you in the best way possible. To my first ever student, Yvonne it was nothing but a pleasure to work with you. I thought I was filled with ambition, courage and dedication until I met you. Never let that spark die, because that is what will make you into a great scientist. I envy the lab that will hire you as a PhD student! Mela, or more like MA GLIPGLOOOOP, I am so happy that you decided to join the IVT Lab as a PhD student. The lab has gained an ambitious and highly motivated PhD student but more importantly I gained a friend in the making. Andrea, I knew from the first day you joined the IVT Lab that we were going to be paired up. I am so thankful that we did because I had nothing but the greatest time with you in the lab. We came up with an amazing/ambitious project while constantly cracking jokes with each other. Will always remember our carbonara and greens night. To a big bundle of joy and energy, Meta thank

you for giving me a bit of life during the hard times in the lab. Because of your hard working and positive energy we were able to clone two viruses in nothing less than 1 week! I am happy that got the chance to go to Brisbane, I am sure the University of Queensland were lucky to have you. Elisa/Topolina/Dandelion, my final student during my PhD! I am truly grateful that you were the last student of mine during this journey, the perfect ending. I am truly amazed how fast you were able to learn things. From someone with zero experience in a lab to leaving the lab knowing how to do cell culture, do *in vitro* AND *in vivo* work is amazing.

To the people at the DPDR that have helped me through my PhD, Saara thanks for being a great friend! I will truly miss our rants at the coffee room and the advice you have always given me. Carmine, I have so many things to thank you for I do not know where to start. Thank you for being a true friend, a basketball mate and someone I have let out almost all my frustrations during my PhD. I will always have that night I beat you 1v1 outside my house! Flavia, thank you for being another scientist to look up to! The work you have done just stuns me and wish to learn from you. Thank you for being a great friend and introducing me to the wonderful men in your life, Otto and Mikko. To Joao (Martins), thank you for making me laugh to a point of almost breaking a rib. The first ever night in Helsinki as a PhD student was unforgettable at the BrewDog because of your humor and positivity. Mariia, thank you for being a friend and making want to live life to the fullest. Seeing all the adventures you take in life has pushed me to also try things out. Riina you are another source of inspiration and bundle of positivity. Thank you for showing me how to be a truly amazing parent and scientist at the same time. Victor and Joao (Santos), even though you guys were not present at the DPDR you have helped me finish this thesis with your endless questions and scientific discussions. Victor eres un cansino pero un referente en la vida, un gran científico y un gran amigo. Joao, all I could remember before meeting you was how people at the UMC (Utrecht) were hyping you and I truly understand why. Thanks for the endless scientific discussion and great beers we have had.

To my basketball teammates at Sykki, I have nothing to say but uff. Uff in a sense of relief because without you guys my days in dark Helsinki would have been such a nightmare. Daniele, tu eres de los mas grandes personajes que e encontrado en esta vida. Tu amor por la cerveza y los amigos me han ayudado bastante con mi PhD. Sin ti, me hubiera muerto del

asco en esta pandemia. Gracias no solo por ser uno de mis mejores amigos pero un referente a la vida. Carlos tu positividad en la vida es una de las grandes virtudes que tienes, gracias por compartirla con nosotros! Tengo mucho que aprender de ti esta vida. Fue un gran placer en conocerte y espero verte en el futuro. Bernardo weyyyyy siempre voy a recordarme de nuestros partidos en myllupuro, hiestu y con Sykki. Gracias por ser un gran amigo y espero que logres todo en tu mente. Federico, I don't know what to say... You surprise me because you break every single stereotype I have. How can someone have that energy, passion, ambition and zealousness while being an academic Prof. Nothing but respect and willingness to learn from you. Will always remember Bergamo and nights at your place (ITS CARMINEEEE, ITS SATURDAY)!

To my zbele friends (Baks and Gee), I have my whole life to thank you for. You guys knew me when I was 14 years old wanting to fight anyone and get into trouble and still wanted to be friends with me. You have seen me and been present at the lowest points in my life and always have been there to support me. I truly don't know where I would be in life without you and your zbele. However, I will never forget how you two shouted at me for not saying that the Lebanese cuisine was the best in San Sebastian. I could not ask for better friends in this world! Let's keep up the travelling experiences.

My sincerest thank you to you, Elina. Amor, I need to thank you for having the ability to listen to my rants without a complain and always being honest with me. You have always been able to change my mood from angry/exhausted to happy/energetic. Because of this, I was able to finish this thesis so quickly. I truly appreciate our long conversations over great food and going through endless tiny desk concerts on Youtube. More importantly, I love that I have gained a partner in life to travel all around the world and embark in life goals together. I know that we will be forming even greater memories and exhilarating adventures. Gracias por todo rakas, te amo.

Mama w Baba, kil shi li 2deret 3amlo b hal hayet min warakon. Into 3alamtune ishte8el b nafse w ikstakshaf 2ouwet. Baba, ma fi minak b hal denye. Ma rah insa 2il lyom le kazaret 2il laptop bil tawle. Hayde kenet lahza b hayet kil shi t8ayar. Min hadan da3ye2 bil hayet, faja2tan seret mrakas bil dares w balashet ebne hayete. Hayda kelo min warak ma rah 2insilak yeha.

Ya mama 2il hanune. Australia kenit min 3as3ab sha8let b hal denye. Ma ken fine 2edar en7e hal fatra law mish men warake. Inte sa2adtine w ntabahte 3aleye. Inte 2ankaste hayete b hal lahza. Bhebkon 2ad hal dinye!

Karim w Hadi shu bade 2elkon 8eir ino telhaso tize b kel ma3na 2il kelme. Hadi 3anjad shu bade 2elak, honestly thank you for setting an example for hard work while growing up. I know that it should be the other way around but we both know who was more responsible during those times. It's crazy that both of us are turning into Drs, mine weighing more than yours but who is counting. Karim, it's crazy to think that from the brothers you are the one who will outsmart us all. A diamond for sure, but in the making.

Firas Hamdan
Helsinki 2023



Abstract

Checkpoint inhibitors have been regarded as a milestone in cancer therapy due to the imminent success in the clinics. Among such checkpoint inhibitors, PD-L1 antibodies have shown outstanding clinical efficacy and have been approved for the treatment of more than 14 different type of cancers. Despite the success, only 14% of patients are eligible for PD-L1 antibody therapy and from them only 44% respond. Therefore, a clear improvement of such therapy is required. Such antibodies are not able to elicit effector mechanisms due to point mutations in the IgG Fc-region removing binding to Fc- γ receptors. This is done because of safety concerns, since PD-L1 expression is not solely limited to the tumor but widely expressed on different types of healthy cells. Nevertheless, *in vivo* studies have shown that arming PD-L1 checkpoint inhibitors with Fc-regions able to elicit effector mechanism leads to increased tumor killing. In need of enhanced PD-L1 checkpoint inhibitors, in this thesis we developed two powerful PD-L1 checkpoint inhibitors able to elicit Fc-effectors mechanisms of both an IgG1 and IgA1. Moreover, to limit side effects we used oncolytic adenoviruses as biological carries to express and limit the secretion of the PD-L1 checkpoint inhibitors to the tumor.

Oncolytic adenoviruses have a specific tumor-tropism that can be utilized to express any desired gene of interest to the tumor microenvironment. Nevertheless, the current methods using homologous recombination to clone oncolytic adenoviruses are time-consuming and inefficient. In Study I, we designed and tested a novel cloning method, called GAMER-Ad, which utilizes the Gibson assembly method rather than homologous recombination for cloning. To test GAMER-Ad, we designed three oncolytic adenoviruses to express CXCL9, CXCL10 or IL-15. GAMER-Ad was shown to be a viable strategy to clone oncolytic adenoviruses in the period of 2-3 days. Also, the cloning method did not affect the oncolytic/replication fitness of the viruses and yielded functioning viruses able to express the corresponding gene. GAMER-Ad was then used in the following studies to clone all oncolytic adenoviruses.

In Study II, we developed an oncolytic adenovirus (Ad-Cab) able to secrete a PD-L1 checkpoint inhibitor able to elicit Fc-effector mechanisms of an IgG1 and IgA1. The expressed checkpoint inhibitor consisted of PD-1 ectodomain (able to bind to murine and human PD-L1) connected to a cross-hybrid IgGA Fc-region (contains heavy chain regions of an IgG1 and IgA1). The virally released cross-hybrid Fc-fusion peptide was able to activate PBMCs, PMNs, complement proteins and macrophages not usually done by either IgG1 or IgA antibodies solely. The engagement of multiple effector mechanisms did lead to an enhanced tumor killing by Ad-Cab compared to PD-L1 antibodies with an IgG1 or IgA Fc-region when all immune components were present. This enhancement was also translated *in vivo* since Ad-Cab outperformed conventional PD-L1 antibodies with various tumor models (4T1, CT26 and A549). This enhancement was attributed to an increased activation of NK cells and reduction of myeloid derived suppressor cells *in vivo*. Moreover, Ad-Cab was shown not to require CD8+ T cells for *in vivo* efficacy unlike the conventional PD-L1 antibodies used. As expected, no signs of toxicity were observed since no reduction in weight was observed in mice and the Fc-fusion peptide was limited to the tumor. Therefore, arming PD-L1 antibodies with Fc-effector mechanisms of an IgG1 and IgA1 leads to higher tumor-killing and safety concerns can be circumvented using oncolytic adenoviruses.

Further building on Ad-Cab, in Study III we designed Ad-Cab FT which had the same Fc-fusion peptide designed in Study II but with four-point mutations in the IgG region. These point mutations increased the affinity towards activating Fc- γ receptors leading to higher NK cell activation. At higher concentrations, Ad-Cab FT had similar levels of tumor lysis as Ad-Cab when PBMCs were added. However, at lower concentrations Ad-Cab FT induced higher tumor killing than Ad-Cab with PBMCs. This enhancement was not shown with PMNs or complement activation. Due to the high activation of PBMCs at lower concentration, Ad-Cab FT outperformed Ad-Cab *in vivo* when low doses and reduced administrations of the virus was given. With Ad-Cab FT treated mice, a higher activation of NK cells in the tumor microenvironment was observed compared to Ad-Cab treated mice. Hence, Ad-Cab FT represents a potentiated therapy with potential use in the clinic.

Taken together, this thesis has highlighted the importance of eliciting multiple immune populations to enhance tumor killing with PD-L1 checkpoint inhibitors and potentially with other therapies. The IgG4 Fc-region may be used in other antibody-based therapies to further increase tumor killing and subsequently clinical efficacy. Finally, oncolytic adenoviruses have demonstrated in this thesis to be excellent biological carriers, limiting the toxicity of dangerous anti-tumor agents.

List of Original publications

The following thesis is based on the following publications which are referred in Roman numerals in the text:

- I. **Hamdan F**, Martins B, Feodoroff M, Giannoula Y, Feola S, Fucciello M, Chiaro J, Antignani G, Grönholm M, Ylösmäki E, Cerullo V. GAMER-Ad: a novel and rapid method for generating recombinant adenoviruses. *Molecular Therapy- Methods & Clinical Development*. 2021 Feb 4;20:625-634. doi: 10.1016/j.omtm.2021.01.014. PMID: 33718513; PMCID: PMC7907680.

- II. **Hamdan F**, Ylösmäki E, Chiaro J, Giannoula Y, Long M, Fucciello M, Feola S, Martins B, Feodoroff M, Antignani G, Russo S, Kari O, Lee M, Järvinen P, Nisen H, Kreutzman A, Leusen J, Mustjoki S, McWilliams TG, Grönholm M, Cerullo V. Novel oncolytic adenovirus expressing enhanced cross-hybrid IgGA Fc PD-L1 inhibitor activates multiple immune effector populations leading to enhanced tumor killing in vitro, in vivo and with patient-derived tumor organoids. *Journal for Immunotherapy of Cancer*. 2021 Aug;9(8):e003000. doi: 10.1136/jitc-2021-003000. Erratum in: *J Immunother Cancer*. 2021 Sep;9(9):1. PMID: 34362830; PMCID: PMC8351494.

- III. **Hamdan F**, Feodoroff M, Russo S, Fucciello M, Feola S, Chiaro J, Antignani G, Greco F, Leusen J, Ylösmäki E, Grönholm M, Cerullo V. Controlled release of enhanced cross-hybrid IgGA Fc PD-L1 inhibitors using oncolytic adenoviruses. *Mol Ther Oncolytics*. 2023 Feb 5;28:264-276. doi: 10.1016/j.omto.2023.01.006. PMID: 36911070; PMCID: PMC9995465.

Personal contribution to original publications

- I. The planning and conceivement of the experiments were done by Hamdan F, Martins B, Ylösmäki E, and Cerullo V. Hamdan F carried out most of the experiments. This project was surprised by Ylösmäki E and Cerullo V. Hamdan F drafter the manuscript and was corrected by Martins B, Ylösmäki E, and Cerullo V. All authors gave critical feedback that shaped the analysis, research and entire manuscript

- II. The planning and conceivement of the experiments were done by Hamdan F, Chiaro J, Ylösmäki E, and Cerullo V. Hamdan F carried out most of the experiments. Long M and McWilliams TG performed the live-cell microscopy. Hee Lee M, Järvinen P, Nisen H and Kreutzman H helped in providing patient material. Grönholm M and Cerullo V surpervised this project. Hamdan F drafted the manuscript and was corrected and shaped by the critical feedback of all authors.

- III. The planning and conceivement of the experiments were done by Hamdan F, Feodoroff M, Ylösmäki E, and Cerullo V. Hamdan F carried out most of the experiments. Grönholm M and Cerullo V surpervised this project. Hamdan F drafted the manuscript and was corrected and shaped by the critical feedback of all authors.

Abbreviations

ACT= Adoptive cell therapy

Ad Pol= Adenovirus polymerase

ADCC= Antibody dependent cell mediated cytotoxicity

ADCP= Antibody dependent cell mediated phagocytosis

APC= Antigen presenting cell

ATCC= American type culture collection

BCR= B cell receptor

BSA= Bovine serum albumin

CAR= Chimeric antigen receptor

CAR= Coxsackie adenovirus receptor

CDC= Complement dependent cytotoxicity

CDR= Complementary determining region

CH= Constant heavy chain

CL= Constant light chain

CMV= Cytomegalovirus

CRS= Cytokine release syndrome

DAB= 3,3'-Diaminobenzidine

DBP= DNA binding protein

DC= Dendritic cell

EGFR= Epidermal growth factor receptor

EMEM= Eagle's minimum essential medium

EpCAM= Epithelial cell adhesion molecule

Fab= Fragment antigen binding

FAP= Fibroblast activation protein

FBS= Fetal bovine serum

Fc= Fragment crystallizable

GM-CSF= Granulocyte-macrophage colony-stimulating factor

GOI= Gene of interest

Gp100= glycoprotein 100

HAMA= Human anti-mouse antibody

HER2= Human epidermal growth factor receptor 2

HRP= Horseradish peroxidase

IFN- γ = Interferon γ

IL-2 = Interleukin 2

ITR= Inverted terminal repeats

LB= Lysogeny broth

MDSC= Myeloid derived suppressor cells

MHC= Major histocompatibility complex

MLP= Major late promoter

MLTU= Major late transcription unit

NF1= Nuclear factor 1

NK= Natural Killer cells

NKT= Natural Killer T cell

OS= Overall survival

OV= Oncolytic virus

PAP= Prostatic acid phosphatase

PBMCs= Peripheral blood mononuclear cells

PMNs= Polymorphonuclear leukocytes

pRB= Retinoblastoma protein

pTP= Precursor terminal protein

RCC= Renal cell carcinoma

RPMI= Roswell park memorial institute

ScFv= Single chain fragment variables

TAA= Tumor associated antigen

TCR= T-cell receptor

Th₂= T helper 2 cell

TIL= Tumor infiltrating lymphocyte

TNF- α = Tumor necrosis factor α

Treg= Regulator T cell

VH= Variable heavy chain

VL= Variable light chain

1. Introduction

The pronunciation of the word cancer may alarm the majority, if not all, of the people. This is simply because of its serious health effects which has brought it to be the second leading cause of death, after cardiac conditions^{1,2}. Scientific surveys from the UK in 2019 have observed that the public's main support for scientific research concerned cancer research³. Analysts perceive this wide support towards the subject as an eager awaited miracle drug that could cure cancer. Yet, as our understanding of cancer grows the discovery of such miracle drug seems to be lost hope.

Cancers have shown to have a dense complexity regarding its biology. In 2000, Hanahan and Weinberg published one of the most cited reviews in the cancer biology field describing the hallmarks of cancer⁴. Six hallmarks were described to oversimplify the needed characteristics for a successful tumor growth. Based on such hallmarks, traditional therapies were developed ranging from radiation, chemotherapy, and targeted therapies.

To this day, radiation and chemotherapy represent one of the most used therapies for the treatment of cancer⁵. The main mode of action of such therapies is the direct tumor cell lysis via different mechanisms. This may be perceived as old fashioned since the mode of action has seen not to be that effective in eradicating full tumors and accompanies serious adverse effects. Moreover, these therapies have a growing list of serious side effects detrimental to patients. In spite of this and as our understanding of cancer biology grew, targeted therapies took the stage since they were more effective and safer⁶. Targeted therapies consist of molecules that exploit certain biological difference among healthy and cancer cells allowing for selective targeting. Nevertheless, advancements in genomic sequencing have demonstrated that cancer is not a monogenic disease yet a complex and heterogenous disease⁷. This explains why the use of targeted therapies targeting single molecules have not shown an overwhelming success as once expected.

After a decade from the Hanahan and Weinberg review, the authors updated the list of hallmarks by adding two new hallmarks: reprogramming energy metabolism and evading immune responses⁸. The latter hallmark consists of a crucial interplay where the immune

system has the capabilities to recognize and kill cancer cells. Hence, tumor cells have developed multiple strategies to overcome immune recognition. Also, tumor cells have shown to induce a tumor-promoting inflammation. As a result of this, a novel era of treatments was developed enhancing the immune system to recognize cancer. In 2013, the world-renowned science journal, *Science*, dubbed such treatment as “breakthrough of the year” due to the significant impact in the clinic⁹. These treatments offer the use of the patient’s own immune system to induce anti-tumor response able to sustain a long-lasting anti-tumor killing.

As successful as immunotherapies have been described, looking at the statistical numbers a very small minority (20-40%) of people do benefit from them¹⁰. Multiple reasons have been formulated over the years concerning why most of the patients do not respond. Nevertheless, a need to improve such treatments is required. This thesis will provide novel strategies to further improve immunotherapies using both antibody structures and oncolytic adenoviruses.

2. Cancer Immunotherapies

Our immune system has a significant role in keeping the integrity of our health. Besides its obvious role in protecting against pathogens, it has a more unobtrusive but highly crucial role in cancer prevention and defence. Already in 1909, Paul Ehrlich postulated that the power of the immune system may be harnessed to control cancer. It was proposed that immune cells are constantly surveilling cells throughout the body, able to recognise and eliminate incipient cancer cells and therefore halt the production of nascent tumours¹¹. This was validated by striking results where immunocompromised individuals had an increased risk in developing certain cancers¹². Furthermore, mice models with defective T cells and NK cells were shown to be more susceptible to cancer¹³. However, according to such logic, tumours that appear and progress in otherwise healthy individuals should be able to somehow resist or evade elimination by the immune system. Further research indeed indicated that the tumour microenvironment was immunosuppressive and cancer cells are able to develop multiple

immune evasion strategies¹⁴. In spite of this, boosting the immune system has been the major target for drug development in the treatment of cancers for the past decade.

Our immune system has a well-known ability to distinguish between self and non-self, especially in the case of infection or malignancy. This process is called immune surveillance and it is crucial in eliminating hundreds of newly formed malignant cells on a daily basis. This process is divided into three parts; elimination, equilibrium and escape¹⁵. The first phase consists of a dynamic process of cancer immunoediting in which immune cells recognize tumor cells expressing immunogenic antigens¹⁶. This then allows the immune cells to recognize and kill tumor cells. However, not all of tumor cells are immunogenic leading them to not be recognized by immune cells. This adds a bottle neck pressure inducing a positive selection of tumor cells with reduced immunogenicity. These cells then enter the final stage of escape since they are unharmed by the immune system and can proliferate uncontrollably¹⁶⁻¹⁸.

In spite of this, the main objective for cancer immunotherapies is to redirect the immune system towards these cells with reduced immunogenicity¹⁹. The current cancer immunotherapies in the clinic can be divided into two groups based on mechanism of actions: passive or active immunotherapies. Active immunotherapies involve the direct activation of a tumor-specific immune response. While passive immunotherapies are molecules that are given to patients that cannot induce them on their own.

2.1. Passive immunotherapies

In many patients, the ability to induce a proper anti-tumor immune response is hindered by factors of immunosuppression. Thus, passive immunotherapies try to overcome such limitation by fighting cancer directly. These molecules endow intrinsic antitumoral activity and can indirectly or directly target tumor cells. In this section these types of molecules will be further explained.

2.1.1. Cytokines

Cytokines are small molecules expressed by both inflammatory and non-inflammatory cells to coordinate inflammation and other immune responses. In cancer, these molecules have been administered to patients in order to stimulate anti-cancer immune responses in an un-specific way. Two main cytokines that will be discussed are interleukin-2 (IL-2) and granulocyte and macrophage colony stimulating factor (GM-CSF).

IL-2 is a pluripotent cytokine able to stimulate the immune system in many ways. However, one of its crucial roles is in the activation of both natural killer (NK) cells²⁰ and T-cells²¹⁻²³. In specific, high levels of IL-2 can induce T cell expansion and activation for interferon gamma (IFN-gamma) production²⁴. A recombinant form of IL-2, marketed as Proleukin[®], has received FDA approval for the use in metastatic renal cell carcinoma (RCC)²⁵ and metastatic melanoma²⁶. Clinical data has shown that from 270 metastatic melanoma patients, 16% of patients showed objective responses while 6% showed complete response²⁷. Similar results also were seen in metastatic RCC, objective responses were seen in 15% of patients and 8% of patients showed complete responses²⁸. Moreover, a clear increase in NK and T cell activation was observed in most of the treated patients. Hence, currently in the clinic Proleukin[®] is still being tested with other potential synergistic molecules to further improve clinical responses. Nevertheless, systemic administration of IL-2 has been associated with several life-threatening toxicities due to an increased inflammation²⁹. In spite of this, several strategies are being developed to ensure a targeted release in the tumor microenvironment.

One other widely used cytokine in the clinic is GM-CSF. Compared to IL-2, GM-CSF works with other types of cells in specific antigen presenting cells (APCs). For example, mice defective in GM-CSF had a decrease proliferation and maturation of dendritic cells (DC) and macrophages leading to an increase susceptibility to bacterial infections³⁰. In 2005, Kurbacher *et al.* treated 19 cancer patients suffering from breast and female reproductive tract carcinomas with recombinant GM-CSF³¹. Only one patient had a complete response while six others had a partial response. The main mode of action was shown to be attributed to the activation of DCs and increased antigen presentation. A recombinant protein of GM-CSF (called Sagramostim) showed a 100% overall response rate with chronic lymphocytic

leukemia patients when combined with chemotherapy³². Yet, with chronic myeloid leukemia it was discontinued in all patients due to severe adverse events³³. Currently, Sagramostim is not used in the treatment of cancer but as a supportive care medicine. Multiple clinical trials are on-going testing Sagramostim with different cancer immunotherapies combination.

2.1.2 Adoptive cell therapy (ACT)

One other form of passive cancer immunotherapy may come in the form of infusing activated immune cells into patients. This is called adoptive cell therapy^{34,35} and can be divided into two subtypes: adoptive tumor-infiltrating lymphocytes (TILs) and genetically engineered T cells expressing specific T cell receptors (TCRs)/chimeric antigen receptors (CARs). Both these therapies share a common step which is the preconditioning lymphodepletion regimen before treatment. With the use of cyclophosphamide, patients undergo lymphopenia and neutropenia in order to prevent such endogenous cells from attacking injected activated immune cells³⁶.

TIL therapy is not a novel form of treatment but can be dated back to 1994 being used in metastatic melanoma³⁷. This therapy consists of isolating tumor-specific T cells within the tumor microenvironment and further expand them *ex-vivo*. Various regimens for expansion have been described, but the most common is the use of high doses of IL-2. Currently such therapy has been approved by the FDA for metastatic melanoma. Yet, multiple clinical trials are undergoing with different type of expansion regimens or in combination with other treatments.

Other than TILs, scientists have tried to increase the armamentarium of T-cells by genetically engineering them to express specific TCRs or CARs³⁸. In both cases, T cells are first isolated through leukapheresis using peripheral blood. Once T cells have been isolated, using a lentiviral vector a transduction is performed to facilitate expression of a TCR or CAR. Following transductions, these cells are then expanded using high doses of IL-2 and are then ready to be re-infused in patients.

Other than the structure, TCRs and CARs give T cells a different way of killing tumor cells. TCRs are made of $\alpha\beta$ heterodimers with each chain consisting of variable and constant region domains. These receptors associate with CD3 in the surface membrane and recognize major histocompatibility complexes (MHC) loaded with an antigen which induces activation and killing of the tumor cell^{39,40}. As for CARs, these receptors consist of an antigen binding domain, consisting of single-chain variable fragment (scFv) from an antibody, which is connected to an intracellular signaling domain causing cell activation⁴⁰. Thus, killing of a tumor cell occurs in a MHC-independent fashion where the scFv portion of the receptor binds to its specific epitope it triggers T cell activation via its signaling domain⁴⁰. This is a clear advantage over the conventional TCR killing since one of the most prominent immune-escape mechanisms a tumor poses the downregulation of MHC from its surface⁴¹. Yet, CAR-based T cells are more toxic than TCR based⁴². Both forms of treatments can cause neurotoxicity and cytokine release syndrome (CRS), yet with CAR-based T cell therapy it is more severe⁴².

From this kind of treatments the only form that has been accepted currently for use in the clinics is a CAR-based T cell, Kymriah[®]. Its consists of a CAR receptor binding to CD19 and is used for B-cell acute lymphoblastic leukemia.

2.2.3 Antibody Therapy

Antibody therapy in cancer has been one of the most successful types of therapies used in the clinic to treat hematological and solid tumors. The advancement of antibodies in cancer therapy can date back to 1890 when first described as neutralizing substances against diphtheria⁴³. It was later seen that these substances had a specific property in recognizing specific epitopes and were secreted by our own cells, in specific plasma B cells^{44,45}. It was then hypothesized that each plasma B cell clone was able to produce one specific antibody⁴⁶. This concept led to the discovery of novel methods able to sequester unique B cell clones in order to obtain monoclonal antibodies^{47,48}. This technology allowed for the screening of thousands of monoclonal antibodies to identify high-affinity monoclonal antibodies against any desired tumor-associated antigen. The first clinical trial using an antibody began in 1980 for lymphoma patients^{49,50}. Sadly, such antibodies provided poor clinical efficacy since a human anti-mouse antibody (HAMA) response was elicited once infused into patients. Therefore, to

optimize antibody therapy, techniques to humanize antibodies originating from mice were developed. These techniques included cloning the murine derived variable chains (chimeric) or complementary determining regions (humanized) into human antibody formats. Recent techniques have now allowed for the generation of full human antibodies by using transgenic mice or yeast-phage display^{51,52}. As a result of such advancements, antibody therapy has become the most type of drug sold for pharmaceutical purposes.

Antibodies are able to directly kill target cells by disrupting or activating receptor signaling. This activity is pertinent to the Fab regions of an antibody which are responsible for binding. However other than direct cell killing, antibodies are also able to orchestrate host-immune response to induced immune-mediated cell death. This dual mechanism of action has made antibody therapy powerful and safe compared to other conventional therapies. This section will describe the structure of an antibody and its use in cancer therapy.

2.2.3.1 Antibody structure

Antibodies are large structures made up of four polypeptides, two heavy and two light chains, joined together via disulfide bonds to give a “Y” shaped structure (Figure 1). Both heavy and light chains are made up of two regions: the variable and constant domains. Light chains consist of one variable domain (V_L) and one constant domain (C_L) while heavy chains comprise of one variable domain (V_H) and four constant domains (C_{H1} , C_{H2} , C_{H3} and C_{H4}). Furthermore, based on structure, antibodies can be classified into two Fab (Fragment antigen-binding) regions and an Fc (Fragment crystallizable) region. The Fab region comprises of the full light chain and part of the heavy chain (V_H and C_{H1}) which give the tips of the “Y” shape. The rest of the constant heavy chain domains make up the Fc region which forms the stalk of the “Y” shape.

The variable regions of both the heavy and light chain are then subdivided into four framework regions and three hypervariable regions. The amino-acid composition of the hypervariable regions is the most varied from antibody-to-antibody. Once these regions fold into three β -strands they are then referred to as complementary-determining regions (CDR) since the shape complements the targeted epitope. The CDRs from the heavy and light chains determine the antibody-binding side but the framework regions also play a minor role. As for the Fc region, it comprises of C_{H2} - C_{H4} and has a vital role for modulating immune cell

activity. Immune effector cells can bind to the Fc-region of an antibody through the Fc-receptors subsequently activating effector functions.

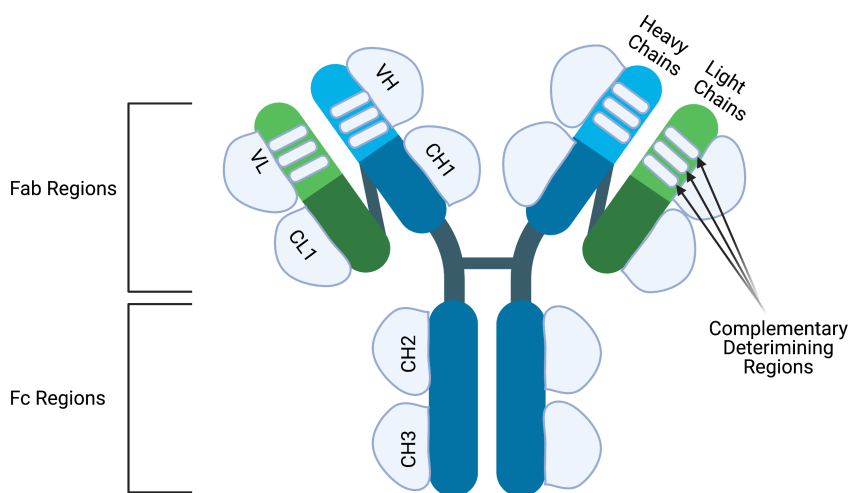


Figure 1. The structure of an antibody. Antibodies are made up of two identical heavy chains and light chains. The heavy chains are connected to each other via disulfide bridge and the light chains are connected to the upper part of the heavy chains. Both heavy and light chains consist of variable (V) and constant regions (C). The heavy chain contains three constant domains (CH1-CH3) and one variable domain (VH) while the light chain has one constant domain (CL) and one variable domain (VL). Moreover, the variable chains have three complementary determining regions which dictate the specificity of the antibody. Antibodies can also be classified into two structures; the Fc and Fab region. The Fc regions contains the CH2 and CH3 domains and is important to elicit Fc-effector mechanisms. The Fab regions compromise of CH1, VH, CL1 and VL regions and are important for epitope binding. Figures were created with BioRender.com.

2.2.3.2 Heavy and Light chains of Antibodies

In mammals, two types of light chains of an antibody exist called lambda and kappa. No functional differences have been described for both these chains which are used to build an antibody complex. However, the antibody complex contains two identical light chains, and no mix of kappa and lambda chains usually occurs within one antibody. The proportions of each chain used varies among species and can serve as markers of abnormal proliferation of B cell clones⁵³.

As for heavy chains, in mammals there exists five different chains called alpha, gamma, delta, epsilon and micro which give rise to five different antibody classes such as IgA, IgG, IgD, IgE and IgM, respectively. Contrary to light chains, the antibody classes differ in many functional activities, biological properties, and location. This is mostly due to the differential binding of different Fc-receptors since IgA, IgG or IgE bind to Fc- α , Fc- γ , or Fc- ϵ receptor respectively. These receptors are distinguished based on what type of immune cells express them and signaling properties, explaining the antibody class functions (Figure 2). For example, Fc- ϵ receptors are found on eosinophils, mast cells and basophils explaining the associated role in allergic responses.


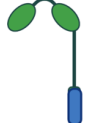
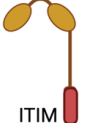
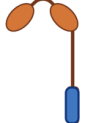
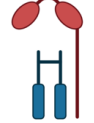
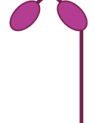
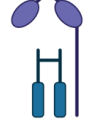
Name	Fc- γ RI CD64	Fc- γ RIIa CD32a	Fc- γ RIIb CD32b	Fc- γ RIIc CD32c	Fc- γ RIIIa CD16a	Fc- γ RIIIb CD16b	Fc- α R CD89
Structure	 ITAM		 ITIM				
Function	Activating	Activating	Inhibitory	Activating	Activating	Inhibitory	Activating
Expression	Monocytes Macrophages Neutrophils Dendritic cells Mast cell	Monocytes Macrophages Neutrophils DC Basophils Mast cell Eosinophil Platelet	B-cell Monocytes Macrophages Neutrophils DC Basophils	Monocytes Macrophages Neutrophils	NK cells Monocytes Macrophages	Basophils Neutrophils	Macrophages Monocytes Neutrophils Eosinophils

Figure 2. The distribution, structure and function of Fc receptors. The different types of Fc- γ and Fc- α receptors found in humans. All activating Fc receptors contain an immunoreceptor tyrosine-based activation motif (ITAM) while inhibitory Fc receptors have an immunoreceptor tyrosine-based inhibitory motif (ITIM) or none. Figures were created with BioRender.com.

2.2.3.3 Direct tumor killing using monoclonal antibodies

As previously mentioned, cancer antibodies have a dual mechanism of action consisting of either direct killing or inducing immune-mediated cell death of opsonized cancer cells. Cancer cells heavily depend on pro-tumor growth and survival signaling provided by different growth factor receptors. Antibodies can perturb such signaling by manipulating the activation or blocking ligand binding subsequently leading to cell death. An example of ligand blocking is the clinically approved Cetuximab, a monoclonal antibody binding to epidermal growth factor

receptor (EGFR). EGFR is highly overexpressed on many different types of cancers and when activated can induce proliferation, migration, and invasion of tumor cells⁵⁴⁻⁵⁷. Cetuximab binding to EGFR has been seen to disrupt ligand binding and consequently lead to apoptosis of tumor cells^{58,59}. Human epidermal growth factor receptor 2 (HER2) is another growth receptor overexpressed by tumor cells to sustain proliferation⁶⁰. In specific, HER2 overexpression has been highly seen in ovarian and breast cancer⁶⁰. Unlike EGFR, HER2 has no known ligand and is activated by heterodimerization to other growth receptors⁶¹. Trastuzumab, a clinically approved monoclonal antibody against HER2, has been shown to disrupt this heterodimerization, consequently leading to tumor cell death⁶². Trastuzumab has been a clinical success in in treating HER2+ breast cancer patients⁶².

2.2.3.4 Complement-dependent cytotoxicity

Antibodies can interact with the complement system through the Fc-region to activate the classical component cascade^{63,64}. Once antibodies bind to the target ligand, the available Fc-regions are then able to bind complement protein, C1q. Hexamerization of near-by antibodies allows for efficient C1q binding, which then activates C1r and C1s^{65,66}. Activation of C1r and C1s leads to the proteolytic cleavage of C4 and C2 to initiate the complement cascade and subsequently complement dependent cytotoxicity (CDC)^{65,66}. However, only IgG and IgM antibodies are able to elicit CDC since they are the only antibody isotypes that have a C1q binding site. Nevertheless, IgA antibodies have also been observed to elicit CDC via the classical pathway, despite not having a C1q site^{67,68}. Yet, this has only been seen in B-cell lymphoma cells and the mechanism has been attributed to other receptors in the B-cell able to bind to C1q.

As an effector function, CDC has been shown to be required for *in vivo* efficacy. Mice having the genes encoding for C1q knocked out showed no clinical efficacy with anti-CD20 antibody, rituximab⁶⁹. Also, follicular lymphoma patients with known polymorphisms in the C1qA gene reducing CDC activity have been correlated with low clinical response to rituximab⁷⁰. Despite these results, Fc-engineering to increase CDC activity has been extensively done and a successful example of this has been anti-CD20 antibody, ofatumumab. Ofatumumab has been engineered to have an increased ability to hexamerize and bind to C1q subsequently leading to higher CDC activity⁷¹. This enhancement translated into better

clinical outcomes since ofatumumab outperformed rituximab in chronic lymphocytic leukemia patients⁷².

2.2.3.5 Antibody-dependent cell phagocytosis

Macrophages express a variety of Fc receptors and in concrete Fc- γ RII (CD32) and Fc- γ RI (CD64) allowing for interaction with IgG antibodies against cancer (Figure 2)⁷³. This interaction can then lead to cell death through a process called antibody-dependent cell mediated phagocytosis (ADCP)⁷⁴. The role of ADCP in clinical efficacy has not been very well studied but there has been some evidence demonstrating a role in antibody efficacy. For example, rats having their macrophages depleted lost significant response towards monoclonal antibody therapy against colon carcinoma⁷⁵. Similar results were also shown with SCID-BEIGE mice transplanted with xenografts and treated with monoclonal antibody therapy⁷⁶. These specific mice do not have B or T cells and defective NK cells which then makes macrophages a primary effector immune cell and ADCP the main effector mechanism. These mice showed an *in vivo* clearance of leukemic cells when treated with daratumumab, an anti-CD38 antibody. ADCP efficacy in the clinic was also shown when 11 out of 12 of multiple myeloma patients showed ADCP when cells were cultured and treated with daratumumab *in vitro*⁷⁶.

A reason for why ADCP has not been so clearly correlated with antibody efficacy could be due to the expression of SIRP α and CD47 on macrophages and tumor cells, respectively. The interaction among both receptors leads to a “don’t eat me” signal which downregulates ADCP activity⁷⁷. Blockage of this axis has been shown to increase antibody therapy by enhancing ADCC activity. Currently, SIRP α and CD47 blockers are being tested in the clinic together with various antibody therapies⁷⁷.

2.2.3.6 Antibody dependent cell mediated cytotoxicity

In 1965, antibody opsonized cancer cells were shown to be killed via a non-phagocytic mechanism termed antibody-dependent cell mediated cytotoxicity (ADCC)⁷⁸. This effector mechanism can be elicited from different types of immune cells such as NK cells, neutrophils, monocytes, and eosinophils⁷⁹. However, the way cell death is elicited differs among cells and can range from release of cytotoxic granules, reactive oxygen species release or Fas/FasL

signaling⁸⁰⁻⁸². The clinical relevance of ADCC was first described in 2000 where Clynes and colleagues showed that rituximab and trastuzumab relied on ADCC for efficacy⁸³. Moreover, it was later seen that mice lacking FcγRs or certain mutations limiting ADCC did not respond to monoclonal antibody therapy⁸⁴. Within the population, polymorphisms in Fc-γRIIA (CD32a)⁸⁵ and Fc-γRIIIA (CD16a)⁸⁶ exist causing an increase in IgG affinity and subsequently ADCC activity. In several clinical trials with rituximab, it was seen that patients with such polymorphisms had a better clinical response⁸⁷⁻⁸⁹. Similar results were also shown with cetuximab⁹⁰ and trastuzumab^{91,92} treating colorectal cancer and metastatic breast cancer, respectively. Further confirming such results, patients with higher response to trastuzumab also demonstrated higher ADCC activity compared to patients not responding⁹³.

Since all the cancer antibodies in the clinic are of the IgG isotype, Fc-γRs are the main receptors that mediate ADCC. In humans there exists six different types of Fc-γRs which can be divided into activating (Fc-γRI, Fc-γRIIA, Fc-γRIIC and Fc-γRIIIA) and inhibitory (Fc-γRIIB and Fc-γRIIIB) receptors⁹⁴. As the name indicates, the activating receptors elicit ADCC while the inhibitory receptors downregulate effector mechanisms. With IgG therapy, NK cells are the main population that elicit ADCC and this due to type of Fc-γR expression (Figure 3). NK cells express only one Fc-γR which is the activating Fc-γRIIIA explaining its importance for ADCC mediated by IgG⁹⁵. Other myeloid and granulocytic cells also express activating Fc-γR but also higher levels of inhibitory Fc-γR. For example, inhibitory Fc-γRIIB expression on neutrophils is seven to five times higher than Fc-γRIIA⁹⁶. This has been shown to have a negative role on mediating ADCC because of the competition with Fc-γRIIA^{97,98}. This heavy reliance on NK cell for ADCC has been shown to limit efficacy. This is because NK cells have been seen to undergo exhaustion fast and not able to elicit ADCC⁹⁹. Only 24 hours later NK cells gain the ability to elicit ADCC again⁹⁹.

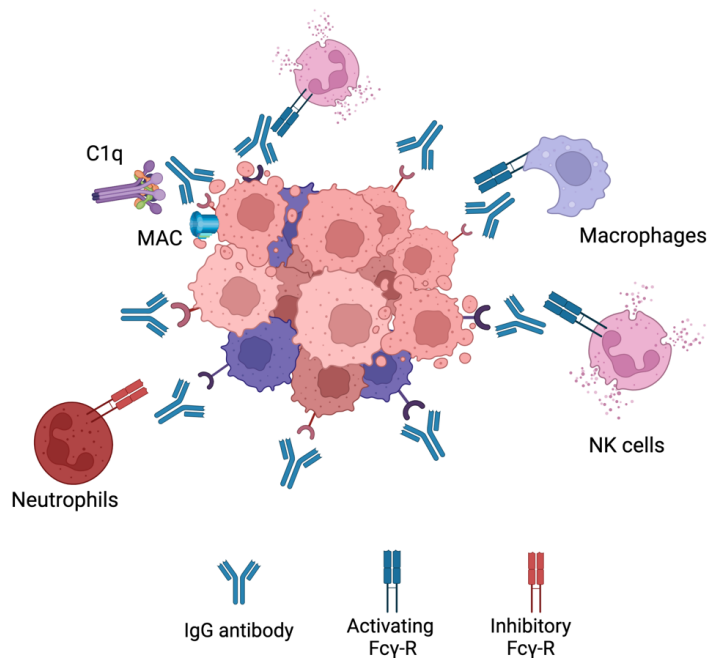


Figure 3. IgG1 effector mechanisms. When an IgG antibody opsonizes a cancer cell it can elicit various effector functions. It can interact with C1q complement protein leading to the formation of membrane attack complex (MAC) leading to CDC. The Fc region can also bind to activating Fc γ -Rs on NK cells or macrophages to elicit ADCC or ADCP, respectively. Neutrophils express a high level of inhibitory Fc γ -Rs leading to very little activation. Figures were created with BioRender.com.

2.2.3.7 IgA for cancer therapy

Due to the limitations the IgG isotype poses, preclinical studies have been conducted on the development of cancer therapeutic mAbs with isotypes different from IgG. A potential candidate isotype is IgA (Figure 4). This antibody is the most prominent immunoglobulin isotype found in mucosal sites and the second most frequent antibody isotype in serum, after IgG¹⁰⁰. It consists of two different isotypes; IgA1 and IgA2 with the latter comprising three allotypes; IgA2m(1), IgA2m(2) and IgA2m(n). IgA interacts with immune cells via binding to Fc α R (CD89)¹⁰⁰. Such receptor is expressed on cells of the myeloid lineage such as neutrophils, monocytes, distinct macrophage populations and eosinophils¹⁰⁰. Initial ADCC experiments with bispecific IgG1-antibodies where one of the F(ab')₂ fragments was directed at the Fc α R receptor and the other to a target antigen highlighted the potential use of IgA antibodies in the context of malignancies¹⁰¹. Various reports have also shown that IgA mAbs

directed at different tumour antigens showed an increased ability to recruit PMNs as effector cells compared to IgG^{102–106}. This emphasises that IgA antibodies are able to employ a distinct effector population of immune cells against tumour cells compared to IgG. Furthermore, IgA antibodies mediate macrophage dependent tumour cell killing comparable to IgG¹⁰⁷. It has been suggested that IgA mAbs are not able to activate the complement system due to the lack of a C1q-binding site¹⁰⁸. However, certain studies have shown that IgA antibodies¹⁰⁹ or IgG-fab fragments directed against CD20¹¹⁰ have been able to elicit CDC of malignant B-cells through the classical pathway. The mechanism behind it is thought to be due to rearrangements in the IgM or IgG B-cell receptor (BCR) of malignant B-cells¹¹⁰ exposing its C1q binding site mediated by the clustering of CD20 after IgA binding. The Fc α R represents an advantage over Fc γ Rs since it does not have any inhibitory receptors and no polymorphisms have been reported. This implies that more predictable responses are

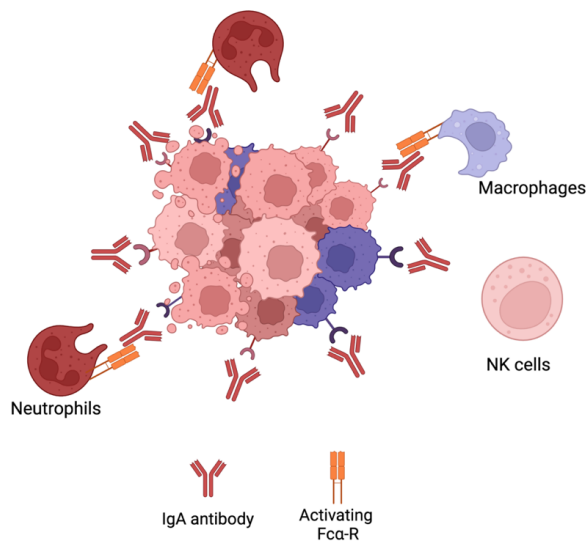


Figure 4. IgA effector mechanisms. IgA effector mechanisms differ from IgG antibodies. IgA antibodies do not activate CDC, since they do not have a C1q binding site, or NK cells since they do not express Fc α -R. The Fc region of IgA binds to Fc α -R on neutrophils cells or macrophages to elicit ADCC or ADCP, respectively. However since NK cells do not express Fc α -R, IgA antibodies do not activate such immune population. Figures were created with BioRender.com.

achievable with IgA. Finally, antibody internalisation occurs less frequently with IgA compared to IgG. These advantages highlight the potential use of the IgA isotype in the development of therapeutic mAbs.

2.2.3.8 IgA and IgG combinational therapy for cancer

Despite the advantage of IgA, this isotype is not able to capitalize on NK cells or complement activation. To maximize on every effector population possible, scientists have tested whether combining IgG and IgA enhanced tumor killing. Bradsma and colleagues showed that using both IgG1 and IgA1 antibodies directed at different TAAs (Tumor Associated Antigens) induced higher killing than the individual antibodies when NK cells and neutrophils were present¹¹¹. However, when the IgG and IgA antibodies were directed towards the same TAA this enhanced effect was not seen. It is hypothesized that it could be due to the competition towards the same TAA leading to one isotype dominating in binding. Further building on this work, TrisomAB was then developed which consisted of an IgG1 antibody directed towards a TAA and Fc- α R¹¹². TrisomAB was shown to increase tumor killing when both NK cells and neutrophils were present. This data then further supports the use of both antibody isotypes in the treatment of cancer.

2.2.3.9 Fc-fusion peptides

Antibodies are large complexes which make them very hard to diffuse into large tumors¹¹³. Moreover, production is very complex and costly which inflate the price in the clinic¹¹³. Regarding such issues, a novel type of antibody-based therapeutics have been developed comprising of peptides fused to an Fc region^{114–116}. These peptides can be of very small size and bind to any desired target. However, when these peptides are administered systemically, they have a very short half-life due to rapid renal filtration. Attaching Fc-regions, in specific of the IgG region, increases the half-life of the peptides due to binding of Fc-neonatal receptors¹¹⁷. Moreover, the Fc-regions can also provide Fc-effector mechanisms such as CDC, ADCC or ADCP. Currently, there are six Fc-fusion peptides approved in the clinic used for thrombocytopenia, kidney transplants and inflammatory diseases such as arthritis or psoriasis¹¹⁴. Currently, no Fc-fusion peptides have been approved for the treatment of cancer.

However, many Fc-fusion peptides against cancer have been described and entered clinical testing. For example, a bispecific peptide fused to a Fc of an IgG against HER-1 or HER-2 has showed high anti-tumor efficacy¹¹⁸. Moreover, the IgG Fc portion was able to elicit Fc-effector mechanisms of a normal IgG antibody.

2.2 Active Immunotherapy

In contrast to passive, active immunotherapies are molecules that are used to induce or revitalize anti-tumor responses *in vivo*. This then requires patients to have an active and responsive immune system for successful treatment.

2.2.1 Checkpoint inhibitory therapy

In the thymus, the life of a T cell begins by proliferating and creating a diverse repertoire of TCRs. In order to maintain homeostasis, the immune system needs to distinguish between self and non-self. T-cells go through an initial selection process called central tolerance. In this process T-cells that strongly react to self-peptides, presented by thymocytes, undergo apoptosis. T-cells that weakly respond to self-peptides are released as naive cells to circulate into secondary lymphoid organs. Antigen presenting cells (APC), specifically dendritic cells (DC), are then able to present naive T-cells either with foreign antigens (under infection conditions) or mutated self-proteins (under malignancy conditions) resulting in T-cell activation. However, some of the activated T-cells have TCRs which are still able to cross-react with self-antigens. To prevent cross-reactivity to self, multiple checkpoint pathways are present during the steps of activation to prevent autoimmunity. Also, checkpoints prevent the immune system to over activate during the course of infection. This process has been termed peripheral tolerance and two main constituents that take the centre of this process are the membrane receptors CTLA-4 and PD-1. Although CTLA-4 and PD-1 have a common function, they are present in different stages of T-cell activation. CTLA-4 is called the “leader” of the immune checkpoints since it regulates the activation of naive T-cells in lymph nodes. Contrary to CTLA-4, PD-1 acts in later stages since it regulates already activated T-cells in the peripheral tissues.

2.2.1.1 The CTLA-4 axis

Activating naive T-cells in the thymus is a complex process that requires more than one signal. In addition to TCR binding to peptide-loaded MHC, several co-stimulatory signals are required for full T-cell activation. An appropriate amount of co-stimulation from either B7-1 (CD80) or B7-2 (CD86), expressed on APCs and binding to CD28 on T cells, is required for activating naive T-cells which then leads to IL-2 production. Stimulatory signals from CD28:B7 also lead to the localisation of CTLA-4 to the surface of T-cells¹¹⁹. Even though CTLA-4 is a homologue to CD28, it has a higher affinity towards B7 providing competitive binding that results in decreased CD28:B7 interactions (Figure 5). The interaction between CTLA4 and B7 does not produce a stimulatory signal required for naive T-cell activation¹²⁰. Some data has suggested that CTLA-4 has signalling capabilities able to counteract CD28:B7 stimulatory signals. Other inhibitory mechanisms have also been proposed such as direct inhibition at the TCR immune synapse¹²⁰ or causing an increased T-cell mobility causing a decreased contact frequency with APCs¹²¹. Thus, CTLA-4 is seen as an inhibitor of the co-stimulation usually supplied by the interaction of CD28 and B7. Whether a naive T-cell undergoes activation or anergy is dependent on the balance between CD28:B7 and B7:CTLA4 signalling. What determines this balance still remains a mystery but multiple mechanisms such as ligand competition between B7 and CTLA-4, regulatory cytokines and CTLA-4 signalling has been proposed¹²². When the balance is tilted towards the negative B7:CTLA-4 signalling, IL-2 production is halted preventing cell cycle progression¹²³.

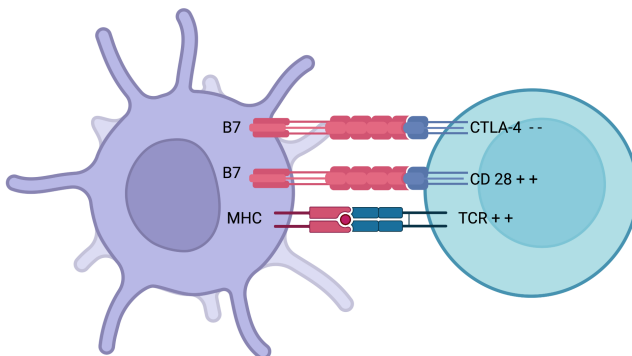


Figure 5: CTLA-4 suppression. Naive T-cells migrate to lymph nodes to become activated. Activation is usually provided by both MHC (loaded with an antigen) and co-stimulation from B7 (interacting with CD28) provided by a DC. After early stimulation, CTLA-4 is translocated to the surface of DCs which then competes with B7 to bind to CD28 and downregulates T-cell activation. Whether a naive T-cells undergoes activation or anergy is dependent on the balance of between CD28:B7 and B7:CTLA4 signalling. Figures were created with BioRender.com.

As previously mentioned, CTLA-4 is upregulated on the surface of naive T-cells after CD28:B7 or TCR:MHC binding. Before such stimulation is provided, CTLA-4 is present in the cytoplasm of the cell within vesicles¹²⁴. CD28 and TCR stimulation causes the exocytosis of the CTLA-4-containing vesicles, leading to the upregulation of CTLA-4 on the surface. This process is under a positive and graded feedback loop where stronger TCR and CD28 stimulation increases CTLA-4 translocation.

The importance of CTLA-4 in maintaining homeostasis was shown in adult mice, where abrogating CTLA-4 expression caused a systemic inflammation and formation of organ-specific autoantibodies. Moreover, congenital CTLA-4 deficient mice died due to lymphoproliferation¹²⁵. Similar observations were also shown in humans where patients with CTLA-4 deficiencies suffer from various autoimmune and autoinflammatory diseases. CTLA-4 is not only expressed on naive T-cells but also on regulatory T cells (Tregs). Unlike in naive T-cells, CTLA-4 is constitutively expressed on Treg cells¹²⁶. This constitutive expression of CTLA-4 makes Treg cells key players in maintaining peripheral tolerance. For example, mice with Treg cells with impaired CTLA-4 had impaired suppressive functions¹²⁵

2.2.1.2 CTLA-4 inhibitor for the treatment of cancer

The rationale behind inhibiting CTLA-4 for treating cancer is not a novel idea but has been reported back in 1996¹²⁷. Using preclinical models, it was shown that the blockade of CTLA-4 led to anti-tumour immunity. Mice administered with CTLA-4 antibodies rejected pre-established or injected tumours. Moreover, the rejection resulted in immunity against a second tumour challenge. This was further supported by other studies where administering CTLA-4 antibodies to mice with a pre-established B16-BL6 melanoma resulted in tumour clearance¹²⁸. Based on such preclinical evidence, two CTLA-4 antibodies, ipilimumab and tremelimumab, were developed and entered clinical development. Despite acceptable tolerance and durable responses in patients^{129,130}, tremelimumab did not show statistical

significance in overall survival (OS) in a phase III trial with advanced melanoma patients¹³¹. However, it is disputed that this may have been due to the crossing over of patients from the chemotherapy-only treatment arm to the chemotherapy and tremelimumab treatment arm. Ipililumab on the other hand has been successful in two phase III trials with advanced melanoma patients^{132,133}. While the median survival improved minimally, the success of ipililumab was in the remarkable increase in landmark survival after treatment. After 2 years, 18% patients treated with ipililumab in combination with vaccination against the cancer-specific protein gp100 were alive compared to 5% of patients receiving gp100 vaccination alone. In addition, pooled data from clinical trials testing ipililumab in advanced melanoma patients showed that 20% of patients had a long-term survival of at least 3 years¹³⁴. Not only confined to advanced melanoma, ipililumab has also succeeded with other malignancies. Pancreatic cancer patients receiving ipililumab had an increase in OS compared to patients receiving chemotherapy only¹³⁵. In addition, it also resulted in responses with prostate cancer patients¹³⁶.

While the anti-tumour mechanisms of CTLA-4 antibodies are not well understood, the generally believed hypothesis is that blocking CTLA-4 causes an increased activation of proliferation of effector T-cells accompanied with a decrease in activated Treg cells¹³⁷. Supporting this hypothesis, good responses in melanoma patients was attributed to a wide and diverse pool of T-cells¹³⁸. However, other studies observed that a baseline T-cell diversity, before treatment, was associated with higher OS in metastatic melanoma patients¹³⁹. Therefore, pre-existing conditions might be prognostic markers for CTLA-4 blockade anti-tumour efficacy rather than post-treatment induced artifacts.

2.2.1.3 PD1/PD-L1 axis

Similar to CTLA-4, PD-1 is part of the CD28/B7 family of co-stimulatory receptors. It is expressed on effector T cells and regulates them by binding to its ligands, PD-L1 and PD-L2, which are expressed by both hematopoietic and non-hematopoietic cells (Figure 6). Activation of PD-1 leads to the phosphorylation of both its intracellular immunoreceptor tyrosine-based switch motif (ITSM) and immunoreceptor tyrosine-based inhibitory motif (ITIM). The phosphorylation of these motifs attracts phosphatases, such as SHP-2, that are

able to terminate signalling cascades of both CD28 and TCR¹⁴⁰. This then inhibits the proliferation and survival of T-cells and production of IL-2, INF- γ and tumour necrosis factor- α (TNF- α). Hence, PD-1 is able to terminate TCR signalling and reduce T-cell activation. PD-1 is not constitutively expressed on T-cells but rather is a marker of “exhaustion”. After high levels of stimulations from CD4+ T-cells, effector T-cells start to express PD-1 in order to prevent over-activation¹⁴¹. This exhaustion state is commonly observed both in chronic infections and cancer. Therefore, this causes the suboptimal control of infections and cancer progression. For example, mice chronically infected with cytomegalovirus had virus specific CD8+ T-cells present. Yet the T-cells were ineffective since they did not produce cytokines upon antigen challenge. This was also shown in metastatic melanoma patients where exhausted CD8+ T-cells were ineffective in tumour clearance.

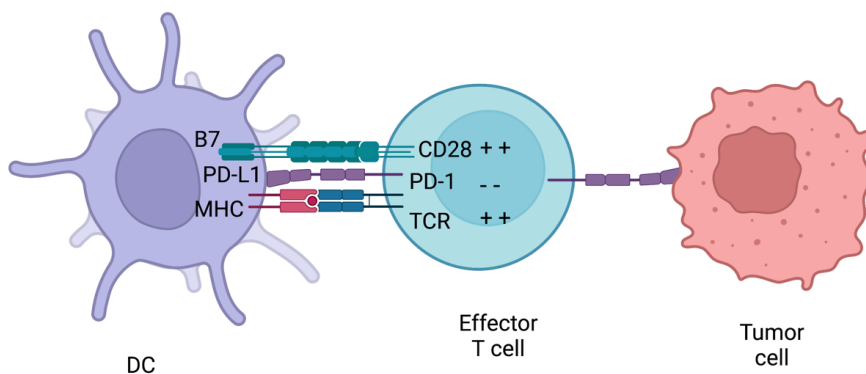


Figure 6: PD-1 inhibition. PD-1 is usually expressed on effector T-cells and binds to either PD-L1 or PD-L2. PD-L1 can be expressed both on immune cells and tumours. Therefore, PD-1 can inhibit effector T-cells at different stages of an immune response. After PD-L1 is activated by the receptor, they can initiate a signalling complex able to counteract MHC and B7 signalling. Figures were created with BioRender.com.

Expression and the location between PD-L1 and PD-L2 are different. PD-L1 is expressed on many types of tumours and associated with poor prognosis and high TILs¹⁴². PD-L2 resides on DC and monocytes but also on non-immune cells depending on the microenvironment. This contrasting distribution of PD-L1 and PD-L2 causes distinct biological effects when each ligand is bound to PD-1. For example, natural killer T cell (NKT) activation under PD-L1 or PD-L2 signalling were opposing¹⁴³. Moreover, PD-L1 and CD80 interaction decreased T-cell response unlike when PD-L2 was blocked, an increased T-helper 2 cell (Th2) activity was

noted¹⁴⁴. These opposing biological effects provide an explanation on the toxicity levels caused by inhibiting PD-1 and has highlighted the use of PD-L1 inhibitors.

Even though CTLA-4 and PD-1 have similar negative effects on T-cells, there are key differences between the checkpoints. CTLA-4 controls the activation of naive T-cells in lymph nodes whereas PD-1 controls T-cells in the effector phase in the periphery tissues. CTLA-4 expression is confined to T-cells, unlike PD-1 that is expressed on T-cells, B-cells and myeloid cells. Furthermore, the expression and distribution of checkpoint ligands differs. B7 is restricted to professional APCs while PD-L1 and PD-L2 are expressed on leukocytes, non-hematopoietic cells, and non-lymphoid tissues¹⁴⁵. These differences indicate that CTLA-4 down regulates T-cell responses early on in an immune response while PD-1 limits T-cell response later during the effector stage. This then causes different effects *in vivo* when each receptor is inhibited. Blocking CTLA-4 causes an increase in activation and proliferation of effector T-cells regardless of TCR specificity while PD-1 inhibition leads to restoring proper T-cell functions.

2.2.1.4 Targeting the PD-1 axis in cancer therapy

After the success in targeting CTLA-4 during cancer, many antibodies have been designed to disturb the PD-1 axis for a similar purpose. Although the antibodies differ in structure (antibody isotype and chimerised/humanised), they can be categorised in two main groups: antibodies targeting the PD-1 receptor and antibodies targeting the ligand PD-L1. PD-1 antibodies such as nivolumab and pembrolizumab were shown in a phase I clinical trial with advanced melanoma, non-small cell lung cancer, renal cell carcinoma and other tumours to be tolerable and result in high durable responses^{146,147}. Results from three phase III clinical trials with advanced melanoma have been published¹⁴⁸⁻¹⁵⁰. In all three trials the OS was significantly higher in patients receiving nivolumab. In addition to melanoma, renal cell carcinoma patients treated with nivolumab had an OS of 25 months compared to 19.6 months in patients receiving the current standard treatment, everolimus (mTOR inhibitor). Similar results were also shown in a phase III trial with non-small cell lung cancer. The mechanism behind the anti-tumour effects of PD-1 blockade, which occurs during the effector stage of T-cells, involves re-activating peripheral T-cells that have been “exhausted” due to the high

exposure of tumour antigens. Many studies have reported that PD-1 is expressed on TILs^{147,151}. Thus, PD-1 inhibition allows the suppressed TILs to gain back their anti-tumour properties. However, a recent study indicated that ipilimumab response was associated with levels of expression of PD-L1 on tumour cells¹⁵². When PD-1 is inhibited, the interaction between PD-1:PD-L1 is blocked yet PD-L1 is still able to inhibit T-cells by binding to CD80, a second receptor for this ligand. To overcome such limitation, PD-L1 antibodies have been generated and are able to disrupt both PD-1:PD-L1 and PD-L1:CD80 interactions. These antibodies are also able to keep intact the interaction between PD-1 and PD-L2, required for self-tolerance and thus leading to lower toxicities. Three PD-L1 antibodies (Atezolizumab, Durvalumab and Avelumab) have been clinically approved and have shown durable responses and less toxicity levels in a variety of tumours¹⁵³.

2.2.1.5 Fc silencing of checkpoint inhibitors

The Fc-region of antibodies provides the ability to elicit Fc-effector mechanisms which are crucial for clinical efficacy. With respect to checkpoint inhibitors, it has been a subject of debate. For CTLA-4 checkpoint inhibitor, ipilimumab, Fc-effector mechanisms pertinent to the IgG1 isotype has been correlated with clinical efficiency. Advanced melanoma patients with Fc- γ IIIa polymorphism V158F increasing IgG1 affinity, have been shown to respond better to ipilimumab¹⁵⁴. Silencing Fc-effector mechanisms by changing the Fc-isotype or adding point mutations have seen to reduce *in vivo* activity of CTLA-4 inhibitors. The mechanism behind this has been argued to be the depletion of immunosuppressive Treg populations. However, opposite results were seen with PD-1 checkpoint inhibitors where Fc-effector mechanisms have lowered the *in vivo* anti-tumour activity¹⁵⁵. PD-1 checkpoint inhibitors with competent Fc regions able to elicit Fc-effector mechanism were shown to deplete crucial CD8+T cell and CD4+ T cell populations¹⁵⁵. These results explain why all of the PD-1 checkpoint inhibitors approved in the clinic are of the IgG4 isotype, an isotype that elicits low levels of ADCC and CDC, and have a S228P mutation decreasing Fc- γ R binding. This reduction in Fc-effector activity then prolongs CD8+T cell binding which subsequently increases anti-tumour activity.

As for PD-L1 checkpoint inhibitors, a safety concern over the addition of Fc-effector mechanisms exists. This is because PD-L1 expression is not solely limited to tumor cells but also can be expressed on healthy cells¹⁵⁶. In result, the opsonisation of healthy cells with an

antibody able to elicit Fc-effector mechanism can be deleterious. Out of the three approved PD-L1 inhibitors, atezolizumab and durvalumab have point mutations in the IgG1 Fc-region that remove Fc- γ R binding. However, *in vivo* data has shown that arming such checkpoint inhibitors can increase anti-tumor efficacy¹⁵⁵. This was attributed to an increased clearance of tumor cells but also immunosuppressive immune populations. Therefore, a strategy to increase Fc-effector mechanism while maintaining safety concerns is required.

2.2.2 Cancer Vaccines

Vaccines have been a major milestone in preventing life threatening infectious diseases. The concept of being able to induce an immune response resulting in a protective immunological memory against cancer is ideal. Not only could this prevent or treat cancer but also help in tumour relapse. Nevertheless, cancer genomics has shown the complexity in achieving this since most of the tumour antigens being highly expressed on tumours are also shared among healthy cells. TAAs such as HER-2, glycoprotein (gp) 100, Telomerase and others are ideal antigen candidates due to their immunogenic properties, yet are expressed on healthy tissue^{157,158}. This lack of specificity is concerning due to the “off-target” effects that can be very toxic to a patient. However, in 2010 the first therapeutic cancer vaccine, Sipuleucel-T, was approved by the FDA for asymptomatic or mildly symptomatic metastatic prostate cancer¹⁵⁹. This vaccine consisted of isolating the patients PBMCs and expanding/activating them *ex-vivo* using the commonly known TAA called prostatic acid phosphatase (PAP). The approval of such cancer vaccine stimulated other vaccine platforms to be investigated in the clinic. For example, BioNTech have developed a novel RNA lipoplex complex, called FixVac, coding for different TAAs¹⁶⁰. Such platforms are able to selectively target dendritic cells to induce an appropriate antigen presentation allowing for an effective T-cell immune response.

The perfect type of cancer vaccine would include an antigen selectively expressed on tumour cells. The genome of cancer cells is unstable and undergoes many genetic modifications such as somatic mutations, deletions, duplications and other processes. Due to such instability, neoantigens arise from cancer cells that are not found in healthy cells. Hence, such antigens then represent ideal targets for cancer vaccines. Nonetheless, these antigens

are not very immunogenic and fail to induce a sustainable immune response. The first clinical trial evaluating a neoepitope based vaccine was with stage III cutaneous melanoma patients. These patients were injected with A*02:01-specific neoepitopes and a specific CD8+ T cell response was observed¹⁶¹. Yet, this activation was modest and was not very effective in controlling tumor growth. This field is still a hot topic with multiple type of strategies trying to further strengthen immunogenicity.

2.2.3 Oncolytic viruses

Oncolytic viruses are able to selectively replicate in tumor cells, while leaving healthy cells unharmed, where malignant pathways have been activated or disrupted¹⁶². Additionally, since these viruses are able to stimulate systemic host immune responses, via the interactions with pathogen pattern receptors¹⁶³, they can modify the immunosuppressive tumor microenvironment and enhance anti-tumor immune responses.¹⁶⁴ This dual mechanism OV possess makes them interesting therapy agents.

These viruses have been genetically modified to conditionally replicate in cells in which specific cellular pathways are disrupted. This then allows OVs to infect both healthy and tumor cells and only replicate in tumor cells in which cellular pathways are compromised, but be recognized and cleared by healthy cells by the intrinsic immune system. However, studies using immunocompetent and immunocompromised mice have shown that the direct oncolysis of such viruses is not enough to induce tumor clearance¹⁶⁵. After tumor lysis, various TAAs are released and made accessible by nearby DCs¹⁶⁶. Such TAAs are then able to be taken up, processed and presented on MHC complexes allowing for adaptive tumor-specific tumor responses to be formed. This mechanism of action has been shown to be key for a successful response. Many different types of DNA and RNA oncolytic viruses have and are currently under clinical development and testing. In this literature review, a specific focus will be drawn into adenoviruses to be used as OVs.

3. Adenoviruses and their roles as cancer therapies

3.1 Adenoviruses

Adenoviruses were first discovered when scientists were investigating adenoid cells¹⁶⁷. They observed that these viruses featured a double-stranded DNA genome of about 36kb packaged into a capsid with an icosahedral shape. Adenoviruses are medium sized, around 100nm, particles with a non-envelope capsid composed of a penton, hexon and fiber knob domain all required for attachment and entry. There has been 57 different serotypes identified to date which can be subdivided into 6 groups (A-F).

Unlike many other viruses, adenoviruses circulate through humans during the whole year and are endemic in children. The mode of transmission of the virus is through water and fomites. Owing to their success of infection, adenoviruses are resilient to harsh environments due to their resistance to chemical and physical agents. For example, the resistance to gastric acid and biliary secretions has allowed such viruses to infect the gastrointestinal tracts¹⁶⁸. Moreover, adenoviruses can withstand being outside the host for up to three weeks. To our advantage, despite causing flu-like symptoms these viruses rarely induce serious disease in healthy human but can be generate illness in immune-compromised patients. No animal reservoirs have been identified making the virus hard to study due to low animal models to mimic disease¹⁶⁹.

The infection process starts off with the protein-interactions between the adenovirus capsid and host-cellular membranes. The adenovirus capsid is comprised of 240 hexons and 12 pentons. Other minor components such as pIX, pVIII, pVI and IIIa are also present in the capsid. The pentons, which consists of complex of five polypeptide III, provide the base for the trimeric fiber to attach. The fiber contains the knob-fiber domain that is then responsible for attaching to host-cellular membranes. The receptor that the fiber binds to depends on the serotype but the main ones include the coxsackie adenovirus receptor (CAR), desmoglein-2 or CD46¹⁷⁰⁻¹⁷³. After initial binding, the pentons in the adenovirus interact with the host-cell integrins ($\alpha_v\beta_3$ or $\alpha_v\beta_5$), leading to activation of certain signaling proteins (GTPases, phosphoinositide-3-OH kinase and MAPK) which induce the uptake of the virus particles via clathrin-coated vesicles¹⁷⁴.

Once inside the vesicles, the acidification of the endosome cues for dismemberment of the viral capsid by proteolytically cleaving protein VI¹⁷⁵. After endosomal escape, the resulting virion is released and transported to the nucleus with the help of dynein and microtubules which interact with capsid proteins (μ , proteins VII and V). Once the adenovirus genome reaches the nucleus, the transcription of genes begins and is divided into two phases; early and late. The early phase consists in the transcription and translation of early gene products (E1A, E1B, E2, E3 and E4) which help in the replication of the adenovirus DNA genome. Moreover, the products of the early genes also then induce the expression of late genes (L1, L2, L3, L4 and L5). The late gene products are required for virion assembly since they represent the structural proteins.

After the genome has been replicated and the structural proteins expressed, virion assembly begins with the hexons and pentons clustering with multiple scaffolding proteins (L4 22-33K)¹⁷⁶. This induces the insert of the viral DNA inside the virion structure and the final maturation of the virus by the release and cleavage of precursor proteins (L1 52-55K)¹⁷⁶. The whole replication process of the adenovirus usually takes 24-36 hours and can yield about 10,000 virions per cell to be released¹⁷⁵.

3.1.1 Adenovirus genome, replication, and machinery behind it

Despite the small genome of 30-36 kb in length, adenoviruses can encode for multiple genes due to the overlapping open reading frames, alternate splicing, and ability of transcription from both strands of the genome.¹⁷⁷ As described previously, the early gene products are responsible for genome replication and mainly consist of the preterminal protein (pTP), DNA polymerase (Ad Pol) and DNA-binding protein (DBP). The late genes of the adenovirus include proteins involved in virion assembly and encapsulation and are only expressed once the early genes are. The multiple late genes are usually arranged in the adenovirus major late transcription unit (MLTU) which consists of five regions, L1-L5, and are under transcriptional control of the major late promoter (MLP)¹⁷⁸⁻¹⁸². Other than the early and late genes, the adenovirus has also two other gene products, pIX and IVa2, which are often described as intermediate genes since they are not in the MLTU but facilitate the expression of the late genes.

The adenovirus genome is flanked by inverted terminal repeats (ITR) which comprise of around 100 bp each. These ITRs contain a ~50 bp origin of replication which is made up of a core origin and auxiliary origin¹⁸³. The core region provides the binding site to pTP and Ad Pol while the auxiliary region provides for cellular transcription factors nuclear factor 1 (NF1) and OCT-1¹⁸⁴. Moreover, near the ITR regions the adenovirus genome has a packaging sequence (ψ) which is required for encapsulation in virions^{185,186}. Finally, to the 5' ends of the genome terminal proteins (TP) is covalently attached which protects the DNA from degradation.

Genome replication starts with the formation of the pre-imitation complex which consists of multiple protein-protein and protein-DNA interactions (Figure 7). Firstly, Ad Pol will covalently attach to pTP via the dCMP nucleotide on its S580 amino acid position^{187,188}. Following Ad pol binding, DBP then binds to the core origin which then further facilitates the binding of Ad Pol and NF1 to core origin and auxiliary origin, respectively. NF1 and OCT-1 are not necessarily required for genome replication but rather enhance replication. After, Ad Pol dissociates from pTP and the formation of the nascent strand can then begin. This is marked with the dissociation of the pre-initiation complex and allowing DBP to unwind the dsDNA and allowing Ad Pol to form the nascent strand. Interestingly, displaced ssDNA can anneal to itself via the intramolecular/intermolecular interactions of the ITR regions which create dsDNA origins of replications. Hence, both dsDNA and ssDNA can be used as replication intermediates to increase the genome copy number.

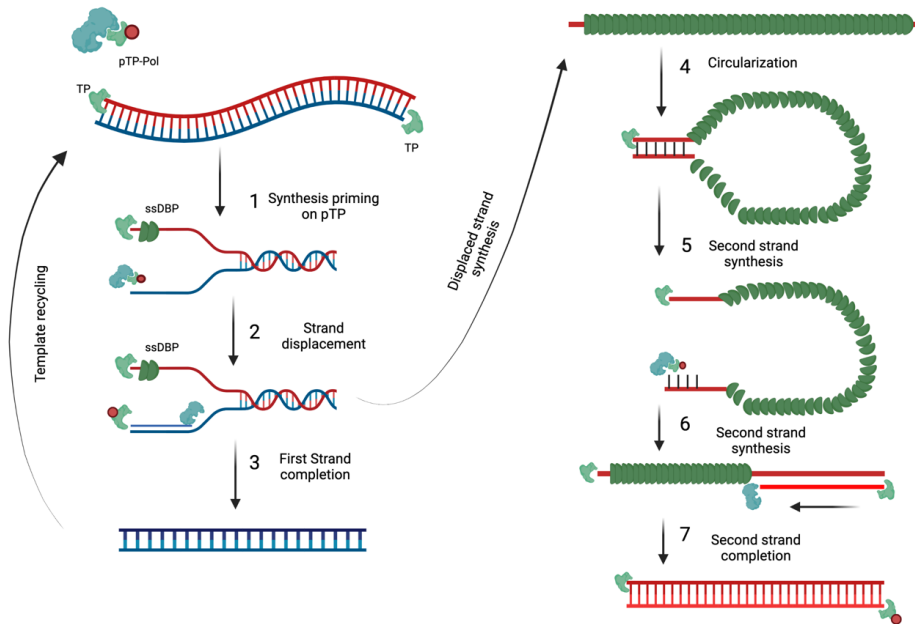


Figure 7. Adenovirus genome replication. DNA replication begins with the pTP-Pol complex invading and serving as a primer to begin DNA replication (1). Pol protein then begins to synthesize the new DNA strand and displaces the original strand (2) which is then coated with DBP. As soon as the first strand is completed it can then be used for template recycling (3). The displaced strand covered in DBP then circularizes because of the complementary ITR regions (4). The circularized DNA strand is then used as a template and evaded by the pTP-Pol complex to begin the synthesis of the complementary strand (5 & 6) until completion (7). Figures were created with BioRender.com.

3.1.2 Adenovirus-host cell interactions and selective replication

Adenoviral replication cycle is facilitated by the interactions between viral and cellular-host proteins. During the replication cycle of adenovirus, the virus must sequester various cellular proteins to help in genome replication, transcription, and translation. Moreover, while doing so it also has to fight off the intrinsic pathways of the host cell that are designed to shut off cell machinery, induce apoptosis and clear the virus. Therefore, adenoviruses have multiple proteins aiding in facilitating all these processes. Due to the understanding of such mechanisms, scientists have been able to come up with genetic modification allowing adenovirus to conditionally replicate in tumor cells¹⁸⁹. This section will describe these crucial interactions and how scientists have taken advantage of them to create conditionally replicating adenoviruses (CrAd).

For the adenovirus to start replicating its genome, the cell must be directed into S-phase¹⁹⁰. The adenovirus expresses E1a protein which is responsible in doing so by interacting with retinoblastoma protein (pRb). Under normal conditions, pRb can control the cell-cycle by interacting with DNA-binding transcription factor E2F¹⁹¹. This interaction restricts E2F from binding to DNA and promoting cell replication. E1a can bind to pRb and restrict its interaction with E2F¹⁹². This then leads to E2F to be dissolved and bind freely to DNA and promoting transition into S-phase. Usually in malignant cells, the mechanisms controlling cell replication are defective to sustain cell growth. The majority of cancers have a deficient pRb protein and consequently an E2F roaming freely¹⁹³. In consequence, adenoviruses do not require E1a to replicate in tumor cells and it becomes non-essential. Therefore, removing or rendering E1A defective can lead to a selective replication of adenoviruses in tumor cells (deficient in pRb proteins) while unable to replicate in healthy cells due to pRb. A 24 base pair deletion in the E1A protein has been previously described causing the protein unable to bind to pRb¹⁹². Various clinically tested oncolytic adenoviruses apport this mutation making them selectively replicate in tumor cells and have been shown to be safe.

After adenovirus infection pushes cells into the S-phase, p53 accumulates as a response to induce apoptosis to control cell growth¹⁹⁴. To circumvent this, adenoviruses express E1B 55k, E4 orf6 and E1B 19K which are all able to interact with p53 directly or indirectly to avoid apoptosis¹⁹⁵. Nevertheless, apoptosis might be disrupted but E1B 19K induces autophagy at the end of the viral replication cycle to release virions. Like pRb, p53 is also mutated in most cancers which prompts for a different strategy to induce selectivity in replication for adenoviruses. Deletion of the E1B gene induces adenoviruses to replicate in tumor cells while leaving healthy cells free¹⁹⁶. This deletion has also been noted to be clinically safe with different oncolytic viruses, such as ONYX-015 and H101, and in some countries they have been approved as therapy^{196,197}.

3.1.3 Arming oncolytic adenoviruses

As mentioned previously, even though oncolytic adenoviruses can directly infect selectively tumor cells and induce oncolysis this is not enough for clinical efficacy. The release of TAAs from oncolysis leading to a vaccination effect is required for a successful treatment. However,

a major limitation from achieving such clinical efficacy is the absence of anti-tumor immune cells and/or preventing their anti-tumor functions. One of the key advantages of using oncolytic adenoviruses is the ability to turn “cold” tumors with poor immune infiltration into “hot” tumors with high immune infiltration¹⁹⁸. Yet, the amount of immune stimulation provided seems not to be enough to sustain clinical efficacy or tumor elimination. Despite this, researchers have armed oncolytic adenoviruses with various molecules ranging from cytokines, antibodies, bi-specific antibodies (BiTEs) and more (Figure 8). Other than expressing adequate levels of immunomodulatory molecules, the oncolytic tropism of the virus may help in circumventing toxicity issues by limiting expression in the tumor microenvironment with minimal leakage to the periphery.

One class of molecules that has been used to arm oncolytic adenoviruses are co-stimulatory molecules. An example is the arming of oncolytic adenoviruses with two immune-activating ligands CD40L and OX40L^{199–202}. CD40L when secreted can interact with CD40 present on APCs and enhance their antigen presentation and co-stimulation capacity²⁰³. Moreover, OX40L binds to OX40 found on T cells and induces the survival and homeostasis of memory T-cells²⁰⁴. Another strategy, was arming oncolytic adenovirus LOAd703 with CD40L and 4-1BBL²⁰⁵. The interaction of 4-1BBL with 4-1BBL among T cells and APC lead to the increase of T-cell proliferation and activation. LOAd703 has been tested in clinical trials against many solid tumors and, interestingly, with pancreatic cancer it has been seen to reduce myeloid derived suppressed cells (MDSC) and increase memory T cells in many patients.

The release of cytokines and chemoattractants from oncolytic viruses are a successful strategy to increase immune cell homing to the tumor. The only FDA approved oncolytic virus in the clinic, T-VEC, comprises of a herpes simplex virus expressing GM-CSF²⁰⁶. This cytokine helps in the maturation and antigen presentation of APC, leading to better induction of T-cell immune responses. A similar version of T-VEC exists, but rather than a herpes simplex virus an adenovirus is used with the 24 base pair deletion in its E1A, previously described, to express GM-CSF²⁰⁷. Such virus, called ONCOS-102, is under clinical evaluation and was seen to increase CD8+T cells circulation but more importantly antigen-specific CD8+ T cells in mesothelioma and multiple peritoneal malignancies²⁰⁸. Many oncolytic adenoviruses have

been used to locally express various cytokine such as IL-2 and tumor necrosis factor α (TNF- α), IL-18, IL-24 or IL-12 in order to potentiate anti-tumor immune responses. Other than cytokines, chemokines such as CXCL9 and CXCL10 have also been cloned in oncolytic adenoviruses to recruit T-cells²⁰⁹.

BiTEs are small molecules which consist of two scFv directed at different tumor antigens. Conventional BiTEs usually have one of their scFV directed towards CD3 while the other towards a TAA. These BiTE's main mechanism of action is bringing CD3+ T cells into close proximity of tumor cells and induce MHC-independent killing²¹⁰. These BiTEs have been shown to be excellent therapies for the treatment of lymphomas and leukaemias. For example, Blinatumomab, against CD3 and CD19, is the first BiTE to be approved by the FDA for the use of B-malignancies²¹¹. However, for solid tumors it has been seen not to be effective since their half-life in blood is short-lived, which consequently requires constant infusion of treatment leading to systemic toxicities. Yet, oncolytic adenoviruses have shown to provide excellent platforms to deliver BiTEs locally and persistently in solid tumors. Enadenotucirev is one of the first oncolytic adenoviruses to express a BiTE, which was directed towards TAA epithelial cell adhesion molecule (EpcAM) and CD3²¹². Other than just targeting TAA, a similar oncolytic adenovirus expressing BiTE was also constructed but directed towards fibroblast activation protein(FAP) which is found on cancer-associated fibroblasts²¹³. The combination of both viruses demonstrated enhanced anti-tumor efficacy and T cell recruitment and function.

The systemic administration of checkpoint inhibitor has been associated with many adverse events. To further improve the safety profile, checkpoint inhibitors have been packaged into the genome of oncolytic adenovirus. Checkpoint inhibitors against CTLA-4²¹⁴ and PD-L1²¹⁵ have been cloned into oncolytic adenoviruses and have shown to be effective in controlling tumor growth with a high safety profile. Yet, a limiting factor that needs to be addressed with this strategy is that adenovirus has low capacity for cloning long transgenes in the genome. Hence, cloning whole antibodies consisting of a heavy and light chain can affect the viral fitness.

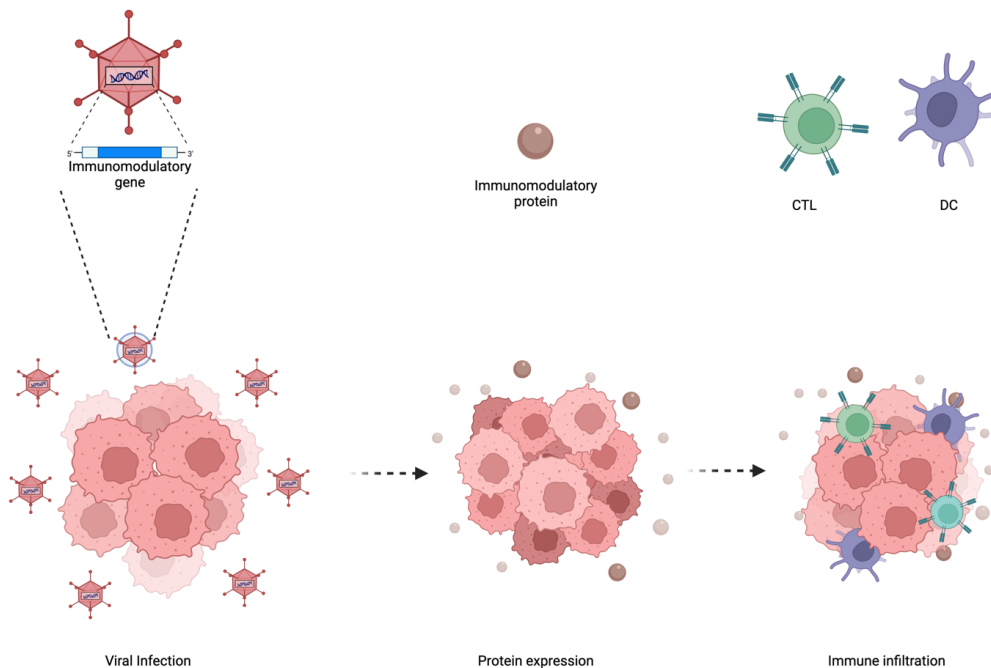


Figure 8. Enhancing oncolytic adenoviral therapy. Oncolytic adenoviruses have a specific tumor-tropism which can be utilized to arm such viruses with immunomodulatory genes. This then leads to the expression and secretion of the immunomodulatory proteins in the tumor microenvironment which increases immune infiltration. Figures were created with BioRender.com.

3.1.4 Construction of adenoviral vectors

The use of adenoviruses for gene therapy, vaccines and cancer immunotherapies has increased throughout the years. This entails the engineering of adenovirus to express any gene of interest (GOI), a process that has been modified several times in order to optimize the procedure. The classical approach that many scientists have used, is the cloning the GOI in a shuttle plasmid containing a 5'-ITR, a packaging signal and sequence of homologous recombination^{216,217}. This shuttle plasmid is then transfected into HEK293 cells with an adenovirus vector for homologous recombination to occur and create an adenovirus genome incorporating the GOI. Another used method is the cloning of the GOI into a similar shuttle plasmid but the homologues recombination sequence is substituted with LoxP site(s)²¹⁸. This shuttle is then transfected into HEK293 cells with an adenovirus genome containing LoxP sites. The shuttle vector and adenovirus genome are then joined via Cre recombinase-mediated recombination. A separate cloning method is the use of shuttle vector containing a

5'-ITR, a packaging signal and sequence of homologous recombination flanking a kanamycin resistance gene. After the GOI is added to this shuttle, it is linearized and transfected into bacterial cells (BJ5183) along with an ampicillin-resistant adenovirus backbone²¹⁹. Colonies are then screened based on kanamycin resistance and the final adenovirus containing the GOI product is linearized and transfected into HEK293 cells.

Each cloning system presented here are well characterized, reproducible and easy to design and carry out. However, these methods are very time consuming and it can take up to 6 months or more to obtain the final product. This is because homologous recombination has very low efficiency and can take multiple rounds for a positive colony. Moreover, secondary recombination can occur leading to the incorporation of unwanted repeated regions or secondary structures. Hence, the need of novel cloning methods that are faster, easier and reliable are required.

4. Aims of the Study

The main goal of this thesis was to further improve oncolytic adenoviruses to be used in cancer immunotherapies by inducing a simultaneous activation of multiple immune effector populations. To achieve this goal, the thesis was divided into three aims:

1. Develop a novel cloning method which is faster, easier, and more practical than traditional methods, to engineer adenoviruses to express any given GOI. (I)
2. Design and engineer an oncolytic adenovirus expressing a cross-hybrid IgGA Fc fusion peptide against PD-L1 able to activate multiple immune-effector populations. (II)
3. Further improve the cross-hybrid IgGA Fc fusion peptide ability to elicit immune effector populations and evaluate its safety and bio-distribution *in vivo*. (III)

5. Methods and Materials

5.1 Cell lines

All the cell lines used in the studies were grown at 37°C and 5% CO₂. A549 (human lung adenocarcinoma) cells were cultured in low glucose Dulbecco's Modified Eagle Medium (DMEM) (Gibco) supplemented with 10% fetal bovine serum (FBS) (Gibco), 1% L-glutamine and 1% penicillin-streptomycin antibiotics (Gibco). B16-K1 (murine melanoma) and MDA-MB-436 (human triple negative breast cancer) cells were cultured in high glucose DMEM supplemented with 10% FBS, 1% L-glutamine and 1% penicillin-streptomycin. B16F10 (murine melanoma) and CT26 (murine colorectal cancer) were grown in low glucose Roswell Park Memorial Institute (RPMI) supplemented with 10% FBS, 1% L-glutamine and 1% penicillin-streptomycin. 4T1 (murine triple negative breast cancer) cells were given high glucose RPMI supplemented with 10% FBS, 1% L-glutamine and 1% penicillin-streptomycin. B16F1 (murine melanoma) cells were grown in Eagle's minimum essential medium (EMEM) supplemented with 10% FBS, 1% L-glutamine and 1% penicillin-streptomycin. These cells were thawed at passage 5-6 and kept in culture until reaching passage 15. Moreover, mycoplasma contaminations were regularly preformed. All cells were purchased from the American Type Culture Collection (ATCC).

5.2 Oncolytic adenoviruses

All the adenoviruses used in these studies were of the human serotype 5. Some of the viruses have the knob domain replaced with the knob-domain of serotype 3, which are termed 5/3²²⁰. Also, all viruses have a 24 base-pair deletion (Δ 24) in the E1A protein which induces a selective tropism towards cells defective in the Rb-pathway. Oncolytic adenoviruses used in the studies can be seen in table 1.

Table 1: Oncolytic adenoviruses used in studies

Virus (Name)	Fiber	Modifications	Transgenes	Study
Ad5/3-(Δ 24)	Ad 5/3	Δ 24 bp in E1A	-	I, II & III
Ad5-(Δ 24) RFP	Ad 5	Δ 24 bp in E1A	RFP	II

Ad5/3-(Δ 24) CXCL9	Ad 5/3	Δ 24 bp in E1A	CXCL9	I
Ad5/3-(Δ 24) CXCL10	Ad 5/3	Δ 24 bp in E1A	CXCL10	I
Ad5/3-(Δ 24) IL-15	Ad 5/3	Δ 24 bp in E1A	IL-15	I
Ad-Cab	Ad 5/3	Δ 24 bp in E1A	IgGA Fc-fusion peptide against PD-L1	II & III
Ad-Cab FT	Ad 5/3	Δ 24 bp in E1A	Enhanced IgGA Fc-fusion peptide against PD-L1	III

5.3 Transgene insertion into Adenovirus genome

To equip oncolytic adenoviruses with a GOI, the gp19k+7.1 region was removed and subsequently replaced by the GOI. First, oncolytic adenovirus 5/3 plasmids (pAd5/3- Δ 24) were cut with *SrfI* (New England Biolabs) and *BamI* (SibEnzyme) to remove the E3 region. After digestion, poly(A) and cytomegalovirus promoters (CMV) were synthesized by ThermoFisher containing a 40-nucleotide overlapping sequence. The poly(A) sequence had an overlapping sequence to the 3' of the cut pAd5/3- Δ 24 while CMV had the overlapping sequence to the 5' end. Moreover, the poly(A) fragment also contained all other E3 regions except for gp19k+7.1. The GOI were then synthesized with a 40-nucleotide sequence that was overlapping to CMV and poly(A) on its 5' and 3' ends, respectively. Following synthesis, CMV, poly(A) and GOI fragments were assembled using the Gibson assembly (GA) master mix (New England Biolabs) according to the manufacturer's guidelines. In the assembly process, a 3:1:1 (polyA: CMV: GOI) molar ratio was used in which 50ng of poly(A) was used. Assembled products were then amplified with PCR and then assembled to the cut pAd5/3- Δ 24 using the GA mix. The molar

ratios used were 3:1 (insert:vector) in which 1.3µg of vector was used. Succeeding the assembly, 2µl of the assemble products were used to transform DH5-alpha *E.coli* (Thermofisher). Since pAd5/3-Δ24 vectors contained a kanamycin resistance gene, transformed bacteria were spread on kanamycin-containing agar plates. Colonies were then grown in liquid lysogeny broth (LB) containing kanamycin and then assembled plasmids were isolated for restriction enzyme analysis and/or sanger sequencing.

5.4 Amplification and purification of oncolytic adenoviruses

Kanamycin resistance gene from the assembled pAd5/3-Δ24 + GOI was removed by *PacI* digestion overnight. After digestion, 3µg of digested linear genomes, isolated using ethanol precipitation, were transfected into A549 cells seeded in T25 flask using Effectene (QIAGEN). In the wake of cytopathic effects, cells were collected and put through four freeze-thaw cycles to liberate viral particles into the supernatant. The virus containing supernatant was then used for the next round amplification by infecting a T175 flask cultured with A549 cells. After cytopathic effects, the same amplification round was done but with a 10-layer cell culture multi-flask.

When cytopathic effects were observed in the multi-flasks, cells were collected and pelleted by centrifugation at 400g for 20 minutes. Cell pellets were resuspended in medium and underwent four freeze-thaw cycles to liberate viral particles into the supernatant. Viral particles were then isolated using a double CsCl gradient and ultracentrifugation. Isolated viral particles were dialyzed overnight with A195 buffer, composed by Evans et al²²¹.

5.5 Particle titering

Viral particles were measured by first mixing viral preparations with virus lysis buffer (VBL) made up of 10 mM Tris-HCL, 1 mM EDTA and 0.5% SDS. Virus preparations and VBL were mixed in 1:2 and 1:3 ratio (virus:VBL) and kept at 95°C for 15 minutes and then absorbance at 260 nm was measured. Using the following the viral particles were determined:

$$\text{Viral particles/ml} = \text{OD}_{260} \times \text{dilution factor} \times 1.1 \times 10^{12}$$

5.6 Infectivity assay

In a 24-well plate, cultured A549 cells were infected with virus in a series of 10-fold dilution and incubated for 48 hours at 37°C. Infected cells were then fixed using ice-cold methanol and washed with 1% bovine serum albumin (BSA) containing PBS. Viral infection was stained using first mouse anti-hexon antibody and then secondary anti-mouse conjugated with horseradish peroxidase (HRP). Binding was then detected by using 3,3' Diaminobenzidine (DAB) solution and color formation was observed under bright field microscope. Infectious titer was then calculated using the following formula:

$$\text{Infectious units/ml} = X \times \frac{A(\text{Well})}{A(\text{Field})} \times \frac{1}{d} \times \frac{1 \text{ ml}}{V}$$

X = Average number of infected cells

A(well)= Area of the well

A(field)= Area of the field in which infected cells were counted

d= Dilution factor used

V= Volume of virus used

5.7 Viability assay

Cells were first seeded at 1×10^4 per well in a 96-well plate overnight and then infected with different viral dilutions. After 3 days, cell viability was then analysed using MTS according to the manufacturer's guidelines (Cell Titer 96 Aqueous One Solution Cell Proliferation Assay: Promega). Optical densities were then read at 490nm using the Varioskan LUX multimode microplate reader (Thermo Fisher).

5.8 PBMC migration assay

Migration of PBMCs was analyzed using a Transwell (Corning) system containing a 5µm pore membrane. In the apical side, cells were cultured and infected with virus at 100 MOI. In the basolateral side, PBMCs stained with calcein green (Thermo Fisher), according to

manufacturer's guidelines, were added. After two days, green PBMC cells in the apical side were counted manually.

5.9 Determining concentrations of biological molecules

Cytokines and Fc-fusion peptide concentrations were determined either from *in vitro* cell cultures or *in vivo* tumor, liver, and blood samples. For *in vitro* samples, 100,000 cells were cultured and infected with virus at 100 MOI. After indicated time points, cell supernatant was taken and frozen at -80°C until further analysis. As for *in vivo* tumor and liver, samples were passed through a 0.22µM cell strainer to create a single cell suspension. Supernatants were then collected from samples centrifuged at 500g for 10 minutes.

Cytokine concentrations were then measured using the respective ELISA Dup set test (R&D Systems) according to manufacturer's guidelines. Since a His tag is found in the C-terminal end, concentrations of Fc-fusion peptides were determined using a HIS-tag ELISA kit (Cell Biolabs).

5.10 Competition assay

In a 96-well, A549 cells were cultured at 100,000 cells per well and then incubated with different concentrations of purified Fc-fusion peptides for 30 minutes on ice. After binding, Atezolizumab was given at 10µg/ml and incubated again for 30 minutes on ice. Atezolizumab binding was then measured by staining samples with anti-human IgG PE (BioLegend) and analyzed using flow cytometry.

5.11 PBMC, PMN, monocyte and complement active serum isolation

For active serum isolation, 40ml of blood was taken from 11 healthy volunteers in BD Vacutainer tubes (BD Biosciences) and allowed to clot for 30 minutes at room temperature. Samples were then centrifuged for 5 minutes at 500g. Serum fractions from blood were isolated and mixed from all volunteers to compensate any complement deficiencies.

As for PBMC and PMN isolation, buffy coats were first diluted in PBS in a 1:1 dilution and then mounted on top of a Ficoll (Cytiva) and Histopaque (Sigma Aldrich) double density

layer. Samples were centrifuged at 400g for 20 minutes with low acceleration and no brakes. PBMCs and PMNs were subsequently collected from the respective layer and cultured in low glucose RPMI.

Monocytes were isolated by seeding 10×10^6 isolated PBMC cells in a T75 flask and cultured for two hours at 37°C. Floating cells were removed and attached monocytes were washed with PBS.

5.12 Mixed leukocyte reaction (MLR)

Isolated monocytes were first differentiated into DC by culturing cells for seven days in low glucose DMEM supplemented with 10% FBS, 500 U/mL of IL-4 (PeproTech) and 250 U/mL of GM-CSF (Abcam). Differentiated DCs were then co-cultured with PBMCs, stained with CFSE (Thermo Fisher), from a different donor for five days and untreated or treated with either 20 µg/ml of Fc-fusion peptides or Atezolizumab. T-cell proliferation was then measured by staining cells with anti-human CD8 (BioLegend) and observing CFSE staining in such cell population with flow cytometry.

5.13 Complement dependent cytotoxicity

In a 96 well plate, 100,000 cells were first seeded and then treated with indicated amounts of antibodies/Fc-fusion peptides or virus. Virally infected cells were incubated for 48 hours and then 15.5% of complement active serum was added. As for cell treated with either antibodies or Fc-fusion peptides, 15.5% of complement active serum was added after 30 minutes of incubation. After 4 hours of incubation with serum, cell lysis was measured by staining with 7AAD (eBioscience) and measured with flow cytometry.

5.14 Antibody dependent cell mediated cytotoxicity

In a 96 well plate, 15,000 of target cells were plated and then treated with antibodies/Fc-fusion peptides or virus. Cell infected with virus were incubated for 48 hours and then PBMCs or PMNs were added at a 100:1 or 40:1 (Effector: Target) ratio, respectively. As for cells treated with antibodies/Fc-fusion peptides, effector populations were added after 30

minutes. Lysis was then measured by quantifying the amount of LDH released into the supernatant using a colorimetric assay (CyQUANT LDH Cytotoxicity Assay). Specific lysis was measured using the following formula:

$$\% \text{Specific lysis} = \frac{\text{Experimental LDH} - \text{No treatment LDH}}{\text{Maximum LDH} - \text{No treatment LDH}} \times 100$$

Experimental LDH= LDH released from treated sample

No treatment LDH= LDH released from samples with effector and target cells but no treatment

Maximum LDH= LDH released from target cells treated with lysis buffer

5.15 Antibody dependent cell mediated phagocytosis

Monocytes were first differentiated into macrophages by culturing cells in RPMI supplemented with 50µg/ml of M-CSF (Sigma Aldrich) for 7 days at 37°C. In a 96 well plate, 10,000 target cells were then plated per well and then stained with CFSE. Stained cells were then infected with virus with either 10 or 100 MOI and incubated for 48 hours. After incubation, unstained differentiated macrophages were added in a 5:1 (Effector: Target) ratio for 4 hours. Phagocytosis was then calculated by measuring uptake of CFSE from macrophages using flow cytometry.

5.16 Trogocytosis

Trogocytosis was performed by first plating 5,000 target cells per well in a 96-well plate and then infecting cells with virus at 100 MOI for 48 hours. The lipid cell membranes were then stained with 5µM of DiO (ChemCruz) for 30 minutes at 37°C. After staining and washing with PBS, PMNs were then added at a 40:1 (Effector:Target) ratio for four hours. Neutrophil uptake of DiO was then measured using flow cytometry

5.17 Real-time quantitative analysis (xCELLigence assay)

Real time killing was assessed using the the xCELLigence system (ACEA Biosciences). Per well, 25,000-100,000 cells were plated for 24 hours. After incubation, designated amount of

antibody/Fc-fusion peptide was added along with PBMCs and PMNs. Cell index was then measured every 5 or 30 minutes. Killing rates was then calculated by drawing a linear trendline and analysing the slope.

5.18 Live cell imaging

For target and effector cell contacts, A549 cells were imaged by first seeding 150,000 cells per well in a 24 well plate overnight. Cells were then imaged for the first 30 minutes and then 10µg/ml of Fc-fusion peptide or antibody was added along with PBMCs at 10:1 (Effector:Target) ratio. Images were then acquired every 5 minutes with the ANDOR Spinning Disc Microscope equipped with a Zyla camera (SR Achromat x100 Objective).

For live-killing videos, 100,000 cells were seeded in a 24 well plate in each well and left to grow overnight. After incubation, 3µM of Incucyte Caspace3/7 green apoptotic assay reagent (Sartorius) was added and cells imaged with the IncuCyte S3 system for one hour. Later, 5µg/ml of Fc-fusion peptides or antibodies were added along with PBMCs and PMN at 100:1 and 40:1 (Effector:Target) ratios, respectively. Cells were imaged for 23 hours, and videos were constructed and processed with the IncuCyte analysis software (IncuCyte Chemotaxis Software).

5.19 Whole blood assays

Blood from 3 healthy volunteers were collected in BD Vacutainer Heparin plasma tubes and 200µl of blood from each volunteer was plated in a 96-well plate. Unmanipulated blood was then treated with 20µg/ml of Fc-fusion peptides or antibodies for 24 hours. After incubation, cells were then stained with CD3 (BioLegend), CD15 (BioLegend), CD14 (BioLegend), CD56 (BioLegend) and CD11c (BioLegend). Moreover, to determine absolute numbers counting beads (BioLegend) were added according to manufacturer's guidelines.

5.20 Patient derived cancer organoid cultures

Renal cell carcinoma samples delivered from Peijas Hospital (Vantaa, Finland) from four patients were collected, dissociated in cell suspension. Cells were first frozen and stored at -80°C until further use.

Frozen dissociate cells were first thawed and grown in ultralow attachment plates (ULA Corning) with DMEM/F12 medium supplemented with 30% Matrigel (Corning). Cells were then split using gentle cell disassociation media (Stemcell) and counted. Then, 10,000 cells were mixed with 30% Matrigel and dome like structure was created in a 24-well plate. Organoid cultures were grown in DMEM/F12 supplemented with 5%FBS, 8,4 ng/ml of cholera toxin (Sigma), 0.4µg/ml hydrocortisone (Sigma), 10ng/ml epidermal growth factor (Corning), 24 µg/ml Adenine (Sigma), 5 µg/ml insulin (Sigma) and 10 µM of Y-27632 RHO inhibitor (Sigma).

5.21 Immunofluorescence and flow cytometry analysis on organoids

For immunofluorescence analysis, organoids were first dissociated with gentle cell disassociation media (Stemcell) and then plated on a 8 well Nunc Lab-Tek II Chamber slides and cultured for 4 days. After culturing, cells were fixed using 4% cold paraformaldehyde and stained with CAIX (Novus), Vimentin (Novus), Cytokeratin pan (Novus) or Alexa Fluor 633 Phalloidin (Invitrogen). Staining was then examined using the EVOS FL cell imaging system (Thermo Fisher).

As for flow cytometry, organoids were dissociated as mentioned previously and stained with anti-human CD3 (Biolegend), anti-human CD4 (Biolegend), anti-human CD8 (Biolegend), anti-human PD-L1(Biolegend) and anti-human CD45 (Biolegend). Staining was analyzed with flow cytometry.

5.22 Organoid viral infection, PBMC co-culture and ADCC experiments

Organoids plated in a 24 well-plated were infected with 100,000 viral particles of Ad-5 Δ24 RFP virus by adding the virus on top of the media. RFP expression was then monitored using the EVOS FL cell imaging system and cell viability was determined by using 1µM of Calcein AM (Thermo fisher).

As for co-culture, PBMCs were first stained with 1 μ M of Calcein AM and 15,000 stained PBMCs were added on top of the media culture. After 4 hours, PBMC infiltration was then seen under the EVOS FL cell imaging system.

ADCC experiments were conducted by first infecting organoids with virus, as previously mentioned, or treating with 10 μ g/ml of antibody. After 72 hours, PBMCs and/or PMNs were added at 100:1 and 40:1 (Effector:Target) ratio, respectively. When four hours of killing was done, supernatants were collected to determine the amount of LDH released using the colometric assay (CyQuant LDH Cytotoxicity Assay).

5.23 Syngenic mousemodels

All mouse experiments performed in this thesis were approved by the Experimental Animal Committee of the University of Helsinki and Provincial Government of Sothern Finland (license number ESAVI/11895/2019). Moreover, all mice used were of 4-6 weeks of age. For Balb-C mice, they were injected with either 500,000 CT26 cells or 300,000 4T1 cells subcutaneously (sc) in the right flank. As for C57BL/6 mice, they were injected with 500,000 B16K1 cells sc in the right flank. Mice were treated with either 1 \times 10⁹ or 1 \times 10⁸ viral particles per dose intratumorally in final volume of 25 μ l or 100 μ g of antibody intraperitoneally in a final volume of 100 μ l. Dosing scheduled depended on the tumor model but are mentioned in the results section. Every second day tumor volumes were measured and calculated using the following formula:

$$\frac{(Long\ side) \times (Short\ side)^2}{2}$$

5.24 *In-vivo* immune cell depletion

One day before treatment, mice were first administered with 500 μ g of depleting CD8 antibody (Bio X cell) and then every two days 100 μ g of the depleting antibody until the end of the experiments. To check for depletion, peripheral blood from the saphenous vein was collected and subjected to ACK lysis buffer (Gibco) to remove red blood cells according to

manufacturer's guidelines. Then, samples were stained with anti-mouse CD3, anti-mouse CD8 and anti-mouse CD4 and analyzed under flow cytometry.

5.25 Humanized mouse studies

Humanized mice were done by injecting 5×10^6 freshly isolated PBMCs intraperitoneally in Nod.CB17-Prkdc^{scid}/NCrCrl purchased from Charles river. Immediately after PBMC injection, mice were also implanted with 5×10^6 A549 sc in the right flank. When tumors were palpable, two rounds, separated by three days of break, of viral treatments were given intratumorally at a concentration of 1×10^8 viral particles per mouse.

5.26 Flow cytometry

Murine and human samples were subjected to two antibody panels. Starting with murine samples, the first antibody panel included FITC anti-mouse NK1.1 (Thermo Fisher), PE anti-mouse PD-1 (BioLegend), PeCy7 anti-mouse CD4 (Thermo Fisher Scientific), PerCp/Cy5.5 anti-mouse CD107a (BioLegend) and Pacific Blue anti-mouse CD3 (BioLegend). The second panel was made up of APC anti-mouse Ly6C (BioLegend), PE anti-Ly6G (BD Biosciences), PerCP Cy5.5 anti-mouse CD11b (Thermo Fisher Scientific), BV650 anti-mouse F4/80 (BD Biosciences) and PECy7 anti-mouse CD11c (Thermo Fisher Scientific). With the human samples the first panel consisted of FITC anti-human CD56 (BioLegend), PerCP anti-human CD8alpha (BioLegend), PE-Cy5 anti-human CD4 (Thermo Fisher Scientific), PE-Cy7 anti-human CD3 (BioLegend), Pacific blue anti-human PD-1 (BioLegend) and APC anti-human CD107a (BioLegend). The second panel had PE-Cy7 antihuman CD3 (BioLegend), APC anti-human CD11c (BioLegend), Pacific Blue anti-human CD15 (BioLegend) and PE anti-human CD14 (BioLegend).

5.27 Statistical analyses

Statistical analyses were all done with GraphPad Prism 7 (GraphPad Software). Statistical tests used were either unpaired t-test or Two-way ANOVAs with a post-hoc (Tukey's multiple comparison test). All $n \geq 3$ and significance were set at * $p < 0.05$, ** $p < 0.01$, *** $p < 0.001$ and **** $p < 0.0001$. Error bars represent standard error of mean (SEM).

6. Results and Discussions

6.1 Study I: GAMER-Ad: An enhanced and faster cloning method for oncolytic adenoviruses

Oncolytic adenoviruses have been shown to be excellent vehicles for selective release of anti-cancer molecules due to the specific tumor tropism. However, the current cloning methods are sub-optimal due to their complexity and are time consuming. The current method used is the AdEasy method which utilizes a shuttle plasmid containing the GOI flanked by homologous regions to the adenovirus genome. Then through homologous recombination, the GOI is added to the genome. In our first study, we designed a novel cloning method which utilizes the Gibson assembly²²². Our method, which we have called GAMER-Ad (Gibson Assembly MEdiated Recombination for Adenovirus), is faster compared to the AdEasy system **(Study 1; figure 1)**. In this study we described the method in detail by engineering three oncolytic adenoviruses (Ad-5/3 Δ 24) to express CXCL9, CXCL10 or IL-15.

6.1.1 Designing and executing the GAMER-Ad cloning method

The GAMER-Ad cloning method consists of removing the gp19k+7.1k region and substituting it with a GOI **(Study 1; figure 2)**. This region encodes for multiple proteins involved in immune evasion by downregulating MHC-1 complexes. Hence, the removal of this region attenuates the virus further from immune evasion which is favorable to be used as a cancer immunotherapy. To do this, firstly the full E3 region of the adenovirus (Ad-5/3 Δ 24) was removed by using *Srf1* and *EcoRI* restriction enzymes since the region is flanked by such sites **(Study 1; figure 3 a)**. To verify that the restriction enzyme digest was successful, products were run in an agarose gel to check for the excised E3 region. The agarose gel indicated a clear band between 3kb and 4kb, showing that the E3 region of 3,398 bases was cut from the genome **(Study 1; figure 3 b)**.

After removing the E3 region, we constructed the GOI that would replace such region. The GOI consisted of a region encoding for IL-15 flanked with a CMV promoter and polyA region. The CMV and polyA region had 40 overlapping nucleotides to the 5' and 3' of the excised adenovirus genome, respectively. As for the IL-15 gene, the 5' and 3' ends were given

40 nucleotides overlapping with the CMV and polyA, respectively. Moreover, the polyA also contains all the essential genes of E3 except for the gp19k+7.1k region. All the regions were first amplified using PCR and then checked using an agarose gel. In lanes 2, 3 and 5 bands were observed corresponding to the sizes of CMV, polyA and IL-15 indicating that the amplification was successful (**Study 1; figure 3 c**). Using the overlapping nucleotides of IL-15, all three fragments were assembled using Gibson Assembly (**Study 1; figure 3 d**). The assembled products were then ran on agarose and a band corresponding to the size of the complete GOI was observed implying that the assembly was successful (**Study 1; figure 3 e**). Also, the ability to assemble the IL-15 gene with the CMV and polyA fragment provides a plug-in/out system. Meaning that IL-15 can be substituted with any desired gene having the 40-nucleotide homology region making GAMER-Ad versatile and adaptable.

As for the final step of the cloning method, the assembled GOI and excised adenovirus genome were assembled together using the Gibson Assembly. This was possible due to the 40 nucleotide overlapping regions to the adenovirus genome found in the polyA and CMV. After assembly, products were transformed, and bacterial cells were plated in agar containing kanamycin since the adenovirus genome contains the kanamycin-resistance gene.

6.1.2 Quality control of assembled adenovirus genome products

After adenovirus genomes assembled with the GOI were transformed into bacteria, eight colonies were picked and underwent colony PCR. Primers used flanked the CMV and polyA region which are not found in the adenovirus genome but only in the GOI. Out of eight colonies, six showed a band with a corresponding size of the GOI (**Study 1; figure 4 a**). To further assess the presence of the GOI, three positive colonies were grown in LB and the isolated DNA was subjected to restriction enzyme analysis and Sanger sequencing. With restriction enzyme analysis, *EcoRI* enzyme was used due to the unique pattern of cutting with assembled adenovirus compared to unassembled adenovirus genomes. With assembled adenovirus genomes, a clear band with a size of 2,075 base pair should be observed while with unassembled adenovirus a band of 2,718 base pairs should be seen when *EcoRI* is added (**Study 1; figure 4 b**). As expected, when *EcoRI* was added all three colonies presented a smaller band compared to wild-type unassembled adenovirus genome (**Study 1; figure 4 c**). To further compliment these results, sanger sequencing also showed that all three colonies

did have the gp19k+7.1k region replaced with the GOI (**Study 1; figure 4 d**). This was then repeated with two different genes, CXCL9 and CXCL10, to demonstrate the versatility of GAMER-Ad. This data implies that GAMER-Ad cloning method is a viable strategy to be used to engineer oncolytic adenoviruses to express any desired gene. Moreover, these results also comment on the efficiency of the assembly since 75% of the colonies chosen had the GOI. This is a clear advantage since with the commonly used homologous recombination-based method the efficiency is much lower compared to GAMER-Ad.

Following assembly, adenovirus genomes were transfected into A549 cells for viral production. Seven days post transfection, plaques could be observed with cells transfected with assembled adenovirus genomes containing IL-15 demonstrating viral production (**Study 1; figure 5 a**). Viral particles were then collected, expanded, and successfully purified using a CsCl gradient. One of the major hurdles with homologous recombination is the possibility of wild-type contamination due to unwanted recombination events. To assess for wild-type contamination in viral products assembled using the GAMER-Ad method, purified viral preparation underwent PCR analysis. Two different PCR reactions were done in which the first reaction primers flanking the gp19k+7.1k regions were used while the second reactions primers binding to CMV and poly-A were added. If no wild-type virus is present then no bands should be found with the first PCR reaction with CXCL9-,CXCL10- and IL-15-expressing virus preparations since the gp19k+7.1k region has been replaced. However, only in the second PCR reaction bands should be found due to the presence of the GOI. As expected, in the first PCR reaction no bands were found in any of the viral preparations but only in the wild-type adenovirus genome. Furthermore, corresponding bands of the GOI were observed in the second reaction with all viral preparations and not in the wild-type adenovirus genome. This then implies that the GAMER-Ad cloning method seems not to lead to wild-type contamination, which could be a vital issue in therapy development.

6.1.3 Oncolytic fitness and functionality of adenovirus engineered by GAMER-Ad

Succeeding viral production, the oncolytic fitness of CXCL9-, CXCL10- and IL-15 expressing viruses was examined to analyze whether GAMER-Ad affected such properties. Viruses engineered with GAMER-Ad have a 24 base pair deletion in the E1A region rendering them to selectively replicate in Rb-deficient tumor cells. Despite this, all three engineered viruses were

used to infect human cancer cell lines, A549 and MDA-MB-436 at different MOIs. Moreover, murine melanoma cancer cells, B16F10 and B16F1, were also infected with such viruses as a negative control since human adenoviruses do not replicate in murine cells. To examine the oncolytic fitness wild-type adenovirus containing the 24-base pair deletion was used to compare. All engineered viruses were able to kill both human cancer cell lines at MOIs of 10 and 100 after three days similarly to wild-type virus. Also, no killing was observed with murine cell lines as expected. This implies that the GAMER-Ad cloning method does not affect the oncolytic fitness of viruses.

Finally, the functionality of the engineered viruses was tested by measuring the expression of cytokines released and PBMC migration. After infecting MDA-MB-436 cells, the amount of cytokines was quantified by ELISA. All viruses expressed the corresponding levels of cytokines ranging from 1ng to 38ng. Since the cytokines cloned in this study can induce PBMC migration, the functionality of the expressed cytokines was then tested using a trans-well system. Calcein-green labeled PBMCs were placed in the apical side while cells infected with cytokine expressing virus were placed in the basolateral side. After 48 hours of incubation, migrated PBMCs on the basolateral side were then manually counted. A clear increase in migrated PBMCs could be seen in all cytokine expressing viruses compared to wild-type virus. The CXCL9 expressing virus was shown to have the highest migrated PBMCs followed by the CXCL10 expressing virus. In conclusion, GAMER-Ad produces oncolytic fit and functional adenoviruses. Previous studies have used Gibson assembly to clone adenoviruses^{223,224}, however what makes this method unique is the site of cloning. The substitution of the gp19k+7.1k region with a GOI is highly desirable for cancer therapies but also vaccine platforms. This is because this regions codes for proteins able to down-regulate MHC-1 which can attenuate any clinical efficacy either for cancer treatment or vaccinations. For example, the novel adenoviruses created in this study can be used in combination with other therapies activating T cell tumor killing (like checkpoint inhibitor therapy) since they increase T-cell infiltration. Yet, with an intact gp19k+7.1k region this could potentially hamper efficacy since MHC-1 is required for checkpoint inhibitory therapy.

6.2 Study II: Activating multiple immune effector populations using a cross-hybrid IgGA Fc fusion peptide against PD-L1

Immune checkpoint inhibitors have had a strong positive impact in the clinic for many cancer patients. In specific, checkpoint inhibitors against PD-L1 have been clinically approved for more than 14 different types of cancer²²⁵. Nevertheless, only 14% of patients benefit from such therapy²²⁶. In need to improve such therapy, a viable strategy would be equipping PD-L1 checkpoint inhibitors with a competent Fc able to activate effector mechanisms. Yet, the expressing of PD-L1 is not limited to the tumor but also to healthy cells. This explains why the majority of the PD-L1 checkpoint inhibitors are not able to induce or have a reduced ability to elicit effector mechanisms. To circumvent this safety issue, oncolytic adenoviruses have been used to limit expression to the tumor microenvironment.

In this study we designed a checkpoint inhibitor against PD-L1 which consists of a PD-1 ectodomain connected to a cross-hybrid IgGA Fc. This IgGA Fc contains regions of both an IgG1 and IgA1 able to induce effector mechanisms of both Fc-regions. Using the novel cloning method developed in study one, we cloned the Fc-fusion peptide against PD-L1 in oncolytic adenovirus to limit its release to the tumor microenvironment and prevent off-target effects.

6.2.1 Characterizing oncolytic adenovirus expressing cross-hybrid IgGA Fc fusion peptide

We designed a novel checkpoint inhibitor consisting of a PD-1 ectodomain connected via a GGGGS linker to a cross-hybrid IgGA Fc. The hybrid IgGA Fc can elicit effector mechanisms of both an IgG1 and IgA potentially leading to higher tumor killing (**Study 2; figure 1 a**). In order to circumvent safety issues, release of the Fc-fusion peptide was restricted to the tumor microenvironment by cloning it into an oncolytic adenovirus using GAMER-Ad. The gp19k+7k region was replaced by the Fc-fusion peptide and the oncolytic adenovirus was called Ad-Cab (Adenovirus-ChimericAntibody). Similar to results from study I, the genetic modifications did not alter the oncolytic fitness of the virus (**Study 2; supplementary figure 1 b**). We then tested the secretion of the Fc-fusion by infecting A549 with Ad-Cab or unarmed oncolytic virus (Ad-5/3 Δ 24) at 100 MOI. After 48 hours, western blot analysis showed a 100kDa band from the supernatant from Ad-Cab infected cells under native conditions (**Study 2; supplementary figure 1 b**). As expected, the Fc-fusion peptide consisted of homodimer since the band shifted

from 100kDa to 50kDa under denaturing conditions (**Study 2; supplementary figure 1 c**). This is to be expected since the Fc heavy chains form a homodimer via disulfide bridges. After observing that the Fc-fusion peptide was released, the amount released into the supernatant was quantified and a clear increase can be observed over time with Ad-Cab. After 24 hours, Ad-cab was able to secrete 2 μ g and reached 7 μ g after 72 hours (**Study 2; figure 1 c**). This amount should be enough to activate immune cells to elicit effector mechanisms. The secreted Fc-fusion peptide was then tested to see it was able to bind to PD-L1. This was done by using a competitive assay where A549 cells expressing PD-L1 were first incubated with various Fc-fusion concentrations and then Atezolizumab, a well-known binder to PD-L1, was added. To quantify Atezolizumab binding, an anti-human IgG tagged with fluorophore PE able to only recognize Atezolizumab and not the Fc-fusion peptide was added. At high concentrations of the Fc-fusion peptide, Atezolizumab binding was not observed but only at lower concentrations (**Study 2; figure 1 d**). This signifies that the secreted Fc-fusion peptide can bind to PD-L1 and compete for binding with Atezolizumab. To finally characterize the Fc-fusion peptide, we performed a mixed leucocyte reaction to assess the ability of the Fc-fusion peptide to block the PD-1/PD-L1 axis. DC from one donor were mixed with CFSE-labelled CD8⁺ T cells from a second donor and proliferation was then assessed due to the existing HLA-mismatch. When samples were untreated very limited proliferation of CD8⁺ T cells was observed due to the PD-1/PD-L1 axis (**Study 2; figure 1 e**). When Atezolizumab was added a higher proliferation was observed due to the disruption of the axis (**Study 2; figure 1 e**). Similar results were also shown when the Fc-fusion peptide was added indicating a disruption of the axis as well (**Study 2; figure 1 e**). Moreover, the expansion index further indicated that both Atezolizumab and Fc-fusion peptide induced CD8⁺ T cell expansion (**Study 2; figure 1 e**). The data demonstrates that Ad-cab secretes a Fc-fusion peptide able to bind to PD-L1 and disrupt the binding to its PD-1 ligand.

6.2.2 Ad-Cab induces Fc-effector mechanisms of both IgG1 and IgA1

Once we observed that Ad-cab can bind PD-L1 and disrupt its axis, the ability to elicit Fc-effector mechanisms was tested. Since the Fc-fusion peptide could bind to both murine and human PD-L1, we chose six different cell lines from both murine (B16F10, B16F1, 4T1 and CT26) and human (MDA-MB-436 and A549) setting expressing varying levels of PD-L1 (**Study**

2: figure 2 a). Cells were infected either with 10 or 100 MOI of unarmed virus or Ad-Cab and incubated for 48 hours to minimize oncolysis from the virus in human cell lines and allow adequate levels of Fc-fusion peptide to be released. Following incubation, effector populations such as complement active serum, PBMCs, PMNs and macrophages were added. IgG1 or IgA1 are not able to activate all effector mechanisms individually but in combination they can. When complement active serum was added, very minimal levels of lysis could be seen with all cell lines infected with Ad-Cab at 10 MOI (**Study 2: figure 2 b**). No lysis was seen with the unarmed virus, attributing the cell lysis to complement activation. When the MOI increased to 100, a higher cell lysis level could then be observed with all cell lines with Ad-Cab (**Study 2: figure 2 b**). This meant that the IgG portion of the Fc-fusion peptide was able to interact with complement proteins and induce CDC.

We then tested the ability of Ad-Cab to activate ADCC by PBMCs and PMNs. With both effector populations, no specific cell lysis could be observed with 10 MOI when cells were infected with either Ad-Cab or unarmed virus (**Study 2: figure 2 c**). Yet when cells were infected with 100 MOI of Ad-Cab, specific cell lysis can be noticed with both PBMCs and PMNs (**Study 2: figure 2 d**). This then indicated that Ad-Cab was able to activate both effector populations which neither IgG1 nor IgA1 antibodies can do individually. The mechanisms in which PBMCs exert ADCC has been extensively characterized by the release of granzymes and perforins. Nevertheless, the mechanism PMNs induce ADCC has not been very well understood. We hypothesize that PMNs can induce ADCC by inducing trogocytosis. This mechanism includes the disruption and endocytosis of the plasma membrane which induces a necrotic type of cell death²²⁷. To explore this, we labelled cells with a lipid dye, DiO, and measured the uptake of DiO from added PMNs. When PMNs were added on their own (**Study 2: figure 3 a**) or exposed to DiO-labelled cells (**Study 2: figure 3 b**), no uptake of DiO was seen, indicating that no transfer of membrane took place. However, when cells were infected with Ad-Cab and incubated for 48 hours a clear uptake of DiO in PMNs was observed (**Study 2: figure 3 c**). This was not seen when cells were infected with unarmed virus which attributes to the transfer of DiO to the released Fc-fusion peptide. This was tested with all six cell lines previously used (**Study 2: figure 3 d**). This data indicates a transfer of DiO inferring the possibility of trogocytosis occurring but does not necessarily assure of the process occurring. The uptake of DiO could have been due to the release of exosomes or pieces of

membrane after apoptosis picked up by the PMNs. Live imaging should be performed to further test this out.

Finally, we tested the ability of macrophages to elicit ADCP with Ad-Cab, by labelling infected cells with CFSE (**Study 2: figure 2 e**). If macrophages elicited ADCP then a transfer in CFSE should be observed. When cells were infected at 100 MOI with Ad-Cab a clear transfer in CFSE was noted and this was not seen with unarmed virus. Overall, the data demonstrates that Ad-Cab can induce Fc-effector mechanisms of both an IgG1 and IgA1. This is in line with other studies showing that different cross-hybrid IgGA formats can be used to elicit effector mechanisms of both antibody isotypes. Yet, what has not been tested whether in the presence of all immune components, could the IgGA activate all effector mechanism synchronously^{228,229}. If that is not possible then there is no use of the hybrid and the combination of IgG1 and IgA antibodies should be used.

6.2.3 Activation of multiple effector mechanisms elicit high tumor killing

Previously, we showed that Ad-Cab can activate multiple effector populations individually. Yet, whether these effector populations could be activated synchronously and lead to higher tumor killing was then tested. Therefore, we repeated the ADCC experiments with the same six cell lines (**Study 2; figure 4 a**) but added different combinations of effector populations; PBMCs+PMNs or PMBCs+PMNs+Serum. Moreover, we also compared the degree of killing of Ad-Cab to PD-L1 antibodies with an IgG1 or IgA1 competent Fc with the six previously tested cell lines. Atezolizumab was also used as a negative control since it contains an N298A mutation removing Fc-effector mechanisms. Firstly, we compared the degree of oncolysis of the viruses and antibodies when each component was added individually. Coinciding with our previous results, Ad-Cab was able to elicit cell lysis with all components and to a similar degree as the IgG1 and IgA antibodies (**Study 2; supplementary figure 3 a-d**). As expected, IgG1 antibodies were only able to induce cell lysis when serum or PBMCs were added. As for IgA, cell lysis was observed only with PMNs and not with either PBMCs or serum. Atezolizumab and unarmed virus were not able to elicit cell lysis. This data aligns with previous studies demonstrating that IgG1 antibodies are not able to activate PMNs²³⁰⁻²³⁵.

After testing killing when each component was added individually, PBMCs and PMNs were added together (**Study 2; figure 4 b**). In B16F10, B16F1, CT26 and A549 there was clear increase in killing with Ad-Cab compared to IgG1 or IgA. This indicates that Fc-fusion peptide was able to activate both PMNs and PBMCs at the same time. With 4T1 and MDA-MB-436 this was not noted since majority of PD-L1 expressing cells were killed. To further explore this, we treated cells with INF- γ before treatment to increase PD-L1 expression. The increase in PD-L1 expression lead Ad-Cab to induce higher tumor killing compared to IgG1 and IgA. This meant that the enhanced tumor killing observed from Ad-Cab requires a certain level of PD-L1 expressing cells. To further examine this enhancement, we then added serum to the combination of PBMCs and PMNs (**Study 2; figure 4 c**). Similar to previous results, Ad-Cab killing was further enhanced, outperforming all other treatment groups. Interestingly, IgG1 antibodies were shown to induce higher killing than IgA. This is mostly likely due to the dual activation of both PBMCs and serum which IgA antibodies lack. Moreover, this demonstrates that the activation of more than one effector mechanism induces higher tumor killing.

Other than using LDH assay to measure tumor killing, we also performed live-cell imaging and impedance-based real-time quantitative analysis (XCELLigence) to quantify Ad-Cab tumor killing. With live-cell imaging, A549 cells were treated with isolated Fc-fusion peptides or IgG1 antibodies and then PBMCs+PMNs were added (**Study 2; Supplementary figure 4 a**). Killing was measured by adding a caspase3/7 dye and measuring the phase area confluence over the space of 24 hours (**Study 2; Supplementary figure 4 b**). As shown before, Ad-Cab induced a higher level of killing compared to IgG1 further reinforcing the tumor-killing enhancement. Carefully examining the videos and pictures, it can be noted that with Ad-Cab treated cells, a large portion of dying cells seem not to be labeled with caspase 3/7. This is not seen as much with IgG1 or Atezolizumab treated cells. This could be due to the induction of trogocytosis by Ad-Cab, which does not signal caspase3/7 cleavage. We then finally tested cell killing with XCELLigence using a similar setup with five different cell lines (**Study 2; Supplementary figure a-f**). Ad-Cab was shown to have a higher level of killing and rate compared to IgG1 or Atezolizumab. In conclusion, we have demonstrated using various methods that Ad-Cab can activate multiple effector populations which enhance its tumor-killing properties.

6.2.4 In-vivo efficacy of Ad-Cab with CT26 and A549 tumor models

In-vitro testing demonstrated the augmented tumor killing of Ad-Cab which prompted us to examine this *in vivo*. Mice do not endogenously express Fc- α R rendering the testing of the IgA region in the Fc-fusion peptide futile. However, mice do express Fc- γ receptors which are able to bind to the Fc of human IgG and be activated²³⁶. Therefore, mice models can be used to test the efficacy of Ad-Cab to a certain extent. We, decided to use a CT26 model since it has been previously shown not to effectively respond to conventional PD-L1 checkpoint therapy^{237,238}. Mice bearing CT26 tumors were either treated with PBS (mock), unarmed virus (Ad-5/3 Δ 24), Ad-Cab or mPD-L1 for a total of seven treatments (**Study 2: figure 5 a**). Ad-Cab demonstrated to have the best tumor control compared to all other treatments with tumors sizes not exceeding 200mm³ (**Study 2: figure 5 b & supplementary figure 7 a**). This tumor control also translated to a better overall survival for Ad-Cab treated mice (**Study 2: figure 5 c**). After sacrificing mice, the biodistribution of the Fc-fusion peptide was tested. No Fc-fusion peptides could be found in the peripheral blood (**Study 2: figure 5 d**) of any treated mice but with Ad-Cab treated mice around 3 μ g/ml of Fc-fusion peptides can be seen in the tumor (**Study 2: figure 5 e**). This bio-distribution seems to reassure safety concerns since no leakage of the Fc-fusion peptide could be detected. The lack of a Fc-neonatal binding region in Ad-Cab could possibly explain why no Fc-fusion peptides could be found in blood due to the rapid clearance²²⁸. Surviving mice from Ad-Cab treated and mPD-L1 treated groups were then re-challenged again with CT26 along with naïve mice (**Study 2: figure 5 f**). Surprisingly, mPD-L1 treated mice had a lower tumor growth compared to naïve mice. Yet, Ad-Cab treated mice completely rejected the CT26 rechallenge. It has been previously mentioned that mice treated with PD-L1 checkpoint inhibitory therapy can induce a specific immune response against the tumor²³⁹. It is hypothesized that the oncolytic effect exerted by Ad-Cab or mPD-L1 led to the release and availability of TAA for APCs. Moreover, the enhanced tumor killing exerted from Ad-Cab could have induced a more robust memory response compared to mPD-L1 treated mice. Future studies should collect the T-cells from the treated mice and investigate if a memory response was formed.

After observing the *in-vivo* efficacy of Ad-Cab in syngenic mice models, we tested the efficacy in a semi-humanized model. We developed a PBMC humanized mouse model by injecting immunocompromised NS (NOD/SCID) mice with human PBMCs (**Study 2: figure 5 g**).

PBMC engraftment was successful since hCD45+ hCD3+ cells were shown to circulate in the peripheral blood of treated mice (**Study 2: supplementary figure 8**). During the same day of PBMC engraftment, mice were also implanted with A549 tumor cells. When tumors were palpable, mice were treated either with PBS (Mock), unarmed virus (Ad-5/3 Δ 24) or Ad-Cab for a total of two treatments. Like CT26, Ad-Cab treated mice had the lowest tumor growth compared to all other treatment groups in A549 bearing mice (**Study 2: figure 5 h**). A similar bio-distribution of the Fc-fusion peptide is seen with no release in the blood (**Study 2: figure 5 i**) but a high amount (4 μ g/ml) present in the tumor (**Study 2: figure 5 j**). We then analyzed the activation status of the human PBMCs engrafted in the mice (**Study 2: figure 5 k**). Ad-Cab treated mice had a higher upregulation of both CD107a and PD1 in the CD8+T cell compartment. CD107a upregulation denotes a degranulation marker of perforins and granzyme while as for PD1 upregulating it signifies an exhausted profile. With NK cells, a high upregulation of CD107a can also be observed in Ad-Cab treated mice. Hence, this data demonstrates the efficacy of Ad-Cab in controlling tumor growth in *xenograft* models which can be attributed to the activation of CD8+ T cells and NK cells.

As a final tumor model, 4T1 cell line was used due to its fast growing, highly metastatic and immunosuppressive model in dire need for novel treatments. With similar treatment groups and schedule to the CT26 model (**Study 2: figure 6 a**), Ad-Cab treated mice had the best tumor growth control compared to the rest of the treatment groups (**Study 2: figure 6 b**). Due to the highly immunosuppressive tumor microenvironment 4T1 models induce, we analyzed the immune infiltration in the treated mice. A high infiltration of both MDSC cells of the granulocytic and monocytic lineage can be seen in most groups (**Study 2: figure 6 c**). To our surprise, a significant reduction in both populations can be observed in Ad-Cab treated mice (**Study 2: figure 6 d & e**). A reduction in TAMs (**Study 2: figure 6 f**), CD4+ T-cells, CD8+ T-cells or DCs was not observed (**Study 2: supplementary figure 9 a**). This specific reduction in MDSCs has been observed with PD-L1 checkpoint inhibitors with competent IgG1 Fc¹⁵⁵. This might be due to the high expression of PD-L1 in MDSCs and the low expression in other immune cells²⁴⁰. Interestingly, in the Ad-Cab treated group a higher infiltration of NK cells was seen which was accompanied with a higher activation due to the upregulation of CD107a (**Study 2: figure 6 h**). Other than NK cells, CD8 +T cells were also more activated in Ad-Cab treated mice since such cells had higher levels of PD1 and CD107a (**Study 2: figure 6 i & j**). All in all, the effectiveness of Ad-Cab can clearly be seen in all three *in-vivo* models with a very

safe bio-distribution. This effectiveness can be attributed to its high degree of activation of NK and CD8+ T cells along with the downregulation of immunosuppressive MDSCs.

6.2.5 Ad-Cab does not solely require CD8+ T cells like conventional checkpoint inhibitory therapy.

Conventional PD-L1 checkpoint inhibitory therapy requires CD8+ T cells to be effective. *In-vivo* data has shown that Ad-Cab can activate NK cell cytotoxicity which prompts us to examine whether CD8+ T cells are also required. We then repeated the same experiment with the 4T1 model but before treatment a high dose of CD8+ T-cells depleting antibody was administered (**Study 2: figure 6 k**). Moreover, CD8+ T cell depletion was sustained by continuous administration of the depleting antibody. Before treatment, mice treated and untreated with the depleting antibody were sacrificed and had their CD8+ T cell compartment examined in the peripheral blood. Mice given the depleting antibody did not have circulating CD8+ T cells while the CD4+ T cells were unharmed (**Study 2: figure 6 l**). After CD8+ T cell depletion was verified, treatment began. As expected, mPD-L1 did not have a therapeutic effect since tumor growth resembled mock mice (**Study 2: figure 6 m**). Yet, Ad-Cab treated mice still were able to control tumor growth and increase the overall survival (**Study 2: figure 5 n**). Intriguingly, the activation of multiple effector populations has allowed Ad-Cab not to solely rely on a single immune population. Further experiments should still be conducted to pinpoint what crucial immune populations are required for Ad-Cab efficacy.

6.2.6 Generation and testing of patient derived organoids with Ad-Cab

As mentioned, mice are not the most appropriate model to test the efficacy of Ad-Cab due to the lack of Fc α -R expression. To test the full efficacy of Ad-Cab, we developed patient derived organoids from renal cell carcinoma (RCC) patient material. Four RCC patients (RCC1-4) undergoing nephrectomies had pieces of their tumor collected and dissociated. RCC1 was the only sample classified as chromophobe RCC while the rest were classified as clear cell RCC. Dissociated tumor cells were then grown on a 2D surface or by embedding it on a Matrigel to allow 3D growth (**Study 2: figure 7 a**). Once the patient-derived organoids, PDOs, were grown, they were dissociated and stained with commonly used RCC stains (Vimentin, CAIX and

Cytokeratin) (**Study 2: figure 7 b**). RCC2-4 were strongly positive for either stain which is consistent with clear cell RCC. However, RCC1 had focal expression or very weak expression of either stain since chromophobe RCC is usually negative for such stains. This then indicated that PDOs consisted of the appropriated tumor cells. To further test this platform, we added Ad-5 $\Delta 24$ expressing RFP on top of the Matrigel to see if viral infection was possible (**Study 2: figure 7 c**). Overnight incubation demonstrated that infection was possible to the expression of RFP in the PDOs and intensified as the incubation increased. Since the adenovirus added was oncolytic, we also analysed the viability of the PDOs by adding a live marker, calcein. Death could be observed at day 4 due to the morphology of the PDOs but also loss of calcein staining. Finally, to test whether immune infiltration was also possible we added on top of the Matrigel T cells labeled in calcein green (**Study 2: figure 7 d**). After 4 hours, T-cells were seen around the PDOs indicating that infiltration was possible.

After seeing that PDOs can be infected with adenoviruses and infiltrated with immune cells, we repeated the ADCC experiments (**Study 2: figure 7 e & f**). When PBMCs and PMNs were added individually it can be seen that Ad-Cab could activate both populations, while IgG and IgA activated PBMCs or PMNs, respectively. When both effector populations were added, Ad-Cab was shown to be more effective in killing PDOs from RCC2-4 further elaborating the advantage of activating multiple effector populations. With RCC1, no enhancement could be seen, and this can be attributed to the low expression of PD-L1. In conclusion, PDOs have further reinforced the added advantage of Ad-Cab in activating Fc-effector mechanisms of an IgG1 and IgA1.

In conclusion, the *in vitro*, *in vivo* and *ex-vivo* data of Ad-Cab indicate the possibility of clinical testing. Nevertheless, further analysis should be done with more other different types of models. For example, the use of transgenic mice expressing Fc α -R should be used to test Ad-Cab. Other than testing efficacy, safety can also be further analyzed since a high activation of neutrophils could induce long lasting inflammations potentially being toxic. Moreover, other models which should be used is the implantation of the PDOs in NS mice to test efficacy.

6.3 Study III: Controlled release of enhanced cross-hybrid IgGA Fc fusion peptide against PD-L1

In Study II, we observed that the use of a cross-hybrid IgGA Fc able to elicit Fc-effector mechanisms of an IgG1 and IgA1 leads to an increased tumor killing. The ability to increase efficacy while maintaining safety is owed to the controlled released of the Fc-fusion peptide to the tumor microenvironment. Using such advantage, we wanted to further build on such progress by increasing the IgG1 Fc-effector mechanisms by adding four well known point mutations increasing NK cell activation. The four-point mutations (H268F/S324T/S239D/I332E) added to the IgG portion of the IgGA Fc increased the affinity towards both activating receptors, Fc- γ Ia and Fc- γ IIIa²⁴¹. CD16a is the only Fc-gamma receptor found on NK cells and expressed relatively at high levels. So, we hypothesized that these mutations would increase tumor killing of the Fc-fusion peptide by increasing the activation of NK cells. Moreover, these mutations also increase the affinity towards C1q, a crucial component required to activate the complement system through the classical pathway.

Therefore, in Study III we characterized the efficacy and biodistribution of the Fc-fusion peptide against PD-L1 in study II with the point mutations in the IgG portion.

6.3.1 Cab FT induces high tumor killing at lower concentrations when PBMCs are added

In study II we developed an Fc-fusion peptide consisting of a cross-hybrid IgGA Fc connected to a PD-1 ectodomain, which we have called Cab (Cross-hybrid Antibody). Cab was shown to be very effective in killing tumor cells by activating Fc-effector mechanisms of an IgG1 and IgA1. To increase efficacy, we added four-point mutations (H268F/S324T/S239D/I332E) in the IgG portion that are well known to increase NK cell activation and called it Cab-FT. To test the enhanced efficacy of Cab FT, we performed ADCC experiments with four different murine (B16K1 and B16F10) and human (A549 and MDA-MB-436) cells and using PBMCs as effector cells (**Study 3: figure 1 a**). We treated cells with different concentrations of Cab and Cab-FT and measured lysis. At high concentrations, Cab and Cab FT induced very similar levels of lysis with all cell lines. Yet, at lower concentrations from 2.5 μ g/ml-0.3125 μ g/ml Cab-FT outperformed Cab. We repeated these experiments but adding PMNs as effector cells (**Study 3: figure 1 b**). Both Cab and Cab-FT induced tumor lysis at very similar levels with all different

concentrations. This was expected since despite PMNs expressing Fc γ -IIa, inhibitory receptors such as Fc γ -IIb and Fc γ -IIIb are overexpressed possibly limiting Fc γ -IIa activation. Interestingly when we added both PBMCs and PMNs (**Study 3: figure 1 c**), Ad-Cab FT induced higher levels of cell lysis at lower concentrations than Ad-Cab. This implied that the enhanced activation of NK cells provided from the point mutations can lead to an increased tumor killing under psychological conditions.

We then finally tested if there was an increased activation of CDC, since the point mutations did increase C1q binding (**Study 3: supplementary figure 1**). To our surprise, no increase in CDC was noted from Ad-Cab FT since the levels of lysis was like Ad-Cab. This could be explained by the fact that the Fab regions of an antibody have been implicated in the aid of activating the complement classical pathway. The Fc-fusion peptides do not possess Fab regions and could subsequently lead to poor activation of CDC, which has been seen with other Fc-fusion peptides.

6.3.2 Cab and Cab FT do not induce cell death of certain leukocyte population while blocking the PD-L1/PD1 axis

Various leukocyte populations such as DCs, monocytes and neutrophils have shown to express PD-L1. We hypothesized that even though Cab and Cab-FT would bind to these cells, no cell death would be induced. This is because the copy-number of an epitope is a key determinant for antibodies to elicit effector mechanisms. The copy number PD-L1 on such immune cells are relatively low which then possibly limits the Fc-fusion peptides from inducing cell death. To test this, we treated whole blood from three healthy volunteers with Cab and Cab-FT for 24 hours. In whole-blood, all effector populations that the Fc-fusion peptide can activate are present allowing us to analyze if any death of certain leukocyte population is possible (**Study 3: figure 2 a**). After incubation, we determined the absolute numbers of various leukocyte populations and compared them to untreated whole-blood or treated with Trastuzumab (IgG1 against Her2, used as a negative control). No difference between cell percentages (**Study 3: figure 2 b**) or absolute numbers (**Study 3: figure 2 c**) could be observed among whole-blood samples untreated or treated with Fc-fusion peptides or Trastuzumab in any of the leukocyte populations (Neutrophils, monocytes, DC, T and NK

cells). This data then indicates that the Fc-fusion peptides does not elicit cell death to certain leukocyte populations which are essential for efficacy.

Once observed that Fc-fusion peptides do not harm important leukocyte populations, we tested whether they could block the PD-L1/PD1 axis by using a MLR test (**Study 3: figure 2 d**). Both Cab and Cab-FT were shown to block the PD-L1/PD1 axis in a similar degree since the expansion index of CD8+T cells were very similar. Also, the level of inhibition also seems to be comparable to the clinically approved PD-L1 blocker, Atezolizumab. Moreover, this data further attributes the enhanced activity of Cab-FT to NK activation. An enhanced PD-L1/PD1 disruption could have caused the enhanced efficacy shown with Cab-FT compared to Cab at low concentrations when PBMCs were added. This is because T cells are present in the PBMC cultures and an enhanced blocking of PD-L1 could induce a higher tumor killing.

6.3.3 Engineering Fc-fusion peptides into oncolytic adenoviruses for controlled release and induction of Fc-effector mechanism

As mentioned previously, the systemic administration of the Fc-fusion peptides could have various off-target effects which could be detrimental to patients. To avoid such side-effects, we decided to clone Cab and Cab FT in oncolytic adenoviruses to restrict the release to the tumor microenvironment. Using the cloning method from Study I, we were able to clone the Fc-fusion peptides into Ad-5/3 Δ 24 genomes and subsequently characterized them. Viruses expressing Cab or Cab-FT were then called Ad-Cab or Ad-Cab FT, respectively. Using an MTS assay, we saw that the genetic manipulation did affect the oncolytic fitness of Ad-Cab or Ad-Cab FT (**Study 3: figure 3 a**). With human cell lines, cell death was only observed with MOIs of 10 and 100 and the level of cell death of Ad-Cab and Ad-Cab FT were like unarmed Ad-5/3 Δ 24. With murine cell lines, as expected no cell death observed was seen with any of the viruses since replication is limited in such settings. This data further assures that the cloning method, GAMER-Ad, does not affect the oncolytic/replication fitness of adenoviruses. We then tested the amount of Fc-fusion peptide released from each virus from murine and human cell lines. With human cell line, A549, around 7 μ g of Fc-fusion peptide was released with both Ad-Cab an Ad-Cab FT (**Study 3: figure 3 b**). A lower amount of Fc-fusion peptide was shown (1.3 μ g) with murine cell line, B16K1, but the levels were almost the same among

Ad-Cab and Ad-Cab FT (**Study 3: figure 3 c**). This implies that both Ad-Cab and Ad-Cab FT can infect and express the corresponding Fc-fusion peptide in human and murine cells lines and with very similar levels. This is mostly since both viruses have the same CMV promoter and poly-A tail controlling the expressing of the Fc-fusion peptide.

Since both viruses expressed similar levels of Fc-fusion peptides, we tested level of cell lysis induced from each virus at different concentrations. We used the same cell lines previously used. When either PMNs (**Study 3: supplementary figure 2 b**) or complement active serum (**Study 3: supplementary figure 2 c**) was added, the level of cell lysis among different MOIs between Ad-Cab and Ad-Cab FT were comparable. This further supported previous data that the four-point mutations in Cab FT did not increase PMN or complement activation. When PBMCs were added, a clear difference in cell lysis can be seen in which Ad-Cab FT had higher levels of cell lysis than Ad-Cab at lower MOIs (**Study 3: supplementary figure 2 a**). With human cell lines (A549 and MDA-MB-436) this enhanced activation could be seen at MOIs from 20-60 while for murine (B16K1 and B16F10) from 100-200. The difference between murine and human cell lines can be explained by the lower levels of Fc-fusion peptides being secreted in murine cells compared to human cells. This increased cell lysis was also shown when both PBMCs and PMNs were added together where Ad-Cab FT had higher cell lysis levels than Ad-Cab at low MOIs (**Study 3: figure 4**). In line with previous data, other than decreasing the amount of Fc-fusion peptide but also decreasing amount of virus can maintain the level of tumor killing with Ad-Cab FT when PBMCs are present.

6.3.4 Kinetics of tumor cell killing with Ad-Cab and Ad-Cab FT using XCELLigence

Having observed the increase killing efficacy of Ad-Cab FT, we further analyzed this by conducting a real-time killing assay using the XCELLigence system (**Study 3: figure 5**). This would allow us to get a detailed look into the kinetics of killing of Ad-Cab FT. We chose A549 and B16K1 as target cells and cells were infected with 30 or 100 MOI of Ad-Cab, Ad-Cab FT or Ad-5/3 Δ 24. Also, PBMCs and PMNs were used as effector cells and added directly after viral infection. With A549 cells, cell death was noted at 18 hours with Ad-Cab FT while no death was seen with the other conditions. After reaching 24 hours, Ad-Cab FT had reached its final level of tumor killing while no cell death was recorded for Ad-Cab. Only after 32 hours was cell death observed with Ad-Cab while for Ad-5/3 Δ 24 at 40 hours. A similar trend was also

observed with B16K1 in which Ad-Cab FT had the highest tumor death levels and occurred faster compared to other conditions. The only difference between A549 and B16K1 cells was that death was noted much later in B16K1 cells. Hence, other than reaching higher killing levels Ad-Cab FT was able to induce faster tumor killing than Ad-Cab. The faster tumor killing kinetics observed could be due to the higher affinity of Cab-FT towards Fcγ-IIa, found on NK cells. This high affinity could then result in lower amounts of the Fc-fusion peptide required for activation.

6.3.5 Lower amounts and dosages are required for Ad-Cab FT for *in vivo* efficacy.

In-vitro data showed that Ad-Cab FT could maintain high levels of tumor killing at low concentrations when PBMCs were present. We then tested whether this was also the case *in vivo*. We used B16K1 as a tumor model and injected mice with a lower dose of virus corresponding to 10^8 viral particles compared to 10^9 viral particles used in Study II. Moreover, previously mice were given 7 doses while in this case we decreased the total amount of doses to four (**Study 3: figure 6 a**). This would then allow to test the efficacy of Ad-Cab and Ad-Cab FT at low concentrations. Mice receiving Ad-Cab FT had the best tumor control compared to all other groups (**Study 3: figure 6 b**). A significant tumor control could still be seen with Ad-Cab but was significantly lower compared to Ad-Cab FT. After sacrificing the mice, the biodistribution of the Fc-fusion peptides was analyzed and no leakage to the liver (**Study 3: figure 6 e**) or serum was noticed but rather an accumulation in the tumor microenvironment was noticed (**Study 3: figure 6 f**). Similar levels of Fc-fusion peptides were present in mice treated with Ad-Cab or Ad-Cab FT. This implied that the improved tumor control of Ad-Cab FT is not caused by higher levels of Fc-fusion peptide. The enhancement could be attributed to the increased NK activation since mice treated with Ad-Cab FT had higher levels of CD107a+ NK cells compared to other groups (**Study 3: figure 6 c**). This was not seen with CD8+ T cells, since the expression of CD107a in such cells was similar among Ad-Cab, Ad-Cab FT or mPD-L1 treated mice (**Study 3: figure 7 d**). This also strengthens the attribution of NK cell activation leading to better tumor control with Ad-Cab since CD8+ T cell activation seems to be similar among treatment groups.

To further confirm such results, we repeated this experiment with a harder tumor model to treat, 4T1 (**Study 3: figure 7 g**). As expected, Ad-Cab FT treated mice had the best

tumor control among all other treatment groups (**Study 3: figure 7 h**). Moreover, Ad-Cab was also shown here to induce some tumor control but still lower than Ad-Cab FT. The level of activation of CD8+ T cells (**Study 3: supplementary figure 4 d & e**) was similar in Ad-Cab, Ad-Cab FT and mPD-L1 treated mice but NK cell activation (**Study 3: supplementary figure 4 c**) was more pronounced in Ad-Cab FT treated mice. Other than higher NK cell activation, Ad-Cab FT treated mice also had a lower infiltration of MDSCs of the granulocytic (**Study 3: figure 6 i**) and monocytic (**Study 3: figure 6 j**) lineage in the tumor microenvironment. Contrary to Study II, Ad-Cab treated mice in this case did not have this decrease in MDSCs seen with Ad-Cab FT. It might have been due to the fact a lower level of NK activation is noticed subsequently leading to lower targeting of such populations.

As a final tumor model to test the efficacy of Ad-Cab FT, we used a humanized murine model. NS mice were implanted with human A549 cells and PBMCs isolated from a healthy control (**Study 3: figure 7 a**). Before treatment, peripheral blood was collected from mice to test whether human PBMC engraftment was successful. Mice injected with human PBMCs were shown to have a hCD45+ and hCD45+ CD3+ cell population in peripheral blood compared to mice not given PBMCs (mock) (**Study 3: figure 7 b**). Mice were then administered with two doses of either PBS (Mock), Ad-5/3 Δ 24, Ad-Cab or Ad-Cab FT and tumor volumes were regularly checked. Similar to syngenic mouse models, Ad-Cab FT clearly controlled the tumor growth better than the other treatment groups with A549 (**Study 3: figure 7 c**). This enhanced tumor control was accompanied with a higher NK cell activation in Ad-Cab FT treated mice (**Study 3: figure 7 d**). Yet, both Ad-Cab and Ad-Cab FT treated mice showed a similar level of CD8+ T cell activation (**Study 3: figure 7 e & f**). Again, further strengthening the attribute of efficacy towards NK cell activation. Other than efficacy, both Ad-Cab and Ad-Cab FT mice showed an excellent safety profile since no Fc-fusion peptide could be found in the serum (**Study 3: figure 7 g**) or liver (**Study 3: figure 7 i**) but only in the tumor microenvironment (**Study 3: figure 6 h**). In conclusion, the addition of for point mutations to the Fc-fusion peptide engineered in Study II increased its efficacy at lower levels in both *in vitro* and *in vivo* settings. Ad-Cab FT is an enhanced version of Ad-Cab which could be potentially used in the clinic. This could help in reducing the dosage since Ad-Cab FT works efficiently at lower concentrations. A dose escalation study should be the first conducted to determine if this is the case in the clinic.

7. Conclusions and Future Prospects

Oncolytic viruses have been regarded as direct tools for tumor lysis due to their tumor-specific tropism. Nevertheless, the oncolytic properties of viruses are not enough for tumor clearance but rather the ability of the virus to activate the immune system. Hence, scientists have equipped oncolytic viruses with multiple immune-stimulatory molecules which have enhanced anti-tumor effects. Other than enhancing anti-tumor effects, this has also had a positive effect regarding limiting toxicities since the expression/release of the molecules is limited to the tumor. Yet, all of these molecules target PBMCs. Many studies have shown that targeting solely PBMCs does not cause full clearance since the cytotoxic effects mediated are finite.

PMNs have been a neglected cell population despite being the largest leukocyte population in blood and highly infiltrated in tumors. This has been mostly due to the use of IgG antibodies which sub-optimally activates neutrophils. This is simply because PMNs highly express CD32b and CD16b which downregulate effector functions or act as a molecular “sink”, respectively. This can be dangerous since immune cells have shown to be malleable depending on the microenvironment and stimulus provided. For example, researchers found relatively normal levels of Treg cells in the joints of rheumatoid arthritis patients compared to healthy individuals²⁴². However rather than promoting immune resolution, Tregs cells from the patients were programmed to secrete a powerful pro-inflammatory cytokine IL-17. The mechanism behind was speculated to be most probably due to the influence of the highly inflammatory microenvironment. Despite this, it could explain why the infiltration of neutrophils to the tumor is associated with a poorer prognosis since they are not adequately activated²⁴³. This then calls for appropriate molecules able to capitalize such population to be used as an effector population.

To address this, in this thesis we equipped oncolytic adenovirus with immune-stimulatory molecules able to activate PBMCs as effector cells as well as PMNs. We were able to activate PMNs by designing PD-L1 checkpoint inhibitors with a cross-hybrid Fc region containing both IgG1 and IgA1 heavy regions. We have further enhanced antibody cytotoxicity by adding IgA1 regions, since PMNs highly express the IgA Fc receptor Fc α -R. Such receptor has been shown to be one of the most powerful activators of PMNs and has shown to increase

tumor cytotoxicity from 20%, using IgG, to 90%, when using IgA to activate it. In this thesis we show that when PMNs and PBMCs are used as effector cells, exhaustion effects are minimized, and full clearance of tumors is achieved. This has been done using various *in vitro*, *in vivo* and *ex-vivo* models. Yet, *in-vivo* murine models are not able to optimally test the efficacy of the IgGA Fc due to the lack of Fc- α receptor expression. In the future, transgenic mice expressing Fc- α receptors should be used to thoroughly investigate the IgGA Fc. Also, with these models it can also be investigated whether the IgGA Fc can re-direct immunosuppressive immune populations towards a tumor-killing phenotype. MDSC of the granulocytic lineages express a high level of Fc- α receptors and with appropriate stimulation could lead to anti-tumor properties. If this is so, the IgGA Fc region should then be used in tumors highly infiltrated with MDSCs in order to achieve efficient clinical responses.

The cross-hybrid IgGA Fc-region was tested in the context of PD-L1 checkpoint inhibitory therapy. A therapy for which almost all approved antibodies have the Fc-effector functions silenced due to safety reasons. The addition of Fc-effector mechanisms of an IgG1 and IgA1 showed to increase the efficacy and with the help of oncolytic viruses limit toxicity. In the future, this cross-hybrid IgGA could be used for any clinical therapy which targets tumors or immunosuppressive populations. For example, one of the main mechanisms of action of CTLA-4 antibodies has been shown to be the targeting of Treg cells. The IgGA Fc could in this instance increase clinical efficacy by enhancing the depletion of Treg cells. Other than just adding point mutations to increase tumor killing, one other strategy to do so is by further engineering the Fc region to contain IgE domains. The use of IgE domains in cancer has been investigated due to its ability to activate eosinophils and basophils against cancer. We have clearly shown that the simultaneous activation of multiple effector populations is optimal for tumor clearance. Therefore, the creation of another cross-hybrid Fc containing regions of an IgG, IgA and IgE can further increase tumor killing.

The path of clinical approval for cancer therapies has yielded many failures where the majority do not reach the clinics. This is no different with immunotherapies and the reasons vary. Ad-Cab and Ad-Cab FT present a strong case for clinical approval since unconventional to majority of cancer immunotherapies, it capitalizes on multiple immune effector mechanisms. This could prevent exhaustion of immune cells which has been attributed to a

reduction in clinical efficacy. Moreover, the safety profile seems to be outstanding since the expression and secretion of the potent Fc-fusion peptides is restricted to the tumor. What would be interesting is to test with what type of tumor could Ad-Cab or Ad-Cab FT be successful in treating clinically. Based on the data, it should be tumors with a high expression of PD-L1 and possibly high PMN and PBMC infiltration. With the further experiments, discussed above, Ad-Cab and Ad-Cab FT should undergo clinical testing.

1. Siegel, R.L., Miller, K.D., and Jemal, A. (2020). Cancer statistics, 2020. *CA Cancer J Clin* *70*, 7–30. 10.3322/CAAC.21590.
2. Heron, M. (2019). National Vital Statistics Reports Volume 68, Number 6, June 24, 2019, Deaths: Leading Causes for 2017.
3. for Business, D., and Strategy, I. (2020). Public attitudes to science 2019.
4. Hanahan, D., and Weinberg, R.A. (2000). The hallmarks of cancer. *Cell* *100*, 57–70. 10.1016/S0092-8674(00)81683-9.
5. Harrington, S.E., and Smith, T.J. (2008). The Role of Chemotherapy at the End of Life: “When Is Enough, Enough?” *JAMA : the journal of the American Medical Association* *299*, 2667. 10.1001/JAMA.299.22.2667.
6. Baudino, T. (2015). Targeted Cancer Therapy: The Next Generation of Cancer Treatment. *Curr Drug Discov Technol* *12*, 3–20. 10.2174/1570163812666150602144310.
7. Meldrum, C., Doyle, M.A., and Tothill, R.W. (2011). Next-Generation Sequencing for Cancer Diagnostics: a Practical Perspective. *Clin Biochem Rev* *32*, 177.
8. Hanahan, D., and Weinberg, R.A. (2011). Hallmarks of cancer: the next generation. *Cell* *144*, 646–674. 10.1016/J.CELL.2011.02.013.
9. Couzin-Frankel, J. (2013). Breakthrough of the year 2013. Cancer immunotherapy. *Science* *342*, 1432–1433. 10.1126/SCIENCE.342.6165.1432.
10. Sharma, P., Hu-Lieskovan, S., Wargo, J.A., and Ribas, A. (2017). Primary, Adaptive, and Acquired Resistance to Cancer Immunotherapy. *Cell* *168*, 707–723. 10.1016/J.CELL.2017.01.017.
11. Hanahan, D., and Weinberg, R.A. (2011). Hallmarks of cancer: the next generation. *Cell* *144*, 646–674. 10.1016/j.cell.2011.02.013.
12. Vajdic, C.M., and van Leeuwen, M.T. (2009). Cancer incidence and risk factors after solid organ transplantation. *Int J Cancer* *125*, 1747–1754. 10.1002/ijc.24439.

13. Smyth, M.J., Thia, K.Y., Street, S.E., MacGregor, D., Godfrey, D.I., and Trapani, J.A. (2000). Perforin-mediated cytotoxicity is critical for surveillance of spontaneous lymphoma. *J Exp Med* *192*, 755–760. 10.1084/JEM.192.5.755.
14. Vinay, D.S., Ryan, E.P., Pawelec, G., Talib, W.H., Stagg, J., Elkord, E., Lichtor, T., Decker, W.K., Whelan, R.L., Kumara, H.M.C.S., et al. (2015). Immune evasion in cancer: Mechanistic basis and therapeutic strategies. *Semin Cancer Biol* *35*, S185–S198. 10.1016/j.semcancer.2015.03.004.
15. Dunn, G.P., Old, L.J., and Schreiber, R.D. (2004). The three Es of cancer immunoediting. *Annu Rev Immunol* *22*, 329–360. 10.1146/ANNUREV.IMMUNOL.22.012703.104803.
16. Kim, R., Emi, M., and Tanabe, K. (2007). Cancer immunoediting from immune surveillance to immune escape. *Immunology* *121*, 1. 10.1111/J.1365-2567.2007.02587.X.
17. Dunn, G.P., Koebel, C.M., and Schreiber, R.D. (2006). Interferons, immunity and cancer immunoediting. *Nature Reviews Immunology* *2006* *6*:11 *6*, 836–848. 10.1038/nri1961.
18. Swann, J.B., and Smyth, M.J. (2007). Immune surveillance of tumors. *Journal of Clinical Investigation* *117*, 1137. 10.1172/JCI31405.
19. Seliger, B. (2005). Strategies of tumor immune evasion. *BioDrugs* *19*, 347–354. 10.2165/00063030-200519060-00002/FIGURES/TAB2.
20. Lehmann, C., Zeis, M., and Uharek, L. (2001). Activation of natural killer cells with interleukin 2 (IL-2) and IL-12 increases perforin binding and subsequent lysis of tumour cells. *Br J Haematol* *114*, 660–665. 10.1046/J.1365-2141.2001.02995.X.
21. Smith, K.A. (1988). Interleukin-2: inception, impact, and implications. *Science* *240*, 1169–1176. 10.1126/SCIENCE.3131876.
22. Gillis, S., Baker, P.E., Ruscetti, F.W., and Smith, K.A. (1978). Long-term culture of human antigen-specific cytotoxic T-cell lines. *J Exp Med* *148*, 1093. 10.1084/JEM.148.4.1093.
23. Gillis, S., and Smith, K.A. (1977). Long term culture of tumour-specific cytotoxic T cells. *Nature* *268*, 154–156. 10.1038/268154A0.
24. Paliard, X., de Waal Malefijt, R., Yssel, H., Blanchard, D., Chrétien, I., Abrams, J., de Vries, J., and Spits, H. (1988). Simultaneous production of IL-2, IL-4, and IFN-gamma by activated human CD4⁺ and CD8⁺ T cell clones. *The Journal of Immunology* *141*.

25. Fyfe, G., Fisher, R.I., Rosenberg, S.A., Sznol, M., Parkinson, D.R., and Louie, A.C. (1995). Results of treatment of 255 patients with metastatic renal cell carcinoma who received high-dose recombinant interleukin-2 therapy. *J Clin Oncol* *13*, 688–696. 10.1200/JCO.1995.13.3.688.
26. Amaria, R.N., Reuben, A., Cooper, Z.A., and Wargo, J.A. (2015). Update on use of aldesleukin for treatment of high-risk metastatic melanoma. *Immunotargets Ther* *4*, 79. 10.2147/ITT.S61590.
27. Davar, D., Ding, F., Saul, M., Sander, C., Tarhini, A.A., Kirkwood, J.M., and Tawbi, H.A. (2017). High-dose interleukin-2 (HD IL-2) for advanced melanoma: A single center experience from the University of Pittsburgh Cancer Institute. *J Immunother Cancer* *5*, 1–10. 10.1186/S40425-017-0279-5/FIGURES/3.
28. Achkar, T., Arjunan, A., Wang, H., Saul, M., Davar, D., Appleman, L.J., Friedland, D., and Parikh, R.A. (2017). High-dose interleukin 2 in patients with metastatic renal cell carcinoma with sarcomatoid features. *PLoS One* *12*. 10.1371/JOURNAL.PONE.0190084.
29. Pachella, RN, MSN, AGPCNP-BC, AOCNP®, L.A., adsen, PhD, RN, AOCNS®, L.T., and Dains, DrPH, JD, RN, FNP-CB, DPNAP, J.E. (2015). The Toxicity and Benefit of Various Dosing Strategies for Interleukin-2 in Metastatic Melanoma and Renal Cell Carcinoma. *J Adv Pract Oncol* *6*, 212. 10.6004/jadpro.2015.6.3.3.
30. Stanley, E., Lieschke, G.J., Grail, D., Metcalf, D., Hodgson, G., Gall, J.A.M., Maker, D.W., Cebon, J., Sinickas, V., and Dunn, A.R. (1994). Granulocyte/macrophage colony-stimulating factor-deficient mice show no major perturbation of hematopoiesis but develop a characteristic pulmonary pathology. *Proc Natl Acad Sci U S A* *91*, 5592. 10.1073/PNAS.91.12.5592.
31. Kurbacher, C., Kurbacher, J., Cramer, E., Rhiem, K., Mallman, P., Reichelt, R., Reinhold, U., Stier, U., and Cree, I. (2005). Continuous low-dose GM-CSF as salvage therapy in refractory recurrent breast or female genital tract carcinoma. *undefined*.
32. Strati, P., Ferrajoli, A., Lerner, S., O'Brien, S., Wierda, W., Keating, M.J., and Faderl, S. (2014). Fludarabine, cyclophosphamide and rituximab plus granulocyte macrophage colony-stimulating factor as frontline treatment for patients with chronic lymphocytic leukemia. *Leuk Lymphoma* *55*, 828–833. 10.3109/10428194.2013.819574.
33. Cortes, J., Quintás-Cardama, A., Jones, D., Ravandi, F., Garcia-Manero, G., Verstovsek, S., Koller, C., Hiteshew, J., Shan, J., O'Brien, S., et al. (2011). Immune

- modulation of minimal residual disease in early chronic phase chronic myelogenous leukemia. *Cancer* 117, 572–580. 10.1002/cncr.25438.
34. Perica, K., Varela, J.C., Oelke, M., and Schneck, J. (2015). Adoptive T Cell Immunotherapy for Cancer. *Rambam Maimonides Med J* 6, e0004. 10.5041/RMMJ.10179.
 35. Rosenberg, S.A., Restifo, N.P., Yang, J.C., Morgan, R.A., and Dudley, M.E. (2008). Adoptive cell transfer: a clinical path to effective cancer immunotherapy. *Nat Rev Cancer* 8, 299. 10.1038/NRC2355.
 36. Proietti, E., Greco, G., Garrone, B., Baccarini, S., Mauri, C., Venditti, M., Carlei, D., and Belardelli, F. (1998). Importance of cyclophosphamide-induced bystander effect on T cells for a successful tumor eradication in response to adoptive immunotherapy in mice. *J Clin Invest* 101, 429–441. 10.1172/JCI1348.
 37. Rosenberg, S.A., Yannelli, J.R., Yang, J.C., Topalian, S.L., Schwartzentruber, D.J., Weber, J.S., Parkinson, D.R., Seipp, C.A., Einhorn, J.H., and White, D.E. (1994). Treatment of patients with metastatic melanoma with autologous tumor-infiltrating lymphocytes and interleukin 2. *J Natl Cancer Inst* 86, 1159–1166. 10.1093/JNCI/86.15.1159.
 38. Rosenberg, S.A., and Restifo, N.P. (2015). Adoptive cell transfer as personalized immunotherapy for human cancer. *Science* 348, 62–68. 10.1126/SCIENCE.AAA4967.
 39. Harris, D.T., and Kranz, D.M. (2016). Adoptive T Cell Therapies: A Comparison of T Cell Receptors and Chimeric Antigen Receptors. *Trends Pharmacol Sci* 37, 220–230. 10.1016/J.TIPS.2015.11.004.
 40. June, C.H., O'Connor, R.S., Kawalekar, O.U., Ghassemi, S., and Milone, M.C. (2018). CAR T cell immunotherapy for human cancer. *Science* 359, 1361–1365. 10.1126/SCIENCE.AAR6711.
 41. Blankenstein, T., Coulie, P.G., Gilboa, E., and Jaffee, E.M. (2012). The determinants of tumour immunogenicity. *Nat Rev Cancer* 12, 307. 10.1038/NRC3246.
 42. Restifo, N.P., Dudley, M.E., and Rosenberg, S.A. (2012). Adoptive immunotherapy for cancer: harnessing the T cell response. *Nat Rev Immunol* 12, 269. 10.1038/NRI3191.
 43. Behring, E. von (2013). Ueber das Zustandekommen der Diphtherie-Immunität und der Tetanus-Immunität bei Thieren.
 44. Fagraeus, A. (1947). Plasma cellular reaction and its relation to the formation of antibodies in vitro. *Nature* 159, 499. 10.1038/159499A0.

45. Van Epps, H.L. (2005). How Heidelberger and Avery sweetened immunology. *J Exp Med* 202, 1306. 10.1084/JEM20210FTA.
46. Nossal, G.J.V., and Lederberg, J. (1958). Antibody production by single cells. *Nature* 181, 1419–1420. 10.1038/1811419A0.
47. Schwaber, J., and Cohen, E.P. (1973). Human x mouse somatic cell hybrid clone secreting immunoglobulins of both parental types. *Nature* 244, 444–447. 10.1038/244444A0.
48. Köhler, G., and Milstein, C. (1975). Continuous cultures of fused cells secreting antibody of predefined specificity. *Nature* 256, 495–497. 10.1038/256495A0.
49. Nadler, L.M., Stashenko, P., Hardy, R., Kaplan, W.D., Button, L.N., Kufe, D.W., Antman, K.H., and Schlossman, S.F. (1980). Serotherapy of a Patient with a Monoclonal Antibody Directed against a Human Lymphoma-associated Antigen. *Cancer Res* 40.
50. Koprowski, H., Steplewski, Z., Herlyn, D., and Herlyn, M. (1978). Study of antibodies against human melanoma produced by somatic cell hybrids. *Proc Natl Acad Sci U S A* 75, 3405–3409. 10.1073/PNAS.75.7.3405.
51. Nelson, A.L., Dhimolea, E., and Reichert, J.M. (2010). Development trends for human monoclonal antibody therapeutics. *Nat Rev Drug Discov* 9, 767–774. 10.1038/NRD3229.
52. Riechmann, L., Clark, M., Waldmann, H., and Winter, G. (1988). Reshaping human antibodies for therapy. *Nature* 332, 323–327. 10.1038/332323A0.
53. Hershberg, U., and Luning Prak, E.T. (2015). The analysis of clonal expansions in normal and autoimmune B cell repertoires. *Philosophical Transactions of the Royal Society B: Biological Sciences* 370. 10.1098/RSTB.2014.0239.
54. Cowley, G.P., Smith, J.A., and Gusterson, B.A. (1986). Increased EGF receptors on human squamous carcinoma cell lines. *Br J Cancer* 53, 223–229. 10.1038/BJC.1986.39.
55. Gusterson, B., Cowley, G., Smith, J.A., and Ozanne, B. (1984). Cellular localisation of human epidermal growth factor receptor. *Cell Biol Int Rep* 8, 649–658. 10.1016/0309-1651(84)90045-6.
56. Downward, J., Yarden, Y., Mayes, E., Scrace, G., Totty, N., Stockwell, P., Ullrich, A., Schlessinger, J., and Waterfield, M.D. (1984). Close similarity of epidermal growth factor receptor and v-erb-B oncogene protein sequences. *Nature* 307, 521–527. 10.1038/307521A0.

57. Ullrich, A., Coussens, L., Hayflick, J.S., Dull, T.J., Gray, A., Tam, A.W., Lee, J., Yarden, Y., Libermann, T.A., Schlessinger, J., et al. (1984). Human epidermal growth factor receptor cDNA sequence and aberrant expression of the amplified gene in A431 epidermoid carcinoma cells. *Nature* 309, 418–425. 10.1038/309418A0.
58. Patel, D., Bassi, R., Hooper, A., Prewett, M., Hicklin, D.J., and Kang, X. (2009). Anti-epidermal growth factor receptor monoclonal antibody cetuximab inhibits EGFR/HER-2 heterodimerization and activation. *Int J Oncol* 34, 25–32. 10.3892/IJO_00000125/HTML.
59. Li, S., Schmitz, K.R., Jeffrey, P.D., Wiltzius, J.J.W., Kussie, P., and Ferguson, K.M. (2005). Structural basis for inhibition of the epidermal growth factor receptor by cetuximab. *Cancer Cell* 7, 301–311. 10.1016/J.CCR.2005.03.003.
60. Slamon, D.J., Godolphin, W., Jones, L.A., Holt, J.A., Wong, S.G., Keith, D.E., Levin, W.J., Stuart, S.G., Udove, J., Ullrich, A., et al. (1989). Studies of the HER-2/neu proto-oncogene in human breast and ovarian cancer. *Science* 244, 707–712. 10.1126/SCIENCE.2470152.
61. Chen, J.S., Lan, K., and Hung, M.C. (2003). Strategies to target HER2/neu overexpression for cancer therapy. *Drug Resist Updat* 6, 129–136. 10.1016/S1368-7646(03)00040-2.
62. Plosker, G.L., and Keam, S.J. (2006). Trastuzumab: a review of its use in the management of HER2-positive metastatic and early-stage breast cancer. *Drugs* 66, 449–475. 10.2165/00003495-200666040-00005.
63. Taylor, R.P., and Lindorfer, M.A. (2016). Cytotoxic mechanisms of immunotherapy: Harnessing complement in the action of anti-tumor monoclonal antibodies. *Semin Immunol* 28, 309–316. 10.1016/J.SMIM.2016.03.003.
64. Melis, J.P.M., Strumane, K., Ruuls, S.R., Beurskens, F.J., Schuurman, J., and Parren, P.W.H.I. (2015). Complement in therapy and disease: Regulating the complement system with antibody-based therapeutics. *Mol Immunol* 67, 117–130. 10.1016/J.MOLIMM.2015.01.028.
65. Wang, G., de Jong, R.N., van den Bremer, E.T.J., Beurskens, F.J., Labrijn, A.F., Ugurlar, D., Gros, P., Schuurman, J., Parren, P.W.H.I., and Heck, A.J.R. (2016). Molecular Basis of Assembly and Activation of Complement Component C1 in Complex with Immunoglobulin G1 and Antigen. *Mol Cell* 63, 135–145. 10.1016/J.MOLCEL.2016.05.016.

66. Diebold, C.A., Beurskens, F.J., De Jong, R.N., Koning, R.I., Strumane, K., Lindorfer, M.A., Voorhorst, M., Ugurlar, D., Rosati, S., Heck, A.J.R., et al. (2014). Complement is activated by IgG hexamers assembled at the cell surface. *Science* (1979) *343*, 1260–1263. 10.1126/SCIENCE.1248943/SUPPL_FILE/DIEBOLDER.SM.PDF.
67. Evers, M., Kruse, E., Hamdan, F., Lebbink, R.-J., and Leusen, J.H.W. (2018). Comment on “Type I CD20 Antibodies Recruit the B Cell Receptor for Complement-Dependent Lysis of Malignant B Cells.” *The Journal of Immunology* *200*, 2515–2516. 10.4049/JIMMUNOL.1800087.
68. Evers, M., Ten Broeke, T., Jansen, J.H.M., Nederend, M., Hamdan, F., Reiding, K.R., Meyer, S., Moerer, P., Brinkman, I., Rösner, T., et al. (2020). Novel chimerized IgA CD20 antibodies: Improving neutrophil activation against CD20-positive malignancies. *MAbs* *12*. 10.1080/19420862.2020.1795505.
69. Di Gaetano, N., Cittera, E., Nota, R., Vecchi, A., Grieco, V., Scanziani, E., Botto, M., Introna, M., and Golay, J. (2003). Complement activation determines the therapeutic activity of rituximab in vivo. *J Immunol* *171*, 1581–1587. 10.4049/JIMMUNOL.171.3.1581.
70. Coiffier, B., Lefebvre, S., Pedersen, L.M., Gadeberg, O., Fredriksen, H., Van Oers, M.H.J., Wooldridge, J., Kloczko, J., Holowiecki, J., Hellmann, A., et al. (2008). Safety and efficacy of ofatumumab, a fully human monoclonal anti-CD20 antibody, in patients with relapsed or refractory B-cell chronic lymphocytic leukemia: a phase 1-2 study. *Blood* *111*, 1094–1100. 10.1182/BLOOD-2007-09-111781.
71. Zhang, B. (2009). Ofatumumab. *MAbs* *1*, 326. 10.4161/MABS.1.4.8895.
72. Coiffier, B., Lefebvre, S., Pedersen, L.M., Gadeberg, O., Fredriksen, H., Van Oers, M.H.J., Wooldridge, J., Kloczko, J., Holowiecki, J., Hellmann, A., et al. (2008). Safety and efficacy of ofatumumab, a fully human monoclonal anti-CD20 antibody, in patients with relapsed or refractory B-cell chronic lymphocytic leukemia: a phase 1-2 study. *Blood* *111*, 1094–1100. 10.1182/BLOOD-2007-09-111781.
73. Nimmerjahn, F., Gordan, S., and Lux, A. (2015). FcγR dependent mechanisms of cytotoxic, agonistic, and neutralizing antibody activities. *Trends Immunol* *36*, 325–336. 10.1016/J.IT.2015.04.005.
74. Hubert, P., Heitzmann, A., Viel, S., Nicolas, A., Sastre-Garau, X., Oppezio, P., Pritsch, O., Osinaga, E., and Amigorena, S. (2011). Antibody-Dependent Cell

- Cytotoxicity Synapses Form in Mice during Tumor-Specific Antibody Immunotherapy. *Cancer Res* 71, 5134–5143. 10.1158/0008-5472.CAN-10-4222.
75. Van Der Bij, G.J., Bögels, M., Otten, M.A., Oosterling, S.J., Kuppen, P.J., Meijer, S., Beelen, R.H.J., and Van Egmond, M. (2010). Experimentally induced liver metastases from colorectal cancer can be prevented by mononuclear phagocyte-mediated monoclonal antibody therapy. *J Hepatol* 53, 677–685. 10.1016/J.JHEP.2010.04.023.
76. Overdijk, M.B., Verploegen, S., Bögels, M., Van Egmond, M., Lammerts Van Bueren, J.J., Mutis, T., Groen, R.W.J., Breij, E., Martens, A.C.M., Bleeker, W.K., et al. (2015). Antibody-mediated phagocytosis contributes to the anti-tumor activity of the therapeutic antibody daratumumab in lymphoma and multiple myeloma. *MAbs* 7, 311–320. 10.1080/19420862.2015.1007813.
77. Murata, Y., Tanaka, D., Hazama, D., Yanagita, T., Saito, Y., Kotani, T., Oldenborg, P.A., and Matozaki, T. (2018). Anti-human SIRP α antibody is a new tool for cancer immunotherapy. *Cancer Sci* 109, 1300. 10.1111/CAS.13548.
78. Möller, E. (1965). CONTACT-INDUCED CYTOTOXICITY BY LYMPHOID CELLS CONTAINING FOREIGN ISOANTIGENS. *Science* 147, 873–879. 10.1126/SCIENCE.147.3660.873.
79. Nimmerjahn, F., and Ravetch, J. V. (2008). Fc γ receptors as regulators of immune responses. *Nat Rev Immunol* 8, 34–47. 10.1038/NRI2206.
80. Eischen, C.M., and Leibson, P.J. (1997). Role for NK-cell-associated Fas ligand in cell-mediated cytotoxicity and apoptosis. *Res Immunol* 148, 164–169. 10.1016/S0923-2494(97)84219-8.
81. Nimmerjahn, F., and Ravetch, J. V. (2008). Analyzing antibody-Fc-receptor interactions. *Methods Mol Biol* 415, 151–162. 10.1007/978-1-59745-570-1_9.
82. De Saint Basile, G., Ménasché, G., and Fischer, A. (2010). Molecular mechanisms of biogenesis and exocytosis of cytotoxic granules. *Nat Rev Immunol* 10, 568–579. 10.1038/NRI2803.
83. Clynes, R.A., Towers, T.L., Presta, L.G., and Ravetch, J. V. (2000). Inhibitory Fc receptors modulate in vivo cytotoxicity against tumor targets. *Nat Med* 6, 443–446. 10.1038/74704.
84. De Haij, S., Jansen, J.H.M., Boross, P., Beurskens, F.J., Bakema, J.E., Bos, D.L., Martens, A., Verbeek, J.S., Parren, P.W.H.I., Van De Winkel, J.G.J., et al. (2010). In vivo cytotoxicity of type I CD20 antibodies critically depends on Fc receptor ITAM signaling. *Cancer Res* 70, 3209–3217. 10.1158/0008-5472.CAN-09-4109.

85. Wu, J., Edberg, J.C., Redecha, P.B., Bansal, V., Guyre, P.M., Coleman, K., Salmon, J.E., and Kimberly, R.P. (1997). A novel polymorphism of FcγRIIIa (CD16) alters receptor function and predisposes to autoimmune disease. *J Clin Invest* 100, 1059–1070. 10.1172/JCI119616.
86. Bibeau, F., Lopez-Crapez, E., Fiore, F. Di, Thezenas, S., Ychou, M., Blanchard, F., Lamy, A., Penault-Llorca, F., Frébourg, T., Michel, P., et al. (2009). Impact of Fc{gamma}RIIIa-Fc{gamma}RIIIa polymorphisms and KRAS mutations on the clinical outcome of patients with metastatic colorectal cancer treated with cetuximab plus irinotecan. *J Clin Oncol* 27, 1122–1129. 10.1200/JCO.2008.18.0463.
87. Hatjiharissi, E., Xu, L., Santos, D.D., Hunter, Z.R., Ciccarelli, B.T., Verselis, S., Modica, M., Cao, Y., Manning, R.J., Leleu, X., et al. (2007). Increased natural killer cell expression of CD16, augmented binding and ADCC activity to rituximab among individuals expressing the Fc{gamma}RIIIa-158 V/V and V/F polymorphism. *Blood* 110, 2561–2564. 10.1182/BLOOD-2007-01-070656.
88. Weng, W.K., and Levy, R. (2003). Two immunoglobulin G fragment C receptor polymorphisms independently predict response to rituximab in patients with follicular lymphoma. *J Clin Oncol* 21, 3940–3947. 10.1200/JCO.2003.05.013.
89. Cartron, G., Dacheux, L., Salles, G., Solal-Celigny, P., Bardos, P., Colombat, P., and Watier, H. (2002). Therapeutic activity of humanized anti-CD20 monoclonal antibody and polymorphism in IgG Fc receptor FcγRIIIa gene. *Blood* 99, 754–758. 10.1182/BLOOD.V99.3.754.
90. Rodríguez, J., Zarate, R., Bandres, E., Boni, V., Hernández, A., Sola, J.J., Honorato, B., Bitarte, N., and García-Foncillas, J. (2012). Fc gamma receptor polymorphisms as predictive markers of Cetuximab efficacy in epidermal growth factor receptor downstream-mutated metastatic colorectal cancer. *Eur J Cancer* 48, 1774–1780. 10.1016/J.EJCA.2012.01.007.
91. Boero, S., Morabito, A., Banelli, B., Cardinali, B., Dozin, B., Lunardi, G., Piccioli, P., Lastraioli, S., Carosio, R., Salvi, S., et al. (2015). Analysis of in vitro ADCC and clinical response to trastuzumab: possible relevance of FcγRIIIA/FcγRIIA gene polymorphisms and HER-2 expression levels on breast cancer cell lines. *J Transl Med* 13. 10.1186/S12967-015-0680-0.
92. Musolino, A., Naldi, N., Bortesi, B., Pezzuolo, D., Capelletti, M., Missale, G., Laccabue, D., Zerbini, A., Camisa, R., Bisagni, G., et al. (2008). Immunoglobulin G fragment C receptor polymorphisms and clinical efficacy of trastuzumab-based

- therapy in patients with HER-2/neu-positive metastatic breast cancer. *J Clin Oncol* 26, 1789–1796. 10.1200/JCO.2007.14.8957.
93. Arnould, L., Gelly, M., Penault-Llorca, F., Benoit, L., Bonnetain, F., Migeon, C., Cabaret, V., Fermeaux, V., Bertheau, P., Garnier, J., et al. (2006). Trastuzumab-based treatment of HER2-positive breast cancer: an antibody-dependent cellular cytotoxicity mechanism? *Br J Cancer* 94, 259–267. 10.1038/SJ.BJC.6602930.
 94. Wallace, P.K., Howell, A.L., and Fanger, M.W. (1994). Role of Fc gamma receptors in cancer and infectious disease. *J Leukoc Biol* 55, 816–826. 10.1002/JLB.55.6.816.
 95. Wang, W., Erbe, A.K., Hank, J.A., Morris, Z.S., and Sondel, P.M. (2015). NK Cell-Mediated Antibody-Dependent Cellular Cytotoxicity in Cancer Immunotherapy. *Front Immunol* 6, 1. 10.3389/FIMMU.2015.00368.
 96. Selvaraj, P., Rosse, W.F., Silber, R., and Springer, T.A. (1988). The major Fc receptor in blood has a phosphatidylinositol anchor and is deficient in paroxysmal nocturnal haemoglobinuria. *Nature* 333, 565–567. 10.1038/333565A0.
 97. van der Kolk, L.E., de Haas, M., Grillo-López, A.J., Baars, J.W., and van Oers, M.H.J. (2002). Analysis of CD20-dependent cellular cytotoxicity by G-CSF-stimulated neutrophils. *Leukemia* 16, 693–699. 10.1038/SJ.LEU.2402424.
 98. Peipp, M., Van Bueren, J.J.L., Schneider-Merck, T., Bleeker, W.W.K., Dechant, M., Beyer, T., Repp, R., Van Berkel, P.H.C., Vink, T., Van De Winkel, J.G.J., et al. (2008). Antibody fucosylation differentially impacts cytotoxicity mediated by NK and PMN effector cells. *Blood* 112, 2390–2399. 10.1182/BLOOD-2008-03-144600.
 99. Gill, S., Vasey, A.E., De Souza, A., Baker, J., Smith, A.T., Kohrt, H.E., Florek, M., Gibbs, K.D., Tate, K., Ritchie, D.S., et al. (2012). Rapid development of exhaustion and down-regulation of eomesodermin limit the antitumor activity of adoptively transferred murine natural killer cells. *Blood* 119, 5758–5768. 10.1182/BLOOD-2012-03-415364.
 100. Pakkanen, S.H., Kantele, J.M., Moldoveanu, Z., Hedges, S., Hakkinen, M., Mestecky, J., and Kantele, A. (2010). Expression of Homing Receptors on IgA1 and IgA2 Plasmablasts in Blood Reflects Differential Distribution of IgA1 and IgA2 in Various Body Fluids. *Clinical and Vaccine Immunology* 17, 393–401. 10.1128/CVI.00475-09.
 101. Valerius, T., Stockmeyer, B., van Spruiel, A.B., Graziano, R.F., van den Herik-Oudijk, I.E., Repp, R., Deo, Y.M., Lund, J., Kalden, J.R., Gramatzki, M., et al. (1997). FcαRI (CD89) as a Novel Trigger Molecule for Bispecific Antibody Therapy. *Blood* 90.

102. Dechant, M., Vidarsson, G., Stockmeyer, B., Repp, R., Glennie, M.J., Gramatzki, M., van De Winkel, J.G.J., and Valerius, T. (2002). Chimeric IgA antibodies against HLA class II effectively trigger lymphoma cell killing. *Blood* *100*, 4574–4580. 10.1182/blood-2002-03-0687.
103. Boross, P., Lohse, S., Nederend, M., Jansen, J.H.M., van Tetering, G., Dechant, M., Peipp, M., Royle, L., Liew, L.P., Boon, L., et al. (2013). IgAEGFR antibodies mediate tumour killing *in vivo*. *EMBO Mol Med* *5*, 1213–1226. 10.1002/emmm.201201929.
104. Huls, G., Heijnen, I.A.F.M., Cuomo, E., Van Der Linden, J., Boel, E., Van De Winkel, J.G.J., and Logtenberg, T. (1999). Antitumor Immune Effector Mechanisms Recruited by Phage Display-derived Fully Human IgG1 and IgA1 Monoclonal Antibodies 1. *Cancer Res* *59*, 5778–5784.
105. Leusen, J.H.W. (2015). IgA as therapeutic antibody. *Mol Immunol* *68*, 35–39. 10.1016/j.molimm.2015.09.005.
106. Lohse, S., Derer, S., Beyer, T., Klausz, K., Peipp, M., Leusen, J.H.W., van de Winkel, J.G.J., Dechant, M., and Valerius, T. (2011). Recombinant Dimeric IgA Antibodies against the Epidermal Growth Factor Receptor Mediate Effective Tumor Cell Killing. *The Journal of Immunology* *186*, 3770–3778. 10.4049/jimmunol.1003082.
107. Lohse, S., Brunke, C., Derer, S., Peipp, M., Boross, P., Kellner, C., Beyer, T., Dechant, M., van der Winkel, J.G.J., Leusen, J.H.W., et al. (2012). Characterization of a mutated IgA2 antibody of the m(1) allotype against the epidermal growth factor receptor for the recruitment of monocytes and macrophages. *J Biol Chem* *287*, 25139–25150. 10.1074/jbc.M112.353060.
108. Bakema, J.E., and van Egmond, M. Immunoglobulin A: A next generation of therapeutic antibodies? *MAbs* *3*, 352–361.
109. Pascal, V., Laffleur, B., Debin, A., Cuvillier, A., van Egmond, M., Drocourt, D., Imbertie, L., Pangault, C., Tarte, K., Tiraby, G., et al. (2012). Anti-CD20 IgA can protect mice against lymphoma development: evaluation of the direct impact of IgA and cytotoxic effector recruitment on CD20 target cells. *Haematologica* *97*, 1686–1694. 10.3324/haematol.2011.061408.
110. Engelberts, P.J., Voorhorst, M., Schuurman, J., van Meerten, T., Bakker, J.M., Vink, T., Mackus, W.J.M., Breij, E.C.W., Derer, S., Valerius, T., et al. (2016). Type I CD20 Antibodies Recruit the B Cell Receptor for Complement-Dependent Lysis of Malignant B Cells. *The Journal of Immunology* *197*, 4829–4837. 10.4049/jimmunol.1600811.

111. Brandsma, A.M., Broeke, T. Ten, Nederend, M., Meulenbroek, L.A.P.M., Van Tetering, G., Meyer, S., Jansen, J.H.M., Buitrago, M.A.B., Nagelkerke, S.Q., Németh, I., et al. (2015). Simultaneous targeting of FcγRs and FcαRI enhances tumor cell killing. *Cancer Immunol Res* 3, 1316–1324. 10.1158/2326-6066.CIR-15-0099-T.
112. Heemskerk, N., Gruijs, M., Robin Temming, A., Heineke, M.H., Gout, D.Y., Hellingman, T., Tuk, C.W., Winter, P.J., Lissenberg-Thunnissen, S., Bentlage, A.E.H., et al. (2021). Augmented antibody-based anticancer therapeutics boost neutrophil cytotoxicity. *J Clin Invest* 131. 10.1172/JCI134680.
113. Strohl, W.R., and Knight, D.M. (2009). Discovery and development of biopharmaceuticals: current issues. *Curr Opin Biotechnol* 20, 668–672. 10.1016/J.COPBIO.2009.10.012.
114. Strohl, W.R. (2009). Optimization of Fc-mediated effector functions of monoclonal antibodies. *Curr Opin Biotechnol* 20, 685–691. 10.1016/J.COPBIO.2009.10.011.
115. Nelson, A.L., and Reichert, J.M. (2009). Development trends for therapeutic antibody fragments. *Nat Biotechnol* 27, 331–337. 10.1038/NBT0409-331.
116. Beck, A., and Reichert, J.M. (2011). Therapeutic Fc-fusion proteins and peptides as successful alternatives to antibodies. *MAbs* 3, 415–416. 10.4161/MABS.3.5.17334.
117. Suzuki, T., Ishii-Watabe, A., Tada, M., Kobayashi, T., Kanayasu-Toyoda, T., Kawanishi, T., and Yamaguchi, T. (2010). Importance of Neonatal FcR in Regulating the Serum Half-Life of Therapeutic Proteins Containing the Fc Domain of Human IgG1: A Comparative Study of the Affinity of Monoclonal Antibodies and Fc-Fusion Proteins to Human Neonatal FcR. *The Journal of Immunology* 184, 1968–1976. 10.4049/JIMMUNOL.0903296.
118. Sioud, M., Westby, P., Olsen, J.K.E., and Mobergslien, A. (2015). Generation of new peptide-Fc fusion proteins that mediate antibody-dependent cellular cytotoxicity against different types of cancer cells. *Mol Ther Methods Clin Dev* 2, 15043. 10.1038/MTM.2015.43.
119. Masteller, E.L., Chuang, E., Mullen, A.C., Reiner, S.L., and Thompson, C.B. (2000). Structural analysis of CTLA-4 function in vivo. *J Immunol* 164, 5319–5327.
120. Parry, R. V., Chemnitz, J.M., Frauwirth, K.A., Lanfranco, A.R., Braunstein, I., Kobayashi, S. V., Linsley, P.S., Thompson, C.B., and Riley, J.L. (2005). CTLA-4 and PD-1 Receptors Inhibit T-Cell Activation by Distinct Mechanisms. *Mol Cell Biol* 25, 9543–9553. 10.1128/MCB.25.21.9543-9553.2005.

121. Schneider, H., Downey, J., Smith, A., Zinselmeyer, B.H., Rush, C., Brewer, J.M., Wei, B., Hogg, N., Garside, P., and Rudd, C.E. (2006). Reversal of the TCR Stop Signal by CTLA-4. *Science* (1979) *313*, 1972–1975. 10.1126/science.1131078.
122. Sansom, D.M. (2000). CD28, CTLA-4 and their ligands: who does what and to whom? *Immunology* *101*, 169–177. 10.1046/J.1365-2567.2000.00121.X.
123. Krummel, M.F., and Allison, J.P. (1996). CTLA-4 engagement inhibits IL-2 accumulation and cell cycle progression upon activation of resting T cells. *J Exp Med* *183*, 2533–2540.
124. Linsley, P.S., Bradshaw, J., Greene, J., Peach, R., Bennett, K.L., and Mittler, R.S. (1996). Intracellular trafficking of CTLA-4 and focal localization towards sites of TCR engagement. *Immunity* *4*, 535–543.
125. Walunas, T.L., Bluestone, J.A., Griffin, M.D., Sharpe, A.H., and Bluestone, J.A. (1998). CTLA-4 regulates tolerance induction and T cell differentiation in vivo. *J Immunol* *160*, 3855–3860.
126. Takahashi, T., Tagami, T., Yamazaki, S., Uede, T., Shimizu, J., Sakaguchi, N., Mak, T.W., and Sakaguchi, S. (2000). Immunologic self-tolerance maintained by CD25(+)CD4(+) regulatory T cells constitutively expressing cytotoxic T lymphocyte-associated antigen 4. *J Exp Med* *192*, 303–310.
127. Leach, D.R., Krummel, M.F., and Allison, J.P. (1996). Enhancement of antitumor immunity by CTLA-4 blockade. *Science* *271*, 1734–1736.
128. van Elsas, A., Hurwitz, A.A., and Allison, J.P. (1999). Combination immunotherapy of B16 melanoma using anti-cytotoxic T lymphocyte-associated antigen 4 (CTLA-4) and granulocyte/macrophage colony-stimulating factor (GM-CSF)-producing vaccines induces rejection of subcutaneous and metastatic tumors accompanied by autoimmune depigmentation. *J Exp Med* *190*, 355–366.
129. Ribas, A., Camacho, L.H., Lopez-Berestein, G., Pavlov, D., Bulanhagui, C.A., Millham, R., Comin-Anduix, B., Reuben, J.M., Seja, E., Parker, C.A., et al. (2005). Antitumor activity in melanoma and anti-self responses in a phase I trial with the anti-cytotoxic T lymphocyte-associated antigen 4 monoclonal antibody CP-675,206. *J Clin Oncol* *23*, 8968–8977. 10.1200/JCO.2005.01.109.
130. Hodi, F.S., Butler, M., Oble, D.A., Seiden, M. V., Haluska, F.G., Kruse, A., MacRae, S., Nelson, M., Canning, C., Lowy, I., et al. (2008). Immunologic and clinical effects of antibody blockade of cytotoxic T lymphocyte-associated antigen 4 in previously

- vaccinated cancer patients. *Proceedings of the National Academy of Sciences* 105, 3005–3010. 10.1073/pnas.0712237105.
131. Ribas, A., Kefford, R., Marshall, M.A., Punt, C.J.A., Haanen, J.B., Marmol, M., Garbe, C., Gogas, H., Schachter, J., Linette, G., et al. (2013). Phase III randomized clinical trial comparing tremelimumab with standard-of-care chemotherapy in patients with advanced melanoma. *J Clin Oncol* 31, 616–622. 10.1200/JCO.2012.44.6112.
 132. Hodi, F.S., O'Day, S.J., McDermott, D.F., Weber, R.W., Sosman, J.A., Haanen, J.B., Gonzalez, R., Robert, C., Schadendorf, D., Hassel, J.C., et al. (2010). Improved Survival with Ipilimumab in Patients with Metastatic Melanoma. *New England Journal of Medicine* 363, 711–723. 10.1056/NEJMoa1003466.
 133. Robert, C., Thomas, L., Bondarenko, I., O'Day, S., Weber, J., Garbe, C., Lebbe, C., Baurain, J.-F., Testori, A., Grob, J.-J., et al. (2011). Ipilimumab plus Dacarbazine for Previously Untreated Metastatic Melanoma. *New England Journal of Medicine* 364, 2517–2526. 10.1056/NEJMoa1104621.
 134. Postow, M.A., Callahan, M.K., and Wolchok, J.D. (2015). Immune Checkpoint Blockade in Cancer Therapy. *J Clin Oncol* 33, 1974–1982. 10.1200/JCO.2014.59.4358.
 135. Le, D.T., Lutz, E., Uram, J.N., Sugar, E.A., Onners, B., Solt, S., Zheng, L., Diaz, L.A., Donehower, R.C., Jaffee, E.M., et al. (2013). Evaluation of Ipilimumab in Combination With Allogeneic Pancreatic Tumor Cells Transfected With a GM-CSF Gene in Previously Treated Pancreatic Cancer. *Journal of Immunotherapy* 36, 382–389. 10.1097/CJI.0b013e31829fb7a2.
 136. Slovin, S.F., Higano, C.S., Hamid, O., Tejwani, S., Harzstark, A., Alumkal, J.J., Scher, H.I., Chin, K., Gagnier, P., McHenry, M.B., et al. (2013). Ipilimumab alone or in combination with radiotherapy in metastatic castration-resistant prostate cancer: results from an open-label, multicenter phase I/II study. *Annals of Oncology* 24, 1813–1821. 10.1093/annonc/mdt107.
 137. Fife, B.T., and Bluestone, J.A. (2008). Control of peripheral T-cell tolerance and autoimmunity via the CTLA-4 and PD-1 pathways. *Immunol Rev* 224, 166–182. 10.1111/j.1600-065X.2008.00662.x.
 138. Robert, L., Tsoi, J., Wang, X., Emerson, R., Homet, B., Chodon, T., Mok, S., Huang, R.R., Cochran, A.J., Comin-Anduix, B., et al. (2014). CTLA4 Blockade Broadens the Peripheral T-Cell Receptor Repertoire. *Clinical Cancer Research* 20, 2424–2432. 10.1158/1078-0432.CCR-13-2648.

139. Khunger, A., Rytlewski, J.A., Fields, P., Yusko, E.C., and Tarhini, A.A. (2019). The impact of CTLA-4 blockade and interferon- α on clonality of T-cell repertoire in the tumor microenvironment and peripheral blood of metastatic melanoma patients. *Oncoimmunology* 8. 10.1080/2162402X.2019.1652538.
140. Kankana Bardhan, Nikolaos Patsoukis, Jessica Weaver, Gordon Freeman, L.L. and V.A.B. (2016). PD-1 inhibits the TCR signaling cascade by sequestering SHP-2 phosphatase, preventing its translocation to lipid rafts and facilitating Csk-mediated inhibitory phosphorylation of Lck. *The Journal of Immunology* 196, 128.15-128.15.
141. Wherry, E.J. (2011). T cell exhaustion. *Nat Immunol* 12, 492–499.
142. Hino, R., Kabashima, K., Kato, Y., Yagi, H., Nakamura, M., Honjo, T., Okazaki, T., and Tokura, Y. (2010). Tumor cell expression of programmed cell death-1 ligand 1 is a prognostic factor for malignant melanoma. *Cancer* 116, 1757–1766. 10.1002/cncr.24899.
143. Akbari, O., Stock, P., Singh, A.K., Lombardi, V., Lee, W.-L., Freeman, G.J., Sharpe, A.H., Umetsu, D.T., and DeKruyff, R.H. (2010). PD-L1 and PD-L2 modulate airway inflammation and iNKT-cell-dependent airway hyperreactivity in opposing directions. *Mucosal Immunol* 3, 81–91. 10.1038/mi.2009.112.
144. Huber, S., Hoffmann, R., Muskens, F., and Voehringer, D. (2010). Alternatively activated macrophages inhibit T-cell proliferation by Stat6-dependent expression of PD-L2. *Blood* 116, 3311–3320. 10.1182/blood-2010-02-271981.
145. Keir, M.E., Butte, M.J., Freeman, G.J., and Sharpe, A.H. (2008). PD-1 and Its Ligands in Tolerance and Immunity. *Annu Rev Immunol* 26, 677–704. 10.1146/annurev.immunol.26.021607.090331.
146. Topalian, S.L., Hodi, F.S., Brahmer, J.R., Gettinger, S.N., Smith, D.C., McDermott, D.F., Powderly, J.D., Carvajal, R.D., Sosman, J.A., Atkins, M.B., et al. (2012). Safety, Activity, and Immune Correlates of Anti-PD-1 Antibody in Cancer. *New England Journal of Medicine* 366, 2443–2454. 10.1056/NEJMoa1200690.
147. Topalian, S.L., Sznol, M., McDermott, D.F., Kluger, H.M., Carvajal, R.D., Sharfman, W.H., Brahmer, J.R., Lawrence, D.P., Atkins, M.B., Powderly, J.D., et al. (2014). Survival, durable tumor remission, and long-term safety in patients with advanced melanoma receiving nivolumab. *J Clin Oncol* 32, 1020–1030. 10.1200/JCO.2013.53.0105.
148. Robert, C., Long, G. v., Brady, B., Dutriaux, C., Maio, M., Mortier, L., Hassel, J.C., Rutkowski, P., McNeil, C., Kalinka-Warzocha, E., et al. (2015). Nivolumab in

- Previously Untreated Melanoma without *BRAF* Mutation. *New England Journal of Medicine* 372, 320–330. 10.1056/NEJMoa1412082.
149. Robert, C., Ribas, A., Schachter, J., Arance, A., Grob, J.-J., Mortier, L., Daud, A., Carlino, M.S., McNeil, C.M., Lotem, M., et al. (2019). Pembrolizumab versus ipilimumab in advanced melanoma (KEYNOTE-006): post-hoc 5-year results from an open-label, multicentre, randomised, controlled, phase 3 study. *Lancet Oncol* 20, 1239–1251. 10.1016/S1470-2045(19)30388-2.
 150. Weber, J.S., D’Angelo, S.P., Minor, D., Hodi, F.S., Gutzmer, R., Neyns, B., Hoeller, C., Khushalani, N.I., Miller, W.H., Lao, C.D., et al. (2015). Nivolumab versus chemotherapy in patients with advanced melanoma who progressed after anti-CTLA-4 treatment (CheckMate 037): a randomised, controlled, open-label, phase 3 trial. *Lancet Oncol* 16, 375–384. 10.1016/S1470-2045(15)70076-8.
 151. Cao, J., Brouwer, N.J., Richards, K.E., Marinkovic, M., van Duinen, S., Hurkmans, D., Verdegaal, E.M.E., Jordanova, E.S., and Jager, M.J. (2017). PD-L1/PD-1 expression and tumor-infiltrating lymphocytes in conjunctival melanoma. *Oncotarget* 8, 54722–54734. 10.18632/oncotarget.18039.
 152. Taube, J.M., Klein, A., Brahmer, J.R., Xu, H., Pan, X., Kim, J.H., Chen, L., Pardoll, D.M., Topalian, S.L., and Anders, R.A. (2014). Association of PD-1, PD-1 Ligands, and Other Features of the Tumor Immune Microenvironment with Response to Anti-PD-1 Therapy. *Clinical Cancer Research* 20, 5064–5074. 10.1158/1078-0432.CCR-13-3271.
 153. Postow, M.A., Callahan, M.K., and Wolchok, J.D. (2015). Immune Checkpoint Blockade in Cancer Therapy. *J Clin Oncol* 33, 1974–1982. 10.1200/JCO.2014.59.4358.
 154. Vargas, F.A., Furness, A.J.S., Litchfield, K., Joshi, K., Rosenthal, R., Ghorani, E., Solomon, I., Lesko, M.H., Ruef, N., Roddie, C., et al. (2018). Fc Effector Function Contributes to the Activity of Human Anti-CTLA-4 Antibodies. *Cancer Cell* 33, 649. 10.1016/J.CCELL.2018.02.010.
 155. Dahan, R., Segal, E., Engelhardt, J., Selby, M., Korman, A.J., and Ravetch, J. V (2015). FcγRs Modulate the Anti-tumor Activity of Antibodies Targeting the PD-1/PD-L1 Axis. 10.1016/j.ccell.2015.08.004.
 156. Yi, M., Niu, M., Xu, L., Luo, S., and Wu, K. (2021). Regulation of PD-L1 expression in the tumor microenvironment. *Journal of Hematology & Oncology* 2021 14:1 14, 1–13. 10.1186/S13045-020-01027-5.

157. Finn, O.J. (2018). The dawn of vaccines for cancer prevention. *Nat Rev Immunol* 18, 183–194. 10.1038/NRI.2017.140.
158. Blass, E., and Ott, P.A. (2021). Advances in the development of personalized neoantigen-based therapeutic cancer vaccines. *Nature Reviews Clinical Oncology* 2021 18:4 18, 215–229. 10.1038/s41571-020-00460-2.
159. Plosker, G.L. (2011). Sipuleucel-T: in metastatic castration-resistant prostate cancer. *Drugs* 71, 101–108. 10.2165/11206840-000000000-00000.
160. Sahin, U., Oehm, P., Derhovannessian, E., Jabulowsky, R.A., Vormehr, M., Gold, M., Maurus, D., Schwarck-Kokarakis, D., Kuhn, A.N., Omokoko, T., et al. (2020). An RNA vaccine drives immunity in checkpoint-inhibitor-treated melanoma. *Nature* 2020 585:7823 585, 107–112. 10.1038/s41586-020-2537-9.
161. Lee, K.L., Schlom, J., and Hamilton, D.H. (2021). Combination therapies utilizing neoepitope-targeted vaccines. *Cancer Immunology, Immunotherapy* 70, 875. 10.1007/S00262-020-02729-Y.
162. Lawler, S.E., Speranza, M.C., Cho, C.F., and Chiocca, E.A. (2017). Oncolytic Viruses in Cancer Treatment: A Review. *JAMA Oncol* 3, 841–849. 10.1001/JAMAONCOL.2016.2064.
163. Lemos de Matos, A., Franco, L.S., and McFadden, G. (2020). Oncolytic Viruses and the Immune System: The Dynamic Duo. *Mol Ther Methods Clin Dev* 17, 349. 10.1016/J.OMTM.2020.01.001.
164. Zhao, Y., Liu, Z., Li, L., Wu, J., Zhang, H., Zhang, H., Lei, T., and Xu, B. (2021). Oncolytic Adenovirus: Prospects for Cancer Immunotherapy. *Front Microbiol* 12, 1951. 10.3389/FMICB.2021.707290/BIBTEX.
165. Grote, D., Russell, S.J., Cornu, T.I., Cattaneo, R., Vile, R., Poland, G.A., and Fielding, A.K. (2001). Live attenuated measles virus induces regression of human lymphoma xenografts in immunodeficient mice. *Blood* 97, 3746–3754. 10.1182/BLOOD.V97.12.3746.
166. Hollingsworth, R.E., and Jansen, K. (2019). Turning the corner on therapeutic cancer vaccines. *npj Vaccines* 2019 4:1 4, 1–10. 10.1038/s41541-019-0103-y.
167. Rekosh, D.M.K., Russell, W.C., Bellet, A.J.D., and Robinson, A.J. (1977). Identification of a protein linked to the ends of adenovirus DNA. *Cell* 11, 283–295. 10.1016/0092-8674(77)90045-9.
168. Hierholzer, J.C. (1992). Adenoviruses in the immunocompromised host. *Clin Microbiol Rev* 5, 262. 10.1128/CMR.5.3.262.

169. Ginsberg, H.S., and Prince, G.A. (1994). The molecular basis of adenovirus pathogenesis. *Infect Agents Dis* 3, 1–8.
170. Marttila, M., Persson, D., Gustafsson, D., Liszewski, M.K., Atkinson, J.P., Wadell, G., and Arnberg, N. (2005). CD46 Is a Cellular Receptor for All Species B Adenoviruses except Types 3 and 7. *J Virol* 79, 14429. 10.1128/JVI.79.22.14429-14436.2005.
171. Wu, E., Trauger, S.A., Pache, L., Mullen, T.-M., Von Seggern, D.J., Siuzdak, G., and Nemerow, G.R. (2004). Membrane Cofactor Protein Is a Receptor for Adenoviruses Associated with Epidemic Keratoconjunctivitis. *J Virol* 78, 3897–3905. 10.1128/JVI.78.8.3897-3905.2004/ASSET/AF57C77A-6685-4943-BEC9-F129244166DA/ASSETS/GRAPHIC/ZJV0080418530004.JPEG.
172. Wang, H., Li, Z.Y., Liu, Y., Persson, J., Beyer, I., Möller, T., Koyuncu, D., Drescher, M.R., Strauss, R., Zhang, X.B., et al. (2011). Desmoglein 2 is a receptor for adenovirus serotypes 3, 7, 11, and 14. *Nat Med* 17, 96. 10.1038/NM.2270.
173. Bergelson, J.M., Cunningham, J.A., Droguett, G., Kurt-Jones, E.A., Krithivas, A., Hong, J.S., Horwitz, M.S., Crowell, R.L., and Finberg, R.W. (1997). Isolation of a common receptor for Coxsackie B viruses and adenoviruses 2 and 5. *Science* 275, 1320–1323. 10.1126/SCIENCE.275.5304.1320.
174. Wickham, T.J., Mathias, P., Cheresch, D.A., and Nemerow, G.R. (1993). Integrins $\alpha\beta 3$ and $\alpha\beta 5$ promote adenovirus internalization but not virus attachment. *Cell* 73, 309–319. 10.1016/0092-8674(93)90231-E.
175. Giberson, A.N., Davidson, A.R., and Parks, R.J. (2012). Chromatin structure of adenovirus DNA throughout infection. *Nucleic Acids Res* 40, 2369. 10.1093/NAR/GKR1076.
176. Ahi, Y.S., and Mittal, S.K. (2016). Components of adenovirus genome packaging. *Front Microbiol* 7, 1503. 10.3389/FMICB.2016.01503/BIBTEX.
177. Hoeben, R.C., and Uil, T.G. (2013). Adenovirus DNA Replication. *Cold Spring Harb Perspect Biol* 5. 10.1101/CSHPERSPECT.A013003.
178. Nevins, J.R., and Chen-Kiang, S. (1981). Processing of adenovirus nuclear RNA to mRNA. *Adv Virus Res* 26, 1–35. 10.1016/S0065-3527(08)60419-4.
179. Nevins, J.R., and Darnell, J.E. (1978). Steps in the processing of Ad2 mRNA: poly(A)⁺ nuclear sequences are conserved and poly(A) addition precedes splicing. *Cell* 15, 1477–1493. 10.1016/0092-8674(78)90071-5.

180. Berget, S.M., Moore, C., and Sharp, P.A. (1977). Spliced segments at the 5' terminus of adenovirus 2 late mRNA. *Proc Natl Acad Sci U S A* *74*, 3171–3175. 10.1073/PNAS.74.8.3171.
181. Chow, L.T., Gelinas, R.E., Broker, T.R., and Roberts, R.J. (1977). An amazing sequence arrangement at the 5' ends of adenovirus 2 messenger RNA. *Cell* *12*, 1–8. 10.1016/0092-8674(77)90180-5.
182. Ramke, M., Lee, J.Y., Dyer, D.W., Seto, D., Rajaiya, J., and Chodosh, J. (2017). The 5'UTR in human adenoviruses: leader diversity in late gene expression. *Sci Rep* *7*. 10.1038/S41598-017-00747-Y.
183. Charman, M., Herrmann, C., and Weitzman, M.D. (2019). Viral and cellular interactions during adenovirus DNA replication. *FEBS Lett* *593*, 3531–3550. 10.1002/1873-3468.13695.
184. De Jong, R.N., Van Der Vliet, P.C., and Brenkman, A.B. (2003). Adenovirus DNA replication: protein priming, jumping back and the role of the DNA binding protein DBP. *Curr Top Microbiol Immunol* *272*, 187–211. 10.1007/978-3-662-05597-7_7.
185. Ahi, Y.S., and Mittal, S.K. (2016). Components of Adenovirus Genome Packaging. *Front Microbiol* *7*. 10.3389/FMICB.2016.01503.
186. Ostapchuk, P., and Hearing, P. (2003). Regulation of adenovirus packaging. *Curr Top Microbiol Immunol* *272*, 165–185. 10.1007/978-3-662-05597-7_6.
187. Smart, J.E., and Stillman, B.W. (1982). Adenovirus terminal protein precursor. Partial amino acid sequence and the site of covalent linkage to virus DNA. *Journal of Biological Chemistry* *257*, 13499–13506. 10.1016/S0021-9258(18)33475-6.
188. Desiderio, S. V., and Kelly, T.J. (1981). Structure of the linkage between adenovirus DNA and the 55,000 molecular weight terminal protein. *J Mol Biol* *145*, 319–337. 10.1016/0022-2836(81)90208-4.
189. Heise, C., and Kirn, D.H. (2000). Replication-selective adenoviruses as oncolytic agents. *Journal of Clinical Investigation* *105*, 847. 10.1172/JCI9762.
190. Sha, J., Ghosh, M.K., Zhang, K., and Harter, M.L. (2010). E1A Interacts with Two Opposing Transcriptional Pathways To Induce Quiescent Cells into S Phase. *J Virol* *84*, 4050–4059. 10.1128/JVI.02131-09/ASSET/B26DCBCF-2ACD-4DCA-8A8C-A418B02E0AE0/ASSETS/GRAPHIC/ZJV9990930500007.JPEG.
191. Heise, C., Hermiston, T., Johnson, L., Brooks, G., Sampson-Johannes, A., Williams, A., Hawkins, L., and Kirn, D. (2000). An adenovirus E1A mutant that demonstrates

- potent and selective systemic anti-tumoral efficacy. *Nature Medicine* 2000 6:10 6, 1134–1139. 10.1038/80474.
192. Hemminki, O., Parviainen, S., Juhila, J., Turkki, R., Linder, N., Lundin, J., Kankainen, M., Ristimäki, A., Koski, A., Liikanen, I., et al. (2015). Immunological data from cancer patients treated with Ad5/3-E2F-Δ24-GMCSF suggests utility for tumor immunotherapy. *Oncotarget* 6, 4467. 10.18632/ONCOTARGET.2901.
 193. Wu, T., and Wu, L. (2021). The Role and Clinical Implications of the Retinoblastoma (RB)-E2F Pathway in Gastric Cancer. *Front Oncol* 11, 1954. 10.3389/FONC.2021.655630/BIBTEX.
 194. Lomonosova, E., Subramanian, T., and Chinnadurai, G. (2005). Mitochondrial localization of p53 during adenovirus infection and regulation of its activity by E1B-19K. *Oncogene* 2005 24:45 24, 6796–6808. 10.1038/sj.onc.1208836.
 195. Piya, S., White, E.J., Klein, S.R., Jiang, H., McDonnell, T.J., Gomez-Manzano, C., and Fueyo, J. (2011). The E1B19K Oncoprotein Complexes with Beclin 1 to Regulate Autophagy in Adenovirus-Infected Cells. *PLoS One* 6, e29467. 10.1371/JOURNAL.PONE.0029467.
 196. Cheng, P.H., Wechman, S.L., McMasters, K.M., and Zhou, H.S. (2015). Oncolytic Replication of E1b-Deleted Adenoviruses. *Viruses* 7, 5767–5779. 10.3390/V7112905.
 197. Heise, C., Sampson-Johannes, A., Williams, A., McCormick, F., Von Hoff, D.D., and Kirn, D.H. (1997). ONYX-015, an E1B gene-attenuated adenovirus, causes tumor-specific cytolysis and antitumoral efficacy that can be augmented by standard chemotherapeutic agents. *Nature Medicine* 1997 3:6 3, 639–645. 10.1038/nm0697-639.
 198. Bramante, S., Kaufmann, J.K., Veckman, V., Liikanen, I., Nettelbeck, D.M., Hemminki, O., Vassilev, L., Cerullo, V., Oksanen, M., Heiskanen, R., et al. (2015). Treatment of melanoma with a serotype 5/3 chimeric oncolytic adenovirus coding for GM-CSF: Results in vitro, in rodents and in humans. *Int J Cancer* 137, 1775–1783. 10.1002/IJC.29536.
 199. Schiza, A., Wenthe, J., Mangsbo, S., Eriksson, E., Nilsson, A., Tötterman, T.H., Loskog, A., and Ullenhag, G. (2017). Adenovirus-mediated CD40L gene transfer increases T effector/Tregulatory cell ratio and upregulates death receptors in metastatic melanoma patients. *J Transl Med* 15. 10.1186/S12967-017-1182-Z.
 200. Malmström, P.U., Loskog, A.S.I., Lindqvist, C.A., Mangsbo, S.M., Fransson, M., Wanders, A., Gårdmark, T., and Tötterman, T.H. (2010). AdCD40L immunogene

- therapy for bladder carcinoma - The first phase I/IIa trial. *Clinical Cancer Research* 16, 3279–3287. 10.1158/1078-0432.CCR-10-0385.
201. Loskog, A., Maleka, A., Mangsbo, S., Svensson, E., Lundberg, C., Nilsson, A., Krause, J., Agnarsdóttir, M., Sundin, A., Ahlström, H., et al. (2016). Immunostimulatory AdCD40L gene therapy combined with low-dose cyclophosphamide in metastatic melanoma patients. *Br J Cancer* 114, 872–880. 10.1038/BJC.2016.42.
202. Pesonen, S., Diaconu, I., Kangasniemi, L., Ranki, T., Kanerva, A., Pesonen, S.K., Gerdemann, U., Leen, A.M., Kairemo, K., Oksanen, M., et al. (2012). Oncolytic immunotherapy of advanced solid tumors with a CD40L-expressing replicating adenovirus: Assessment of safety and immunologic responses in patients. *Cancer Res* 72, 1621–1631. 10.1158/0008-5472.CAN-11-3001.
203. Piechutta, M., and Berghoff, A.S. (2019). New emerging targets in cancer immunotherapy: the role of Cluster of Differentiation 40 (CD40/TNFR5). *ESMO Open* 4, e000510. 10.1136/ESMOOPEN-2019-000510.
204. Croft, M., So, T., Duan, W., and Soroosh, P. (2009). The Significance of OX40 and OX40L to T cell Biology and Immune Disease. *Immunol Rev* 229, 173. 10.1111/J.1600-065X.2009.00766.X.
205. Eriksson, E., Milenova, I., Wenthe, J., Hle, M.S., Leja-Jarblad, J., Ullenhag, G., Dimberg, A., Moreno, R., Alemany, R., and Loskog, A. (2017). Shaping the tumor stroma and sparking immune activation by CD40 and 4-1BB signaling induced by an armed oncolytic virus. *Clinical Cancer Research* 23, 5846–5857. 10.1158/1078-0432.CCR-17-0285.
206. Liu, B.L., Robinson, M., Han, Z.Q., Branston, R.H., English, C., Reay, P., McGrath, Y., Thomas, S.K., Thornton, M., Bullock, P., et al. (2003). ICP34.5 deleted herpes simplex virus with enhanced oncolytic, immune stimulating, and anti-tumour properties. *Gene Ther* 10, 292–303. 10.1038/SJ.GT.3301885.
207. Cerullo, V., Pesonen, S., Diaconu, I., Escutenaire, S., Arstila, P.T., Ugolini, M., Nokisalmi, P., Raki, M., Laasonen, L., Särkioja, M., et al. (2010). Oncolytic adenovirus coding for granulocyte macrophage colony-stimulating factor induces antitumoral immunity in cancer patients. *Cancer Res* 70, 4297–4309. 10.1158/0008-5472.CAN-09-3567.
208. Ranki, T., Pesonen, S., Hemminki, A., Partanen, K., Kairemo, K., Alanko, T., Lundin, J., Linder, N., Turkki, R., Ristimäki, A., et al. (2016). Phase I study with ONCOS-102

- for the treatment of solid tumors – an evaluation of clinical response and exploratory analyses of immune markers. *J Immunother Cancer* 4. 10.1186/S40425-016-0121-5.
209. Ylösmäki, E., and Cerullo, V. (2020). Design and application of oncolytic viruses for cancer immunotherapy. *Curr Opin Biotechnol* 65, 25–36. 10.1016/J.COPBIO.2019.11.016.
210. Scott, E.M., Duffy, M.R., Freedman, J.D., Fisher, K.D., Seymour, L.W., Scott, E.M., Duffy, M.R., Freedman, J.D., Fisher, K.D., and Seymour, L.W. (2018). Solid Tumor Immunotherapy with T Cell Engager-Armed Oncolytic Viruses. *Macromol Biosci* 18, 1700187. 10.1002/MABI.201700187.
211. Goebeler, M.E., and Bargou, R. (2016). Blinatumomab: a CD19/CD3 bispecific T cell engager (BiTE) with unique anti-tumor efficacy. *Leuk Lymphoma* 57, 1021–1032. 10.3109/10428194.2016.1161185.
212. Yu, F., Wang, X., Guo, Z.S., Bartlett, D.L., Gottschalk, S.M., and Song, X.T. (2014). T-cell Engager-armed Oncolytic Vaccinia Virus Significantly Enhances Antitumor Therapy. *Molecular Therapy* 22, 102–111. 10.1038/MT.2013.240.
213. Freedman, J.D., Hagel, J., Scott, E.M., Psallidas, I., Gupta, A., Spiers, L., Miller, P., Kanellakis, N., Ashfield, R., Fisher, K.D., et al. (2017). Oncolytic adenovirus expressing bispecific antibody targets T-cell cytotoxicity in cancer biopsies. *EMBO Mol Med* 9, 1067–1087. 10.15252/EMMM.201707567.
214. Dias, J.D., Hemminki, O., Diaconu, I., Hirvinen, M., Bonetti, A., Guse, K., Escutenaire, S., Kanerva, A., Pesonen, S., Löskog, A., et al. (2011). Targeted cancer immunotherapy with oncolytic adenovirus coding for a fully human monoclonal antibody specific for CTLA-4. *Gene Therapy* 2012 19:10 19, 988–998. 10.1038/gt.2011.176.
215. Wang, G., Kang, X., Chen, K.S., Jehng, T., Jones, L., Chen, J., Huang, X.F., and Chen, S.Y. (2020). An engineered oncolytic virus expressing PD-L1 inhibitors activates tumor neoantigen-specific T cell responses. *Nature Communications* 2020 11:1 11, 1–14. 10.1038/s41467-020-15229-5.
216. Stratford-Perricaudet, L.D., Makeh, I., Perricaudet, M., and Briand, P. (1992). Widespread long-term gene transfer to mouse skeletal muscles and heart. *J Clin Invest* 90, 626–630. 10.1172/JCI115902.
217. Mittal, S.K., McDermott, M.R., Johnson, D.C., Prevec, L., and Graham, F.L. (1993). Monitoring foreign gene expression by a human adenovirus-based vector using the

- firefly luciferase gene as a reporter. *Virus Res* 28, 67–90. 10.1016/0168-1702(93)90090-A.
218. Hardy, S., Kitamura, M., Harris-Stansil, T., Dai, Y., and Phipps, M.L. (1997). Construction of adenovirus vectors through Cre-lox recombination. *J Virol* 71, 1842–1849. 10.1128/JVI.71.3.1842-1849.1997.
219. He, T.C., Zhou, S., Da Costa, L.T., Yu, J., Kinzler, K.W., and Vogelstein, B. (1998). A simplified system for generating recombinant adenoviruses. *Proc Natl Acad Sci U S A* 95, 2509. 10.1073/PNAS.95.5.2509.
220. Li, J.-H., Shi, W., Li, A., Mocanu, J., and Liu, F.-F. (2005). Generation of adenovirus 5/3 chimera for improving transduction of lymphocytes. *Cancer Res* 65.
221. Evans, R.K., Nawrocki, D.K., Isopi, L.A., Williams, D.M., Casimiro, D.R., Chin, S., Chen, M., Zhu, D.M., Shiver, J.W., and Volkin, D.B. (2004). Development of stable liquid formulations for adenovirus-based vaccines. *J Pharm Sci* 93, 2458–2475. 10.1002/JPS.20157.
222. Gibson, D.G., Young, L., Chuang, R.Y., Venter, J.C., Hutchison, C.A., and Smith, H.O. (2009). Enzymatic assembly of DNA molecules up to several hundred kilobases. *Nature Methods* 2009 6:5 6, 343–345. 10.1038/nmeth.1318.
223. Ni, N., Deng, F., He, F., Wang, H., Shi, D., Liao, J., Zou, Y., Wang, H., Zhao, P., Hu, X., et al. (2021). A one-step construction of adenovirus (OSCA) system using the Gibson DNA Assembly technology. *Mol Ther Oncolytics* 23, 602–611. 10.1016/J.OMTO.2021.11.011.
224. Pan, H., Yan, Y., Zhang, J., Zhao, S., Feng, L., Ou, J., Cao, N., Li, M., Zhao, W., Wan, C., et al. (2018). Rapid Construction of a Replication-Competent Infectious Clone of Human Adenovirus Type 14 by Gibson Assembly. *Viruses* 10. 10.3390/V10100568.
225. Liu, J., Chen, Z., Li, Y., Zhao, W., Wu, J.B., and Zhang, Z. (2021). PD-1/PD-L1 Checkpoint Inhibitors in Tumor Immunotherapy. *Front Pharmacol* 12. 10.3389/FPHAR.2021.731798.
226. Haslam, A., and Prasad, V. (2019). Estimation of the Percentage of US Patients With Cancer Who Are Eligible for and Respond to Checkpoint Inhibitor Immunotherapy Drugs. *JAMA Netw Open* 2. 10.1001/JAMANETWORKOPEN.2019.2535.
227. Valgardsdottir, R., Cattaneo, I., Klein, C., Introna, M., Figliuzzi, M., and Golay, J. (2017). Human neutrophils mediate trogocytosis rather than phagocytosis of CLL B cells opsonized with anti-CD20 antibodies. *Blood* 129, 2636–2644. 10.1182/BLOOD-2016-08-735605.

228. Kelton, W., Mehta, N., Charab, W., Lee, J., Lee, C.H., Kojima, T., Kang, T.H., and Georgiou, G. (2014). IgGA: A “Cross-Isotype” Engineered Human Fc Antibody Domain that Displays Both IgG-like and IgA-like Effector Functions. *Chem Biol* 21, 1603–1609. 10.1016/J.CHEMBIOL.2014.10.017.
229. Brandsma, A.M., Broeke, T. Ten, Nederend, M., Meulenbroek, L.A.P.M., Van Tetering, G., Meyer, S., Jansen, J.H.M., Buitrago, M.A.B., Nagelkerke, S.Q., Németh, I., et al. (2015). Simultaneous Targeting of FcγRs and FcαRI Enhances Tumor Cell Killing. *Cancer Immunol Res* 3, 1316–1324. 10.1158/2326-6066.CIR-15-0099-T.
230. Lohse, S., Brunke, C., Derer, S., Peipp, M., Boross, P., Kellner, C., Beyer, T., Dechant, M., Van Der Winkel, J.G.J., Leusen, J.H.W., et al. (2012). Characterization of a Mutated IgA2 Antibody of the m(1) Allotype against the Epidermal Growth Factor Receptor for the Recruitment of Monocytes and Macrophages *. *Journal of Biological Chemistry* 287, 25139–25150. 10.1074/JBC.M112.353060.
231. Kelton, W., Mehta, N., Charab, W., Lee, J., Lee, C.H., Kojima, T., Kang, T.H., and Georgiou, G. (2014). IgGA: A “Cross-Isotype” Engineered Human Fc Antibody Domain that Displays Both IgG-like and IgA-like Effector Functions. *Chem Biol* 21, 1603–1609. 10.1016/J.CHEMBIOL.2014.10.017.
232. Evers, M., Ten Broeke, T., Jansen, J.H.M., Nederend, M., Hamdan, F., Reiding, K.R., Meyer, S., Moerer, P., Brinkman, I., Rösner, T., et al. (2020). Novel chimerized IgA CD20 antibodies: Improving neutrophil activation against CD20-positive malignancies. *MAbs* 12. 10.1080/19420862.2020.1795505/SUPPL_FILE/KMAB_A_1795505_SM2346.ZIP.
233. Evers, M., Ten Broeke, T., Jansen, J.H.M., Nederend, M., Hamdan, F., Reiding, K.R., Meyer, S., Moerer, P., Brinkman, I., Rösner, T., et al. (2020). Novel chimerized IgA CD20 antibodies: Improving neutrophil activation against CD20-positive malignancies. *MAbs* 12. 10.1080/19420862.2020.1795505.
234. Brandsma, A.M., Bondza, S., Evers, M., Koutstaal, R., Nederend, M., Marco Jansen, J.H., Rösner, T., Valerius, T., Leusen, J.H.W., and Ten Broeke, T. (2019). Potent Fc receptor signaling by IgA leads to superior killing of cancer cells by neutrophils compared to IgG. *Front Immunol* 10, 704. 10.3389/FIMMU.2019.00704/BIBTEX.
235. Treffers, L.W., Van Houdt, M., Bruggeman, C.W., Heineke, M.H., Zhao, X.W., Van Der Heijden, J., Nagelkerke, S.Q., Verkuijlen, P.J.J.H., Geissler, J., Lissenberg-Thunnissen, S., et al. (2019). FcγRIIIb restricts antibody-dependent destruction of

- cancer cells by human neutrophils. *Front Immunol* *10*, 3124. 10.3389/FIMMU.2018.03124/BIBTEX.
236. Bruhns, P. (2012). Properties of mouse and human IgG receptors and their contribution to disease models. *Blood* *119*, 5640–5649. 10.1182/BLOOD-2012-01-380121.
237. Deng, L., Liang, H., Burnette, B., Beckett, M., Darga, T., Weichselbaum, R.R., and Fu, Y.X. (2014). Irradiation and anti-PD-L1 treatment synergistically promote antitumor immunity in mice. *J Clin Invest* *124*, 687–695. 10.1172/JCI67313.
238. Maute, R.L., Gordon, S.R., Mayer, A.T., McCracken, M.N., Natarajan, A., Ring, N.G., Kimura, R., Tsai, J.M., Manglik, A., Kruse, A.C., et al. (2015). Engineering high-affinity PD-1 variants for optimized immunotherapy and immuno-PET imaging. *Proc Natl Acad Sci U S A* *112*, E6506–E6514. 10.1073/PNAS.1519623112/-/DCSUPPLEMENTAL.
239. Yamauchi, T., Hoki, T., Oba, T., Jain, V., Chen, H., Attwood, K., Battaglia, S., George, S., Chatta, G., Puzanov, I., et al. (2021). T-cell CX3CR1 expression as a dynamic blood-based biomarker of response to immune checkpoint inhibitors. *Nat Commun* *12*. 10.1038/S41467-021-21619-0.
240. Noman, M.Z., Desantis, G., Janji, B., Hasmim, M., Karray, S., Dessen, P., Bronte, V., and Chouaib, S. (2014). PD-L1 is a novel direct target of HIF-1 α , and its blockade under hypoxia enhanced: MDSC-mediated T cell activation. *Journal of Experimental Medicine* *211*, 781–790. 10.1084/JEM.20131916.
241. Wang, X., Mathieu, M., and Brezski, R.J. (2018). IgG Fc engineering to modulate antibody effector functions. *Protein Cell* *9*, 63. 10.1007/S13238-017-0473-8.
242. Komatsu, N., Okamoto, K., Sawa, S., Nakashima, T., Oh-hora, M., Kodama, T., Tanaka, S., Bluestone, J.A., and Takayanagi, H. (2014). Pathogenic conversion of Foxp3⁺ T cells into TH17 cells in autoimmune arthritis. *Nat Med* *20*, 62–68. 10.1038/nm.3432.
243. Masucci, M.T., Minopoli, M., and Carriero, M.V. (2019). Tumor Associated Neutrophils. Their Role in Tumorigenesis, Metastasis, Prognosis and Therapy. *Front Oncol* *9*, 1146. 10.3389/FONC.2019.01146.

STUDY I

GAMER-Ad: a novel and rapid method for generating recombinant adenoviruses

Firas Hamdan,^{1,2,3} Beatriz Martins,^{1,2,3} Michaela Feodoroff,^{1,2,3} Yvonne Giannoula,^{1,2,3} Sara Feola,^{1,2,3} Manlio Fuscillo,^{1,2,3} Jacopo Chiaro,^{1,2,3} Gabriella Antignani,^{1,2,3} Mikaela Grönholm,^{1,2,3,4} Erkko Ylösmäki,^{1,2,3} and Vincenzo Cerullo^{1,2,3,4,5}

¹Laboratory of Immunovirotherapy (IVTlab), Drug Research Program, Faculty of Pharmacy, University of Helsinki, Viikinkaari 5E, 00790 Helsinki, Finland; ²Drug Research Program, Division of Pharmaceutical Biosciences, Faculty of Pharmacy, University of Helsinki, Helsinki, Finland; ³TRIMM, Translational Immunology Research Program, University of Helsinki, Helsinki, Finland; ⁴iCAN Digital Precision Cancer Medicine Flagship, University of Helsinki, Helsinki, Finland; ⁵Department of Molecular Medicine and Medical Biotechnology and CEINGE, Naples University 24 Federico II, 80131 Naples, Italy

Oncolytic adenoviruses have become ideal agents in the path toward treating cancer. Such viruses have been engineered to conditionally replicate in malignant cells in which certain signaling pathways have been disrupted. Other than such oncolytic properties, the viruses need to activate the immune system in order to sustain a long-term response. Therefore, oncolytic adenoviruses have been genetically modified to express various immune-stimulatory agents to achieve this. However, genetically modifying adenoviruses is very time consuming and labor intensive with the current available methods. In this paper, we describe a novel method we have called GAMER-Ad to genetically modify adenovirus genomes within 2 days. Our method entails the replacement of the gp19k gene in the E3 region with any given gene of interest (GOI) using Gibson Assembly avoiding the homologous recombination between the shuttle and the parental plasmid. In this manuscript as proof of concept we constructed and characterized three oncolytic adenoviruses expressing CXCL9, CXCL10, and interleukin-15 (IL-15). We demonstrate that our novel method is fast, reliable, and simple compared to other methods. We anticipate that our method will be used in the future to genetically engineer oncolytic but also other adenoviruses used for gene therapy as well.

INTRODUCTION

In the clinic, anti-cancer agents target rapidly dividing cells or single genetic mutations. Advancements in genome sequencing have led us to understand that cancer is not monogenic but rather a complex and heterogeneous disease.¹ This explains why the use of single genetic mutation agents over the past decades have not yielded significant full response rates or cures as once expected. Therefore, scientists have stopped hunting for individual tumor suppressor genes or oncogenes and started investigating methods in disrupting whole tumorigenic biological pathways.² Oncolytic viruses are the ideal agents in achieving this, because such viruses are able to thrive in tumor cells, where such malignant pathways have been activated or disrupted, and exploit metabolic pathways that characterize tumorigenesis.² Also, oncolytic viruses have extensively been shown to stimulate systemic host immune responses. The tumor microenvironment is immunosuppressive and

boosting the immune system has been observed to have significant anti-tumor effects.² Hence, the dual mechanism oncolytic viruses possess makes them interesting therapy agents.

To date, only one oncolytic virus has been granted US Food and Drug Administration (FDA) approval for treatment despite years of extensive investigation.³ One of the reasons is that oncolytic viruses have been generally seen as direct tools for killing cancer due to their tumor-specific tropism. A growing body of evidence has shown that the ability of the virus to activate the immune system is a key attribute with regard to long-term antitumor effects.⁴ Therefore, to make more significant advances with such therapies there has been a shift in focus from viewing oncolytic viruses not solely as direct oncolytic tools but also as immunotherapies. Scientists have equipped oncolytic viruses with multiple immune-stimulatory molecules that have enhanced anti-tumor effects. For example, oncolytic viruses have been engineered to express molecules like interleukins (IL-2, IL-12, IL-15, and IL-18), chemokines (CCL5, CCL19, CCL20, and CCL21), immune-activating ligands (CD40L), bi-specific T cell engager molecules, and much more (all reviewed in Ylösmäki et al.²).

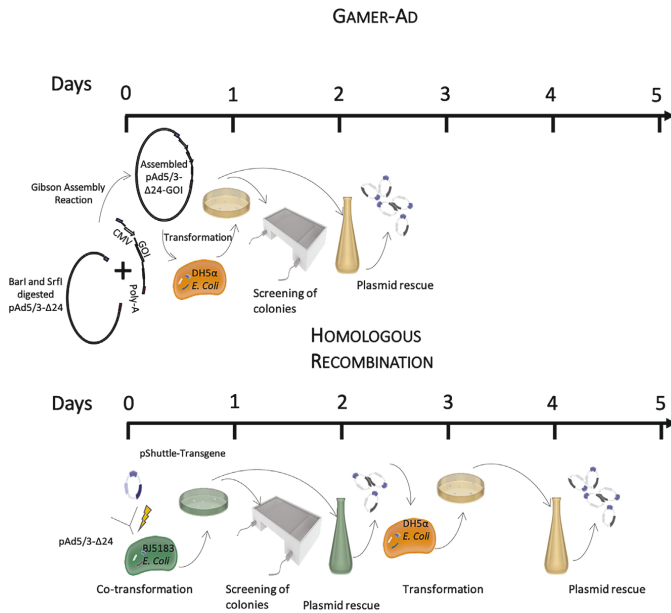
Such oncolytic viruses range from adenoviruses, herpes simplex viruses, vaccinia, Newcastle disease virus, and much more. However, adenoviruses have drawn much of the attention due to their numerous advantages. First, the adenoviral genome is highly stable, which leads to easier large-scale production.⁵ Also, they are able to infect most human cells due to the high expression of the viral coxsackievirus and adenovirus receptor (CAR) throughout the human body. This high infectivity subsequently leads to higher expression levels and sustainability of transgenes. Moreover, anti-adenovirus immunity can be circumvented by attenuating adenovirus vectors. In

Received 19 November 2020; accepted 27 January 2021;
<https://doi.org/10.1016/j.omtm.2021.01.014>

Correspondence: Vincenzo Cerullo, Laboratory of Immunovirotherapy (IVTlab), Drug Research Program, Faculty of Pharmacy, University of Helsinki, Viikinkaari 5E, 00790 Helsinki, Finland.

E-mail: vincenzo.cerullo@helsinki.fi





addition, because of the extensive research done on adenoviruses, the safety dosing and routes of administrations have been established.⁶ Finally, the tropism of the virus can be easily manipulated by modifying its viral capsid.⁷ For example, Zsolt and colleagues^{8,11} were able to redirect adenoviruses to expand solely in tumor cells by replacing the adenoviral fiber knob (responsible for binding to CAR on target cells) with a T cell receptor specific to a unique class of tumor antigens.

Despite all the advantages, starting from a cDNA of interest to modifying an adenovirus able to express such genes involves many steps and significant time to be invested. The most common method used is homologous recombination using a shuttle plasmid and the full adenovirus genome. However, this methodology is very time consuming, inefficient, and labor intensive. Here we present GAMER-Ad (Gibson Assembly Mediated Recombination), a novel method for engineering recombinant viruses that is simple, highly efficient, and takes around 4 days to obtain an adeno full genome with the gene of interest (GOI) inserted (Figure 1). Our method is based on directly substituting the GOI into the E3-gp19k region via the well-known molecular cloning method Gibson Assembly (GA).^{9,10} Gibson Assembly is a molecular cloning method allowing the assembly of multiple DNA fragments in one isothermal reaction containing three enzymes: exonuclease, DNA polymerase, and DNA ligase. The method requires a base overlap of 20–40 nucleotides among the fragments to be assembled. This overlap will allow the exonucleases to chew the 5' ends, allowing the seamless joining of

Figure 1. GAMER-Ad versus homologous recombination

A schematic representation comparing the time required to genetically engineer adenoviruses using GAMER-Ad or the commonly used homologous recombination. The GAMER-Ad method starts by first excising E3 using *Bam*I and *Srf*I following the amplification and insertion of 40 overlapping nucleotides to the fragment to be inserted (GOI) into the adenovector. Both components are then assembled using the Gibson Assembly (GA) reaction and transformed in competent *E. coli*. To select positive colonies, screening of recombinant plasmids can be done using a colony PCR. This technique considerably simplifies and speeds up the process and shows very high efficiency. As for homologous recombination, the optimized procedure requires the cloning of the shuttle plasmid with homologous arms by PCR, linearization of the shuttle plasmid, transformation of *E. coli* BJ5183 (a recombination proficient *E. coli* strain) with the shuttle plasmid and backbone plasmid by electroporation, screening for positive bacteria colonies, and finally transformation of the successfully recombined plasmid into a recombination-incompetent strain of *E. coli* to obtain high yields of plasmid DNA.

adjacent fragments. In this study, we added overlapping regions of the adenovector backbone into the 3' and 5' ends of the GOI, and, using the already commercially available GA Master Mix,

we were able to replace the gp19k gene in the E3 region of the adenovector backbone with our GOI. In this paper, we describe the use of this method for the creation of three genetically modified adenoviruses to express CXCL9, CXCL10, and IL-15.

RESULTS

Excising the E3 region and constructing the GOI

The genetic modification of the described viruses was possible by using a vector containing the Ad5/3-Δ24-E3+ genomic DNA. Our novel methodology consists of replacing the gp19k region of the E3 gene with our GOI using the GA method. First, the E3 region from the adenovirus was removed by taking advantage of the convenient and inherent restriction enzymes flanking the gene, *Bam*I and *Srf*I (Figure 3A). After digestion, products were loaded on an agarose gel, and a clear band between 3 kb and 4 kb can be observed, indicating that the E3 gene (3,398 bp) was excised successfully (Figure 3B).

The GOI to replace the gp19k region consisted of a Citomegalovirus (CMV), coding sequence of IL-15, and a poly(A). The CMV and poly(A) entailed 40 overlapping nucleotides to the 5' and 3' ends of the excised Ad-5/3-Δ24-E3+, respectively, to ensure a correct assembly. Additionally, the poly(A) fragment also contained all the coding sequences of the E3 region except for the gp19k gene. As shown in Figure 2, all three components were amplified via PCR. Moreover, using our primers, 40 overlapping nucleotides were added to the 5' and 3' ends of the IL-15 fragment allowing assembly with poly(A) and CMV fragments (Figure 3C). Using the GA Master Mix, all three

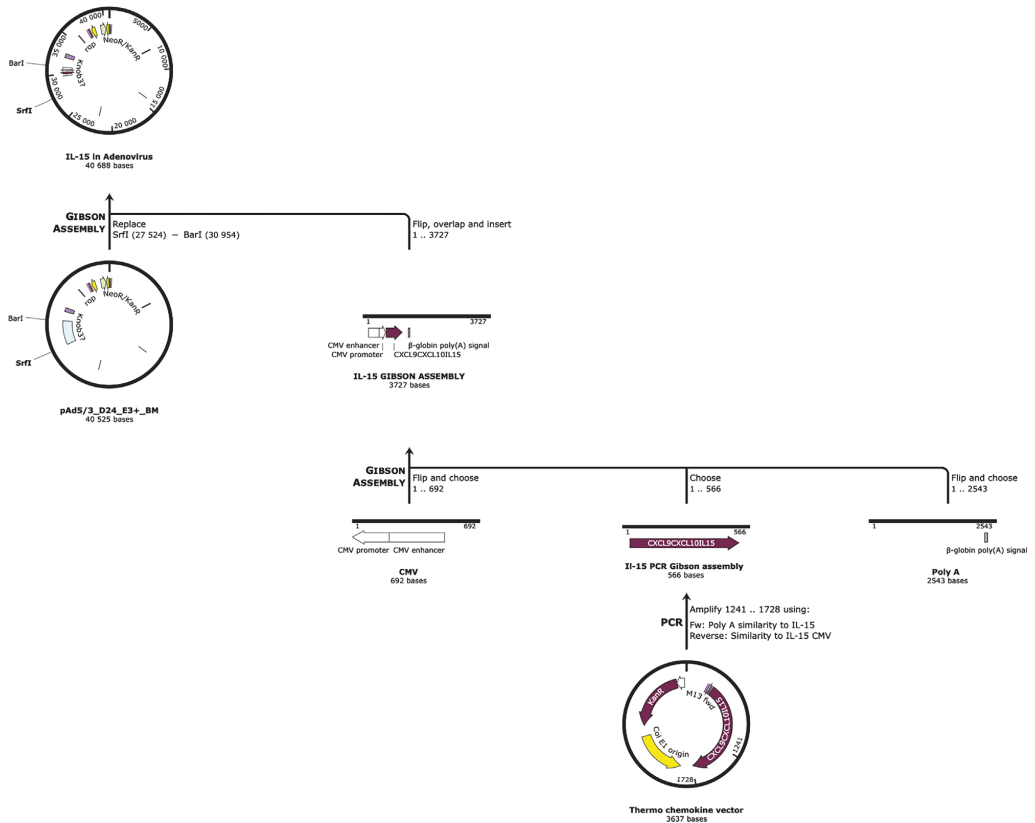


Figure 2. Cloning strategy of GAMER-Ad

The GOI was constructed made up of three components: a CMV starting sequencing, followed by the coding sequencing of the chemokines, and finally ending in a poly(A) tail. The chemokine coding sequences contained 40 nucleotides in their 5' and 3', which are homologous to the ends of the CMV and poly(A) fragment, respectively. The CMV and poly(A) tail also contain all the genes required for E3 except the gp19k gene. All three fragments were then assembled together using the GA method. The Ad-5/3 genome was excised with BarI and SrfI to liberate the E3 region. The GOI was then inserted into the excised genome, again using the GA.

components were assembled together. A PCR using a forward primer flanking the 5' end of the CMV and reverse primer flanking the 3' of poly(A) demonstrated that assembly was successful and in the correct orientation (Figure 3D).

Assembling the GOI into the adenovirus genome

Following adenovector digestion and GOI construction, the two components were assembled together using again the GA Master Mix. The GA products were transformed in *E. coli* cells, and eight colonies were taken for colony PCR. Using primers flanking the CMV and poly(A) tail (only found in the GOI), we saw that from eight colonies, six of them had the GOI (Figure 4A). Three positive colonies (based on colony PCR) were selected, grown in Lysogeni Broth (LB) medium,

and the DNA was isolated. To further check whether replacement of E3 with the GOI in the adenovector was successful, constructs underwent restriction enzyme analysis and Sanger sequencing. Isolated DNA from the three colonies and unmodified adenovector were digested using EcoRI. In case of success in replacing gp19k with the GOI, a band should be observed at 2,075 bp, compared to a 2,718 bp band when gp19k remains (Figure 4B). Digestion with EcoRI demonstrated that gp19k was replaced in all three selected colonies (Figure 4C). Sanger sequencing was then performed and confirmed that all the three selected clones had the gp19k gene replaced by the GOI (Figure 4D). To further illustrate the rapidness and simplicity of our method, we engineered two new Ad5/3 viruses expressing CXCL9 and CXCL10. The same process was used, and each virus took an average of 2 days to be cloned.

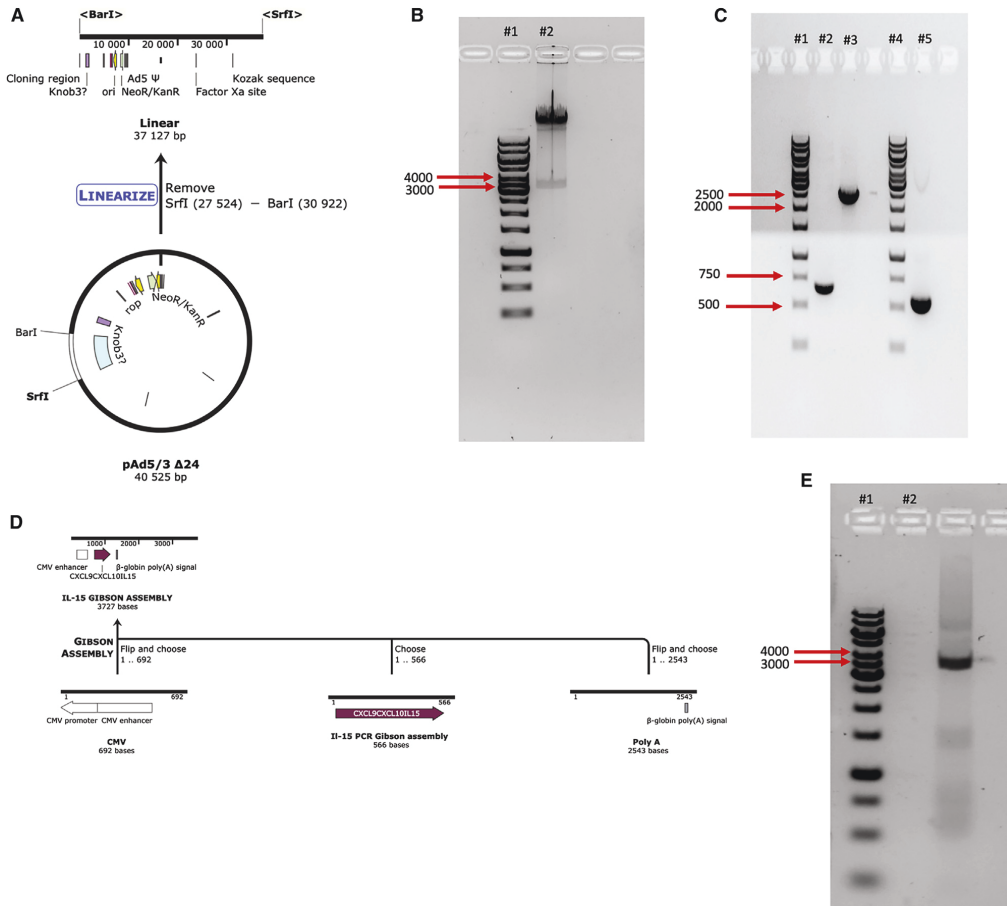


Figure 3. Releasing the E3 region and constructing the GOI

(A) A schematic representation of the linearization of the Ad5/3 genome using BarI and SrfI. (B) Ad5/3 was linearized using the mentioned restriction enzymes and loaded onto an agarose gel in lane 2. Lane 1 represents a 1 kb gene ruler from Thermo Fisher. (C) The CMV, poly(A), and chemokine fragments were amplified and loaded onto an agarose gel in lanes 2, 3, and 5, respectively. Lanes 1 and 4 were loaded with 1 kb gene ruler from Thermo Fisher. (D) Schematic representation of the assembly of the GOI. (E) After assembling all three fragments of the GOI using the GA, the final fragment containing CMV-cytokine-poly(A) was amplified using PCR and loaded on a gel. Lane 2 represents the amplified GOI, while lane 1 represents a 1 kb gene ruler from Thermo Fisher.

Viral production and Ad5/3- Δ 24 contamination check

After successfully constructing adenovectors expressing CXCL9, CXCL19, and IL-15, we linearized the genomes with PacI to release the vector sequence and expose the viral ITRs required for the initiation of the viral DNA replication in the host cell. The digestion product was transfected into A549. Viral plaques appeared on the cell layer 7 days post transfection, suggesting successful rescue of recombinant viruses (Figure 5A). Packaging cells

were lysed to release the virus, and the viral crude was utilized for further amplification of the virus. Viruses were successfully purified using CsCl, and the viral particle titer and infectious unit titer were determined.

After, we sought to determine whether there was an Ad5/3- Δ 24 contamination in the purified preparations of the cloned chemokine expressing Ad-5/3. We designed two different PCR protocols, with

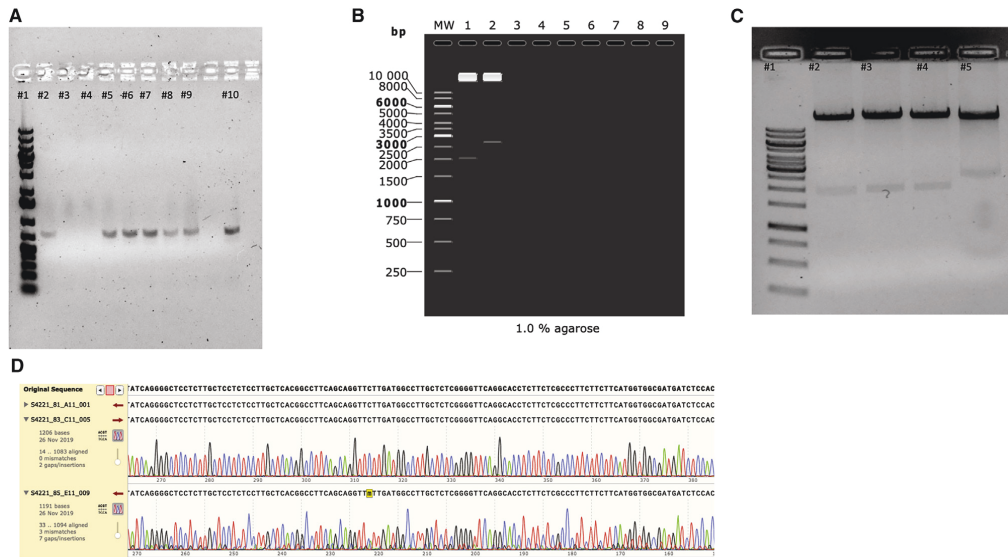


Figure 4. Screening for positive colonies for the IL-5-expressing virus

(A) After transformation of GA products, eight colonies were chosen (lanes 2–9) and a colony PCR was conducted. Primers flanking the CMV and IL-15 coding region were used. As a positive control, the GA of CMV-IL-5-poly(A) (lane 10) was used. Lane 1 represents a 1 kb gene ruler from Thermo Fisher. (B) Simulation of expected lanes where unmodified adenovector is cut with EcoRI (lane 3) compared to positive adenovirus clones successfully having the gp19k replaced with the GOI (lane 2). Lane 1 represents a 1 kb gene ruler from Thermo Fisher. (B) Actual representation of three colonies transformed with the assembled adenovirus containing the GOI (lanes 2, 3, and 4). Lane 5 represents wild-type adenovirus cut with EcoRI, while lane 1 represents a 1 kb gene ruler from Thermo Fisher. (C) Three samples of Sanger sequencing from one of the positive sequences. Original sequence represents the reference sequence of IL-15.

the first protocol having primers flanking the gp19k gene and the second having primers binding to CMV and poly(A) (only found in the cloned Ad5/3-Δ24) (Figure 5B). Purified virus samples from the cytokine-expressing viruses and unmodified Ad5/3-Δ24 were boiled to release the DNA from the viral capsid and were used as template for the PCRs. When primers flanking the gp19k gene were used, a band was only seen with the Ad5/3-Δ24 virus. As expected, when primers binding to the CMV and poly(A) were added, corresponding bands were seen in all cloned Ad-5/3 viruses, but no band was observed with the Ad-5/3-Δ24 virus (Figure 5C). Hence, this demonstrates that our method does lead to Ad5/3-Δ24 virus contamination.

Viral replication and fitness of cloned viruses

Following the cloning and purification of Ad-5/3 viruses expressing CXCL9, CXL10, or IL-15, we wanted to check that method and modification used did not affect the oncolytic fitness or replication of the viruses. All viruses have a well-known 24-bp deletion in the E1A region conditioning such viruses to replicate only in Rb-deficient cells. As a result, two tumor models, lung carcinoma cell (A549) and triple-negative breast cancer cells (MDA-MB-436), were infected with our cloned viruses and unmodified Ad5/3-Δ24 virus. Oncolysis was

observed at day 3 post infection in a dose-dependent fashion in both cell lines (Figures 6A and 6B). Oncolysis levels of the cloned viruses resembled those of the unmodified virus, indicating that our cloning method did not affect oncolytic potency or virus replication. To further corroborate this, two murine cell lines, B16F10 and 4T1, were also studied. Human adenoviruses serotype 5 can infect murine cell lines but are unable to replicate. As expected, no cell death was observed with either murine cell line when infected with the unmodified and cytokine-expressing Ad-5/3 viruses (Figures 6C and 6D). These data illustrate that our novel cloning methodology does not affect oncolytic fitness or replication.

Chemokine expression and migration induction from cloned viruses

The next step of the cloned viruses' *in vitro* characterization was to investigate the levels of expression of the cytokine upon virus infection. MDA-MB-436 cells were infected with the unarmed and the cytokine viruses, separately. The cell's supernatant was collected at day 2 post infection. All cloned viruses were able to induce expression and secretion of the designated chemokine or cytokine at levels ranging from 0.9–37 ng (Figure 7A).

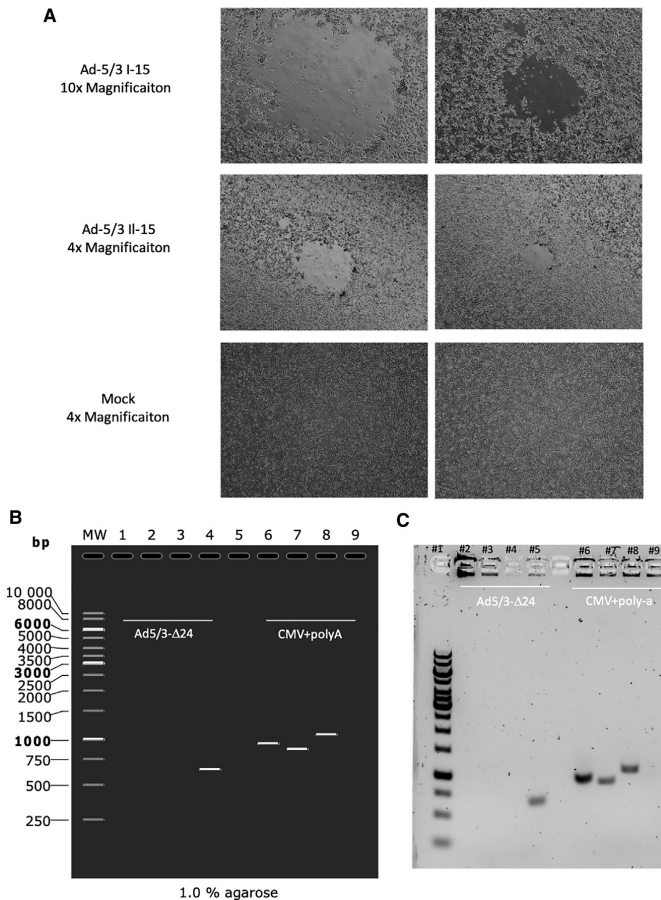


Figure 5. Viral production with lack of Ad5/3- Δ 24 contamination

(A) Representative images of A549 cells transfected with IL-15-expressing adenovirus and wild-type virus. Images were taken 9 days post-transfection at two different magnification, 10 \times and 40 \times . (B) Ad5/3- Δ 24 contamination was checked by amplifying the gp19k region (Ad5/3- Δ 24) or the CMV and poly(A) region (GOI). A simulation of what should be expected is presented and type of samples are annotated. Lane MW represents a 1 kb gene ruler from Thermo Fisher. Lanes 4 and 9 represent Ad5/3- Δ 24 virus. Lanes 1 and 6 represent CXCL9-expressing adenovirus. Lanes 2 and 7 represent CXCL10-expressing adenovirus. Lanes 3 and 8 represent IL-15-expressing adenovirus. (C) The actual representation of the wild-type contamination PCR assay. Lane 1 represents a 1 kb gene ruler from Thermo Fisher. Lanes 5 and 9 represent the unmodified Ad5/3- Δ 24 virus. Lanes 2 and 6 represent CXCL9-expressing adenovirus. Lanes 3 and 7 represent CXCL10-expressing adenovirus. Lanes 4 and 8 represent IL-15-expressing adenovirus.

DISCUSSION

Oncolytic adenoviruses have become ideal agents to treat cancer due to their specific tumor tropism. To achieve a long-term response, such viruses need to induce an anti-tumor response.⁴ In doing so, scientist have armed oncolytic adenoviruses with various immune-stimulating agents. Yet, the current methods to genetically modify the adenoviruses are rather complex, time consuming, and expensive. In spite of this, we adapted a novel method to genetically modify oncolytic adenoviruses using GA, which is faster, cheaper, and more convenient than other methods.

GA has been previously used, to a certain extent, to construct adenovirus genomes. However, the novelty of GAMER-Ad is that it can be done with routinely used Ad-5, Ad-5/3, and Ad-3 viruses.

Moreover, the method entails replacing the gp19k gene from E3 region with a GOI, which has not been done before by using GA. Usually, genetic manipulations are done in limited regions that are not essential for viral production, such as E1, E2A, E3, and E4.^{5,11,12} Yet, much attention has been drawn to the E3 region for genetic manipulation. The E3 region is a complex region, with multiple-gene transcription units expressing around seven different E3 proteins.¹³ This complexity causes such proteins to be expressed at varying times and levels during the course of infection. If these genes were to be substituted by a therapeutic GOI, this would provide a flexible system in which multiple transgenes could be expressed in varying and predictable levels.¹⁴ Additionally, the E3 proteins have well-known roles in immunomodulation; hence, removing such genes creates an opportunity to direct the immune responses to synergize with the therapeutic GOI.¹⁵

CXCL9, CXCL10, and IL-15 have a common role in T cell migration. To test whether the secreted chemokines/cytokines from our viruses were functional, we infected MDA-MB-436 cells with the cytokine-encoding viruses and tested peripheral blood mononuclear cell (PBMC) migration using a Transwell system. Calcein green-labeled PBMCs were placed on top of Transwells and migrated green PBMCs were then counted on the lower chamber. When MDA-MB-436 cells were infected with our cloned viruses, an increase in migratory PBMCs was observed compared to uninfected cells or cells infected with the unarmed virus (Figures 7B and 7C). The highest increase in PBMC migration was observed with Ad5/3-CXCL9, followed by Ad5/3-CXCL10. In conclusion, our cloned viruses are able to express functional chemokines/cytokines that induce lymphocyte migration.

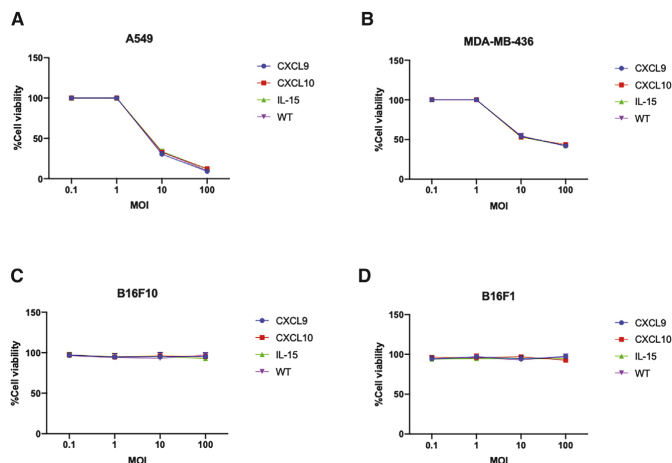


Figure 6. Oncolytic fitness

(A–D) Cell viability assay of (A) A549, (B) MDA-MB-436, (C) B16F10, and (D) B16F1 cell lines. Cell lines were infected with CXCL9 (blue), CXCL10 (red), and IL-15 (green)-expressing adenoviruses along with wild-type virus (purple). Cell viability was checked after 3 days using an (3-(4,5-dimethylthiazol-2-yl)-5-(3-carboxymethoxyphenyl)-2-(4-sulfophenyl)-2H-tetrazolium) (MTS) assay. The data are presented as mean \pm SD (n = 3).

be inconvenient with respect to time and economic efficiency. To help overcome this, we amplified the CMV and poly(A) fragments separately and assembled them with the three different cytokine/chemokine coding sequences. This was done to demonstrate the flexibility of this method and the adaptability of it where only the coding sequence of the therapeutic gene is required for future manipulations.

Beyond being one of the most widely studied viruses in clinical development for cancer therapy (source: [ClinicalTrials.gov](https://clinicaltrials.gov/), URL: <https://clinicaltrials.gov/>; search criteria: condition or disease: cancer; other terms: oncolytic virus; search date: November 26, 2019), adenoviruses have taken the main stage as the most effective vector for gene delivery due to their numerous advantages. Due to the appealing advantages adenoviruses provide, they have become the most-used gene-delivery vectors in clinical trials, accounting for more than 20% of all gene therapy trials.²² Due to the presence of the inherent restriction enzymes SrfI and BarI on multiple adenovirus serotypes (such as Ad5, Ad3, Ad6, and Ad2), our method can be applied in most adenoviruses used for gene therapy.

In conclusion, we have demonstrated a novel method to replace the gp19k gene with a therapeutic GOI. The present work compiles and describes the main steps necessary, from cloning to the production of three novel armed oncolytic adenoviruses, followed by an extensive characterization of the constructed viruses. Considering the discussed improvements, this methodology can be adopted for the generation of a limitless range of viruses to be used for different applications. We believe that our method will help the scientific community progress in the design and construction of novel armed oncolytic adenoviruses.

MATERIAL AND METHODS

Cell lines and viral genomes

Human lung cancer cell line A549, human breast cancer cell line MDA-MB-436, and murine skin cancer cell lines B16F1 and B1610 were purchased from the American Type Culture Collection (ATCC). All cell lines were cultured under appropriate conditions and regularly checked for mycoplasma contamination. In brief, A549 and MDA-MB-436 cells were cultured in Dulbecco's modified Eagle's medium (DMEM), while B16F1 and B16F10 were cultured in Roswell Park Memorial Institute (RPMI) 1640 medium. All media were supplemented with 10% fetal bovine serum and 1% penicillin/streptomycin.

Currently, many labs replace the adenoviral genes with GOI via homologous recombination using a shuttle plasmid and full-length adenoviral backbones.¹⁶ However, this process has a low efficiency, has wild-type (WT) contamination, and is time and labor intensive. Moreover, recombination takes place in a specialized *E. coli* strain, BJ5183, containing a Rec-A deficiency.^{17,18} Even though higher yields of homologous recombination are achieved, there is also a higher chance of secondary recombination events giving rise to unwanted repeat regions or secondary structures to the adenoviral genome. Hence, scientists have directed their efforts in developing easier and more efficient methods for generating recombinant adenoviruses. These methods include directly ligating cDNA into E1-deleted adenoviral genomes using Cre-loxP shuttles¹⁹ and *E. coli*-recombinant systems.²⁰ These methods have simplified this process and fixed wild-type viral DNA input problems. Nevertheless, these methods are still time consuming and not very efficient and require several steps in planning.

We have shown that our method is robust, with minimal false positives during the screening stage. An average of 75% of the colonies from the transformed GA products of Ad5/3-IL-15 tested had IL-15 assembled to the excised adenovirus genome. Usually, the official GA method entails that the overlapping ends have around 15–20 bp.²¹ In our method, 40 overlapping nucleotides seem to be very efficient in assembling products onto the adenovirus genome. Whether this could be further optimized by increasing or decreasing the overlapping region remains to be tested. Moreover, we have shown that no Ad5/3- Δ 24 contamination is found while expanding the viruses. Finally, with three different viruses we demonstrated that our method is rapid and time efficient.

The full GOI fragments to be inserted into the adenovirus genome had a size of more than 4,000 bp. Designing a GOI every time can

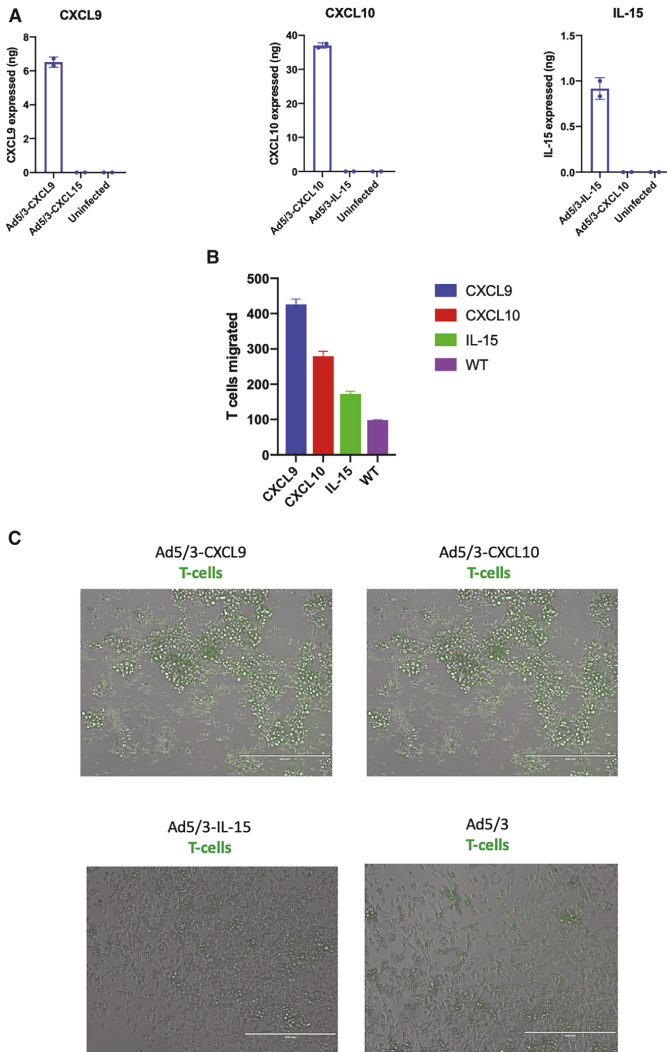


Figure 7. Functional activity of chemokine-expressing viruses

(A) Chemokines from CXCL9, CXCL10, and IL-15-expressing viruses were measured using an ELISA. A549 cells were infected with 100 MOI of the viruses indicated, and at day 2 post-infection the supernatant was collected and tested. (B) Migration was assessed using a Transwell system. Chemokine-expressing viruses were added to MDA-MB-436 cells at MOI 100 at the lower chamber. To the top chamber, calcein green-labeled PBMCs were added, and at day 2 the number of cells at the bottom (migrated cells) were counted manually. (C) Visual representation of migrated green labeled PBMCs. Scale bar, 400 nm.

Plasmid construction

A schematic of the plasmid construction can be found in Figure 2. First, poly(A) and CMV sequences were synthesized by Thermo Fisher. The poly(A) and CMV sequences contained 40 overlapping nucleotides to the adenovirus genome in the 3' and 5' ends, respectively. Also, the poly(A) fragment contained in all the genes of the E3 region except for the gp19k gene. Sequences of the poly(A) and CMV fragments can be found in Figure S1. The poly(A) and CMV fragments were amplified with CMV-Fwd and poly(A)-reverse (Rv) primers Phusion High-Fidelity DNA Polymerase (Thermo Fisher). Coding sequences of CXCL9, CXCL10, and IL-5 were synthesized and cloned in pcDNA 3.3 topo vector by Thermo Fisher. CXCL9, CXCL10, and IL-5 were then amplified, and 40 overlapping nucleotides to the CMV and poly(A) fragments were added to the 5' and 3' ends, respectively, using the primers mentioned in Table 1 using Phusion High-Fidelity DNA Polymerase (Thermo Fisher). Each chemokine fragment was then assembled with the poly(A) and CMV fragments as one fragment using the GA Master Mix (New England Biolabs) and according to manufacturer's instructions. Products were added in a 3:1:1 (poly[A]:CMV:chemokine) molar ratio, where 50 ng of poly(A) was added. The assembled products were further amplified with the CMV-Fwd and poly(A)-Rv using Phusion High-Fidelity DNA Polymerase (Thermo Fisher) to produce enough DNA quantities to proceed to the next step.

In this study, a plasmid containing the adenovirus genome pAd5/3-Δ24-E3+ was used as starting material. The plasmid contains all machinery necessary for plasmid amplification, including kanamycin resistance gene, and the genome of adenovirus serotype 5. This plasmid in particular contains a 24 bp deletion in the viral early gene E1A (Δ24) that enables the virus to replicate in Rb-deficient cells, and the knob of the fiber in the late gene L5 is replaced by the knob of a serotype 3 adenovirus.

At the same time, the pAd5/3-Δ24-E3+ was then linearized with SrfI (New England Biolabs) and BarI (SibEnzyme), releasing the E3 region, and DNA was recovered by ethanol precipitation. The assembled CMV-cytokine-poly(A) fragments were inserted into the linearized adenovirus genome using the GA Master Mix (New England

Table 1. Primers used for cloning the chemokine-expressing viruses

Primer name	Primer sequence, 5'–3'	Product (bp)	Aim
Fw-CXCL9	GATAGGCAGCCTGCACCTGAGGAGTGGCGCCGCTTTATCAGGTGGTCTTCTTCGCTT	461	amplify CXCL9 sequence and add overlaps
Rv-CXCL9	ggtaggcgtgtacgtggaggctataaagcagagctgGCCACCATGAAGAAGAGCGCGGTGCT		
Fw-CXCL10	GATAGGCAGCCTGCACCTGAGGAGTGGCGCCGCTTTATCAGGGGCTCCTCTTGCTCCT	374	amplify CXCL10 sequence and add overlaps
Rv-CXCL10	cggtgacgtggaggctctataaagcagagctgGCCACCATGAACCAGACCCGCATC		
Fw-IL15	GATAGGCAGCCTGCACCTGAGGAGTGGCGCCGCTTTATCAGCTGGTGTGATGAACAT	568	amplify IL-15 sequence and add overlaps
Rv-IL15	cggtgacgtggaggctctataaagcagagctgGCCACCATGAGGATCAGCAAGCCCA		
Rv-CMV	ATAGTGGGTGCGGATGGACAG	692	amplify CMV sequence
Fw-CMV	cagctctcttatataagctccaccg		
Fw-PolyA	GCCGAAGTTCAGATGACTAACTCAG	2,543	amplify poly(A) sequence
Rv-polyA	TGATAAAGCGCCGCACTCCTCAGGTGC		

Biolabs) according to manufacturer's instructions. A 3:1 (insert:vector) molecular ratio was used, where 1.3 µg of the linearized adenovirus genome was added. Approximately 2 µL of assembled products were transformed into DH5-*alpha E. coli* cells, spread on kanamycin-containing LB agar and incubated overnight at 37°C. Positive colonies were picked and grown on kanamycin selection LB medium. Plasmid DNA was isolated from each colony and analyzed using Sanger sequencing or restriction enzyme analysis using EcoRI.

Packaging and amplification of adenoviruses

Adenovirus genomes were first digested with PacI to release the kanamycin resistance gene. The linearized genome was then rescued by ethanol precipitation, and approximately 3 µg was transfected into A549 cells seeded in a T25 cell culture flask using Effectene (QIAGEN). When cytopathic effect (CPE) was observed, cultures were harvested, subjected to four freeze-thaw cycles, and centrifuged to remove the cellular debris, and the supernatant was preserved at 80°C and used as the seed virus. The next round of amplification was performed similarly, but this time using a T175 cell culture flask, and the last round of amplification was performed in a 10-layer cell culture multi-flask.

Purification of adenoviruses

Cells infected with the different adenoviruses were observed under the microscope daily, and once they displayed a clear CPE, cells were further detached from the flask by strongly tapping the cell culture flask. Cells were collected by centrifugation, and the cell pellets were resuspended in 7 mL of cultured medium and subjected to four freeze-thaw cycles. The lysates were further centrifuged to remove cell debris, and supernatant was collected. Viruses were purified using a two-stage CsCl gradient procedure followed by ultracentrifugation. The purified adenoviruses were dialyzed overnight against A195 buffer, formulated by Evans et al.²³ Dialyzed viruses were aliquoted and stored at –80°C for further use.

Colony PCR

Single colonies were picked and added to 20 µL of MilliQ (MQ) water. Samples were then boiled at 95°C for 5 min. One microliter was used as a DNA template, and the following primers were used to conduct the PCR:

Forward (FW) primer: 5'-TGATGTCTCTCTCCAGC-3'

RV primer: 5'-ATTATGCCAGTACATGACC-3'

Viral particle titering

Viral particles were titered by measuring the optical density (OD) at 260 nm. First, virus preparations were mixed with virus lysis buffer (VBL) containing 10 mM Tris-HCL, 1 mM EDTA, and 0.5% SDS in a 1:3 (virus:VBL) ratio. Samples were incubated at 95°C for 15 min and absorbance at 260 nm was measured. VP was calculated using the following formula:

$$\text{Viral particle / ml} = \text{OD}_{260} \times \text{dilution factor} \times 1.1 \times 10^{12}.$$

Infectious titer determination

A549 cells were seeded in a 24-well plate and infected with series of 10-fold dilutions of the virus. After 48 h of incubation at 37°C, cells were fixed with ice-cold methanol and washed with PBS containing 1% bovine serum albumin. Cells were incubated with mouse anti-hexon antibody, followed by secondary horseradish peroxidase (HRP)-conjugated antibody against mouse. Cells were incubated with 3,3' Diaminobenzidine (DAB) solution according to manufacturer's instructions until a clear color formation was detected by naked eye. At this point, the reaction was quenched with PBS and the stained cells were counted under a BF microscope. The calculations of the infectious titer were done using the following formula:

$$\text{Infectious units / mL} = x \times \frac{A(\text{well})}{A(\text{field})} \times \frac{1}{d} \times \frac{1 \text{ mL}}{V},$$

where x is the average of infected cells per field, $A(\text{well})$ is the surface area of the well (in this case is equal to 190 mm²), $A(\text{field})$ is the surface area of the field, d is the dilution factor used, and V is the volume of virus dilution applied per well in milliliters.

Cell viability assay

Cells were plated in a 96-well plate, and on the following day cells were infected at different multiplicities of infection (MOIs). Three-day post-infection cell viability was assessed using a MTS assay and

performed according to manufacturer's protocol (CellTiter 96 AQueous One Solution Cell Proliferation Assay, Promega) according to manufacturer's instructions. Absorbance was measured at 490 nm using Varioskan LUX multimode microplate reader (Thermo Fisher).

Wild-type contamination assay

Virus preparations were first incubated at 95°C for 15 min to release the genomic DNA from the viral capsid. A PCR was performed using DreamTaq Polymerase (Thermo Fisher).

To analyze wild-type viruses, the following primers were used: 5'-tttcctaataagctgcgtc-3' (reverse) and 5'-attcaagcaactctacgggct-3' (forward). To analyze genetically modified viruses, the following primers were used: 5'-ccagtagcatgacattatg-3' (reverse) and 5'-ttgtccagccaatcag-3' (forward).

Transwell migration assays

Migration was tested using a Transwell (Corning) with a 6.5 µm pore membrane. In the bottom (apical side) 100,000 MDA-MB-436 cells were added and infected at MOI 100. On the top (basolateral side), 10⁵ PBMCs stained with calcein green (Thermo Fisher) according to manufacturer's instructions, were added. After two days, green-labeled PBMCs that translocated to the bottom of the Transwell were counted manually.

Concentrations of cytokines

A549 cells were infected with 100 MOI of virus, and supernatant was collected. From the supernatant, the concentrations of CXCL9, CXCL10, and IL-15 were measured using the respective ELISA Duo Set test (R&D Systems) according to the manufacturer's instructions.

SUPPLEMENTAL INFORMATION

Supplemental Information can be found online at <https://doi.org/10.1016/j.omtm.2021.01.014>.

ACKNOWLEDGMENTS

F.H. thanks the Research Foundation of the University of Helsinki for funding his doctoral studies at the Faculty of Pharmacy, Helsinki University. E.Y. acknowledges the Academy of Finland (project no. 1317206). V.C. acknowledges the European Research Council under the Horizon 2020 framework (<https://erc.europa.eu>); ERC consolidator grant (agreement no. 681219); Jane and Aatos Erkko Foundation (project no. 4705796); HiLIFE Fellow (project no. 797011004); Cancer Finnish Foundation (project no. 4706116); and Magnus Ehrnrooth Foundation (project no. 4706235).

AUTHOR CONTRIBUTIONS

F.H., B.M., E.Y., and V.C. conceived and planned all the experiments. F.H., M.F., and Y.G. carried out most of the experiments. E.Y., M.F., S.F., J.C., B.M., M.F., and M.G. helped in carrying out most of the experiments. E.Y. and V.C. supervised the project. F.H., B.M., E.Y., M.G., and V.C. wrote and corrected the paper. All authors provided critical feedback and helped shape the research, analysis, and manuscript.

DECLARATION OF INTERESTS

The authors declare no competing interests.

REFERENCES

- Hyman, D.M., Taylor, B.S., and Baselga, J. (2017). Implementing Genome-Driven Oncology. *Cell* 168, 584–599.
- Ylösmäki, E., and Cerullo, V. (2020). Design and application of oncolytic viruses for cancer immunotherapy. *Curr. Opin. Biotechnol.* 65, 25–36.
- Pitt, J.M., Marabelle, A., Eggermont, A., Soria, J.C., Kroemer, G., and Zitvogel, L. (2016). Targeting the tumor microenvironment: removing obstruction to anticancer immune responses and immunotherapy. *Ann. Oncol.* 27, 1482–1492.
- Andtbacka, R.H.L., Kaufman, H.L., Collichio, F., Amatruda, T., Senzer, N., Chesney, J., Delman, K.A., Spitzer, L.E., Puzanov, I., Agarwala, S.S., et al. (2015). Talmogene laherparepvec improves durable response rate in patients with advanced melanoma. *J. Clin. Oncol.* 33, 2780–2788.
- Marelli, G., Howells, A., Lemoine, N.R., and Wang, Y. (2018). Oncolytic viral therapy and the immune system: A double-edged sword against cancer. *Front. Immunol.* 9, 866.
- Kennedy, M.A., and Parks, R.J. (2009). Adenovirus virion stability and the viral genome: size matters. *Mol. Ther.* 17, 1664–1666.
- Wold, W.S., and Toth, K. (2013). Adenovirus vectors for gene therapy, vaccination and cancer gene therapy. *Curr. Gene Ther.* 13, 421–433.
- Yoon, A.R., Hong, J., Kim, S.W., and Yun, C.O. (2016). Redirecting adenovirus tropism by genetic, chemical, and mechanical modification of the adenovirus surface for cancer gene therapy. *Expert Opin. Drug Deliv.* 13, 843–858.
- Gibson, D.G., Young, L., Chuang, R.Y., Venter, J.C., Hutchison, C.A., 3rd, and Smith, H.O. (2009). Enzymatic assembly of DNA molecules up to several hundred kilobases. *Nat. Methods* 6, 343–345.
- Lee, C.S., Bishop, E.S., Zhang, R., Yu, X., Farina, E.M., Yan, S., Zhao, C., Zheng, Z., Shu, Y., Wu, X., et al. (2017). Adenovirus-mediated gene delivery: Potential applications for gene and cell-based therapies in the new era of personalized medicine. *Genes Dis.* 4, 43–63.
- Sebestyen, Z., de Vrij, J., Magnusson, M., Debets, R., and Willemsen, R. (2007). An oncolytic adenovirus redirected with a tumor-specific T-cell receptor. *Cancer Res.* 67, 11309–11316.
- Flint, S.J., Wewerka-Lutz, Y., Levine, A.S., Sambrook, J., and Sharp, P.A. (1975). Adenovirus transcription. II. RNA sequences complementary to simian virus 40 and adenovirus 2DNA in AD2+ND1- and AD2+ND3-infected cells. *J. Virol.* 16, 662–673.
- Kelly, T.J., Jr., and Lewis, A.M., Jr. (1973). Use of nondefective adenovirus-simian virus 40 hybrids for mapping the simian virus 40 genome. *J. Virol.* 12, 643–652.
- Berkner, K.L., and Sharp, P.A. (1983). Generation of adenovirus by transfection of plasmids. *Nucleic Acids Res.* 11, 6003–6020.
- Wold, W.S.M., Tollefson, A.E., and Hermiston, T.W. (1995). E3 transcription unit of adenovirus. *Curr. Top. Microbiol. Immunol.* 199, 237–274.
- Hawkins, L.K., Johnson, L., Bauzon, M., Nye, J.A., Castro, D., Kitzes, G.A., Young, M.D., Holt, J.K., Trown, P., and Hermiston, T.W. (2001). Gene delivery from the E3 region of replicating human adenovirus: evaluation of the 6.7 K/gp19 K region. *Gene Ther.* 8, 1123–1131.
- Wold, W.S.M., Doronin, K., Toth, K., Kuppuswamy, M., Lichtenstein, D.L., and Tollefson, A.E. (1999). Immune responses to adenoviruses: viral evasion mechanisms and their implications for the clinic. *Curr. Opin. Immunol.* 11, 380–386.
- He, T.C., Zhou, S., Da Costa, L.T., Yu, J., Kinzler, K.W., and Vogelstein, B. (1998). A simplified system for generating recombinant adenoviruses. *Proc. Natl. Acad. Sci. USA* 95, 2509–2514.
- West, S.C. (1994). The processing of recombination intermediates: mechanistic insights from studies of bacterial proteins. *Cell* 76, 9–15.
- Camerini-Otero, R.D., and Hsieh, P. (1995). Homologous recombination proteins in prokaryotes and eukaryotes. *Annu. Rev. Genet.* 29, 509–552.
- Hardy, S., Kitamura, M., Harris-Stansil, T., Dai, Y., and Phipps, M.L. (1997). Construction of adenovirus vectors through Cre-lox recombination. *J. Virol.* 71, 1842–1849.
- Tan, R., Li, C., Jiang, S., and Ma, L. (2006). A novel and simple method for construction of recombinant adenoviruses. *Nucleic Acids Res.* 34, e89.
- Evans, R.K., Nawrocki, D.K., Isopi, L.A., Williams, D.M., Casimiro, D.R., Chin, S., Zhu, D.M., Shiver, J.W., and Volkin, D.B. (2004). Development of stable liquid formulations for adenovirus-based vaccines. *J. Pharm. Sci.* 93, 2458–2475.

STUDY II

Novel oncolytic adenovirus expressing enhanced cross-hybrid IgG A Fc PD-L1 inhibitor activates multiple immune effector populations leading to enhanced tumor killing in vitro, in vivo and with patient-derived tumor organoids

Firas Hamdan ^{1,2,3} Erko Ylösmäki ^{1,2,3} Jacopo Chiaro,^{1,2,3} Yvonne Giannoula,¹ Maeve Long,⁴ Manlio Fucciello ^{1,2,3} Sara Feola ^{1,2,3} Beatriz Martins,^{1,2,3} Michaela Feodoroff,^{1,2,3} Gabriella Antignani,^{1,2,3} Salvatore Russo,^{1,2,3} Otto Kari,³ Moon Hee Lee,^{2,5} Petrus Järvinen,⁶ Harry Nisen,⁶ Anna Kreutzman,^{1,2,3} Jeanette Leusen ⁷ Satu Mustjoki ^{2,5,8,9} Thomas G McWilliams,^{4,10} Mikaela Grönholm,^{1,2,3,8} Vincenzo Cerullo ^{1,2,3,8,11}

To cite: Hamdan F, Ylösmäki E, Chiaro J, *et al.* Novel oncolytic adenovirus expressing enhanced cross-hybrid IgG A Fc PD-L1 inhibitor activates multiple immune effector populations leading to enhanced tumor killing in vitro, in vivo and with patient-derived tumor organoids. *Journal for ImmunoTherapy of Cancer* 2021;**9**:e003000. doi:10.1136/jitc-2021-003000

► Additional supplemental material is published online only. To view, please visit the journal online (<http://dx.doi.org/10.1136/jitc-2021-003000>).

EY and JC contributed equally.

Accepted 21 July 2021



© Author(s) (or their employer(s)) 2021. Re-use permitted under CC BY-NC. No commercial re-use. See rights and permissions. Published by BMJ.

For numbered affiliations see end of article.

Correspondence to
Professor Vincenzo Cerullo;
vincenzo.cerullo@helsinki.fi

ABSTRACT

Background Despite the success of immune checkpoint inhibitors against PD-L1 in the clinic, only a fraction of patients benefit from such therapy. A theoretical strategy to increase efficacy would be to arm such antibodies with Fc-mediated effector mechanisms. However, these effector mechanisms are inhibited or reduced due to toxicity issues since PD-L1 is not confined to the tumor and also expressed on healthy cells. To increase efficacy while minimizing toxicity, we designed an oncolytic adenovirus that secretes a cross-hybrid Fc-fusion peptide against PD-L1 able to elicit effector mechanisms of an IgG1 and also IgA1 consequently activating neutrophils, a population neglected by IgG1, in order to combine multiple effector mechanisms.

Methods The cross-hybrid Fc-fusion peptide comprises of an Fc with the constant domains of an IgA1 and IgG1 which is connected to a PD-1 ectodomain via a GGGG linker and was cloned into an oncolytic adenovirus. We demonstrated that the oncolytic adenovirus was able to secrete the cross-hybrid Fc-fusion peptide able to bind to PD-L1 and activate multiple immune components enhancing tumor cytotoxicity in various cancer cell lines, in vivo and ex vivo renal-cell carcinoma patient-derived organoids.

Results Using various techniques to measure cytotoxicity, the cross-hybrid Fc-fusion peptide expressed by the oncolytic adenovirus was shown to activate Fc-effector mechanisms of an IgA1 (neutrophil activation) as well as of an IgG1 (natural killer and complement activation). The activation of multiple effector mechanism simultaneously led to significantly increased tumor killing compared with FDA-approved PD-L1 checkpoint inhibitor (Atezolizumab), IgG1-PDL1 and IgA-PDL1 in various in vitro cell lines, in

vivo models and ex vivo renal cell carcinoma organoids. Moreover, in vivo data demonstrated that Ad-Cab did not require CD8 + T cells, unlike conventional checkpoint inhibitors, since it was able to activate other effector populations.

Conclusion Arming PD-L1 checkpoint inhibitors with Fc-effector mechanisms of both an IgA1 and an IgG1 can increase efficacy while maintaining safety by limiting expression to the tumor using oncolytic adenovirus. The increase in tumor killing is mostly attributed to the activation of multiple effector populations rather than activating a single effector population leading to significantly higher tumor killing.

INTRODUCTION

Immune checkpoint inhibitor (ICI) therapies have been established as a potent treatment option for a plethora of tumor types and have significantly expanded the therapeutic armamentarium in oncology. Such agents target immune inhibitory receptors and interrupt coinhibitory signaling pathways, abrogating their immunosuppressive function and consequently revitalizing anti-tumor immune response. The consequent restoration of immune-mediated elimination of tumor cells leads to long-term, sustained tumor responses,^{1,2} resulting in their approval as first-line treatments for a growing list of malignancies.³ Nevertheless, accumulating evidence indicate that checkpoint inhibitors can only benefit a fraction of patients.⁴

In spite of such limitations, there has been a shift of focus in improving ICIs therapeutic efficacy. All clinically approved ICIs are antibodies that primarily act as antagonizing agents with their main mechanism of action being the reconstitution of a T-cell response by disrupting an immunosuppressive axis.⁵ Nevertheless, ICIs are either limited or entirely not able to elicit crucial antibody-dependent effector mechanisms⁶ such as complement-dependent cytotoxicity (CDC) or antibody-dependent cell cytotoxicity/phagocytosis (ADCC/ADCP) which are pertinent to an antibody. Based on clinical data, activation of effector mechanisms are a necessity for therapeutic antibodies to achieve tumor clearance.⁷ Moreover, effector mechanisms such as ADCC and CDC have been noticed to be an essential requirement for enhanced antitumor responses for some modified ICIs against CTLA-4⁸ or PD-L1.^{9,10} Thus, equipping or enhancing ICIs with such effector mechanism via the Fc-fragment may lead to improved efficacy, resulting in higher response rates in the clinic.

In the clinic, all therapeutic antibodies against cancer are of the IgG isotype and predominantly of the IgG1 subtype. This is primarily due to the ability of an IgG to activate the complement system and natural killer cells (NK), leading to tumor killing. Yet, IgG fails to efficiently activate the most abundant leukocyte population able to infiltrate solid tumors, neutrophils. This is mostly due to the relatively high expression of inhibitory Fc- γ IIB (CD32B)¹¹ and Fc- γ IIIB (CD16B),¹² which do not contain any signaling motif yet has been seen to block the activation of ADCC.¹³ In order to capitalize on such a promising population, IgA antibodies have been used since they bind to the Fc- α receptor, CD89, which is highly expressed on neutrophils, monocytes and macrophages consequently eliciting ADCC or ADCP.^{14,15} In addition, the Fc- α -mediated activation of neutrophils by IgA antibodies has been shown to be more effective in tumor killing than the Fc- γ -mediated effector mechanisms by IgG antibodies in multiple types of cancers.¹⁶ However, it has been shown that the addition of both IgG and IgA antibodies further enhances tumor cytotoxicity.¹⁷

Here, we have developed a Fc-fusion peptide against PD-L1 consisting of a cross-hybrid Fc region containing constant regions of an IgG1 and an IgA1, termed IgGA,¹⁸ connected to a PD-1 ectodomain, carrying mutations that increase its affinity towards PD-L1 via a glycine linker. However, carrying a competent/functional Fc region can be a double-edged sword since immune checkpoints are expressed ubiquitously and such antibodies are systemically administered, frequently causing irAEs.¹⁹ To circumvent this obstacle, we limited the expression of the Fc-fusion peptide directly into the tumor microenvironment by cloning it into an oncolytic adenovirus. Oncolytic viruses have become ideal gene therapy vehicles because they are able to selectively infect and kill tumor cells while leaving healthy tissues intact, as shown in preclinical trials and patients.²⁰ Moreover, preclinical and clinical research has demonstrated that these agents specifically express

their transgenes to the tumor microenvironment with limited leakage.^{21,22}

We demonstrated that the cross-isotype Fc region gives the ICI the ability to elicit effector mechanisms of both an IgA and an IgG isotype in various tumor cell lines. The subsequent activation of multiple effector mechanisms further enhanced tumor killing and was shown to be superior than a PD-L1 IgG1 antibody or Atezolizumab, a currently approved FDA ICI. To further evaluate the efficacy of the Fc fusion peptide, we tested our engineered adenovirus (named Ad-Cab) in multiple *in vivo* tumor models and showed significantly enhanced tumor growth control as compared with unarmed adenovirus or ICI against murine PD-L1. Finally, to examine the oncolytic efficacy of the Ad-Cab in a testing platform with high clinical response predictability, we used renal cell carcinoma patient-derived organoids (RCC PDO). In this model, we showed significantly enhanced tumor cell lysis as compared with Atezolizumab or an anti-PD-L1 IgG antibody with functional Fc region.

Cell lines and antibodies

Human lung cancer cell line A549 ((ATCC Cat# CRM-CCL-185, RRID:CVCL_0023), human breast cancer cell line MDA-MB-436 ((ATCC Cat# HTB-130, RRID:CVCL_0623), murine colon adenocarcinoma CT26 (ATCC Cat# CRL-2638, RRID:CVCL_7256), murine breast cancer cell line 4T1 (ATCC Cat# CRL-2539, RRID:CVCL_0125) and murine skin cancer cell lines B16F1 (ATCC Cat# CRL-6323, RRID:CVCL_0158) and B1610 (ATCC Cat# CRL-6475, RRID:CVCL_0159) were purchased from the American Type Culture Collection (ATCC) after 2013. Cell lines were thawed at passage 5 and kept in culture until reaching passage 15. All cell lines were authenticated by the ATCC, cultured under appropriate conditions and regularly checked for mycoplasma contaminations. Atezolizumab and IgG1-PD-L1 were purchased from Invivogen. IgA-PD-L1 was kindly provided by Dr Jeanette Leusen of Utrecht University Medical University.

Preparation of conditionally replicating adenovirus and transgene modifications

All adenoviruses were generated as conditionally replicating adenoviruses using standard protocols previously described.²³ Ad-Cab and unarmed viruses are of the chimeric 5/3 serotype with a 21-nucleotide deletion in the E1A region resulting in selective replication in Rb-deficient pathway cells. Ad-RFP has the same genetic modification in E1A but originates from the serotype 5. All transgenes were cloned by replacing the gp19K+7.1K region in the E3 gene using Gibson-Assembly previously described.²⁴

Generation of Fc-fusion peptide

The Fc-Fusion peptide consists of a chimeric Fc containing constant domains of an IgG1 and IgA connected to an enhanced PD-1 ectodomain via five GGGS linkers. The

cross-hybrid Fc has been described¹⁸ as well as the PD-1 ectodomain.²⁵

Cell viability assays

A total of 10,000 cells were plated in a 96-well plate overnight and subsequently infected at different MOIs. Three-day postinfections cell viability was determined by MTS according to the manufacturer's protocol (Cell Titer 96 AQueous One Solution Cell Proliferation Assay; Promega, Nacka, Sweden). Spectrophotometric data were acquired with Varioskan LUXMultimode Reader (Thermo Scientific, Carlsbad, C, USA) operated by SkanItsoftware.

Competition assay

A total of 100,000 A549 cells were plated in a 96-well, washed with PBS and incubated with various concentrations of purified Fc-fusion peptide for 45 min on ice. Next, 10 µg/mL of Atezolizumab (Invivogen, Cat# hpd11-mab12) was added and incubated for 30 min on ice. Atezolizumab was then detected by staining with a PE labeled antihuman IgG (BioLegend Cat# 409303, RRID:AB_10900424). Cells were then washed and resuspended in PBS. Competition was then quantified by flow cytometry using the BD Accuri 6 plus (BD Biosciences) and analyzed using the FlowJo software (FlowJo, V.10.7.1, RRID:SCR_008520).

PBMCs, PMN and serum collection

A total of 40 mL of blood was collected from healthy volunteers in BD Vacutainer collection tubes (BD Bioscience) and allowed to clot for 30 min at room temperature. After clotting, clots were removed, and samples centrifuged for 5 min at 2500 rpm. Separated serum was collected and samples from 15 volunteers were pooled together. Polymorphonuclear cells (PMNs) and peripheral blood mononuclear cells (PBMCs) were isolated from buffy coats as previously described.¹⁸ The PBMC and PMN layers were subsequently removed between serum and Ficoll or in the Histopaque layer, respectively, and cultured in 1xRPMI (Roswell Park Memorial Institute, Gibco, Cat# 21875034)-

Mixed leukocyte reaction

Monocytes were first isolated from PBMCs as previously described. Following isolation, monocytes were differentiated using DMEM low glucose supplemented with 10% FBS, 500 U/mL of IL-4 (PeproTech, #200-04) and 250 U/mL of GM-CSF (Adcam, ab88382) for 7 days. PBMCs from a different donor were freshly isolated, labeled with CFSE and incubated with monocyte-derived dendritic cells for 5 days at a ratio of 1:10 in the presence of 1 µg/mL of Atezolizumab or isolated IgG A Fc-fusion peptide. Cells from the supernatant were then collected and using flow cytometry CFSE was measured in CD3 + CD8+ T cells.

Complement-dependent cytotoxicity assay

A total of 100,000 cancer cells were plated per well to a 96-well plate and infected with 10 or 100 MOI of virus

for 48 hours at 37°C. Then, complement active pooled human serum or heat inactivated serum (by incubating serum at 56°C for 30 min) was added to a final concentration of 15.5% and incubated for 4 hours. Subsequently, lysis was quantified by washing cells and stained with 7-amino-actinomycin D (7-AAD) (eBioscience, Cat# 00-6993-50) and measured by flow cytometry.

Antibody-dependent cell cytotoxicity assays

ADCC assays were performed through measuring cell killing by determining the amount of LDH released using a colorimetric assay (CyQUANT LDH Cytotoxicity Assay, Cat# C20303). A total of 15,000 cells were then seeded and infected with 10 or 100 MOI of virus for 48 hours at 37°C. Afterwards, PBMCs or PMNs were added in a 100:1 or 40:1 ratio (E: T), respectively, and incubated for 4 hours at 37°C. LDH was measured using the mentioned kit and percent cytotoxicity was calculated as follows: Percent cytotoxicity = ("experimental" – "effector plus target spontaneous") / ("target maximum" – "target spontaneous") × 100%, where "experimental" corresponds to the signal measured in a treated sample, "effector plus target spontaneous" corresponds to the signal measured in the presence of PMN or PBMC and tumor cells alone and "target maximum" corresponds to the signal measured in the presence of detergent lysed tumor cells

Antibody-dependent cell phagocytosis

Around 2,000,000 freshly isolated PBMCs were cultured in a T25 culture flask for 2 hours at 37°C. Floating cells were removed, and adherent monocytes were differentiated into macrophages by culturing in RPMI supplemented with 50 µg/mL of M-CSF (Sigma Aldrich, Cat# M6518) for 7 days at 37°C. 10,000 cells were incubated and infected with indicated viruses at 10 and 100 MOI for 48 hours. Cells were then labeled with CFSE (ThermoFisher), according to the manufactures instructions and monocyte-differentiated macrophages were added at a 5:1 effector:target ratio. After 4 hours, supernatant containing macrophages were removed and CFSE was measured using flow cytometry.

Trogocytosis

Trogocytosis was performed as previously described.²⁶ In brief, 5000 cells were infected with 100 MOI of virus and incubated for 48 hours at 37°C. Cell's lipid membrane were labeled with 5 µm of DiO (ChemCruz, Cat# sc-214168), a lipophilic membrane dye, for 30 min at 37°C. Cells were washed and incubated with PMNs at a 40:1 (E:T) ratio. Samples were fixed using Paraformaldehyde (Sigma Aldrich) and measured using flow cytometry. Trogocytosis was measured by first gating on the neutrophil population and measuring the mean fluorescent intensity (MFI) of cells positive for DiO.

Real-time quantitative analysis (xCELLigence assay)

The ability to induce ADCC was analyzed using the impedance-based real-time cytotoxicity assay with the xCELLigence system (ACEA Biosciences, San Diego,

California, USA). In each well, 25,000–100,000 cells were plated for 24 hours. Five $\mu\text{g}/\text{mL}$ of designated antibody or purified Fc-fusion peptide was added along with PBMCs and PMNs at a 10:1 and 4:1 effector:target ratio. Cell index was measured every 5 min for a period of 6 hours. Killing rate was obtained by constructing a linear trend-line and calculating the slope.

Live cell imaging

Imaging target to effector cell contacts, 15,000 A549 cells were plated per well of a 24 well plate (Corning) overnight. Cells were imaged for 30 min and subsequently treated with 10 $\mu\text{g}/\text{mL}$ of indicated Fc-fusion peptides and PBMCs were added at 10:1 E:T ratio. The videos were acquired using an ANDOR Spinning Disc Microscope equipped with a Zyla camera (SRApochromat $\times 100$ objective, NA 1.49). Images were acquired every 5 min over the course of 2 hours 20 min.

Live-cell killing assay was performed by plating 100,000 A549 cells per well of a 24 well plate (Corning) overnight. Fifteen minutes prior to imaging, cells were incubated with 3 μM of IncuCyte Caspace3/7 green apoptosis assay reagent (Sartorius, Cat# C10423). Cells were imaged using the IncuCyte S3 live cell analysis system equipped with a 10 \times air objective for a total of 24 hours. Images were acquired every 15 min and four fields of view were imaged per well. After 1 hour of imaging, cells were treated with indicated antibodies at 5 $\mu\text{g}/\text{mL}$ and PMNs and PBMCs were added at 100:1 and 40:1 E:T ratios, respectively. Treated cells were returned to the IncuCyte S3 and imaged for the remainder 23 hours. Videos were processed with the IncuCyte analysis software (IncuCyte Chemotaxis Software, RRID:SCR_017316) and are displayed as four fields of view per second.

Whole blood assay

Blood was collected from three healthy volunteers in BD Vacutainer Heparin plasma tubes. A total of 200 μL of unprocessed blood was then incubated with 20 $\mu\text{g}/\text{mL}$ of Tratzuzumab or IgGA Fc-fusion peptide for 24 hours. After incubation, samples were treated with ACK lysing buffer (Gibco) to remove red blood cells. Cells were then stained with CD3, CD15, CD14, CD56 and CD11c to determine immune cell populations. Absolute numbers were calculated by using precision count beads (Biolegend, Cat# 424902) and following the manufacturers instructions.

Renal cell carcinoma patient-derived samples and ethical considerations

Renal cell carcinoma samples were obtained from four patients that underwent surgical removal of the tumors. Tumor samples were collected and delivered directly from the Peijas Hospital. The study was conducted in accordance with the declaration of Helsinki and patients gave their written consent.

Syngeneic animal experiments

All animal experiments were reviewed and approved by the Experimental Animal Committee of the University of Helsinki and the Provincial Government of Southern Finland (license number ESAVI/11895/2019). Around 4–6-week-old immunocompetent female BALB/c mice, purchased from Envigo (Venray, Netherlands), injected in the right flank with either 500,000 CT26 cells or 300,000 4T1 cells and were treated 7, 9, 11, 13, 19 and 21-days post-tumor implantation with 1×10^9 viral particles of virus intratumorally or 100 $\mu\text{g}/\text{mL}$ of mPD-L1 (Bio X Cell Cat# BE0101, RRID:AB_10949073) intraperitoneally. Viral treatments were administered in 25 μL volume while antibodies were given in 100 μL . Tumor size was measured every second day and calculated using the following formula: (long side) \times (short side)²/2. Mice were sacrificed when any side of the tumor reached 16 mm.

As for in vivo CD8 depletion, mice were initially injected intraperitoneally with 500 μg of depleting CD8 antibody (Bio X Cell Cat# BE0061, RRID:AB_1125541) 1 day prior to treatment and then 100 μg every 2 days for the duration of the experiment.

At day 23 (CT26) and 15 (4T1) post-tumor implantation, two animals from each group were sacrificed and blood and tumors were collected. Blood was allowed to clot, then centrifuged at 500 g for 15 min and serum was subsequently collected. Tumors were crushed through a 0.22 μm cell strainer, centrifuged at 500 g for 10 min and supernatant collected. His-tagged proteins from serum and tumor supernatant was tested using a His-tag ELISA kit (Cell Biolabs, Cat#AKR-130).

Immune deficient NS (NOD/SCID) mice

Four–six-week-old Nod.CB17-Prkdc^{scid}/NCrCrI mice were purchased from Charles River and were injected with 5×10^6 A549 cells in the right flank. Subsequently, 5×10^6 freshly isolated PBMCs were then injected intraperitoneally. After tumors were palpable, mice were treated two times (with a 3-day break in between) with 1×10^8 viral particles intratumorally.

Flow cytometry analysis

Flow cytometry analysis was done with either BD Accuri 6 plus (BD Bioscience) or Fortessa (BD Bioscience). Antibodies used include APC antimouse Ly6C (BioLegend Cat# 128015, RRID:AB_1732087), FITC antimouse NK1.1 (Thermo Fisher Scientific Cat# 11-5941-85, RRID:AB_465319), PE antimouse PD-1 (BioLegend Cat# 135206, RRID:AB_1877231), PE anti-Ly6G (BD Biosciences Cat# 551461, RRID:AB_394208), PerCP Cy5.5 antimouse CD11b (Thermo Fisher Scientific Cat# 45-0112-82, RRID:AB_953558), BV650 antimouse F4/80 (BD Biosciences Cat# 743282, RRID:AB_2741400), PeCy7 antimouse CD4 (Thermo Fisher Scientific Cat# 25-0041-82, RRID:AB_469576), PerCp/Cy5.5 antimouse CD107a (BioLegend Cat# 121626, RRID:AB_2572055), Pacific Blue antimouse CD3 (BioLegend Cat# 100214, RRID:AB_493645), PECy7 antimouse CD11c (Thermo

Fisher Scientific Cat# 25-011482, RRID:AB_469590), FITC antihuman CD56 (BioLegend Cat# 304604, RRID:AB_314446), PerCP antihuman CD8alpha (BioLegend Cat# 300922, RRID:AB_1575072), PE-Cy5 antihuman CD4 (Thermo Fisher Scientific Cat# 15-0049-42, RRID:AB_1582251), PE-Cy7 antihuman CD3 (BioLegend Cat# 300316, RRID:AB_314052), Pacific blue antihuman PD-1 (BioLegend Cat# 329915, RRID:AB_1877194), APC antihuman CD107a (BioLegend Cat# 328620, RRID:AB_1279055), APC antihuman CD11c (BioLegend Cat# 371505, RRID:AB_2616901), Pacific Blue antihuman CD15 (BioLegend Cat# 323021, RRID:AB_2105361) and PE antihuman CD14 (BioLegend Cat# 301805, RRID:AB_314187).

Renal cell carcinoma patient-derived organoid culturing

Frozen dissociated cells were grown in DMEM/F12 media in 30% Matrigel (Corning, Cat# 354230) on ultralow attachment plates (ULA Corning, Cat# 3473). Cells were split and washed with gentle cell dissociation media (Stemcell, Cat# 07174) and 10,000 cells mixed with 30% Matrigel and grown for 1 week before the experiment. DMEM/F12 media was supplemented with 5% FBS, 8,4ng/mL of cholera toxin (Sigma, Cat# C8052), 0.4 µg/mL hydrocortisone (Sigma, Cat# H4001), 10ng/mL epidermal growth factor (Corning, Cat# 354052), 24 µg/mL Adenine (Sigma, Cat# A8626), 5 µg/mL insulin (Sigma, 91077C) and 10 µM of Y27632 RHO inhibitor (Sigma, Cat# SCM075).

Immunofluorescence and flow-cytometry on renal cell carcinoma patient-derived organoids

Gentle cell dissociation media was used on organoid cultures, and cells washed and carefully pipetted to dissociate cells. Cells were plated on 8 well Nunc; Lab-Tek; II Chamber Slides and cultured for 4 days. Cells were fixed in 4% cold paraformaldehyde and stained with CAIX (Novus Cat# NBP1-51691, RRID:AB_11011250), Vimentin (2D1) (Novus, Cat# 92687AF647), or Cytokeratin pan (AE-1/AE-3) (Novus Cat# NBP2-33200AF750, RRID:AB_2868569) or Alexa Fluor 633 Phalloidin (Invitrogen, Cat# A22284) Microscopy pictures were taking using an EVOS FL cell imaging system (Thermo Fisher Scientific).

Ad-RFP infection and PBMC co-culture with renal cell carcinoma patient-derived organoids

A total of 100,000 VPs of Ad5-RFP were added on top of the media of already cultured organoids and RFP expression was then monitored. Cell viability of PDOs was monitored by adding 1 µM of Calcein AM (Thermo Fisher Scientific, Cat# C1430).

As for coculturing, a total of 15,000 isolated PBMCs were first stained with 1 µM Calcein AM and added on top of the media of RCC PDOs and cultured for 4 hours at 37°C. PBMC invasion was then visualized using the EVOS FL cell imaging system

Antibody-dependent cell cytotoxicity assays with renal cell carcinoma patient-derived organoid

RCC PDOs were infected with viruses at 10 or 100 MOI by adding it on top of the supernatant media and incubated for 72 hours at 37°C. PBMCs and PMNs were then added individually or combined at 100:1 and 40:1 (E:T), respectively. The number of cells in the organoids were assumed to be 10,000. After 4 hours of incubation at 37°C, cell killing was measured by determining the amount of LDH released using a colorimetric assay (CyQUANT LDH Cytotoxicity Assay, Cat# C20303). Specific lysis was then calculated as stated before.

Statistical analysis

Statistical analysis was performed using GraphPad Prism 7 (GraphPad Software, La Jolla, California, USA). Data were analyzed using an unpaired t-test where $n \geq 3$. Levels of significance were set at * $p < 0.05$, ** $p < 0.01$, *** $p < 0.001$ and **** $p < 0.0001$. Error bars represent SEM.

RESULTS

Characterization of an oncolytic adenovirus expressing IgA-chimeric anti-PD1 Fc-fusion peptides

In this study, we generated an oncolytic adenovirus, Ad-Cab (Adenovirus-ChimericAntibody), expressing a chimeric IgG-IgA (IgGA) Fc linked to an enhanced PD-1 ectodomain via a glycine linker able to bind to PD-L1 (figure 1A). This was cloned in the gp19K+7.1K region of the E3A gene (figure 1B) and with an MTS cell viability assay, we could show that the genetic modification did not affect the oncolytic fitness or replication of the virus (online supplemental figure S1A).

First, the Fc-fusion peptide production was tested by western blot analysis. Ad-Cab was able to secrete a 100 kDa Fc-fusion peptide, under native conditions, in the supernatant of A549 cells at 48 hours after incubation (online supplemental figure S1B). As expected, the Fc-fusion peptide comprised of a homodimer connected via a sulfide bridge, since a 50 kDa band was observed under denaturing conditions (online supplemental figure S1B). Next, we assessed the amount of Fc-fusion peptide secreted at different time points of infection. After 1 day of infection in A549 cells, Ad-Cab secreted approximately 2 µg of the Fc-fusion peptide and production kept increasing till day 3 reaching 7 µg (figure 1C). To assess whether the produced Fc-fusion peptide could bind to PD-L1, we performed a competition assay with a commercially available anti-PD-L1 (Atezolizumab), a well-established binder of PD-L1 and disruptor of the PD-1/L1 axis. To this end, we cocubated A549 cells with increasing concentrations of Fc-fusion peptides, purified from the supernatant of infected cells, followed by the addition of 10 µg/mL of Atezolizumab. Detection of bound Atezolizumab to PD-L1 was then analyzed by adding a secondary PE labeled antihuman IgG not able to recognize the Fc-fusion peptide. When no Fc-fusion peptide was added Atezolizumab was able to bind to PD-L1 (figure 1D). Yet, as the concentration

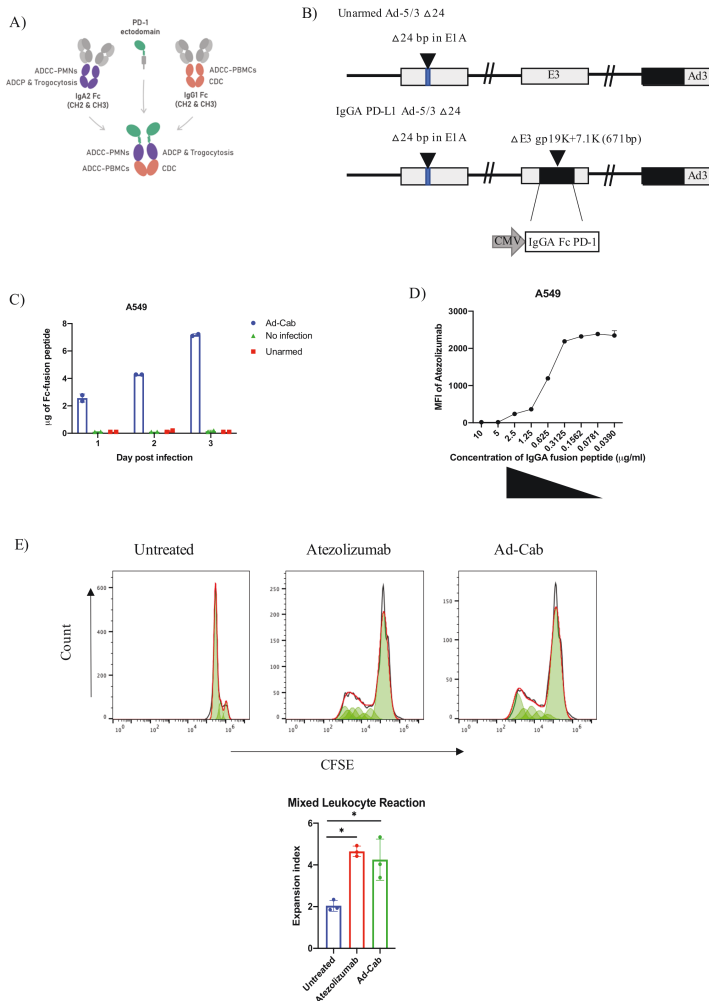


Figure 1 Characterization of Ad-Cab. (A) Graphical representation of the IgGA Fc-fusion protein; the cross-isotype Fc is made up of the CH chains 2 and 3 of an IgA2 (purple) and IgG1 (orange) attached to an PD-1 ectodomain (green) via a glycine linker. The IgGA Fc employs effector mechanism of both an IgG1 and IgA2. (B) Schematic representation of oncolytic adenovirus 5/3 delta 24 (Ad5/3 Δ24) constructs with modifications in the E1, E3 and fiber regions. Black inverted triangles represent deletions. Both unarmed Ad5/3 Δ24 (Unarmed) and IgGA PD-L1 Ad-5/3 Δ24 (Ad-Cab) have a 24 base-pair deletion in the E1 region, leading to conditionally replicate in Rb-deficient cells, and a serotype 5 fiber knob with serotype 3 knob. The IgGA PD-L1 fusion protein cassette consisted of CMV promoter and enhancer and was cloned into the gp19k+71.k region. (C) Quantification of IgGA Fc-fusion proteins over time. A549 cells were infected with 100 MOI of Ad-Cab and Unarmed virus and supernatants were collected at different indicated time points. IgGA Fc-fusion proteins were purified, and concentration was assessed by measuring absorbance at 280 nm. (D) Competitive assay between Atezolizumab and Ad-Cab. A549 cells were incubated with different concentrations of purified IgGA Fc-fusion proteins from Ad-Cab and followed by addition of 10 μg/mL Atezolizumab. Atezolizumab binding was then analyzed using a PE-labeled antihuman IgG not recognizing IgGA Fc-fusion proteins. (E) Coincubation of monocyte-derived dendritic cells with allogeneic CFSE stained T cells, at a 1:10 ratio, in the presence of 1 μg/mL of Atezolizumab or isolated IgGA Fc-fusion peptide. CFSE was then measure from CD3 + CD+ 8T cells and the expansion index was calculated. CH, constant heavy; CMV, cytomegalovirus.

of the Fc-fusion peptide increased, Atezolizumab binding decreased substantially (figure 1D). Moreover, to further demonstrate PD-L1 binding, we conducted live cell imaging to observe whether the Fc-fusion peptide could mediate close cell-contacts when PBMC were cocultured with lung carcinoma A549 cells. When Ad-Cab (online supplemental movie S1) was added, PBMCs were shown to be in clear proximity to A549 compared with when we added Atezolizumab, a clinical PD-L1 antibody holding a N298A mutation abrogating Fc-binding (online supplemental movie S2). To test the ability for the Fc-fusion peptide to activate CD8 + T cells, an allogenic mixed leukocyte reaction was performed. In this assay, monocytic-differentiated dendritic cells from one donor were mixed with isolated CFSE stained PBMCs from another donor to mimic the immunosuppressive effects of PD-L1/PD1 interactions. Samples were treated with or without Atezolizumab or purified IgG_A Fc-fusion peptide to test whether the blocking of PD-L1 could induce a T cells expansion (figure 1E). When Atezolizumab and IgG_A Fc-fusion peptide were added, a clear expansion of CD8 + T cells was observed, correlating with a decrease in CFSE compared with untreated. When calculating their expansion index, both Atezolizumab and IgG_A Fc-fusion peptide were higher than the mock. Taken together, we demonstrated that Ad-Cab can secrete high levels of Fc-fusion peptide that is able to bind to PD-L1, outcompete Atezolizumab and activate CD8 + T cells.

The secreted Fc-fusion peptides activate effector mechanisms of an IgG1 and an IgA1

After testing expression and binding, we examined the ability of the Fc-fusion peptides to activate antibody effector mechanisms. Since the Fc entails a hybrid of an IgG1 and an IgA1, CDC and ADCC were tested with both PMN and PBMCs on six different human and murine tumor cell lines expressing varying levels of PD-L1 (figure 2A). Murine breast cancer (4T1), murine colon carcinoma (CT26) and murine melanoma cell lines (B16F10 and B16F1) were used since oncolytic human adenoviruses cannot induce oncolysis and cytotoxicity in most murine cell lines and thus the effects seen can then be attributed to the Fc-activation of effector mechanisms. Cells were first infected with either Ad-Cab or unarmed oncolytic adenovirus (Ad-5/3 Δ24) at two different MOIs (10 and 100) for 2 days to limit oncolysis with human cell lines (MDA-MB-436 and A549). Subsequently, when complement active serum was added, cell lysis could be observed with Ad-Cab infected cells (figure 2B). Already at MOI 10, cell lysis was occurring and was further augmented as the MOI increased to 100 in all six cell lines. As expected, cell lysis was not shown with the control virus (Ad5/3-delta 24) in all conditions, further attributing cell death to CDC induction, especially in the human cell lines where viral oncolysis can be induced.

ADCC assays were then tested with two different immune populations: PBMCs (figure 2C) and PMNs (figure 2D). In contrast to CDC, at MOI 10 minimal or

no induction of ADCC could be seen with all cell lines infected with Ad-Cab when PBMCs or PMNs were added. Nevertheless, when the MOI increased to 100, cell lysis was observed with both populations. Interestingly, both PMNs and PBMCs were able to elicit similar levels of cytotoxicity with all the cells.

Finally, we wanted to test the ability of Ad-Cab to activate macrophages and induce ADCP. The ability to elicit ADCP was determined by the uptake of CFSE by macrophages from the tumor cell lines labeled with CFSE. At MOI 10, no uptake of CFSE was observed with any condition yet at MOI 100, an increase of CFSE uptake by the macrophages could be observed in all cell lines when Ad-Cab was added (figure 2E). Overall, the data demonstrate that the secreted Fc-fusion peptide can induce the effector mechanisms of both an IgG1 and an IgA.

Trogocytosis drives the PMN-mediated ADCC

It has been previously shown that in order to initiate ADCC *in vitro*, PMNs adhere to the target cells establishing an immunological synapse with the antibody-opsinized tumor cells.²⁷ This subsequently causes the disruption of their plasma membrane and the endocytosis of cytoplasmic fragments, leading to a necrotic type of cell death termed trogocytosis. In order to explore the possible nature of the cytotoxic mechanism during PMN-mediated ADCC, we quantified the transfer of membrane from tumor cells to PMNs by flow cytometry. Virally infected cells had their lipid membrane labeled with 3,3'-diiodo-4,4'-oxydiphenylacetylene perchlorate (DiO), after which unstained neutrophils were added to the cell culture. Neutrophils were first gated using the side and forward scatter since they are smaller than a tumor cell and also confirmed with neutrophil markers such as CD15 + and CD14- (online supplemental figure S2). The MFI of DiO was then measured on these neutrophils after incubation in three different conditions: without exposure to the target cells (figure 3A), with exposure to uninfected stained cells (figure 3B) and with exposure to Ad-Cab infected stained cells (figure 3C). When neutrophils were examined on their own, without former exposure to the target cells or when they were added to uninfected stained tumor cells, there was no DiO measured, and no membrane transfer had happened. Yet, when the neutrophils were added to Ad-Cab infected cells, an uptake of DiO was observed by PMNs. This implies the uptake of the lipid membrane of the infected tumor cells by the neutrophils, which is a characteristic of trogocytosis. The same procedure was performed using all six cell lines and an increase in DiO MFI in the neutrophils was noted only when neutrophils had previously been exposed to cancer cells infected with the Ad-Cab and not with the other controls used (figure 3D). Hence, these findings add evidence in support that one of the mechanisms in which PMNs employ ADCC with Ad-Cab is trogocytosis.

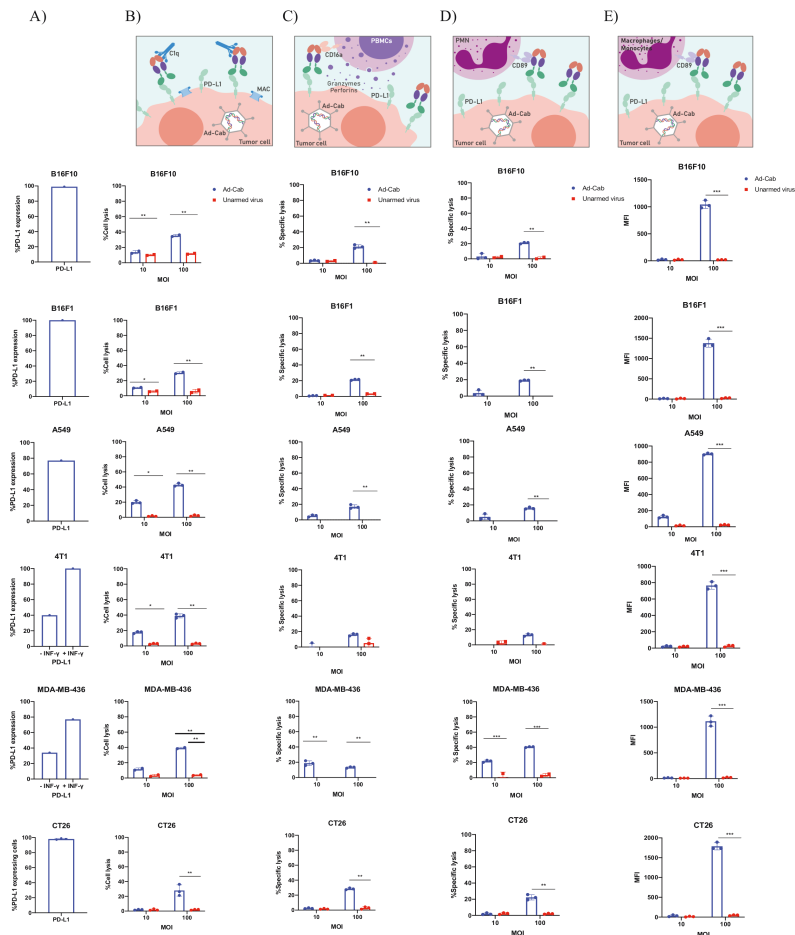


Figure 2 Activation of multiple branches of the immune system. (A) The percentage of PD-L1 expression on all cell lines used in the assays. (B) FACS-based CDC assay against all six different cell lines with Ad-Cab and Unarmed virus. Cells were infected at two indicated MOIs, incubated for 48 hours and pooled serum from healthy volunteers was then added at a final concentration of 15.5%. After 4 hours at 37°C, cell lysis was measured using 7-AAD. ADCC against five different cell lines using either (C) PBMCs or (D) PMN as effector cells. Indicated viruses were added at 10 and 100 MOI and incubated for 48 hours. Subsequently, PBMCs and PMNs were added at an E:T ratio of 100:1 and 40:1, respectively, and lysis was by quantifying LDH release after 4 hours at 37°C. (E) ADCP was measured by incubating target cells with 10 or 100 MOI of Ad-Cab or unarmed virus for 48 hours. Then, cells were labeled with CFSE and macrophages were added at a 5:1 (effector:target) ratio. Phagocytosis was quantified by measuring the uptake of CFSE by macrophages. Levels of significance were set at * $p < 0.05$, ** $p < 0.01$, *** $p < 0.001$ and **** $p < 0.0001$. Error bars represent SD. AAD; amino-actinomycin D; ADCC, antibody-dependent cell cytotoxicity; ADCP, antibody-dependent cell phagocytosis; CDC; complement-dependent cytotoxicity; PBMC; peripheral blood mononuclear cell; PMN, polymorphonuclear.

Ad-Cab induces higher tumor cytotoxicity with multiple immune populations while leaving myeloid cells untouched
We hypothesized that a synchronous activation of the multiple branches of the immune system would lead to enhanced tumor cell killing and complete clearance of the

tumor. To test this, we again performed the ADCC assays with different combinations of immune components such as PBMCs+PMNs or PBMCs+PMNs+serum with the same cell lines as previously expressing PD-L1 (figure 4A). Also, to further examine this, we used Atezolizumab, which

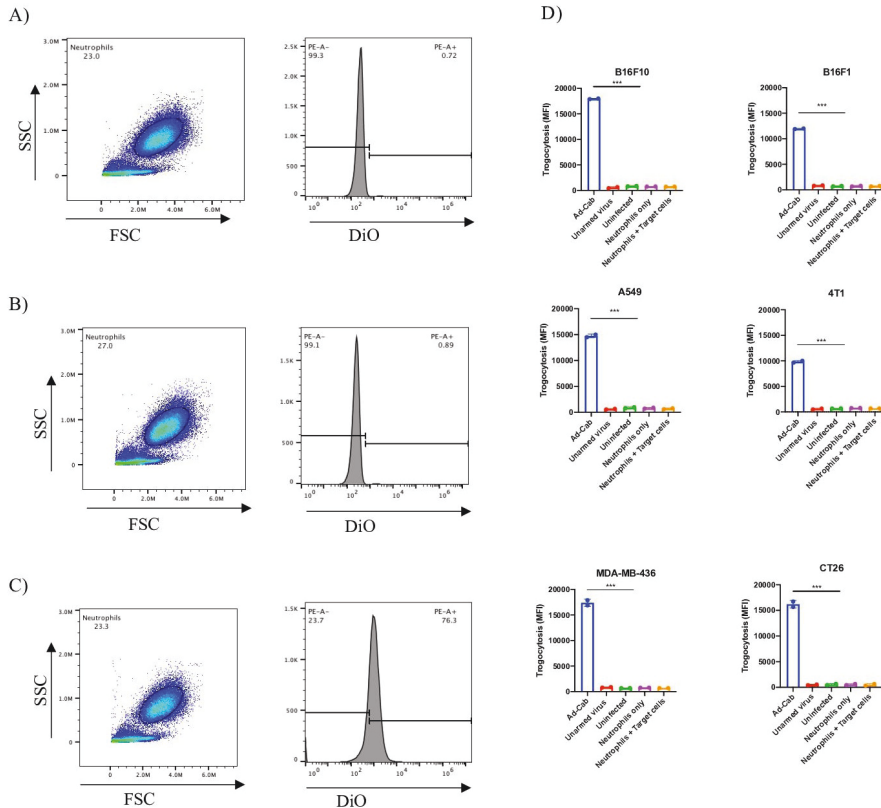


Figure 3 PMN's mode of action during ADCC. Gating strategy (left) and histogram (right) of neutrophils incubated alone (A), with DiO stained A549 cells (B) or DiO stained A549 cells infected with 100 MOI of Ad-Cab (C). Trophocytosis of six different cell lines infected at 100 MOI (D) for 48 hours with indicated virus and PMNs added. Neutrophils alone or neutrophils coincubated with DiO stained target cells were used as controls. PMNs were added at an E:T ratio of 40:1. DiO +PMNs were then calculated using flow cytometry. ADCC, antibody-dependent cell phagocytosis; PMN, polymorphonuclear.

holds a N298A mutation abrogating its effector mechanisms, Atezolizumab without the mutation, designated IgG1-PD-L1, able to elicit effector mechanisms of an IgG1 and an IgA-PD-L1. When each immune component was added individually (online supplemental figure S3B–D), Atezolizumab carrying the N298A mutation was not able to induce cell lysis. Interestingly, the functional IgG1 PD-L1 antibody was able to induce similar cell lysis levels as the Fc-fusion peptides when the complement system or PBMCs were added. Nevertheless, the IgG1 PD-L1 was able to induce only minimal cell lysis with PMNs compared with the Fc-fusion peptides. As expected, IgA-PD-L1 was only able to activate PMNs and not PBMCs or the complement system.

When PBMCs and PMNs were added together, a significant cytotoxicity augmentation, compared with the cell

populations alone, was observed with Ad-Cab (figure 4B). This was not seen with IgG1- or IgA-PD-L1 where cell lysis levels remained like when PBMCs or PMNs were added alone, respectively. Meanwhile, when all three components (fresh human serum, PBMCs and PMNs) were added together, enhanced cytotoxicity could again be noticed with Ad-Cab and IgG1-PD L1 (figure 4C). Interestingly, IgG1 PD-L1 showed a significant increase in cell lysis compared with when serum or PBMCs were added together. This again further reinforced the added benefit of activating multiple immune branches. Moreover, the addition of serum to the combination of PBMCs+PMNs also significantly increased cell lysis with Ad-Cab. This increase in cell lysis almost reached full clearance of PD-L1 expressing cells. Notably, this synergistic effect was demonstrated with B16F10, B16F1 and

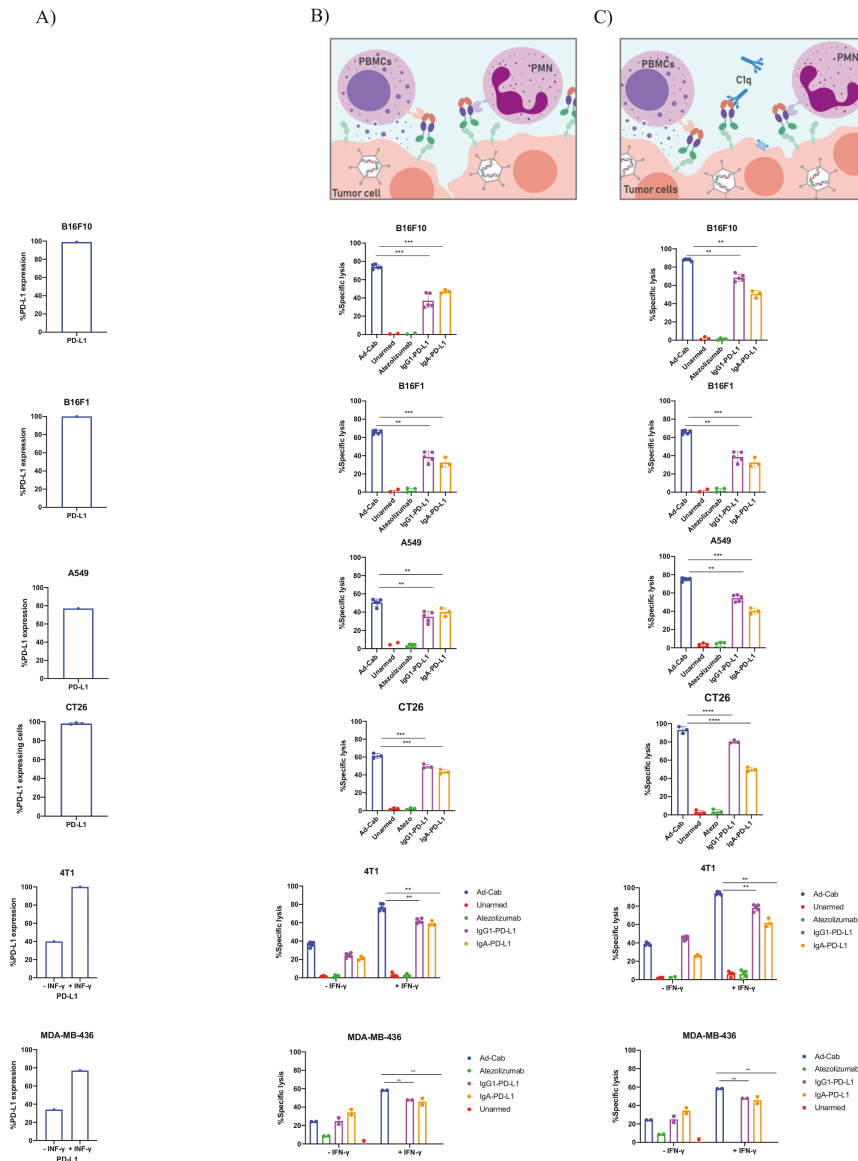


Figure 4 Activation of multiple branches works in synergy leading to enhanced cytotoxicity. (A) Histograms demonstrating the percentage PD-L1 expression on all cell lines used in the assays. Cell lysis of tumor cell lines in the presence of (B) PBMCs and PMNs and (C) PBMCs+serum. PBMCs and PMNs were added at an E:T ratio of 40:1 and 100:1, respectively, while serum was added at 15.5%. Cells were infected with viruses at 100 MOI and incubated for 48 hours or 10 μ g/mL of antibody were added 30 min prior to adding immune components. Lysis was then detected using an LDH release assay. Levels of significance were set at * $p < 0.05$, ** $p < 0.01$, *** $p < 0.001$ and **** $p < 0.0001$. Error bars represent SD. PBMC; peripheral blood mononuclear cell; PMN, polymorphonuclear.

A549 cells but not with 4T1 and MDA-MB-436 cells. We speculated that this was because most of the PD-L1 expressing 4T1 and MDA-MB-436 cells had already been eliminated when each component of the immune system was added individually. To examine this, PD-L1 expression on 4T1 and MDA-MB-436 cells was further increased by treating cells overnight with IFN-gamma before setting the ADCC assays.²⁸ As anticipated, a higher tumor killing could be observed with all immune components added individually or in combination with IFN-gamma treated 4T1 and MDA-MB-436 cells. Like the other cell lines, with the IFN-gamma treated cells, Ad-Cab was able to activate PMNs and induce higher killing with both combinations (PBMc+PMN and PBMcs+PMNs+serum) compared with IgG1 PD-L1.

To further verify such data, we performed both live-cell microscopy and impedance-based real-time quantitative analysis (XCELLigence) to track target cells treated with purified Fc-fusion peptide (Ad-Cab) or therapeutic antibodies (Atezolizumab and IgG1-PDL1) following the addition of PBMcs and PMNs. With live-cell microscopy, A549 cells were monitored for 12 hours, and death was determined using a Caspase-3/7 Green Reagent and phase confluency. At E:T ratios of 10:1 and 4:1, PBMcs and PMNs, respectively, live-cell imaging supported the LDH release data since apoptosis was observed when IgG1-PD-L1 or Ad-Cab was added (online supplemental figure S4A and online supplemental movie S3-5). Moreover, cell death was further enhanced with Ad-Cab compared with IgG1-PDL1 (online supplemental file 4). Using XCELLigence, we analyzed cell-killing in real time (online supplemental figure S5A–E) and calculated the rate of cell death for each therapeutic antibody (IgG1- or IgA-PD-L1) and purified Fc-fusion peptide. The purified Fc-fusion peptide (Ad-Cab) had the highest killing rate in all cell lines, ranging from 0.0361 to 0.0482, compared with IgG-PD-L1 (0.0221–0.0289) and IgA-PD-L1 (–0.0186 to 0.0282) (online supplemental figure S5F). Hence, we demonstrated that the Fc-fusion peptide augment immune-mediated apoptosis compared with IgG1-PD-L1, IgA-PD-L1 and the clinically used Atezolizumab in real time analysis.

Other than cancer cells, immune cells also express PD-L1, especially myeloid cells. To test whether Ad-Cab could affect such cells, purified IgG1 Fc fusion peptide was added in unprocessed whole blood of three healthy donors and incubated for 24 hours. In these conditions, we would be able to test whether the Fc-fusion peptide could induce lysis of any immune population in the presence of all physiological effector populations (NK cells, neutrophils or complement system). After 24 hours, samples were processed and stained, and counting beads were added to determine the absolute numbers of DCs, NK cells, neutrophils, T cells and monocytes (online supplemental figure S6A). Ad-Cab was shown not to induce cytotoxicity to any cell population since the percentages and absolute numbers were similar to untreated or Trastuzumab (anti Her-2 IgG) treated

samples in all three donors (online supplemental figure S6B).

In vivo efficacy of Ad-Cab with CT26 and A549 tumor model

Based on the in vitro data, we decided to test the efficacy of Ad-Cab in vivo using a syngeneic mice model. Mice do not express Fc- α receptors, hence not allowing to test the full efficacy of the Fc-fusion peptide. Nevertheless, due to the homology of human and murine Fc- γ receptors, the IgG portion of the Fc-fusion can be tested. The colon carcinoma CT26 model was used since it has been reported not to respond effectively to PD-L1 checkpoint therapy and the advantages of Ad-Cab could be more apparent in this model.^{29,30} After 7 days postengraftment, mice were treated either with PBS, Ad-5/3 Δ 24, Ad-Cab or mPD-L1 for a total of 7 times (figure 5A). As expected, Ad-Cab was shown to be the most effective group in controlling tumor growth (figure 5B). Also, mice treated with mPD-L1 were shown to control tumor growth better than mock; however, this was not statistically significant. We also calculated a therapeutic threshold based on the average of the tumor growth of mice treated with Ad-5/3 Δ 24 and mPD-L1 since Ad-Cab represents a combination of both treatments. Based on this, all the mice treated with Ad-Cab were responders showing a superior efficacy compared with mPD-L1 (online supplemental figure S7A). The efficacy of Ad-Cab could also be translated to an enhanced overall survival compared with all the other treatment groups (figure 5C). Due to toxicity concerns, we analyzed the weight of the mice and distribution of the antibody for each group. No significant weight changes could be seen among the groups (online supplemental figure S7B). Moreover, because the Fc fusion peptide was tagged with an 8xHis, we monitored the distribution in the blood and tumor. After the mice had received four treatments, two mice from each group were sacrificed and their blood and tumors were collected to detect the Fc-fusion peptide. In blood (figure 5D), undetectable levels of his-tagged Fc-fusion peptide could be observed in all groups. However, in the tumor (figure 5E), only in the Ad-Cab group an average of 2 μ g/mL of his-tagged Fc-Fusion peptide could be found. After observing that from the Ad-Cab and mPD-L1 treated groups, some mice were tumor free, we decided to rechallenge the mice with CT26 to assess if a memory response had been formed. Mice previously treated with mPD-L1 had a successful tumor implantation, yet the growth was reduced compared with naïve mice injected with CT26 (figure 5F). Interestingly, mice treated with Ad-Cab rejected the tumor since no tumor was visible up to 30 days. This indicated that the surviving mice from the Ad-Cab group had formed a memory response able to control a rechallenge of CT26.

We went on to further characterize Ad-Cab in a human tumor xenograft model with immune deficient NS (NOD/SCID) mice reconstituted with a human immune system. NS mice were first implanted with A549 cells and also injected with freshly isolated PBMcs from the same donor (figure 5G). After tumors had been

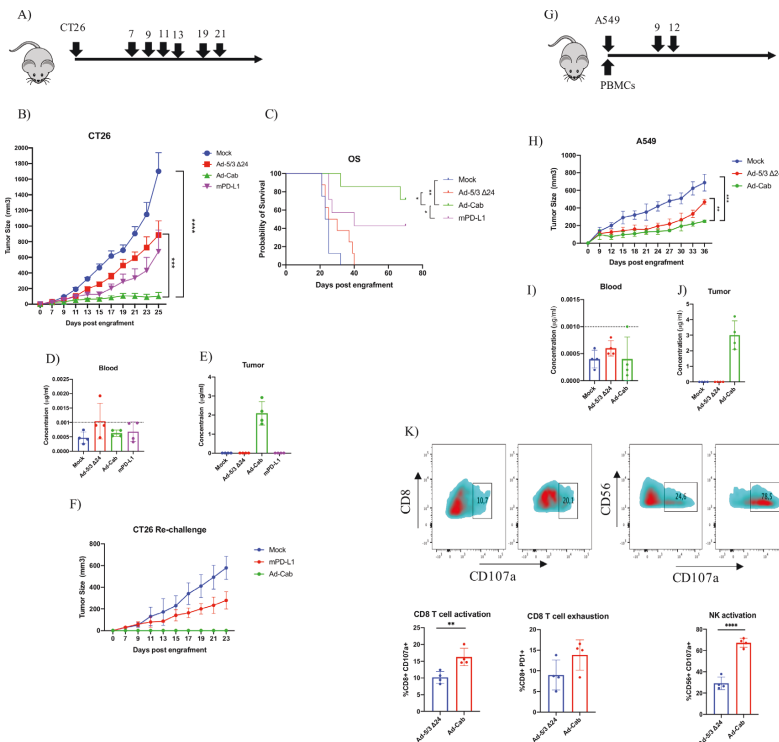


Figure 5 Tumor efficacy and biodistribution of Ad-Cab in syngeneic mouse model CT26 colon carcinoma and xenograft model A549. (A) Schematic diagram of treatment schedule. Mice were treated either with PBS (mock), Ad-5/3Δ24, Ad-Cab or mPD-L1 after 7 days postengraftment of 5×10^5 cells in the right flank of the mice. Treatments were given on days 7, 9, 11, 13, 17, 19 and 21. Ad-5/3Δ24 and Ad-Cab were given intratumorally at a dose of 1×10^9 viral particles while $100 \mu\text{g}$ of mPD-L1 was given intraperitoneally. (B) Summary data for average tumor growth for all treatment Fc groups for CT26 tumor model. (C) Kaplan-Meier survival curve for the treatment groups. Concentration of His-tagged PD-L1 Fc-fusion peptide in blood (D) and tumor (E) from two mice per each group. Dotted line represents the detection limit of the kit. (F) CT26 tumor free mice were rechallenged with 500,000 CT26 cells and tumor growth was recorded. (G) Schematic diagram of treatment schedule A549 model. Mice were implanted with tumors and human PBMCs and then treated with PBS (mock), Ad-5/3Δ24 or Ad-Cab. Treatments were given on days 9 and 12 at a dose of 1×10^9 viral particles intratumorally. (H) Summary data for average tumor growth for all treatments with A549 bearing mice. Concentration of His-tagged PD-L1 Fc-fusion peptide in blood (I) and tumor (J) from two mice per each group. (K) CD8 + T cell and NK cell degranulation (CD107a) and exhaustion (PD-1) markers were examined in the tumor microenvironment. A two-way ANOVA was conducted along with a Dunnett's test to test significance. The number of mice per each group was 9–10. Levels of significance were set at * $p < 0.05$, ** $p < 0.01$, *** $p < 0.001$ and **** $p < 0.0001$. Error bars represent SD. ANOVA, analysis of variance; NK, natural killer; PBMC; peripheral blood mononuclear cell.

engrafted, peripheral blood was taken from the mice to check for human immune cells engraftment. It was seen that human CD45 and CD3 cells were circulating in the peripheral blood of the mice, suggesting that the engraftment with human PBMCs was successful (online supplemental figure S8). Mice were treated with either PBS, Ad-5/3 Δ24 or Ad-Cab for two treatments. Mice treated with unarmed oncolytic adenovirus had a better tumor control compared with mock (figure 5H). Yet, mice treated with Ad-Cab had a statistically significant

tumor control compared with all other groups. Similar with the CT26 mice, his-tagged Fc-fusion peptide was not found in the blood (figure 5I) in any group but in the tumors of Ad-Cab treated mice around 2–4 μg of his-tagged protein was observed (figure 5J). By analyzing the tumor microenvironment, we observed that mice treated with Ad-Cab had an increase in both NK and CD8 + T cells which were positive for CD107a (figure 5K). This indicated that these cells had been activated and degranulated perforins and granzymes. These data demonstrate



the enhanced *in vivo* efficacy and good safety profile of Ad-Cab.

Ad-Cab controls 4T1 tumor growth despite CD8+ T cell depletion

After observing that Ad-Cab was successful in controlling CT26 and A549 tumors *in vivo*, we decided to test it against 4T1 which is a highly immunosuppressive, fast growing and metastatic tumor. Mice bearing 4T1 tumors were treated with the same treatments and dosing as with the CT26 mice (figure 6A). Mice treated with Ad-Cab showed the best tumor control over all other groups. mPD-L1 treated mice also showed a degree of tumor control, yet it was not significant compared with mock (figure 6B). After sacrificing the mice, the tumor micro-environment was analyzed for different immune populations and activation/exhaustion markers. As expected, 4T1 tumors were highly infiltrated with both immunosuppressive monocytic (CD11b+Ly6Chi Ly6G-) and granulocytic (CD11b+Ly6Ghi Ly6C-) myeloid-derived suppressor cells (MDSC) which is in line with previous reports (figure 6C). Surprisingly, there was a significant reduction in both granulocytic MDSC (figure 6D) and monocytic MDSC (figure 6E) cell populations in the Ad-Cab treated group compared with other groups. Moreover, this reduction in the Ad-Cab treated group was accompanied with a higher infiltration of NK cells compared with the rest of the groups (online supplemental figure S9). No increase of other cell types such as dendritic cells, CD8 T-cells, CD4 T-cells (online supplemental figure S9) or tumor-associated macrophages (TAMs) (figure 6F) was observed since the percentage of cells was similar among all groups. We then analyzed the activation of both CD8 + T cells and NK cells using the cytotoxic degranulation marker CD107a (figure 6G). A clear increase of NK activation and degranulation could be observed in Ad-Cab treated groups (figure 6H). This was also seen with the CD8 T cells with the Ad-Cab treated group but as well with the mPD-L1 treated group (figure 6I). Other than being activated, CD8 T-cells displayed an exhausted phenotype in both Ad-Cab and mPD-L1 group with the latter being higher in expressing exhaustion marker PD1 (figure 6J). This implies that both Ad-Cab and mPD-L1 were able to activate and degranulate CD8 + T cells against the tumor but Ad-Cab was also able to do so with NK cells as well.

Having observed that Ad-Cab was able to strongly activate NK cells, we wanted to further characterize their mechanism of action *in vivo* by repeating the same experiment with 4T1 but depleting CD8 T cells. Mice were first given a high dose of CD8 depleting antibody before starting treatment and kept receiving the depleting antibody during the treatment schedule to make sure CD8 T cells were absent during the treatment schedule (figure 6K). After the first treatment, peripheral blood was taken from mice to check that no circulating CD8 T cells were present. Depletion was shown to be successful as no circulating CD8 T cells could be observed in mice receiving CD8 depleting antibody compared with those

that were not (figure 6L). As expected, mPD-L1 treated mice showed a similar tumor growth compared with mock and Ad-5/3 Δ 24 treated mice. Nevertheless, Ad-Cab treated mice had a significantly lower tumor growth compared with all other groups (figure 6M). This was also translated to higher overall survival in the Ad-Cab treated group (figure 6N). This indicates that, in contrast to checkpoint inhibitors, Ad-Cab does not solely require CD8 T cells to induce tumor killing *in vivo*.

Characterization of patient-derived RCC organoids as testing platforms for Ad-Cab

To further study the contribution of the IgA portion of Ad-Cab, we developed a novel testing platform using RCC PDOs. Freshly dissociated tumor tissue from four patients (RCC1-4) undergoing radical nephrectomies were obtained. Samples were grown either as 2D in 3D by embedding cells in Matrigel (figure 7A). In order to assess the heterogeneity of the PDOs and to compare them to the corresponding tumor tissue that they originated from, we stained PDO cells that were allowed to grow as 2D on plastic with three commonly used stains to differentiate RCC (CAIX, Vimentin and Cytokeratin) and with an F-actin stain (Phalloidin) (figure 7B). Both CAIX and vimentin are highly sensitive and specific for clear cell renal cell carcinoma (ccRCC).³¹ This is consistent with the staining since RCC2, RCC3 and RCC4 samples were shown to be positive for CAIX and vimentin and were characterized as ccRCC at the time of diagnosis. Surprisingly, RCC1 was both CAIX and vimentin positive despite being classified as a chromophobe RCC, a subtype that usually is not CAIX or vimentin positive. Yet, RCC1 had a focal expression of CAIX and lower expression of vimentin compared with the other samples, where staining was more diffused.

Subsequently, we tested whether oncolytic adenoviruses had the ability to pass through the Matrigel and infect the organoids. To this end, we infected PDOs with an oncolytic adenovirus expressing the red fluorescent protein (Ad5- Δ 24-RFP) to visualize the infection and the replication of the virus (figure 7C, online supplemental figure S10A-C). The virus was added on top of the supernatant of the PDO cultures and after 1 day PDOs were already infected and expressing RFP. Expression kept increasing until reaching a maximum on day 3. To confirm whether the virus could induce oncolysis, a viability cell stain, Calcein AM, was added and monitored (figure 7C). Oncolysis was observed to start at day 3 with minimal death occurring, and by day 4, most cells were shown to be dead. To finalize the testing platform, we tested whether isolated PBMCs could travel through the Matrigel and surround the organoids. Before their addition to the organoid cultures, PBMCs were labeled with Calcein green and then added on top of the media (figure 7D). Within hours, they could be seen to pass through the Matrigel and surround organoids. Finally, PD-L1 expression was then tested by dissociating the PDOs into single cells and evaluating expression using flow cytometry (figure 7E).

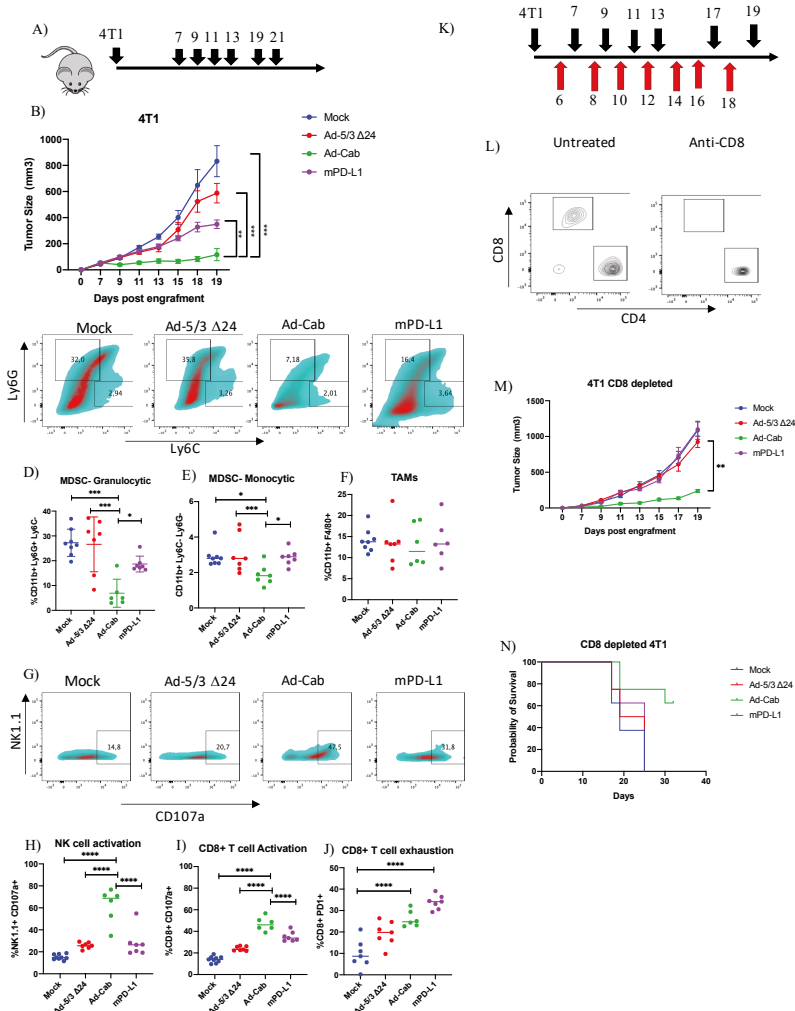


Figure 6 Ad-Cab induces 4T1 tumor control in vivo in presence and absence of CD8 + T cells. (A) Schematic diagram of treatment schedule for 4T1 bearing mice. Mice were treated either with PBS (mock), Ad-5/3Δ24, Ad-Cab or mPD-L1 after 7 days postengraftment of 3×10^5 cells in the right flank of the mice. Treatments were given on days 7, 9, 11, 13, 17, 19 and 21. Ad-5/3Δ24 and Ad-Cab were given intratumorally at a dose of 1×10^9 viral particles while $100 \mu\text{g}$ of mPD-L1 was given intraperitoneally. (B) Summary data for average tumor growth for all treatment groups for 4T1 tumor model. (C) Granulocytic (CD11b+Ly6G⁺Ly6C⁻) and monocytic (CD11b+Ly6G⁻Ly6C⁺) MDSC infiltration in 4T1 tumor microenvironment. Cell percentages of granulocytic (D), monocytic (E) MDSC and TAM (F). NK cell activation (G,H) and CD8 (I) cell activation was determined using the CD107a degranulation marker. CD8 + T cell exhaustion was also measured using PD1 (J). (K) Schematic diagram of treatment (black arrows) and CD8 depletion (red arrows) schedule for 4T1 bearing mice. Treatment scheduled was the same as previously but 1 day before treatment $500 \mu\text{g}$ of CD8 depleting antibody was given and then every 2 days $100 \mu\text{g}$ was given. (L) CD8 and CD4 cell staining on CD3 gated peripheral blood from mice treated with or without depleting CD8 antibody. (M) Summary data for average tumor growth for all treatment groups for CD8 depleted 4T1 tumor model. (N) Kaplan-Meier survival curve for the treatment groups for CD8 depleted 4T1 bearing mice. MDSC, myeloid-derived suppressor cell; TAM, tumor-associated macrophage.

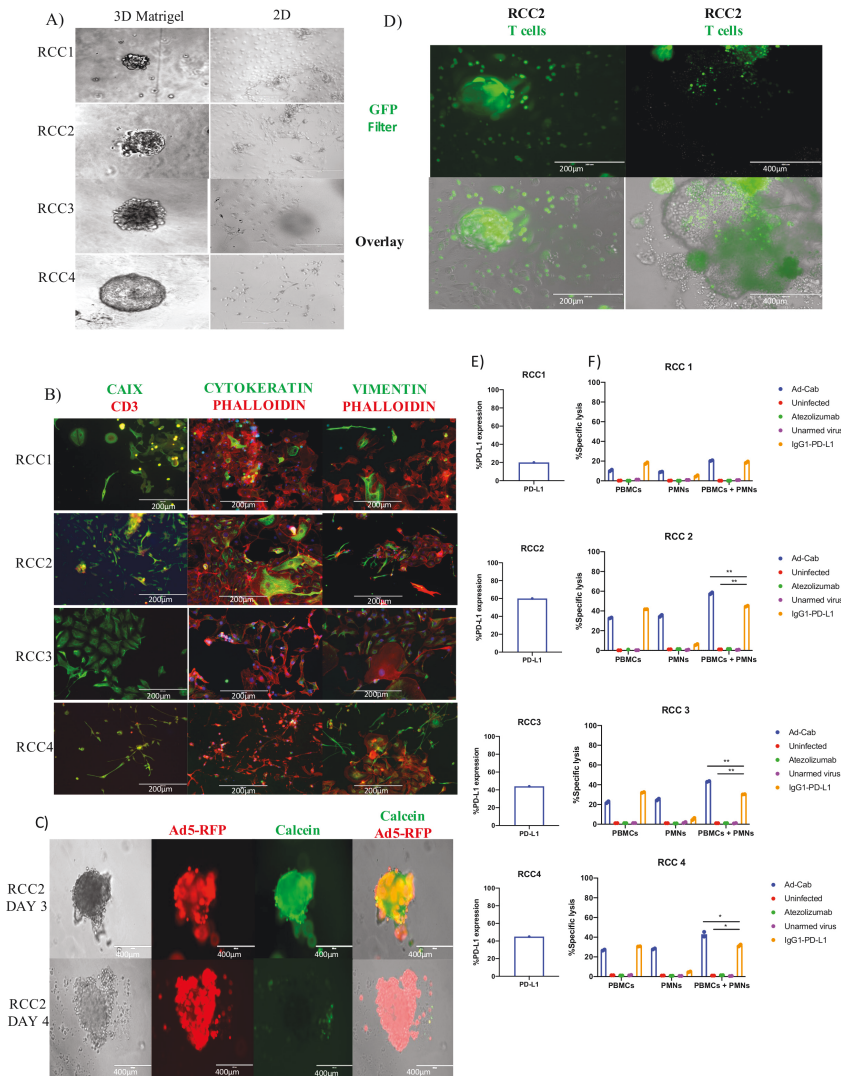


Figure 7 Characterization of Ad-Cab in RCC patient-derived organoids. (A) Representative imaging of renal cancer cell tissue grown in Matrigel as 3D (left) and 2D (right). Immunofluorescence staining of dissociated RCC PDOs using CAIX, Cytokeratin, Vimentin, CD3 and Phalloidin. Scale bar 500 or 200 μm . (C) RCC2 PDOs were infected with 5×10^5 vp of Ad5-RFP $\Delta 24$. Cell viability was visualized using Calcein green. Scale bars 200 μm . (D) Images of RCC2 PDOs infiltrated by Calcein green stained PBMCs. 10^5 PBMCs, stained with Calcein green, were added on top of Matrigel and after 4 hours images were taken using an EVOS FL cell imaging system. Scale bars 400 or 200 μm . (E) FACS analysis of PD-L1 expression of dissociated RCC PDOs. (F) ADCC assays with RCC1, RCC2, RCC3 and RCC4 PDOs. RCC PDOs were infected with viruses at 100 MOI and incubated for 48 hours or 10 $\mu\text{g}/\text{mL}$ of antibody were added 30 min prior to adding immune components. PBMCs and PMNs were added at an E:T ratio of 40:1 and 100:1, respectively. LDH release assays were performed 4 hours after addition of immune effector cells. ADCC, antibody-dependent cell cytotoxicity; PBMC, peripheral blood mononuclear cell; PDO, patient-derived organoid; PMN, polymorphonuclear; RCC, renal cell carcinoma.



Varying levels of expression of CD3-/PD-L1 +positive cell were shown from the samples, from 20% to 66%. Hence, we demonstrate that the RCC PDOs can be used as testing platforms for the Ad-Cab virus, and since they express PD-L1, they can be infected by oncolytic adenoviruses and infiltrated by PBMCs.

After optimizing the RCC organoids as a functional testing platform for the Ad Cabs, we used them to perform the ADCC experiments with PBMCs and PMNs (figure 7F). RCC organoids were first infected with the viruses or treated with the antibodies and incubated for 3 days. As evident from the ADCC results, when PBMCs were added to the organoids, similar levels of cytotoxicity were observed with the Ad-Cab and the IgG1 PD-L1 antibody. Consistent with *in vitro* data, cytotoxicity could only be observed with the Ad-Cab and not with the IgG1 PD-L1 antibody when PMNs were added as the effector cells (figure 7F). When both populations of effector cells were added simultaneously, there was an enhanced cell killing with Ad-Cab compared with when each population was added individually (figure 7F), with all samples except RCC1 (figure 7F). This could be explained by the fact that all PD-L1 expressing cells were killed when each effector population was added individually. The added benefit of activating an additional effector population with Ad-Cab was evident since the killing efficiency in RCC2, 3 and 4 patient samples were greater when PBMCs and PMNs were added together. Thus, the PDOs further reinforced the efficacy of Ad-Cab and the significance of the synergism of the immune system for tumor eradication.

DISCUSSION

ICIs have emerged as a major clinical milestone for the treatment of cancer. However, recent data have revealed that the *in vivo* activity of such antibodies solely depend on the Fab-mediated inhibition of inhibitory immune checkpoints and also the effector mechanisms mediated by the Fc portion.^{32–34} In this study, we designed a novel PD-L1 ICI with a cross-hybrid Fc region mediating effector mechanisms of both an IgG and an IgA. To minimize unwanted cytotoxicity, the novel ICI was cloned into a conditionally replicating adenovirus to limit release only to the tumor microenvironment. Ad-Cab secreted the cross-hybrid IgGA Fc-fusion peptide able to bind to PD-L1 and activate multiple immune pathways, not activated when IgG or IgA antibody is added alone, resulting in enhanced tumor killing in various *in vitro*, *in vivo* and *ex vivo* models.

As expected, the additive effector mechanisms of the Fc-fusion peptide increased tumor killing when compared with the FDA approved IgG, Atezolizumab, containing an N298A mutation abrogating Fc- γ binding. In line with other studies, the additive effector functions of the Fc-fusion peptides against PD-L1 holds potential into greater clinical results.^{9,10} Based on *in vitro* and *in vivo* analysis, a crucial mechanism of action of several therapeutic antibodies against cancer is to elicit tumor cell killing via ADCC

and CDC.³⁵ As for ICIs, including a functional Fc region may not always be beneficial and depends on the immune checkpoint receptor targeted. For example, equipping CTLA-4⁸ and PD-L1 ICIs^{9,10} with a competent Fc region able to elicit ADCC has been shown to enhance efficacy yet with PD-1 antibodies, it reduced efficacy. Coinciding with previous results, we also show that incorporating effector mechanisms to PD-L1 ICIs increases efficacy due to enhanced tumor killing. Our results demonstrate that mice bearing CT26 and 4T1 tumors responded better to Ad-Cab compared with mPD-L1. This superiority is hypothesized to be due to the enhanced Fc-effector mechanisms since the Fc-fusion peptide is partly human IgG1 and such isotype induces greater ADCC compared with IgG2a (isotype of mPD-L1) in mice.¹² This coincides with our data showing an enhanced activation of NK cells when treated with Ad-Cab compared with mPD-L1. Moreover, when CD8 T cells were depleted, mPD-L1 was not able to control anymore the tumor growth yet Ad-Cab was able. This is mostly due to the engagement of other immune cells such as NK cells as an effector population by Ad-Cab. Other than augmenting tumor cell killing, Ad-Cab was also shown to stimulate an antitumor memory response since CT26 recovered mice treated with Ad-Cab did not engraft a second challenge of CT26. The augmented tumor cell killing could have resulted in the excess release of tumor antigens being picked up by infiltrated dendritic cells. Therefore, other than having a local impact, the increased tumor cell killing by the engagement of multiple effector population could lead to a systemic effect.

Interestingly, Ad-Cab was able to affect the tumor micro-environment by reducing highly immunosuppressive cell populations such as monocytic MDSCs and granulocytic MDSCs in 4T1 bearing mice. Such cell populations have been attributed to enhanced tumor growth, suppressing pre-existing antitumor responses and impeding the efficacy of many cancer immunotherapies. It is believed that Ad-Cab was able to reduce such immunosuppressive immune populations due to their abnormally high expression of PD-L1. Even though other myeloid cells such as dendritic cells, macrophages, monocytes or neutrophils express PD-L1, they were unharmed by Ad-Cab both *in vitro* and *in vivo*. These results fall in line with previous studies and have contributed to the number of PD-L1 molecules expressed on the cell membrane which is a key determinant for antibody effector functions. Hence, other than increasing tumor cell killing, Ad-Cab is also able to counteract suppressive immune populations highly expressing PD-L1.

Despite the fact that neutrophils express activating Fc- γ IIA, able to trigger ADCC, the cells also express one log more of Fc- γ IIIB.³⁶ Unlike other Fc- γ receptors, the Fc- γ IIIB receptor does not contain either activating (ITAM) or inhibitory (ITIM) motifs and its role has been questioned. Nevertheless, with therapeutic antibodies against cancer, it has been attributed to act as a molecular “sink” by competitively binding to IgG with

no resulting activation.^{12 13 37} Yet, the Fc-fusion peptide was able to capitalize on such a neglected cell population due to their high expression of Fc- α . Neutrophils are the most abundant leukocyte population in blood and tumorigenesis skews hematopoiesis towards neutrophil production by secreting granulocyte-colony stimulating factor (G-CSF) and granulocyte-macrophage-colony stimulating factor (GM-CSF) leading to tumor infiltration.^{38–40} Regardless of their high tumor infiltration, these cells have shown to be protumorigenic and their tumor infiltration has been associated with a low clinical prognosis.⁴¹ This associated low prognosis is due to the lack of effective neutrophil-activating stimulus and the immunosuppressive tumor microenvironment polarizes the cells towards pro-tumorigenic.³⁹ Many studies have shown that the tumor microenvironment can direct the fate of neutrophils towards either antitumorigenesis or protumorigenesis.^{42–44} Hence, the ability of Fc-fusion peptide to activate neutrophils can polarize already tumor-infiltrated neutrophils from tumor-promoting to tumor-killing cells. Subsequently, the activation of neutrophils can lead to the release of multiple cytokines and chemokines to recruit other effector immune cells⁴⁵ that the Fc-fusion peptide can further activate. Unfortunately, since mice do not express endogenous Fc-alpha receptors, the full efficacy of Ad-Cab could not be studied *in vivo*. In the future, transgenic mice expressing Fc-alpha receptors should be used to fully assess the efficacy of Ad-Cab. Other than eliminating, it would be interesting to examine whether the activation of Fc-alpha receptors on granulocytic or monocytic MDSC could help polarize such cell to be antitumorigenic.

To extensively evaluate the efficacy of the Fc-fusion peptide, we used RCC PDOs. PDOs have revolutionized the study of cancer since analysis of patient-derived tissue can be done without invasive procedures. Additionally, PDO cultures have allowed to test individual responses of patients *ex vivo* with a high sensitivity and specificity in multitude types of tumors.^{46 47} This is because the PDOs can mimic tumor heterogeneity with respect to genetics and architecture often lacking with *in vitro* cell lines and animal models.⁴⁸ To our knowledge, currently there are only two published studies that have evaluated the efficacy of oncolytic viruses using PDOs.^{49 50} This is the first study where the efficacy of the oncolytic virus was tested and an ADCC assay was performed. PDO data further demonstrated the added efficacy of the Fc-fusion peptide by eliciting ADCC with PBMCs and PMNs. This dual activation of both populations was also shown to augment tumor killing compared with when each population was added individually, or one population was only activated by the IgG1 PD-L1. Hence, these data have broadly evaluated the preclinical efficacy of the Fc-fusion peptide.

This synergistic effect by simultaneously engaging Fc- α and Fc- γ was also shown by Brandsma and colleagues,¹⁷ when IgA and IgG antibodies against two different tumor-associated antigens (TAAs) were added and a higher tumor killing was observed compared with when each

antibody was used individually. Interestingly, this effect was only seen when the antibodies were directed towards two different TAAs and diminished when they were directed towards the same TAA. From data presented in this study, it can be deduced that this diminished effect could have been due to the competitive binding between the IgG and IgA antibodies towards the same epitope, since this synergistic effect was shown in the Fc-fusion peptide that incorporated both an IgG and IgA.

In conclusion, here we demonstrate a novel ICI, with enhanced tumor killing efficacy, expressed from an oncolytic adenovirus to limit toxicities. We have shown that the Fc-fusion peptide is able to activate PBMCs, usually activated by IgG1 antibodies, and engage a neglected but important population, PMNs. This coengagement of both populations was shown to work in synergy augmenting tumor killing in various PD-L1 expressing cell lines and RCC PDOs. Such preclinical results prompt the further investigation of Ad-Cab towards the path of clinical development.

Author affiliations

¹Laboratory of Immunovirotherapy, Drug Research Program, University of Helsinki Faculty of Pharmacy, Helsinki, Uusimaa, Finland

²TRIMM, Translational Immunology Research Program, University of Helsinki, Helsinki, Uusimaa, Finland

³Drug Delivery, Drug Research Program, Division of Pharmaceutical Biosciences, Faculty of Pharmacy, University of Helsinki, Helsinki, Finland

⁴Translational Stem Cell Biology & Metabolism Program, Research Programs Unit, Department of Anatomy, Faculty of Medicine, Biomedicum Helsinki, University of Helsinki, Helsinki, Finland

⁵Hematology Research Unit Helsinki, University of Helsinki, Helsinki, Uusimaa, Finland

⁶Abdominal Center, Urology, Helsinki University Central Hospital, Helsinki, Uusimaa, Finland

⁷Center for Translational Immunology, UMC Utrecht, Utrecht, Netherlands

⁸iCAN Digital Precision Cancer Medicine Flagship, University of Helsinki, Helsinki, Finland

⁹Department of Clinical Chemistry and Hematology, University of Helsinki, Helsinki, Finland

¹⁰Department of Anatomy, University of Helsinki, Helsinki, Finland

¹¹Department of Molecular Medicine and Medical Biotechnology and CEINGE, Naples University 24 Federico II, 80131, Naples, Italy

Correction notice This paper has been updated since first published to amend author name 'Moon Hee Lee'.

Twitter Satu Mustjoki @hruh_research and Vincenzo Cerullo @vincersurf

Acknowledgements We thank H Ibrahim for helping us with live cell microscopy. We also thank L Pietilä for helping us with collecting serum.

Contributors FH, EY, JC and VC conceived and planned all the experiments. FH and YG carried out most of the experiments. EY, MF, SF, JC, BM, MF, SR, OKK, AK and MG helped in carrying out most of the experiments. ML and TGM helped in carrying out live-cell microscopy. ML, P.J, HN, AK, MG and SM helped with providing patient material and conducting related experiments. MG and VC supervised the project. FH, EY, MG and VC wrote and corrected the paper. All authors provided critical feedback and helped shape the research, analysis and manuscript.

Funding FH thanks the Research Foundation of the University of Helsinki for funding his doctoral studies at the Faculty of Pharmacy, Helsinki University. VC acknowledges the European Research Council under the Horizon 2020 framework (<https://erc.europa.eu>), ERC-consolidator Grant (Agreement no. 681219), Jane and Aatos Erkkö Foundation (Project no. 4705796), HiLIFE Fellow (Project no. 797011004), Cancer Finnish Foundation (Project no. 4706116), Magnus Ehrnrooth Foundation (Project no. 4706235), Academy of Finland and Digital Precision Cancer Medicine Flagship iCAN. SM received funding from the Cancer Foundation



Finland, the Sigrid Juselius Foundation, the Relander Foundation, state funding for university-level research in Finland and HiLife fellow funds from the University of Helsinki.

Competing interests None declared.

Patient consent for publication Not required.

Ethics approval This study was approved by the Helsinki University Hospital Ethical committee (Renal Cell Carcinoma patients DNRO 115/13/03/02/15).

Provenance and peer review Not commissioned; externally peer reviewed.

Data availability statement All data relevant to the study are included in the article or uploaded as supplementary information. All data relevant to the study are included in the article or uploaded as supplementary information.

Supplemental material This content has been supplied by the author(s). It has not been vetted by BMJ Publishing Group Limited (BMJ) and may not have been peer-reviewed. Any opinions or recommendations discussed are solely those of the author(s) and are not endorsed by BMJ. BMJ disclaims all liability and responsibility arising from any reliance placed on the content. Where the content includes any translated material, BMJ does not warrant the accuracy and reliability of the translations (including but not limited to local regulations, clinical guidelines, terminology, drug names and drug dosages), and is not responsible for any error and/or omissions arising from translation and adaptation or otherwise.

Open access This is an open access article distributed in accordance with the Creative Commons Attribution Non Commercial (CC BY-NC 4.0) license, which permits others to distribute, remix, adapt, build upon this work non-commercially, and license their derivative works on different terms, provided the original work is properly cited, appropriate credit is given, any changes made indicated, and the use is non-commercial. See <http://creativecommons.org/licenses/by-nc/4.0/>.

ORCID iDs

Firas Hamdan <http://orcid.org/0000-0003-4678-7382>
 Erko Ylismäki <http://orcid.org/0000-0001-9678-2614>
 Manlio Fucsiello <http://orcid.org/0000-0002-7166-3018>
 Sara Feola <http://orcid.org/0000-0002-4012-4310>
 Jeanette Leusen <http://orcid.org/0000-0003-4982-6914>
 Satu Mustjoki <http://orcid.org/0000-0002-0816-8241>
 Vincenzo Cerullo <http://orcid.org/0000-0003-4901-3796>

REFERENCES

- Hodi FS, O'Day SJ, McDermott DF, *et al*. Improved survival with ipilimumab in patients with metastatic melanoma. *N Engl J Med* 2010;363:711–23.
- Tsao H, Atkins MB, Sober AJ. Management of cutaneous melanoma. *N Engl J Med Overseas Ed* 2004;351:998–1012.
- Zhang B, Song Y, Fu Y, *et al*. Current status of the clinical use of PD-1/PD-L1 inhibitors: a questionnaire survey of oncologists in China. *BMC Cancer* 2020;20:86.
- Topalian SL, Sznol M, McDermott DF, *et al*. Survival, durable tumor remission, and long-term safety in patients with advanced melanoma receiving nivolumab. *J Clin Oncol* 2014;32:1020–30.
- Pardoll DM. The blockade of immune checkpoints in cancer immunotherapy. *Nat Rev Cancer* 2012;12:252–64.
- Chen X, Song X, Li K, *et al*. FcγR-Binding is an important functional attribute for immune checkpoint antibodies in cancer immunotherapy. *Front Immunol* 2019;10:292.
- Brezski RJ, Georgiou G. Immunoglobulin isotype knowledge and application to Fc engineering. *Curr Opin Immunol* 2016;40:62–9.
- Simpson TR, Li F, Montalvo-Ortiz W, *et al*. Fc-Dependent depletion of tumor-infiltrating regulatory T cells co-defines the efficacy of anti-CTLA-4 therapy against melanoma. *J Exp Med* 2013;210:1695–710.
- Dahan R, Segal E, Engelhardt J, *et al*. FcγRs modulate the anti-tumor activity of antibodies targeting the PD-1/PD-L1 axis. *Cancer Cell* 2015;28:285–95.
- Goletz C, Lischke T, Harnack U, *et al*. Glyco-engineered anti-human programmed death-ligand 1 antibody mediates stronger CD8 T cell activation than its normal glycosylated and non-glycosylated counterparts. *Front Immunol* 2018;9.
- Bournazos S, Wang TT, Ravetch JV. The role and function of Fcγ receptors on myeloid cells. *Microbiol Spectr* 2016;4.
- Treffers LW, van Houdt M, Bruggeman CW, *et al*. FcγRIIb restricts antibody-dependent destruction of cancer cells by human neutrophils. *Front Immunol* 2018;9:3124.
- Derer S, Glorius P, Schlaeth M, *et al*. Increasing FcγRIIIa affinity of an FcγRIII-optimized anti-EGFR antibody restores neutrophil-mediated cytotoxicity. *MAbs* 2014;6:409–21.
- Brandsma AM, Bondza S, Evers M, *et al*. Potent Fc receptor signaling by IgA leads to superior killing of cancer cells by neutrophils compared to IgG. *Front Immunol* 2019;10.
- Lohse S, Brunke C, Derer S, *et al*. Characterization of a Mutated IgA2 Antibody of the m(1) Allotype against the Epidermal Growth Factor Receptor for the Recruitment of Monocytes and Macrophages. *J Biol Chem* 2012;287:25139–50.
- Dechant M, Valerius T. IgA antibodies for cancer therapy. *Crit Rev Oncol Hematol* 2001;39:69–77.
- Brandsma AM, Ten Broeke T, Nederend M, *et al*. Simultaneous targeting of FcγRs and FcαRI enhances tumor cell killing. *Cancer Immunol Res* 2015;3:1316–24.
- Kelton W, Mehta N, Charab W, *et al*. IgGA: A “cross-isotype” engineered human Fc antibody domain that displays both IgG-like and IgA-like effector functions. *Chem Biol* 2014;21:1603–9.
- Feng Y, Roy A, Masson E, *et al*. Exposure-Response relationships of the efficacy and safety of ipilimumab in patients with advanced melanoma. *Clin Cancer Res* 2013;19:3977–86.
- Dias JD, Hemminki O, Diaconu I, *et al*. Targeted cancer immunotherapy with oncolytic adenovirus coding for a fully human monoclonal antibody specific for CTLA-4. *Gene Ther* 2012;19:988–98.
- Höti N, Li Y, Chen C-L, *et al*. Androgen receptor attenuation of Ad5 replication: implications for the development of conditionally replication competent adenoviruses. *Mol Ther* 2007;15:1495–503.
- Nemunaitis J, Tong AW, Nemunaitis M, *et al*. A phase I study of telomerase-specific replication competent oncolytic adenovirus (telomelysin) for various solid tumors. *Mol Ther* 2010;18:429–34.
- Kanerva A, Zinn KR, Chaudhuri TR, *et al*. Enhanced therapeutic efficacy for ovarian cancer with a serotype 3 receptor-targeted oncolytic adenovirus. *Mol Ther* 2003;8:449–58.
- Hamdan F, Martins B, Feodoroff M, *et al*. GAMER-Ad: a novel and rapid method for generating recombinant adenoviruses. *Mol Ther Methods Clin Dev* 2021;20:625–634.
- Maute RL, Gordon SR, Mayer AT, *et al*. Engineering high-affinity PD-1 variants for optimized immunotherapy and immuno-PET imaging. *Proc Natl Acad Sci U S A* 2015;112:E6506–14.
- Treffers LW, Ten Broeke T, Rösner T, *et al*. IgA-Mediated killing of tumor cells by neutrophils is enhanced by CD47–SIRPA checkpoint inhibition. *Cancer Immunol Res* 2020;8:120–30.
- Matlung HL, Babes L, Zhao XW, *et al*. Neutrophils kill Antibody-Opsonized cancer cells by Trogoptosis. *Cell Rep* 2018;23:3946–59.
- Garcia-Diaz A, Shin DS, Moreno BH, *et al*. Interferon receptor signaling pathways regulating PD-L1 and PD-L2 expression. *Cell Rep* 2017;19:1189–201.
- Dosset M, Vargas TR, Lagrange A, *et al*. Pd-1/Pd-L1 pathway: an adaptive immune resistance mechanism to immunogenic chemotherapy in colorectal cancer. *Oncimmunology* 2018;7:e1433981.
- Sagiv-Barfi I, Kohrt HEK, Czerwinski DK, *et al*. Therapeutic antitumor immunity by checkpoint blockade is enhanced by ibrutinib, an inhibitor of both BTK and ITK. *Proc Natl Acad Sci U S A* 2015;112:E966–72.
- Yu W, Wang Y, Jiang Y, *et al*. Distinct immunophenotypes and prognostic factors in renal cell carcinoma with sarcomatoid differentiation: a systematic study of 19 immunohistochemical markers in 42 cases. *BMC Cancer* 2017;17.
- Chan HT, Hughes D, French RR, *et al*. CD20-induced lymphoma cell death is independent of both caspases and its redistribution into Triton X-100 insoluble membrane rafts. *Cancer Res* 2003;63:5480–9.
- Diebold CA, Beurskens FJ, de Jong RN, *et al*. Complement is activated by IgG hexamers assembled at the cell surface. *Science* 2014;343:1260–3.
- Nimmerjahn F, Ravetch JV. Fcγ receptors as regulators of immune responses. *Nat Rev Immunol* 2008;8:34–47.
- Desjarlais JR, Lazar GA. Modulation of antibody effector function. *Exp Cell Res* 2011;317:1278–85.
- Wang Y, Jönsson F. Expression, role, and regulation of neutrophil Fcγ receptors. *Front Immunol* 2019;10:1958.
- Peipp M, Lammerms van Bueren JJ, Schneider-Merck T, *et al*. Antibody fucosylation differentially impacts cytotoxicity mediated by NK and PMN effector cells. *Blood* 2008;112:2390–9.
- Kowanetz M, Wu X, Lee J, *et al*. Granulocyte-Colony stimulating factor promotes lung metastasis through mobilization of Ly6G+Ly6C+ granulocytes. *Proc Natl Acad Sci U S A* 2010;107:21248–55.
- Casbon A-J, Reynaud D, Park C, *et al*. Invasive breast cancer reprograms early myeloid differentiation in the bone marrow to

- generate immunosuppressive neutrophils. *Proc Natl Acad Sci U S A* 2015;112:E566–75.
- 40 Coffelt SB, Kersten K, Doornebal CW, *et al.* IL-17-Producing $\gamma\delta$ T cells and neutrophils conspire to promote breast cancer metastasis. *Nature* 2015;522:345–8.
- 41 Wang J, Bo X, Suo T, *et al.* Tumor-Infiltrating neutrophils predict prognosis and adjuvant chemotherapeutic benefit in patients with biliary cancer. *Cancer Sci* 2018;109:2266–74.
- 42 Braster R, O'Toole T, van Egmond M. Myeloid cells as effector cells for monoclonal antibody therapy of cancer. *Methods* 2014;65:28–37.
- 43 Albanesi M, Mancardi DA, Jönsson F, *et al.* Neutrophils mediate antibody-induced antitumor effects in mice. *Blood* 2013;122:3160–4.
- 44 Uchida J, Hamaguchi Y, Oliver JA, *et al.* The innate mononuclear phagocyte network depletes B lymphocytes through Fc receptor-dependent mechanisms during anti-CD20 antibody immunotherapy. *J Exp Med* 2004;199:1659–69.
- 45 Mantovani A, Cassatella MA, Costantini C, *et al.* Neutrophils in the activation and regulation of innate and adaptive immunity. *Nat Rev Immunol* 2011;11:519–31.
- 46 Maru Y, Tanaka N, Itami M, *et al.* Efficient use of patient-derived organoids as a preclinical model for gynecologic tumors. *Gynecol Oncol* 2019;154:189–98.
- 47 Boj SF, Hwang C-I, Baker LA, *et al.* Organoid models of human and mouse ductal pancreatic cancer. *Cell* 2015;160:324–38.
- 48 Fusco P, Parisatto B, Rampazzo E, *et al.* Patient-Derived organoids (PDOs) as a novel in vitro model for neuroblastoma tumours. *BMC Cancer* 2019;19.
- 49 Heideman DAM, Steenbergen RDM, van der Torre J, *et al.* Oncolytic adenovirus expressing a p53 variant resistant to degradation by HPV E6 protein exhibits potent and selective replication in cervical cancer. *Molecular Therapy* 2005;12:1083–90.
- 50 Zhu Z, Gorman MJ, McKenzie LD, *et al.* Zika virus has oncolytic activity against glioblastoma stem cells. *J Exp Med* 2017;214:2843–57.

STUDY III

Controlled release of enhanced cross-hybrid IgGA Fc PD-L1 inhibitors using oncolytic adenoviruses

Firas Hamdan,^{1,2,3,8} Michaela Feodoroff,^{1,2,3,4,5,8} Salvatore Russo,^{1,2,3} Manlio Fucsiello,^{1,2,3} Sara Feola,^{1,2,3} Jacopo Chiaro,^{1,2,3} Gabriella Antignani,^{1,2,3} Francesca Greco,¹ Jeanette Leusen,⁶ Erkki Ylösmäki,^{1,2,3} Mikaela Grönholm,^{1,2,3,5} and Vincenzo Cerullo^{1,2,3,5,7}

¹Laboratory of Immunovirotherapy, Drug Research Program, Faculty of Pharmacy, University of Helsinki, Helsinki, Finland; ²Translational Immunology Research Program (TRIMM), University of Helsinki, Helsinki, Finland; ³Drug Delivery, Drug Research Program, Division of Pharmaceutical Biosciences, Faculty of Pharmacy, University of Helsinki, Helsinki, Finland; ⁴Institute for Molecular Medicine Finland (FIMM), Helsinki Institute of Life Science (HiLIFE), University of Helsinki, Helsinki, Finland; ⁵CAN Digital Precision Cancer Medicine Flagship, University of Helsinki, Helsinki, Finland; ⁶Center for Translational Immunology, University Medical Center Utrecht, Utrecht, the Netherlands; ⁷Department of Molecular Medicine and Medical Biotechnology and CEINGE, Naples University Federico II, Naples, Italy

Immune checkpoint inhibitors have clinical success in prolonging the life of many cancer patients. However, only a minority of patients benefit from such therapy, calling for further improvements. Currently, most PD-L1 checkpoint inhibitors in the clinic do not elicit Fc effector mechanisms that would substantially increase their efficacy. To gain potency and circumvent off-target effects, we previously designed an oncolytic adenovirus (Ad-Cab) expressing an Fc fusion peptide against PD-L1 on a cross-hybrid immunoglobulin G (IgGA) Fc. Ad-Cab elicited antibody effector mechanisms of IgG1 and IgA, which led to higher tumor killing compared with each isotype alone and with clinically approved PD-L1 checkpoint inhibitors. In this study, we further improved the therapy to increase the IgG1 Fc effector mechanisms of the IgGA Fc fusion peptide (Ad-Cab FT) by adding four somatic mutations that increase natural killer (NK) cell activation. Ad-Cab FT was shown to work better at lower concentrations compared with Ad-Cab *in vitro* and *in vivo* and to have better tumor- and myeloid-derived suppressor cell killing, likely because of higher NK cell activation. Additionally, the biodistribution of the Fc fusion peptide demonstrated targeted release in the tumor microenvironment with minimal or no leakage to the peripheral blood and organs in mice. These data demonstrate effective and safe use of Ad-Cab FT, bidding for further clinical investigation.

INTRODUCTION

Our immune system has a significant role in maintaining the integrity of our health. Besides its role in protecting against pathogens, it is also crucial in cancer prevention and defense. Research has indicated that immunocompromised individuals have an increased risk for developing certain cancers¹ and that mouse models with defective T cells and natural killer (NK) cells bear higher susceptibility for the disease.² Moreover, the tumor microenvironment in patients with cancer has been shown to be immunosuppressive, with tumor cells able to

develop multiple immune evasion strategies.³ Therefore, a major target in drug development for the treatment of cancer has been to boost the immune system.

An integral inhibitory pathway, the checkpoint pathway, exists within our body to modulate activation of the immune system. These checkpoints prevent the immune response from overactivation, with potential consequences being autoimmune and autoinflammatory diseases and collateral immune-mediated tissue damage. One strategy tumor cells exhibit to evade an immune response is to overexpress the negative checkpoint regulator PD-L1.^{4,5} PD-L1 is a PD-1 ligand that, upon interaction, leads to T cell exhaustion and tumor evasion. Clinical trials with PD-L1 inhibitors have demonstrated enhanced overall survival outcomes with melanoma, non-small cell lung cancer, renal cell carcinoma, and bladder cancer.⁵ However, a substantial group of patients, 66%, do not respond to such therapy, and some responders develop acquired resistance during the course of treatment.⁶ Hence, a crucial improvement in PD-L1 checkpoint inhibitors is required.

Currently, the majority of the PD-L1 inhibitors in the clinic are monoclonal antibodies (of the immunoglobulin G [IgG] isotype) that mainly act as antagonizing agents. Their pertinent effector mechanisms, such as complement-dependent cytotoxicity (CDC) or antibody-dependent cell cytotoxicity (ADCC)/antibody-dependent cell phagocytosis (ADCP), are limited or abrogated. The subsequent limitation in Fc effector mechanisms is mostly due to safety issues because PD-L1 expression is ubiquitous and can lead to killing of healthy cells. However, such effector mechanisms of many antibodies

Received 31 August 2022; accepted 31 January 2023;
<https://doi.org/10.1016/j.omto.2023.01.006>.

⁸These authors contributed equally

Correspondence: Vincenzo Cerullo, Laboratory of Immunovirotherapy, Drug Research Program, Faculty of Pharmacy, University of Helsinki, Helsinki, Finland.
E-mail: vincenzo.cerullo@helsinki.fi



are required for full tumor clearance. Moreover, addition of Fc effector mechanisms has been shown to increase efficacy with PD-L1 antibodies.^{7,8} This has also been shown with the approval of avelumab, which is the only IgG1 PD-L1 checkpoint inhibitor with Fc effector mechanisms in the clinic.

We previously developed a novel PD-L1 checkpoint inhibitor consisting of a PD-1 ectodomain connected to an IgGA cross-hybrid Fc, comprising regions of an IgG1 and IgA (termed Ad-Cab).⁹ All therapeutic anti-cancer antibodies in the clinic are of the IgG isotype, which is excellent in activating the complement system and NK cells. However, they fail to activate the most abundant leukocyte population, neutrophils, because of the expression pattern of Fc gamma receptors (Fc- γ). Although neutrophils express the activating receptor Fc- γ RIIA (CD32A), they have far more abundant expression of the non-signaling Fc- γ RIIB (CD16B)¹⁰ and some expression of inhibitory Fc- γ RIIB (CD32B).¹¹ Contrary to IgG antibodies, IgA antibodies are able to exploit neutrophils because of expression of the activating Fc- α (CD89) receptor.^{10,12,13} However, they cannot activate the complement system (because of a lack of a C1q binding site) or NK cells (which do not express Fc- α). Therefore, the IgGA cross-hybrid Fc is able to generate effector functions of IgG1 and IgA, which leads to enhanced tumor killing and a decrease in immune effector population exhaustion.^{9,14}

Here, to further improve such therapy, we added certain point mutations in the IgG1 region of the IgGA Fc to increase NK cell activation (called Ad-Cab FT). Moreover, to circumvent toxicity issues, we cloned such a construct into an oncolytic adenovirus genome. Oncolytic adenoviruses have been shown to be ideal gene therapy vehicles because of their selective tropism and replication toward tumor cells while leaving healthy cells unharmed.^{15,16} This allows local and controlled release of our enhanced PD-L1 Fc fusion inhibitor in the tumor bed.

In this study, we demonstrated that the oncolytic adenoviruses were able to release substantial amounts of the Fc fusion peptides when infecting tumor cells. Our improved Ad-Cab FT was more potent in NK cell activation at lower concentrations compared with Ad-Cab but had a similar potency with activating the complement system and neutrophils. This also translated to higher potency with Ad-Cab FT when all effector components were added, mimicking physiological parameters. Ad-Cab FT also showed a good safety profile *in vivo* with humanized mouse models; mice did not lose weight, and release of the Fc fusion peptide was limited to the tumor with no leakage to the peripheral blood. Interestingly, other than superior tumor control, Ad-Cab FT was also able to remodel the suppressive microenvironment by reducing the presence of myeloid-derived suppressor cells (MDSCs).

RESULTS

Cab FT activates higher ADCC with peripheral blood mononuclear cells (PBMCs) at lower concentrations than Cab

Previously, we designed a novel Fc fusion peptide (Cab) consisting of a PD-1 ectodomain (binding to PD-L1) connected to a cross-hybrid

IgGA Fc via a GGGG linker. This Fc fusion peptide was able to display effector mechanisms of IgG1 and IgA, which increased tumor killing compared with clinically approved PD-L1 antibodies or IgG1 or IgA backbones alone. To further improve Cab, four point mutations (H268F/S324T/S239D/I332E) were added to the IgG1 portion of the cross-hybrid IgGA Fc (Cab FT) to increase activation of NK cells.¹⁷ We performed ADCC experiments with isolated PBMCs using different concentrations (20–0.15625 μ g/mL) of Cab and Cab FT. These experiments were performed with two murine (B16F10 and B16K1) and two human cell lines (A549 and MDA-MB-439) because the PD-1 ectodomain is able to bind to murine and human PD-L1. Moreover, we have previously tested the expression of PD-L1 and correlated the expression to specific lysis.⁹ With all cell lines, a clear trend can be observed in which Cab FT was more potent at lower concentrations (between 2.5–0.3125 μ g/mL) compared with Cab (Figure 1A). However, at high concentrations of 5–20 μ g/mL, Cab and Cab FT had similar efficiency in tumor killing (Figure 1A).

We then repeated the experiments using polymorphonuclear leukocytes (PMNs) as the effector population. No difference in killing was observed between Cab and Cab FT because IgG1 sub-optimally activates neutrophils (Figure 1B). No increase in tumor killing was observed when serum was added, even though the point mutations in Cab FT have been shown to increase C1q binding¹⁷ (Figure S1).

After seeing increased NK cell activation with Cab FT, we wanted to see whether we could observe such an effect under more physiological conditions where PBMCs and PMNs would be present. Similar to previous data, Cab FT was again superior to Cab at lower concentrations, further emphasizing the added gain in tumor killing (Figure 1C). Overall, the data demonstrate that the point mutations in Cab FT increase ADCC killing with PBMCs at lower concentrations.

Cab and Cab FT do not induce leukocyte killing and block the PD-L1/PD-1 axis

PD-L1 expression is not limited to tumor cells but can also be expressed by many immune cells, such as macrophages, dendritic cells (DCs), and monocytes. However, expression of PD-L1 has been documented to be lower compared with tumor cells. This is to our advantage because the copy number of a target epitope on the cell membrane is an essential requirement for antibody effector mechanisms to be activated. Hence, despite expression of PD-L1 on immune cells, Cab and Cab FT could not induce killing of such cell populations. To test that Cab and Cab FT do not harm crucial immune cells, we performed a whole-blood assay where unmanipulated blood from three different donors was incubated with 20 μ g/mL of both Cab and Cab FT. In the presence of all effector populations, we analyzed whether a decrease in cell percentage or absolute number was observed with T cells, NK cells, DCs, monocytes, and neutrophils (Figure 2A). No significant differences in percentages (Figure 2B) or absolute numbers (Figure 2C) were observed among samples treated with Fc fusion peptides, trastuzumab (binding to Her-2 and not found on immune cells)

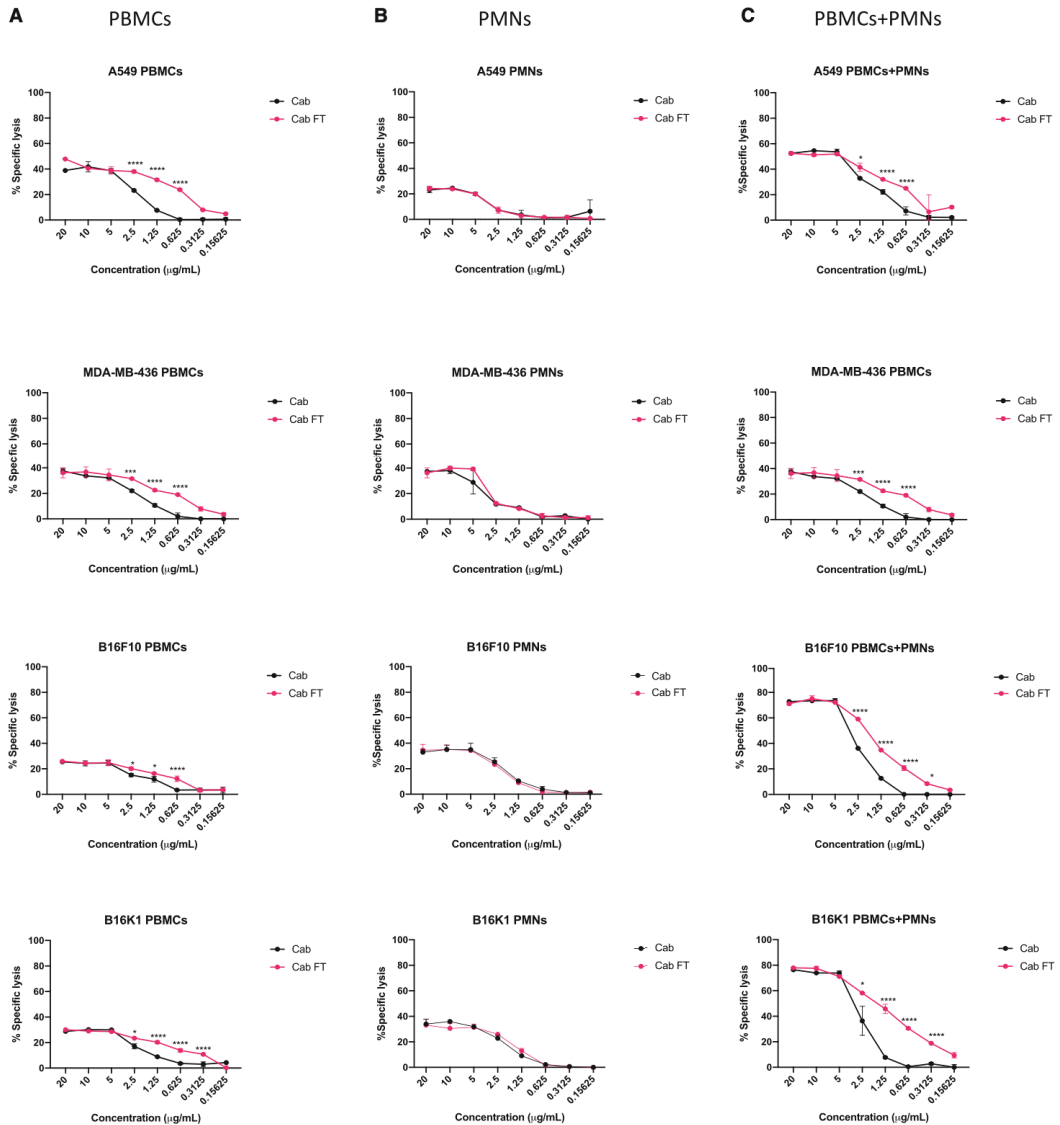


Figure 1. Cab versus Cab FT in inducing ADCC with different effector populations

(A–C) Cells were treated with different concentrations of Fc fusion peptides and had either PBMCs (A; 100:1, E:T), PMNs (B; 40:1, E:T), or PBMCs and PMNs (C) added for a 4-h incubation. Lysis was then quantified by measuring release of endogenous LDH. All $n \geq 3$, and significance levels were set at * $p < 0.05$, ** $p < 0.01$, *** $p < 0.001$, and **** $p < 0.0001$. Error bars represent SEM.

or untreated samples. This indicates that, even though Cab and Cab FT induce high tumor killing, they do not kill low-PD-L1-expressing immune cells.

Some studies have shown that increasing Fc effector functions of PD-L1 checkpoint inhibitors can lead to a higher disruption of the PD-L1/PD1 axis.¹⁸ To test whether the enhanced killing of Ad-Cab FT was

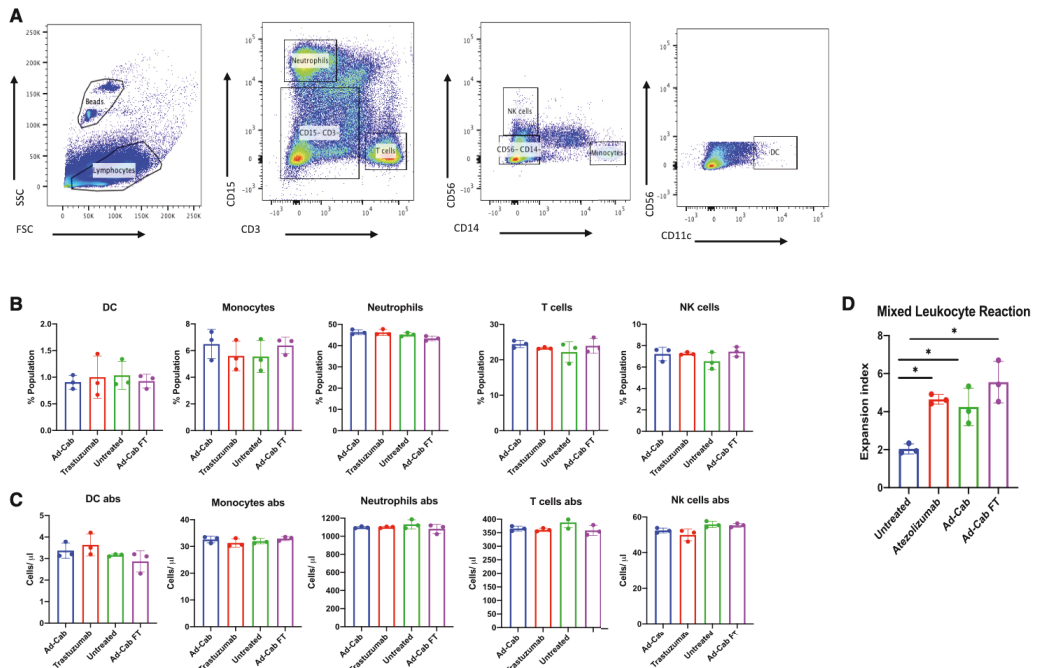


Figure 2. Whole-blood and mixed-leukocyte assay with Cab and Cab FT

Unmanipulated blood from 3 donors was treated with 20 $\mu\text{g}/\text{mL}$ of Fc fusion peptides and incubated for 24 h. (A–C) Immune populations were then gated (A) and quantified by percentage (B) and absolute number (C). DCs and CFSE-labeled PBMCs from different donors were incubated with 10 $\mu\text{g}/\text{mL}$ of Fc fusion peptides or antibody for 5 days. (D) PBMCs were then collected, and CD8+ T cells had their expansion index calculated based on CFSE staining. All $n \geq 3$, and significance levels were set at * $p < 0.05$, ** $p < 0.01$, *** $p < 0.001$, and **** $p < 0.0001$. Error bars represent SEM.

due to the point mutations and not increased PD-L1/PD1 disruption, we performed a mixed leukocyte reaction assay. In this assay, the PD-L1/PD1 axis is analyzed by co-incubating monocyte-derived DCs from one donor with carboxyfluorescein succinimidyl ester (CFSE)-stained PBMCs from another donor. Because of the presence of PD-L1 and PD1, we expect to see very little proliferation. However, in the presence of a PD-L1 checkpoint inhibitor, an increase in the expansion should be observed. Cab and Cab FT had expansion indices very similar to each other and to the clinically approved PD-L1 checkpoint inhibitor atezolizumab (Figure 2D). Hence, Cab and Cab FT have similar levels of PD-L1/PD-1 axis inhibition.

Ad-Cab and Ad-Cab FT have similar oncolytic activity and expression levels of the Fc fusion peptide

To reduce safety concerns, Cab and Cab FT were cloned into an oncolytic adenovirus-5/3 named Ad-Cab and Ad-Cab FT, respectively. After isolating the cloned viruses, a colorimetric method for determining cell viability (3-(4,5-dimethylthiazol-2-yl)-5-(3-carboxymethoxyphenyl)-2-(4-sulfophenyl)-2H-tetrazolium [MTS] assay) was

performed to assess oncolytic fitness. In human cell lines (MDA-MB-436 and A549), clear cell lysis was observed as the multiplicity of infection (MOI) increased up to 100. Ad-Cab and Ad-Cab FT had very similar levels of cell lysis, also when compared with unarmed Ad-5/3 $\Delta 24$ (Figure 3A), which is identical to Ad-Cab viruses but lacks the Fc fusion peptide gene. This indicated that Ad-Cab and Ad-Cab FT had similar oncolytic fitness and that the gene manipulation did not affect fitness/oncolysis/functionality. As expected, no cell lysis was observed in any of the murine cell lines (B16F10, B16K1, and 4T1) (Figure 3A). This is due to the lower replication of human Ad-5 viruses in murine cells.

We then tested whether Ad-Cab and Ad-Cab FT could express and secrete the Fc fusion peptides into the supernatant. Cab and Cab FT had a His tag, allowing such quantification. When A549 cells were infected at 100 MOI, a clear secretion of Fc fusion peptide was observed. This secretion level increased until reaching day 3 post infection, when around 7 $\mu\text{g}/\text{mL}$ of released peptides was detected (Figure 3B). Similar results were shown with B16K1 but with lower

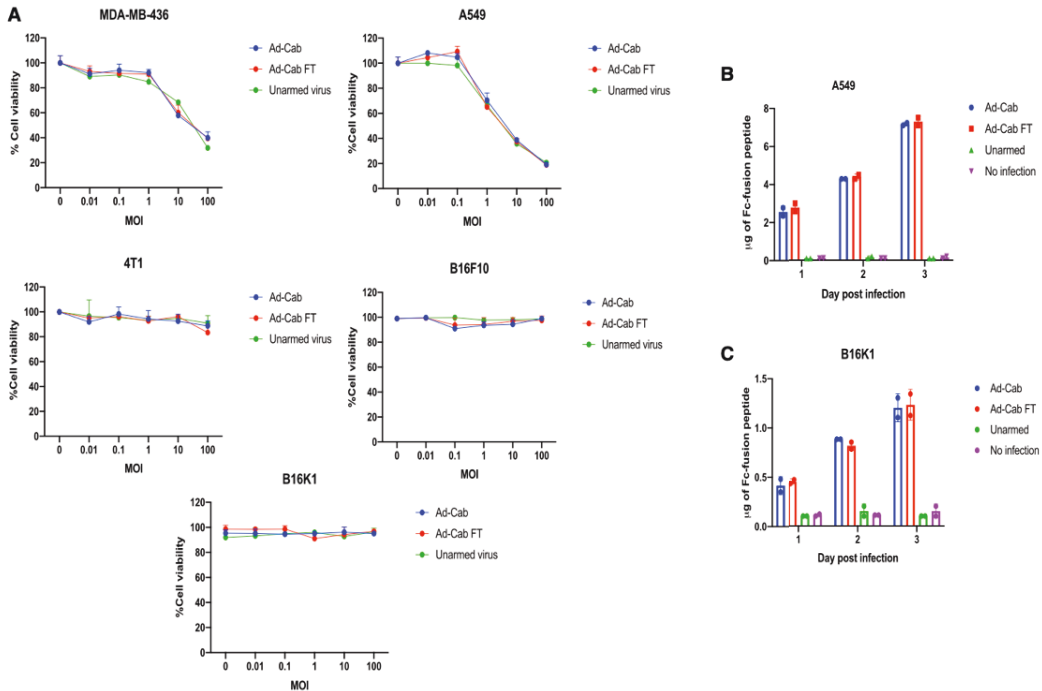


Figure 3. Oncolytic fitness and expression of Ad-Cab and Ad-Cab FT

(A–C) Different cell types were infected with the indicated MOIs of virus and incubated for 3 days. Using an MTS assay, cell viability (A) was determined. A549 (B) and B16K1 (C) cells were infected with 100 MOI of virus, and the amount of Fc fusion peptides was measured using a His tag ELISA.

amounts of secreted peptide (Figure 3C). Lower peptide levels in B16K1 are mostly due to lower adenoviral replication of Ad-5 in murine cells compared with human cells¹⁹ (Figure 3C). Together, these results indicate that Ad-Cab and Ad-Cab FT are able to express and secrete adequate levels of the Fc fusion peptide in human and murine settings.

Ad-Cab FT induces higher levels of killing at lower concentrations when PBMCs are added

To test whether the secreted Fc fusion peptides from the adenovirus were functional, we infected target cells with Ad-Cab and Ad-Cab FT and again performed ADCC assays. When human cells were infected at different MOIs ranging from 10–100, Ad-Cab FT outperformed Ad-Cab when PBMCs were added as an effector population at lower MOIs (Figure S2A). Moreover, no death was observed with Ad-5/3 Δ 24, indicating that cell lysis was due to the Fc fusion peptide and not because of viral oncolysis. With murine cells, higher MOIs were added because secretion of the Fc fusion peptide is lower compared with human cells. Similar to human cells, higher specific cell lysis could be observed with Ad-Cab FT at lower MOIs compared with

Ad-Cab. We then repeated the same experiments by adding either PMNs (Figure S2B) or complement-active serum (Figure S2C). As expected, when PMNs or serum was added, clear cell lysis was observed among Ad-Cab and Ad-Cab FT but not Ad-5/3 Δ 24. Additionally, similar specific cell lysis levels were seen with Ad-Cab and Ad-Cab FT at different MOIs.

We then performed the same experiments but with effector populations combined: PBMCs and PMNs (Figure 4). Ad-Cab FT demonstrated higher tumor cell killing levels compared with Ad-Cab at lower concentrations. Hence, Ad-Cab FT can secrete functional Cab FT and induce high tumor killing at lower MOIs when PBMCs are used as effector cells.

Ad-Cab FT induces faster killing than Ad-Cab

To further elucidate the advantages of Ad-Cab FT, we examined the kinetics of tumor killing using an impedance-based real-time quantitative analysis (XCELLigence). A549 cells were infected at 30 MOI and co-incubated with PBMCs and PMNs (Figure 5A). Cell killing was analyzed in real time, and at around 18 h, killing could be

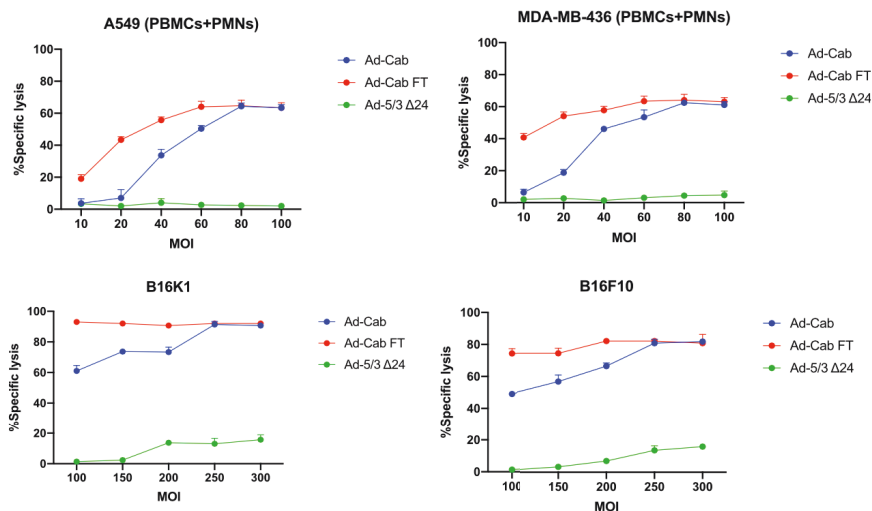


Figure 4. ADCC of Ad-Cab and Ad-Cab FT in the presence of PBMCs and PMNs

Cells were infected at various MOIs with virus and incubated for 48 h. PBMCs (100:1, E:T) and PMNs (40:1, E:T) were then added. After 4 h, lysis was quantified based on endogenous LDH release.

observed in A549 cells with Ad-Cab FT. No death was recorded at this time point with either Ad-Cab or Ad-5/3 Δ24. Cell killing for Ad-Cab and Ad-5/3 Δ24 started at around 32 and 40 h, respectively. Moreover, within 24 h, Ad-Cab FT had reached its final cell killing capacity, much earlier than the effects of viral oncolysis that were recorded with Ad-5/3 Δ24 or Ad-Cab, for which it took more than 36 h. The level of cell killing was superior with Ad-Cab FT compared with Ad-Cab, which corresponds with our previous data. In agreement with the A549 data, similar kinetics were also observed with B16K1 (Figure 5B). However, cell killing was observed later, at around 27 h for Ad-Cab FT, while for Ad-Cab, it was seen at around 42 h. These data clearly indicate that Ad-Cab FT not only kills tumor cells at a higher efficiency but also does so at a faster pace than Ad-Cab.

Ad-Cab FT controls tumor growth *in vivo* with B16K1 and 4T1

Following the *in vitro* data, we assessed the efficacy of Ad-Cab and Ad-Cab FT *in vivo* with different tumor models. For the first tumor model, we used B16K1 because of its high expression of PD-L1. Mice were sub-divided into five treatment groups receiving different treatments: PBS (mock), Ad-5/3 Δ24, Ad-Cab, Ad-Cab FT, and mPD-L1. Four injections of each treatment were given intratumorally (viruses or PBS) or intraperitoneally (antibodies), with a 2-day break between the injections (Figure 6A). Usually, 10^9 viral particles are administered per mouse for oncolytic adenovirus therapy. However, because Ad-Cab FT was shown to work at lower MOIs, each mouse was administered a one-tenth lower dose, 10^8 viral particles. As expected, Ad-Cab FT outperformed all other treatment groups

(Figures 6B and S4A). Two days after the last dose, mice were sacrificed to investigate the tumor microenvironment. Interestingly, as *in vitro*, higher NK cell activation was seen with Ad-Cab FT, explaining better tumor control than with Ad-Cab (Figure 6C). High upregulation of CD107a was observed with NK cells from the Ad-Cab FT group, which signifies a release of cytotoxic molecules such as perforins and granzymes. Upregulation of CD107a was also seen with CD8+ T cells in the Ad-Cab, Ad-Cab FT, and mPD-L1 groups because of PD1/PD-L1 inhibition (Figure 6D). Analyzing the tumor microenvironment indicates a clear increase in NK cell infiltration in Ad-Cab FT-treated groups (Figure S4B), while similar levels of CD8+ T cells (Figure S4C) and CD4+ T cells (Figure S4D) can be seen in all groups. We then tested the biodistribution of the Fc fusion peptide in the tumor and liver. In both Ad-Cab and Ad-Cab FT treated groups (Figure 6E), 1 μg/mL of Fc-fusion peptide could be observed in the tumor and undetectable levels were measured in the liver (Figure 6F). Overall, Ad-Cab FT was able to control tumor growth at lower dosages than Ad-Cab, with a safe biodistribution.

After observing the added benefit of Ad-Cab FT with B16K1, we repeated the same experiment but with a highly immunosuppressive and fast-growing tumor model, 4T1. Similar groups, schedules, and dosages were used (Figure 6G). Comparable with B16K1, Ad-Cab FT groups had the best tumor control compared with other groups (Figures 6H and S5A). Ad-Cab was also able to control tumor growth better than mPD-L1 or mock. After sacrificing the mice, we evaluated different immune cell populations. One of the main reasons why 4T1

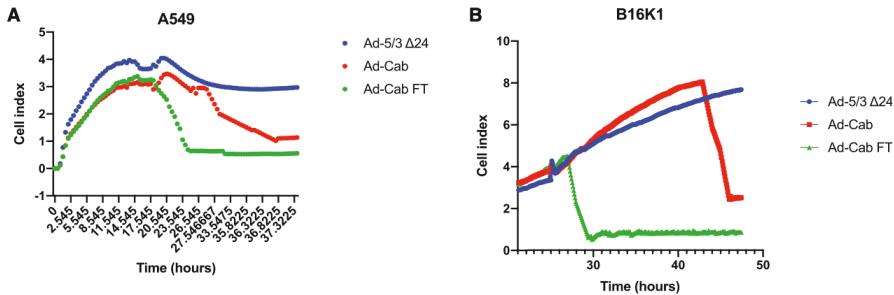


Figure 5. Real-time killing of A549 and B16K1 cells with Ad-Cab and Ad-Cab FT

(A and B) A549 (A) and B16K1 (B) cells were first seeded for 24 h. Then viruses were added at 30 MOI (A549) and 100 MOI (B16K1), along with PBMCs (100:1, E:T) and PMNs (40:1, E:T). The cell index was then measured every 30 min for the indicated times.

tumors are immunosuppressive is high infiltration of MDSCs. A decrease in MDSC granulocytic (Figure 6I) and MDSC monocytic (Figure 6J) cells can be seen in Ad-Cab FT groups, most likely because of the high expression of PD-L1. Furthermore, an increase in NK cells (Figure S5B) can be seen in Ad-Cab FT-treated groups, along with high activation (CD107a+) (Figure S5C) of such cells. Nevertheless, no changes in infiltration were seen with other immune populations, like CD8+ (Figure S5D) or CD4+ (Figure S5E) T cells, among the treated groups. Finally, a similar biodistribution was observed with around 1 $\mu\text{g}/\text{mL}$ of Fc fusion peptide in the tumor microenvironment (Figure 6K) and below-detection levels in the liver (Figure 6L). In conclusion, Ad-Cab FT was able to control 4T1 tumor growth, mostly because of NK cell activation and downregulation of MDSC populations.

Ad-Cab FT is effective in controlling the A549 tumor xenograft model *in vivo*

As a final tumor model to assess efficacy, we used nonobese diabetic (NOD)/severe combined immunodeficiency (SCID) (NS)-deficient mice with a reconstituted human immune system and A549 tumor xenografts. NS mice were first implanted with A549 tumor cells and then injected with freshly isolated PBMCs from a healthy donor (Figure 7A). Before treatment, two mice injected with or without PBMCs were sacrificed. Mice injected with PBMCs could be seen to have engrafted human CD45+ cells and human CD3+ T cells (Figure 7B). Mice were then treated with PBS (mock), Ad-5/3 $\Delta 24$, Ad-Cab, or Ad-Cab FT for a total of two injections. Two injections were given instead of four, as done previously with B16K1 and 4T1 tumor models, because a higher amount of Fc fusion peptide can be obtained with the human cell line A549 compared with murine cells because of replication kinetics. As expected, mice receiving Ad-Cab FT had the best tumor control compared with any of the other groups (Figures 7C and S6). Ad-Cab did exert a therapeutic effect, but it was low and comparable with mice receiving Ad-5/3 $\Delta 24$. When examining the tumor microenvironment, the Ad-Cab and Ad-Cab FT groups had upregulation of CD107a on NK cells, indicating activation (Figure 7D). This upregulation was nevertheless higher for Ad-Cab

FT compared with Ad-Cab, which coincides with *in vitro* data. As for CD8+ T cells, similar levels of CD107a (Figure 7E) and PD1 (Figure 7F) can be seen between Ad-Cab and Ad-Cab FT. These levels were higher compared with the Ad-5/3 $\Delta 24$ group, indicating an increase in T cell activation and exhaustion. Finally, we checked the biodistribution of the Fc fusion peptides. No Fc fusion peptides were found in the blood (Figure 7G), but a high amount could be observed in the tumor (Figure 7H) and very minimal levels in the liver (Figure 7I). This indicated that most of the Fc fusion peptide can be found in the tumor microenvironment, with no leakage to the blood and liver. Thus, xenograft data further showed the effectiveness of Ad-Cab FT.

DISCUSSION

Previously, we engineered a cross-hybrid Fc fusion peptide binding to PD-L1 that consisted of an Fc region made up of an IgA1- and IgG1-constant heavy domain.⁹ The inclusion of IgA1 and IgG1 supplemented the Fc fusion peptide with Fc effector mechanisms of both isotypes, resulting in higher tumor killing *in vitro*, *in vivo*, and *ex vivo*. To further improve this therapy, we supplemented the IgG1 region with four point mutations shown previously to increase NK cell killing¹⁷ (Ad-Cab FT). Ad-Cab FT was shown to activate higher NK cell tumor killing than Ad-Cab and to result in better *in vivo* tumor control with various tumor models when lower amounts were administered.

The attribute of efficacy in antibody therapy for cancer has been the ability to elicit Fc effector mechanisms.²⁰ Checkpoint inhibitors (atezolizumab and durvalumab) in the clinic have a reduced ability to elicit such mechanisms because of the antibody isotype or single-point amino acid mutations. However, *in vitro* and *in vivo* data have shown that cancer therapeutic antibodies require Fc effector mechanisms to be effective.⁸ This does not seem to apply to all checkpoint inhibitors and primarily depends on the checkpoint receptor. For example, when CTLA-4²¹ and PD-L1^{7,8} checkpoint inhibitors had a competent Fc able to elicit effector mechanisms, it enhanced anti-tumor efficacy *in vivo*. However, for PD-1 checkpoint inhibitors,

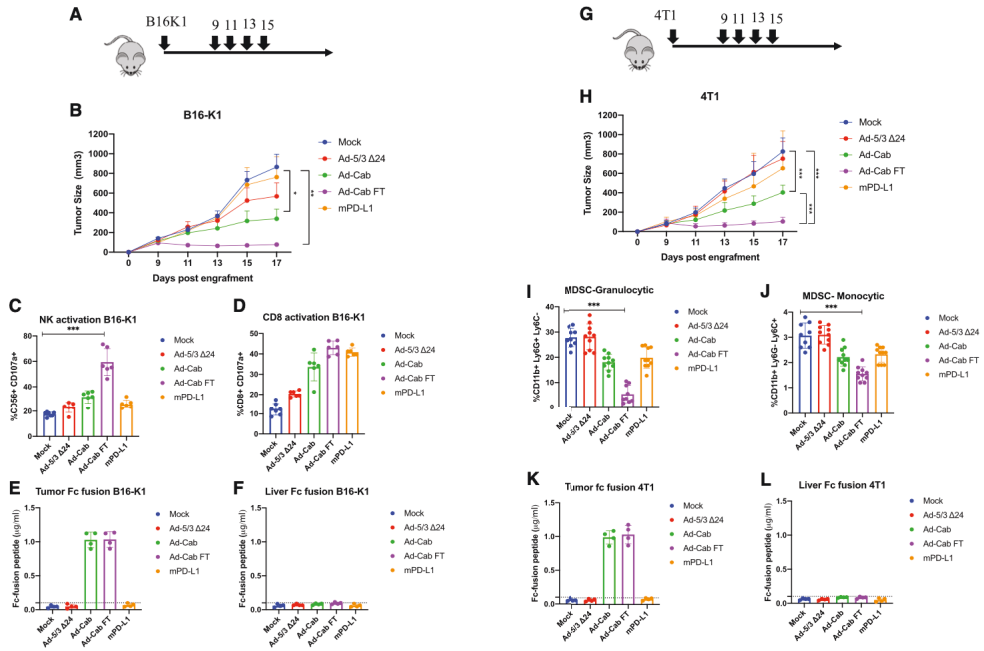


Figure 6. In vivo efficacy of Ad-Cab and Ad-Cab FT (A) Schematic of B16K1 tumor implantation and the treatment schedule. Mice were implanted with 500,000 cells in the right flank and then treated either with PBS (mock), Ad-5/3 Δ24, Ad-Cab, Ad-Cab FT, or mPD-L1. (B) Tumor growth was then recorded. (C and D) After mice were sacrificed, NK cell activation (C) and T cell activation (D) were measured with flow cytometry. (E and F) Biodistribution of the Fc fusion peptide was then checked in the tumor (E) and liver (F). (G) Schematic of the treatment schedule for mice implanted with 300,000 4T1 cells. The same treatment groups as for the 4T1 tumor model were used with B16K1 mice. (H) Tumor growth was recorded for 17 days. (I and J) After mice were sacrificed, suppressive immune cell populations, MDSC-granulocytic (I) and MDSC-monocytic (J), were analyzed with flow cytometry. (K and L) The biodistribution of Fc fusion peptides was analyzed in the tumor (K) and liver (L). All $n \geq 3$, and significance levels were set at * $p < 0.05$, ** $p < 0.01$, *** $p < 0.001$, and **** $p < 0.0001$. Error bars represent SEM.

having a competent Fc had negative effects on efficacy because of a reduction of effector CD8+ T cells.⁸ The contrasting effects can be attributed to expression patterns of immune checkpoints that differ among immune cells.

Coinciding with previous results, we show that incorporating effector mechanisms into PD-L1 immune checkpoint inhibitors (ICIs) increases efficacy and enhances tumor killing. Moreover, in syngeneic mouse models, PD-L1 ICIs with ADCC capabilities did not reduce or deplete neutrophils, DCs, NK cells, T cells, or B cells despite expressing PD-L1.⁸ Nevertheless, the enhanced efficacy was due to depletion of two major immunosuppressive populations: MDSCs and F4/80+ tumor-associated macrophages (TAMs). Contrary to our results, we did not see a decrease in TAMs. This can be explained by the fact that TAMs are a heterogeneous group of cells that can be polarized to either M1 or M2.²² M1 cells usually express a lower

amount of PD-L1 compared with M2, and the frequency of infiltration among these cell types can differ from that of tumor models. However, our results confirm that Fc-competent PD-L1 checkpoint inhibitors lead to a decrease in MDSC populations.

IgG antibodies can orchestrate immune cell killing of tumor cells by binding to their respective receptors, Fc-γ receptors. Six of these receptors are found in humans and can be divided into activating and inhibitory receptors. The mutations added in Ad-Cab FT selectively increase the binding of two activating Fc-γ receptors, Fc-γIIa (CD32A) and Fc-γIIIa (CD16A).¹⁷ NK cells only possess two Fc-γ receptors, CD16A and CD32C, which are both activating. This could potentially explain why Ad-Cab FT outperformed Ad-Cab at lower concentrations in lysing tumor cells in the presence of PBMCs. This phenomenon was not seen when PMNs were added, despite expression of CD32A on such cells. This is most likely because the

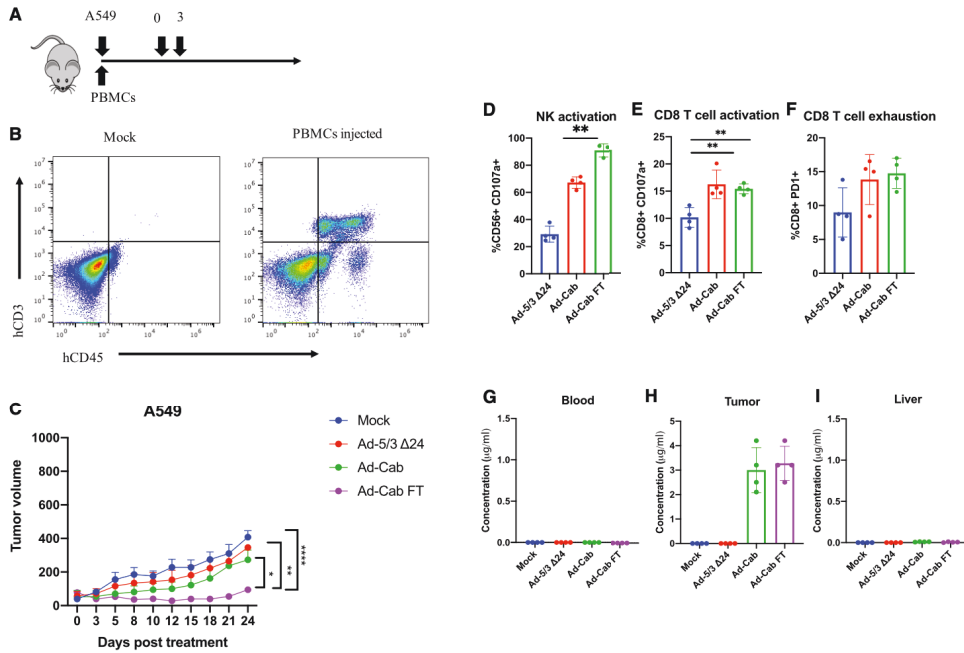


Figure 7. Efficacy of Ad-Cab and Ad-Cab FT in xenograft *in vivo* models

(A) Schematic of treatment schedules given to NS mice. Mice were first implanted in the right flank with 5×10^6 A549 cells subcutaneously and 5×10^6 PBMCs intraperitoneally. Treatment groups were divided into mice receiving Ad-5/3 Δ 24, Ad-Cab, or Ad-Cab FT. (B) Before treatment, two mice implanted with PBMCs or not were sacrificed, and human CD3+ and CD45+ cells were analyzed in the peripheral blood. (C) Tumor growth was recorded. (D–F) After mice were sacrificed, NK cell activation (D), T cell activation (E), and T cell exhaustion (F) were analyzed in the tumor microenvironment. (G–I) Biodistribution of the Fc fusion peptide was then checked in the blood (G), tumor (H), and liver (I). All $n \geq 3$, and significance levels were set at * $p < 0.05$, ** $p < 0.01$, *** $p < 0.001$, and **** $p < 0.0001$. Error bars represent SEM.

mutations in Ad-Cab FT also increase the affinity toward inhibitory receptor CD32B by 9.9-fold.¹⁷ Moreover, PMNs also express a higher level of CD16B, which does not possess a signaling motif but has been seen to serve as an inhibitory receptor in cancer therapy. Similarly, no increase in CDC activation was observed with Ad-Cab FT, despite the mutations being reported to increase the affinity for C1q. Induction of the classical pathway in complement activation does not solely require the Fc; the Fab regions are required, too.²³ The Fc fusion peptides lack the Fab regions, and this could explain why an increase in CDC activation was not observed.

Studies have demonstrated that the armamentarium of the immune system in the fight for cancer is finite.²³ The phenomenon of immune cell exhaustion has rendered many cancer immunotherapies ineffective in tumor clearance. Hence, activation of multiple immune effector populations seems to be a viable solution to overcome exhaustion. Along with previous studies,^{9,24} activation of multiple effector populations by simultaneously stimulating Fc- γ and Fc- α receptors has led to

higher tumor killing and less immune cell exhaustion. This study further confirms such findings as well as builds on the use of point mutations to further increase Fc effector mechanisms and tumor killing. Nevertheless, administering such potent Fc fusion peptides intravenously could be very toxic because PD-L1 is expressed all over healthy cells. Hence, to increase efficacy while maintaining the safety of PD-L1 checkpoint inhibitors, use of oncolytic viruses is favorable. In this study, we have shown that Ad-Cab and Ad-Cab FT were able to release the Fc fusion peptides and maintain them in the tumor. Very minimal or low detection levels of the Fc fusion peptides were found in the blood or liver. Usually, IgG antibodies have a half-life of 4–6 days in mice because of the presence of neonatal Fc receptors.²⁵ However, the Fc fusion peptides lack the binding domain to these neonatal Fc receptors, explaining why they were not detected in the blood. Moreover, Ad-Cab FT requires low doses to be effective, leading to low levels of the Fc fusion peptide being released. However, as mentioned, Ad-5 viruses do not replicate efficiently in murine settings, which could explain why the Fc-fusion peptide was not found outside of the tumor.

Further biodistribution studies are required, using more appropriate models, such as Syrian gold hamsters and non-human primates. These data show an encouraging safety profile of Ad-Cab and Ad-Cab FT and encourage clinical testing.

One of the main advantages of using adenoviruses as a therapeutic treatment is the feasibility of upscaling large amounts for clinical therapy. However, the purification process of adenoviruses has been an issue because the amount of adenovirus increases. For a therapeutic effect, 10^{13} viral particles of oncolytic viruses are given per patient, which causes purification to be an obstacle. In this study, we have shown that Ad-Cab FT requires a lower concentration to be administered to mice to control tumor growth. This could also translate into lower dosages of Ad-Cab used in the clinic with patient and as result ease purification issues with adenovirus production. In the future, Ad-Cab FT should undergo phase I/IIb clinical testing to investigate whether lower dosages of the virus is as effective compared to higher dosages of Ad-Cab.

One of the main limitations of Ad-Cab and Ad-Cab FT is long-term tumor control because oncolytic adenoviruses are usually administered intratumorally. For tumor types such as melanoma or other easily accessible tumors, repeated injections can be possible and can help with long-term tumor control. However, for tumors that are in deep tissues, this can pose a problem; guided surgical instruments are required, and repeated injections might be inconvenient for patients and pose a possible health risk. As for metastatic tumors, Ad-Cab or Ad-Cab FT would have very little effect because of the poor biodistribution of the Fc fusion peptides. One way to overcome this limitation is by adding a vaccine effect to the platform, such as attachment and/or genetic cloning of tumor peptides.

Conclusion

In this work, we further improved a previously designed PD-L1 Fc fusion peptide consisting of a cross-hybrid IgGA Fc (Ad-Cab) by adding four point mutations (Ad-Cab FT), leading to an increase in IgG effector mechanisms. At low concentrations, Ad-Cab FT was shown to secrete adequate levels of the Fc fusion peptide able to induce higher tumor killing when PBMCs were added compared with Ad-Cab. Moreover, other than higher tumor killing, Ad-Cab FT was able to induce tumor cell death faster than Ad-Cab. The effectiveness of Ad-Cab FT was also seen in different *in vivo* models, displaying better tumor control and higher activation of NK cells. Other than tumor control, Ad-Cab FT was also able to downregulate MDSC populations that have been correlated with poor prognosis and tumor growth. Finally, biodistribution analysis revealed that the oncolytic adenoviruses restricted release of the toxic Fc fusion peptides to the tumor, reducing safety concerns. In conclusion, the efficacy and safety profile of Ad-Cab FT prompt further investigation for clinical use.

MATERIALS AND METHODS

Cell lines

All cell lines in this study were purchased from the American Type Culture Collection (ATCC) and cultured in appropriate medium at

37°C and 5% CO₂. Cell lines used in this study were human lung cancer A549, human triple negative breast cancer MDA-MB-436, murine triple negative breast cancer 4T1, and murine skin cancer B16K1 and B16F10. All cell lines were cultured until reaching passage 15 and routinely checked for mycoplasma infection.

Virus transgene modifications

Adenoviruses were made to be conditionally replicating, using protocols described previously.²⁶ All adenoviruses are of serotype 5 with a fiber of serotype 3 (Ad-5/3) and contain a 24-bp deletion in the E1A region. The Fc fusion peptide transgenes were produced using the GeneArt gene synthesis service (Thermo Fisher Scientific). The Fc fusion peptide genes were then added to the adenovirus genome using protocols described previously.²⁷ In short, the gp19K + 7.1k region was substituted with the Fc fusion peptides using Gibson assembly. Moreover, the Fc fusion peptides were under a cytomegalovirus (CMV) promoter.

Cell viability assays

Cell viability was assessed by plating 10,000 cells and infecting them with various MOIs (0.01–100) for 3 days. Death was then assessed by MTS according to the manufacturer's protocol (Cell Titer 96 AQueous One Solution Cell Proliferation Assay, Promega, Naccka, Sweden) Spectrophotometric data were read using the Varioskan LUXMultimode Reader (Thermo Scientific, Carlsbad, CA, USA).

Serum collection

Ten volunteers had 40 mL of their blood taken in BD Vacutainer collection tubes (BD Bioscience), which was left to clot for 30 min at room temperature. Following clotting, blood samples were centrifuged for 5 min at 2,500 rpm. Serum was then collected and frozen at –80°C until further use.

PBMC, PMN, and monocyte collection

PBMCs and PMNs were separated and isolated from buffy coats as described previously²⁸ and cultured in Roswell Park Memorial Institute (RPMI) 1640 medium (Gibco, catalog number 21875034). From PBMCs, monocytes were further collected as described previously.¹³

Mixed leukocyte reaction

Monocytes were first differentiated into DCs by culturing in DMEM low glucose supplemented with 10% fetal bovine serum (FBS), 500 U/mL of interleukin-4 (IL-4) (PeproTech, 200-04), and 250 U/mL (Abcam, ab88382) for 7 days. After differentiation, PBMCs from a different donor were labeled with CFSE (Thermo Fisher Scientific) according to the manufacturer's protocol, cocultured at a 1:10 ratio, and treated with 1 µg/mL of either atezolizumab (InvivoGen) or Fc fusion peptide. After 5 days, supernatants were collected, and CFSE was measured in gated CD3+ CD8+ T cells by flow cytometry.

CDC assay

CDC assays were performed either with purified Fc fusion peptides or viruses. For viruses, 100,000 cells were plated and infected at the

indicated MOIs for 48 h. For Fc fusion peptides, different concentrations as indicated were added and incubated for 30 min. After incubation, 15.5% of complement-active serum was added for 4 h. Cells were then stained with 7-aminoactinomycin D (7-AAD) (eBioscience), and lysis was measured using flow cytometry.

ADCC assays

ADCC assays were performed using either purified Fc fusion peptides or viruses. Similar to the CDC assays, 15,000 cells were infected with the indicated MOIs for 48 h, while for Fc-fusion peptides, the indicated concentration was added for 30 min. After incubation, effector cells were added at a ratio of 100:1 and 40:1 (effector:target) for PBMCs and PMNs, respectively. After 4 h of incubation at 37°C, cell lysis was measured by calculating the release of endogenous lactate dehydrogenase (LDH) using a commercial kit (CyQUANT LDH Cytotoxicity Assay, catalog number C20303). Specific percent cell lysis was calculated using the following formula: (“experimental LDH release” – “effector plus target spontaneous”)/ (“target maximum” – “effector plus target spontaneous”) × 100. “Experimental LDH release” corresponds to the signal measured by the treated samples, “effector plus target spontaneous” corresponds to the release of LDH when effectors and targets are incubated, and “target maximum” corresponds to when target cells are treated with cell lysis buffer.

Whole-blood assay

Whole blood was collected from three healthy volunteers in BD Vacutainer heparin plasma tubes (BD Bioscience). Healthy volunteers were defined as volunteers with no underlying pathologies. 200 μ L of unmanipulated blood was then incubated with 20 μ g/mL of antibody or Fc fusion peptides for 24 h at 37°C. After 24 h, samples were treated with ammonium-chloride-potassium (ACK) buffer to lyse red blood cells and then stained with CD3, CD15, CD14, CD56, and CD11c (BioLegend) to differentiate immune populations. Counting beads were then added before performing flow cytometry to calculate absolute numbers (BioLegend, catalog number 424902).

Animal experiments

For syngeneic mouse experiments, 4- to 8-week-old BALB/c or C57BL/6 immunocompetent mice, purchased from Envigo, were injected with 300,000 4T1 or 500,000 B16K1 cells in the right flank, respectively. After 9 days, tumors were palpable, and then followed a treatment schedule of 4 treatments separated by 2 days of break between. Viruses or PBS were injected intratumorally at a final volume of 25 μ L, while antibodies were administered intraperitoneally at a final volume of 100 μ L. Viruses were administered at a concentration of 1×10^8 viral particles per mouse, while 100 μ g of antibody was administered per mouse. Tumor size was calculated using the following formula: (long side) × (short side)²/2.

For xenograft mice models, 4- to 6-week-old immunodeficient Nod.CB17-Prkdcscid/NCrCrl mice were purchased from Charles River Laboratories. For tumor implantation, mice were injected with 5×10^6 A549 cells subcutaneously in the right flank. On the same

day, 5×10^6 PBMCs extracted from the same donor were injected intraperitoneally for engraftment. After tumors were palpable, mice were given 2 doses of virus at a concentration of 1×10^8 viral particles per mouse.

All animal experiments were approved and reviewed by the Experimental Animal Committee of the University of Helsinki and Provincial Government of Southern Finland (license ESAVI/11895/2019). Tumor growth across all experimental groups was regularly measured throughout the experiment. All injections and tumor measurements were performed under isoflurane anesthesia.

Biodistribution analysis

After animals were sacrificed, tumors, livers, and peripheral blood were collected for processing. Tumors and livers were passed through a 0.22- μ m cell strainer to create a single-cell suspension. Samples were then centrifuged for 10 min at $500 \times g$ to pellet cells and collect the supernatant for further processing. For blood, samples were centrifuged for 30 min at $500 \times g$, and serum was collected. Because the Fc fusion peptides contain a C-terminal His tag, a His tag ELISA was used to determine concentrations from the supernatant and serum samples collected (Cell Biolabs, catalog number AKR-130).

Flow cytometry analysis

All flow cytometry samples were run either with the BD Accuri 6 plus (BD Bioscience) or Fortessa (BD Bioscience). Human and murine samples had two antibody panels each that were used. Panel 1 includes fluorescein isothiocyanate (FITC) anti-mouse NK1.1 (Thermo Fisher Scientific, catalog number 11-5941-85, RRID: AB_465319), phycoerythrin (PE) anti-mouse PD-1 (BioLegend, catalog number 135206, RRID: AB_1877231), PerCPy7 anti-mouse CD4 (Thermo Fisher Scientific, catalog number 25-0041-82, RRID: AB_469576), PerCP/Cy5.5 anti-mouse CD107a (BioLegend, catalog number 121626, RRID: AB_2572055), and Pacific Blue anti-mouse CD3 (BioLegend, catalog number 100214, RRID: AB_493645). Panel 2 included allophycocyanin (APC) anti-mouse Ly6C (BioLegend, catalog number 128015, RRID: AB_1732087), PE anti-Ly6G (BD Biosciences, catalog number 551461, RRID: AB_394208), PerCP Cy5.5 anti-mouse CD11b (Thermo Fisher Scientific, catalog number 45-0112-82, RRID: AB_953558), BV650 anti-mouse F4/80 (BD Biosciences, catalog number 743282, RRID: AB_2741400), and PECy7 anti-mouse CD11c (Thermo Fisher Scientific, catalog number 25-0114-829, RRID: AB_469590). For humans, the first panel included FITC anti-human CD56 (BioLegend, catalog number 304604, RRID: AB_314446), PerCP anti-human CD8alpha (BioLegend, catalog number 300922, RRID: AB_1575072), PE-Cy5 anti-human CD4 (Thermo Fisher Scientific, catalog number 15-0049-42, RRID: AB_1582251), PE-Cy7 anti-human CD3 (BioLegend, catalog number 300316, RRID: AB_314052), Pacific Blue anti-human PD-1 (BioLegend, catalog number 329915, RRID: AB_1877194), and APC anti-human CD107a (BioLegend, catalog number 328620, RRID: AB_1279055). The second panel for human samples included PE-Cy7 anti-human CD3 (BioLegend, catalog number 300316, RRID: AB_314052), APC anti-human CD11c (BioLegend, catalog number

371505, RRID: AB_2616901), Pacific Blue anti-human CD15 (BioLegend, catalog number 323021, RRID: AB_2105361), and PE anti-human CD14 (BioLegend, catalog number 301805, RRID: AB_314187).

Statistical analysis

All statistical analysis were performed with GraphPad Prism 7 (GraphPad, La Jolla, CA, USA). Statistical tests used were either unpaired t test or two-way ANOVA with a post hoc test (Tukey's multiple comparisons tests). All $n \geq 3$, and significance levels were set at * $p < 0.05$, ** $p < 0.01$, *** $p < 0.001$, and **** $p < 0.0001$. Error bars represent standard error of the mean (SEM).

DATA AVAILABILITY

The authors confirm that all data supporting the manuscript findings are available in the main text and supplemental figures. Raw data of this study are available upon reasonable request from the corresponding author.

SUPPLEMENTAL INFORMATION

Supplemental information can be found online at <https://doi.org/10.1016/j.omto.2023.01.006>.

ACKNOWLEDGMENTS

F.H. thanks the Research Foundation of the University of Helsinki for funding his doctoral studies at the Faculty of Pharmacy, University of Helsinki. V.C. acknowledges the European Research Council under the Horizon 2020 framework (<https://erc.europa.eu>), ERC-consolidator grant (agreement 681219), the Jane and Aatos Erkkö Foundation (project 4705796), HiLIFE Fellow (project 797011004), the Finnish Cancer Foundation (project 4706116), the Magnus Ehrnrooth Foundation (project 4706235), the Academy of Finland, and Digital Precision Cancer Medicine Flagship iCAN.

AUTHOR CONTRIBUTIONS

F.H., J.L., E.Y., and V.C. planned and conceived the experiments. F.H. and M.Feodoroff carried out most of the experiments. S.R., M.Fusciello, S.F., J.C., G.A., F.G., E.Y., and M.G. helped to carry out the experiments and interpret results. J.L. provided significant expertise. F.H. wrote the manuscript. All authors provided critical feedback and helped shape the research, analysis, and manuscript.

DECLARATION OF INTERESTS

V.C. is a co-founder and shareholder of Valo Therapeutics LTD (not related to this study).

REFERENCES

- Vajdic, C.M., and Van Leeuwen, M.T. (2009). Cancer incidence and risk factors after solid organ transplantation. *Int. J. Cancer* 125, 1747–1754. <https://doi.org/10.1002/IJC.24439>.
- Smyth, M.J., Thia, K.Y., Street, S.E., MacGregor, D., Godfrey, D.I., and Trapani, J.A. (2000). Perforin-mediated cytotoxicity is critical for surveillance of spontaneous lymphoma. *J. Exp. Med.* 192, 755–760. <https://doi.org/10.1084/JEM.192.5.755>.
- Vinay, D.S., Ryan, E.P., Pawelec, G., Talib, W.H., Stagg, J., Elkord, E., Lichter, T., Decker, W.K., Whelan, R.L., Kumara, H.M.C.S., et al. (2015). Immune evasion in can-

cer: mechanistic basis and therapeutic strategies. *Semin. Cancer Biol.* 35, S185–S198. <https://doi.org/10.1016/j.semcancer.2015.03.004>.

- Ishida, Y., Agata, Y., Shibahara, K., and Honjo, T. (1992). Induced expression of PD-1, a novel member of the immunoglobulin gene superfamily, upon programmed cell death. *EMBO J.* 11, 3887–3895. <https://doi.org/10.1002/J.1460-2075.1992.TB05481.X>.
- Chen, L., and Han, X. (2015). Anti-PD-1/PD-L1 therapy of human cancer: past, present, and future. *J. Clin. Invest.* 125, 3384–3391. <https://doi.org/10.1172/JCI80011>.
- Jácóme, A.A., Castro, A.C.G., Vasconcelos, J.P.S., Silva, M.H.C.R., Lessa, M.A.O., Moraes, E.D., Andrade, A.C., Lima, F.M.T., Farias, J.P.F., Gil, R.A., et al. (2021). Efficacy and safety associated with immune checkpoint inhibitors in unresectable hepatocellular carcinoma. *JAMA Netw. Open* 4, e2136128. <https://doi.org/10.1001/JAMANETWORKOPEN.2021.36128>.
- Goletz, C., Lischke, T., Harnack, U., Schiele, P., Danielczyk, A., Rühmann, J., and Goletz, S. (2018). Glyco-engineered anti-human programmed death-ligand 1 antibody mediates stronger CD8 T cell activation than its normal glycosylated and non-glycosylated counterparts. *Front. Immunol.* 9, 1614. <https://doi.org/10.3389/FIMMU.2018.01614/BIBTEX>.
- Dahan, R., Segal, E., Engelhardt, J., Selby, M., Korman, A.J., and Ravetch, J.V. (2015). FcγRs modulate the anti-tumor activity of antibodies targeting the PD-1/PD-L1 Axis. *Cancer Cell* 28, 285–295. <https://doi.org/10.1016/j.ccell.2015.08.004>.
- Hamdan, F., Ylösmäki, E., Chiaro, J., Giannoula, Y., Long, M., Fusciello, M., Feola, S., Martins, B., Feodoroff, M., Antignani, G., et al. (2021). Novel oncolytic adenovirus expressing enhanced cross-hybrid IgGα Fc PD-L1 inhibitor activates multiple immune effector populations leading to enhanced tumor killing in vitro, in vivo and with patient-derived tumor organoids. *J. Immunother. Cancer* 9, e003000. <https://doi.org/10.1136/JITC-2021-003000>.
- Bournazos, S., Wang, T.T., and Ravetch, J.V. (2016). The role and function of Fcγ receptors on myeloid cells. *Microbiol. Spectr.* 4.
- Treffers, L.W., Van Houdt, M., Bruggeman, C.W., Heineke, M.H., Zhao, X.W., Van Der Heijden, J., Nagelkerke, S.Q., Verkuiljen, P.J.J.H., Geissler, J., Lissenberg-Thunnissen, S., et al. (2018). FcγRIIIB restricts antibody-dependent destruction of cancer cells by human neutrophils. *Front. Immunol.* 9, 3124. <https://doi.org/10.3389/FIMMU.2018.03124/BIBTEX>.
- Brandsma, A.M., Bondza, S., Evers, M., Koutstaal, R., Nederend, M., Jansen, J.H.M., Rösner, T., Valerius, T., Leusen, J.H.W., and Ten Broeke, T. (2019). Potent Fc receptor signaling by IgA leads to superior killing of cancer cells by neutrophils compared to IgG. *Front. Immunol.* 10, 704. <https://doi.org/10.3389/FIMMU.2019.00704/BIBTEX>.
- Evers, M., Ten Broeke, T., Jansen, J.H.M., Nederend, M., Hamdan, F., Reiding, K.R., Meyer, S., Moerer, P., Brinkman, I., Rösner, T., et al. (2020). Novel chimerized IgA CD20 antibodies: improving neutrophil activation against CD20-positive malignancies. *MAbs* 12. <https://doi.org/10.1080/19420862.2020.1795505>.
- Kelton, W., Mehta, N., Charab, W., Lee, J., Lee, C.H., Kojima, T., Kang, T.H., and Georgiou, G. (2014). IgGA: a "cross-isotype" engineered human Fc antibody domain that displays both IgG-like and IgA-like effector functions. *Chem. Biol.* 21, 1603–1609. <https://doi.org/10.1016/j.chembiol.2014.10.017>.
- Feng, Y., Roy, A., Masson, E., Chen, T.T., Humphrey, R., and Weber, J.S. (2013). Exposure-response relationships of the efficacy and safety of ipilimumab in patients with advanced melanoma. *Clin. Cancer Res.* 19, 3977–3986. <https://doi.org/10.1158/1078-0432.CCR-12-3243>.
- Höft, N., Li, Y., Chen, C.L., Chowdhury, W.H., Johns, D.C., Xia, Q., Kabul, A., Hsieh, J.T., Berg, M., Ketner, G., et al. (2007). Androgen receptor attenuation of Ad5 replication: implications for the development of conditionally replication competent adenoviruses. *Mol. Ther.* 15, 1495–1503. <https://doi.org/10.1038/SJ.MT.6300223>.
- Moore, G.L., Chen, H., Karki, S., and Lazar, G.A. (2010). Engineered Fc variant antibodies with enhanced ability to recruit complement and mediate effector functions. *MAbs* 2, 181–189. <https://doi.org/10.4161/MABS.2.2.11158>.
- Sun, L., Li, C.W., Chung, E.M., Yang, R., Kim, Y.S., Park, A.H., Lai, Y.J., Yang, Y., Wang, Y.H., Liu, J., et al. (2020). Targeting glycosylated PD-1 induces potent anti-tumor immunity. *Cancer Res.* 80, 2298–2310. <https://doi.org/10.1158/0008-5472.CAN-19-3133>.

19. Blair, G.E., Dixon, S.C., Griffiths, S.A., and Zajdel, M.E. (1989). Restricted replication of human adenovirus type 5 in mouse cell lines. *Virus Res.* *14*, 339–346. [https://doi.org/10.1016/0168-1702\(89\)90026-9](https://doi.org/10.1016/0168-1702(89)90026-9).
20. Desjarlais, J.R., and Lazar, G.A. (2011). Modulation of antibody effector function. *Exp. Cell Res.* *317*, 1278–1285. <https://doi.org/10.1016/j.yexcr.2011.03.018>.
21. Simpson, T.R., Li, F., Montalvo-Ortiz, W., Sepulveda, M.A., Bergerhoff, K., Arce, F., Roddie, C., Henry, J.Y., Yagita, H., Wolchok, J.D., et al. (2013). Fc-dependent depletion of tumor-infiltrating regulatory T cells co-defines the efficacy of anti-CTLA-4 therapy against melanoma. *J. Exp. Med.* *210*, 1695–1710. <https://doi.org/10.1084/JEM.20130579>.
22. Wu, L., and Zhang, X.H.F. (2020). Tumor-associated neutrophils and macrophages—heterogenous but not chaotic. *Front. Immunol.* *11*, 553967. <https://doi.org/10.3389/FIMMU.2020.553967>.
23. Mortensen, S.A., Sander, B., Jensen, R.K., Pedersen, J.S., Golas, M.M., Jensenius, J.C., Hansen, A.G., Thiel, S., and Andersen, G.R. (2017). Structure and activation of C1, the complex initiating the classical pathway of the complement cascade. *Proc. Natl. Acad. Sci. USA* *114*, 986–991. <https://doi.org/10.1073/PNAS.1616998114/-/DCSUPPLEMENTAL>.
24. Brandma, A.M., Ten Broeke, T., Nederend, M., Meulenbroek, L.A.P.M., Van Tetering, G., Meyer, S., Jansen, J.H.M., Beltrán Buitrago, M.A., Nagelkerke, S.Q., Németh, I., et al. (2015). Simultaneous targeting of FcγRs and FcγRI enhances tumor cell killing. *Cancer Immunol. Res.* *3*, 1316–1324. <https://doi.org/10.1158/2326-6066.CIR-15-0099-T>.
25. Vieira, P., and Rajewsky, K. (1988). The half-lives of serum immunoglobulins in adult mice. *Eur. J. Immunol.* *18*, 313–316. <https://doi.org/10.1002/EJL.1830180221>.
26. Kanerva, A., Zinn, K.R., Chaudhuri, T.R., Lam, J.T., Suzuki, K., Uil, T.G., Hakkarainen, T., Bauerschmitz, G.J., Wang, M., Liu, B., et al. (2003). Enhanced therapeutic efficacy for ovarian cancer with a serotype 3 receptor-targeted oncolytic adenovirus. *Mol. Ther.* *8*, 449–458. [https://doi.org/10.1016/S1525-0016\(03\)00200-4](https://doi.org/10.1016/S1525-0016(03)00200-4).
27. Hamdan, F., Martins, B., Feodoroff, M., Giannoula, Y., Feola, S., Fuscillo, M., Chiaro, J., Antgnani, G., Grönholm, M., Ylösmäki, E., and Cerullo, V. (2021). GAMER-Ad: a novel and rapid method for generating recombinant adenoviruses. *Mol. Ther. Methods Clin. Dev.* *20*, 625–634. <https://doi.org/10.1016/j.omtm.2021.01.014>.
28. Cui, C., Schoenfelt, K.Q., Becker, K.M., and Becker, L. (2021). Isolation of polymorphonuclear neutrophils and monocytes from a single sample of human peripheral blood. *STAR Protoc.* *2*, 100845. <https://doi.org/10.1016/j.xpro.2021.100845>.